IDENTIFICATION OF A NOVEL, RAPID MECHANISM TO ALLEVIATE THE NUCLEOSOME BARRIER TO TRANSCRIPTION

A Dissertation

Presented to the Faculty of the Graduate School

of Cornell University

In Partial Fulfillment of the Requirements for the Degree of

Doctor of Philosophy

by

Steven Joseph Petesch

May 2012

IDENTIFICATION OF A NOVEL, RAPID MECHANISM TO ALLEVIATE THE NUCLEOSOME BARRIER TO TRANSCRIPTION

Steven Joseph Petesch, Ph. D.

Cornell University 2012

To efficiently transcribe genes, RNA Polymerase II (Pol II) must overcome the barrier imposed by nucleosomes and higher order chromatin structure. Many genes, including *Drosophila melanogaster Hsp70*, undergo changes in chromatin structure upon activation. It has long been thought that changes to chromatin structure occur co-transcriptionally as a result of Pol II movement through the gene and recruitment of Pol II associated factors that disrupt chromatin structure. In this dissertation, I demonstrate that, upon activation, the changes in chromatin structure of *Drosophila melanogaster's Hsp70* gene occur in an extremely rapid manner that is independent of active transcription of the gene. In addition, these changes extend beyond the gene encoding unit to natural chromatin insulating elements. From a series of targeted RNAi screens I indentified four proteins necessary for the rapid, transcription-independent loss of nucleosomes at the *Hsp70* locus following heat shock and an ordered mechanism through which they function. The first factor identified, heat shock factor (HSF), is the master transcriptional activator of heat shock genes and is rapidly recruited to the gene within seconds of heat shock, and

binds cooperatively with the second factor, GAGA Factor, already bound to the gene. HSF is necessary for the recruitment of the third identified factor, dTip60, a histone acetyltransferase that acetylates histone H2A lysine 5. This acetylation is necessary for the enzymatic activation of the fourth and final factor, Poly(ADP)-Ribose Polymerase (PARP), which catalyzes the formation Poly(ADP-ribose). PARP is associated with the 5' end of *Hsp70* before heat shock, and its enzymatic activity is rapidly induced by heat shock. This activation causes PARP to redistribute throughout the *Hsp70* loci and Poly(ADP-ribose) to concurrently accumulate in the wake of PARP's redistribution. Both the protein PARP and its catalytic activity are necessary for the rapid loss in nucleosome structure of *Hsp70* upon heat shock and full transcriptional activation of *Hsp70*. In this dissertation I propose a novel mechanism to overcome the nucleosome barrier to achieve full transcriptional activation through the enzymatic activation of PARP which results in a rapid, transcription-independent, locus-wide disruption of chromatin structure.

BIOGRAPHICAL SKETCH

I was born on August 24, 1983 in Seattle, WA to two accountants, Doug and Mary Anne Petesch. I grew up in Seattle and infamously did not speak much of my early life, as my older sister Anne did most of the talking for me. I was said to be content sitting and doing puzzles quietly. As I grew older, and my younger sister Julie appeared I found myself most happy doing math homework, both teaching it to my classmates and sometimes to my sisters as well. I graduated from St. Mark's Catholic Grade School as the class valedictorian where I convinced my 8th grade math teacher, without the support of my classmates, to teach the entirety of our math textbook for the first time in twenty years. I followed my sister to Seattle Preparatory High School where at the end of my freshman year I met my wife-to-be, Krissy Hope, as I helped manage the school's girl's volleyball team. It was here that I was the editor-in-chief of our school's newspaper, was the first student to take the BC AP Calculus test and helped convince the school to implement a BC AP Calculus class, and received the math award and class valedictorian at graduation. I decided to leave Washington for Harvey Mudd College in southern California mainly because I wanted to attend a challenging math and science college as I thought that I wanted to be an engineer and also because I still had far-fetched dreams of becoming a volleyball player. By my second year of college I realized that engineering was no longer rewarding enough for me and there was no chance of me ever becoming a professional volleyball

player. It was also at this time that I took an inspiring organic chemistry class that convinced me I would be most happy transferring into the chemistry department. Harvey Mudd College hired a new Biochemistry professor, Dr. Haushalter, the following year that had just finished a post doc in Jim Kadonaga's lab, working with single-molecule techniques, chromatin, and DNA repair proteins. It was in Dr. Haushalter's lab that I first gained laboratory experience in biochemistry and molecular biology research, was introduced into chromatin biology, and I fell in love with it all. After spending four years apart in college, I decided that I would follow Krissy to Cornell to do my graduate school work, where she was already in her first year of graduate school. It was here at Cornell that I was first able to experience all things that I am most passionate about at once: science, teaching, Krissy, and volleyball. As I leave Cornell and head back to Seattle I hope to continue pursuing science in creative ways, challenging others when it comes to what they are capable of achieving, and maybe, if there is still time, become a better volleyball player.

I would like to dedicate this work to my family, friends, and particularly my wife, who, through perseverance, is now appropriately named Dr. Hope.

ACKNOWLEDGMENTS

I would first, and foremost, like to acknowledge my advisor, John Lis, for accepting me into his lab and being incredibly supportive of allowing me to investigate the things that most interested me. John is an advisor whose enthusiasm and passion for science is nothing short of infective. John is an incredibly creative thinker that always is looking towards developing unique techniques that allow us to visually observe and quantitatively measure the many aspects of transcription. I have learned a lot from him throughout the years as to how to go about picking interesting questions to answer and to push the limits of a technology's current capabilities to provide the most comprehensive and accurate answer to those questions. In my years of being in the lab with John I can honestly say that after every time I spoke with him about my project I came away from those discussions more inspired and always looking at some aspect of my project from a different perspective than before. I attribute much of the success of my project to his critical thinking and providing a creative soundboard through which this project was cultivated and grew into the story it is today.

I would also like to acknowledge my two committee members, Eric Alani and Michelle Wang. I had the privilege of rotating through Eric's lab as a first year graduate student and learned a lot from him, and his class, about how to think about a problem from a geneticist's point of view. His discussions of how to identify the target of PARP's actions at *Hsp70* were always very

helpful. I also would like to thank him for his cheery disposition as I looked forward to updating him about my recent progress and developments in my project and future career goals. I would also like to thank Michelle for her added expertise about how to think about this project through the prospective of a physicist. Her continued suggestions of how to improve the temporal and spatial resolution of my assays to better describe the potential models for how nucleosomes could be lost or how PARP redistributes were very beneficial. I could not have asked for a better committee as their background and input complimented each other greatly.

In addition to thanking all the members of the John's lab that I have overlapped with in my time, I would like to mention a few in particular. Upon rotating through the lab, I was guided by both Behfar Ardehali and Nicholas Fuda. Throughout the years they have provided me with exceptional technical guidance and some of the most useful experimental suggestions throughout our many subgroup and group meetings. Their selfless, thoughtful, and critical perspectives provided me with role models as to how to think and approach science in a laboratory setting. I would also like to thank Abbie Saunders for her willingness to help edit and revise my first publication and to help me achieve a writing style that was more "sexy" for publication purposes. I lastly have to thank Janis Werner, John's lab manager, who has provided an easy, organized, and efficient lab work environment while I was here.

I finally have to thank my family, friends, and wife. I first have to thank my parents for their willingness to send me to a great college and pay for my

education, even after telling them that I no longer wanted to be an engineer but would rather pursue chemistry. I would also like to acknowledge my friends, both scientists and nonscientists, for being able to share in my excitement and celebrate with me my accomplishments. Finally, I would like to thank my wife, Krissy Hope, who, as a scientist, has provided me with just as much feedback, insights, and criticisms regarding my project than the members of my lab.

I would like to end my acknowledgements with an explanation of how John's patience and creative input helped mold this project from the beginning. After joining John's lab in June of my first year, he and I talked almost every day for multiple months about potential ideas or questions that we had surrounding the interface of chromatin and transcription. Besides an ongoing RNAi screen in the lab, I did not pick up a pipette for my own project for virtually months. Instead, my many ideas that were presented were met with either fair criticisms or tepid responses. Although frustrated, and slightly concerned that John might soon regret his decision to let me join the lab, I always felt inspired from my discussions with John to think of a new idea and grateful for his patience with me. It was ultimately after one group meeting that a discussion with him resulted in us both excited about the prospect probing the chromatin landscape near the paused polymerase of *Hsp70* both before and after heat shock to understand the fate of transcribed nucleosomes at high resolutions. I look back and acknowledge that these first few months in the lab of critically thinking and talking with John as what truly helped me

develop a project that, regardless of the results of the experiments, would provide answers to relatively unanswered, interesting questions.

This work was supported by an NIH grant GM25232 to J.T.L and a predoctoral training grant T32-GM70723 to S. J. P.

TABLE OF CONTENTS

LIST OF FIGURES

LIST OF TABLES

LIST OF ABBREVIATIONS

Asf1: anti-silencing factor 1

BEAF-32: boundary element associated factor, 32 kDa

bp: base pairs

BPTF: bromodomain PHD-finger transcription factor

CAF-1: chromatin assembly factor 1

CHD: chromodomain-helicase-DNA-binding protein

ChIP: chromatin immunoprecipitation

Chz1: chaperone for H2A.Z-H2B

CBP: CREB (cAMP-response-element-binding protein)-binding protein

Daxx: death domain associated protein

DRB: 5,6-dichloro-1-beta-d-ribofuranosylbenzimidazole

DSIF: DRB sensitivity inducing factor

ERCC3: excision repair cross-complementing rodent repair deficiency, complementation group 3

FACT: facilitates chromatin transcription

FRAP: fluorescence recovery after photobleaching

FRET: fluorescence resonance energy transfer

GAF: GAGA associated factor

Gcn5: general control non-derepressible 5

H2A: histone H2A

H2B: histone H2B

H3: histone H3

H4: histone H4

HDAC3: histone deacetylase 3

HIRA: histone regulator A protein

HS: heat shock

HSF: heat shock factor

Hsp70: heat shock protein, 70 kDa

INO80: inositol-requiring 80

IP: immunoprecipitation

ISWI: imitation switch

kDa: kilo Daltons

LacZ: beta-galactosidase encoding gene

Med15: mediator of RNA polymerase II transcription subunit 15

Med23: mediator of RNA polymerase II transcription subunit 23

MI-2: idiopathic inflammatory myopathy nuclear antigen 2

Min: minute

MNase: micrococcal nuclease

NAD^+: nicotinamide adenine dinucleotide

Nap1: nucleosome assembly protein 1

NHS: non heat shock

Nurf301: nucleosome remodeling factor, 301 kDa

P-TEFb: positive transcription elongation factor b

Paf1: RNA polymerase II associated factor

PAR: poly(ADP-ribose)

PARP: poly(ADP-ribose) polymerase

PHD: plant homeodomain

Pol II: RNA polymerase II

PTM: post-translational modification

qPCR: quantitative polymerase chain reaction

rcf: rate centrifugal force

RNAi: RNA interference

Rp49: ribosomal protein gene RpL32

Rpm: revolutions per minute

RSC: remodels the structure of chromatin

RT-qPCR: reverse transcription-quantitative polymerase chain reaction

scs/scs´: specialized chromatin structure elements

sec: seconds

S2: *Drosophila* Schneider 2

SWI/SNF: switch/sucrose nonfermentable

SWR1: SWI/SNF related protein 1

Spt3: suppressor of ty homolog 3

Spt6: suppressor of ty homolog 6

Tip60: TAT interactive protein, 60 kDa

Topo1: topoisomerase 1

Topo2: topoisomerase 2

Tra1: transformation/transcription domain–associated protein 1

Ubp8: ubiquitin specific protease 8

Zw5: zeste white 5

LIST OF SYMBOLS

´: minutes

´´: seconds

°C: degrees Celsius

M: molar

mg: milligrams

mL: milliliters

mM: millimolar

U: units

µg: micrograms

µL: microliters

µM: micromolar

x g: times the acceleration due to gravity

CHAPTER 1 AN INTRODUCTION TO OVERCOMING THE NUCLEOSOME BARRIER DURING TRANSCRIPT ELONGATION[1]

RNA Polymerase II (Pol II) must break the nucleosomal barrier to gain access to DNA and efficiently transcribe genes. New single molecule techniques have elucidated many molecular details of nucleosome disassembly and what happens once Pol II encounters a nucleosome. This introduction highlights mechanisms that Pol II utilizes to transcribe through nucleosomes including the roles of chromatin remodelers, histone chaperones, post-translational modifications of histones, incorporation of histone variants into nucleosomes, and activation of the Poly(ADP-Ribose) Polymerase enzyme. Future studies need to assess the molecular details and the contribution of each of these mechanisms, individually and in combination, to transcription across the genome to understand how cells are able to regulate transcription in response to developmental, environmental, and nutritional cues.

1.1 The Nucleosome is a Natural Barrier to Transcript Elongation of Pol II

Eukaryotic organisms efficiently package their genetic information into the nucleus by compacting DNA into chromatin. The fundamental repeating unit of chromatin is the nucleosome which is comprised of 147 base pairs (bp) of DNA bound to a central octamer of histone proteins, consisting of two H2A-

[1] Parts taken from (Petesch and Lis, 2012b)

H2B dimers and one H3-H4 tetramer (Figure 1a). The primary effect of nucleosome formation is a six fold compaction of DNA, which subsequently, can form yet higher order chromatin structures (Li and Reinberg, 2011).

Although DNA compaction into the nucleosome serves an important structural necessity for packaging genetic information into the nucleus, it also presents an inherent obstacle to any cellular process that requires DNA access, such as gene expression (Kulaeva et al., 2007). Transcription of mRNA encoding genes by Pol II can be regulated at many distinct steps (Fuda et al., 2009). Although nucleosomes can inhibit the stage of transcription initiation by occupying key regulatory DNA sequences near the promoter and transcriptional start sites of genes, these DNA regions are often depleted of nucleosomes in vivo (Yuan et al., 2005) and the rules that dictate nucleosome positioning and occupancy near these regions are an area of active research (Jiang and Pugh, 2009; Segal and Widom, 2009). Nucleosomes, however, occupy the coding region of nearly all genes and have been shown to severely inhibit the rate of transcription and processivity of purified Pol II complexes in vitro (Izban and Luse, 1991; Knezetic and Luse, 1986; Lorch et al., 1987). More recent in vitro studies have shown that the magnitude of the nucleosome barrier to Pol II transcription is dictated by the strength of local histone-DNA interactions and by the positions of these interactions within the nucleosome (Bondarenko et al., 2006). Surprisingly, Pol II transcript elongation rates in vitro on naked DNA are comparable to the rates that have been measured in vivo on genes (~1-4 kb/min) where nucleosomes should, in principle, impede

its path (Ardehali and Lis, 2009). Additionally, nucleosomes that contain DNA sequences that have strong local interactions and impose a polar barrier to transcription in vitro do not greatly affect transcription when inserted into the genome in vivo (Gaykalova et al., 2011). These results indicate that the cell utilizes mechanisms to abrogate the inherent barrier that the nucleosome poses to transcribing Pol II.

1.2 Single-Molecule Analysis of Nucleosome Disassembly and Transcription through Nucleosomes

The nucleosome assembles through the addition of an H3-H4 tetramer to DNA followed by sequential addition of each H2A-H2B dimer, and disassembles through the reverse reaction. However, less understood are the intermediate structures formed during this reversible process and the mechanisms by which Pol II and its associated factors facilitate the formation of such intermediates. Recent single-molecule *f*luorescence *r*esonance *e*nergy *t*ransfer (FRET) studies using donor or acceptor tags on histones or DNA have uncovered two important findings regarding how the nucleosome disassembles. First, the frequency of DNA breathing (i.e. spontaneous, localized release of DNA contact with histones) of the first ~20 bp occurs once every 250 ms (Li et al., 2005), but the frequency of DNA breathing ~40 bp into the nucleosome progressively and rapidly decreases to once every 10 minutes and even longer closer to the nucleosome dyad (Tims et al., 2011) (Figure 1a). Second, nucleosome disassembly occurs initially through an opening of the

H3-H4 tetramer/H2A-H2B dimer interface followed by the release of H2A-H2B dimers from the DNA (Bohm et al., 2011; Gansen et al., 2009) (Figure 1b). These results indicate that Pol II is likely able to gain access to the first segment of nucleosomal DNA through its breathing but is unlikely to be able to spontaneously access the DNA that is in direct contact with an H2A-H2B dimer, although these experiments have yet to be reported with transcriptionally engaged Pol II. Additionally, one rate-limiting step that might be facilitated by Pol II's traversal of the nucleosome is the loosening of the H3-H4 tetramer/H2A-H2B dimer interface. This is supported by the fact that a single round of Pol II transcription through a nucleosome can remove an H2A-H2B dimer and the resulting hexamer of histones is now more conducive to Pol II transcription (Bintu et al., 2011; Kireeva et al., 2002).

Single-molecule optical trap experiments have also provided additional high-resolution insight into the DNA-histone interactions and the outcomes of transcriptionally engaged Pol II encountering a nucleosome (Killian et al., 2011). Molecular unzipping experiments in which DNA is peeled away from the histone octamer reveal interactions with the DNA every 5 bp with the strongest interactions occurring at the nucleosome dyad, nearest the H3-H4 tetramer, and to a lesser extent 40 bp on either side of the dyad, where DNA contacts the H2A-H2B dimers (Hall et al., 2009). These techniques have also been used to measure the effects a nucleosome has on Pol II transcription and, as expected, the nucleosome greatly impeded Pol II's transcription, especially at physiological salt conditions, sometimes resulting in complete

Figure 1 The nucleosome contains specific interactions that provide a barrier to transcript elongation and can be disassembled through chromatin remodelers

(a) The crystal structure of the nucleosome as visualized from PDBid 1AOI [72]. The nucleosome consists of 147 bp of DNA (strands colored black) wrapped 1.7 times around a core octamer of histone proteins with 2 H2A (yellow) H2B (red) dimers associated with an H3 (blue) H4 (green) tetramer. All the subsequent depictions of nucleosomes will use the color coordination depicted here unless otherwise noted. The strongest DNA contacts that exist between the DNA and histones are marked by asterisks with the first being 30 bp into the nucleosome where DNA contacts the H2A-H2B dimer interface and 70 bp into the nucleosome at the nucleosome dyad. This perspective of the nucleosome also shows the direction of DNA movement when breathing, a process whereby DNA spontaneously breaks contact with the histones, which occurs once every 250 ms 20 bp into the nucleosome but once every 10 minutes 40 bp into the nucleosome. The figure on the right is rotated to show the same nucleosome looking at the nucleosome dyad, which is the perspective Pol II takes when it engages the nucleosome. This is the perspective sketched in (b) and subsequent figures.

(b) Diagram depicting the reversible process of nucleosome disassembly/assembly as determined by FRET assays. The first step depicts the H2A-H2B dimers breaking contact with the H3-H4 tetramer in the intact nucleosome state (i) and opening up to form the intermediate shown in (ii). The second step shows the dissociation of the H2A-H2B dimers from the DNA template leaving just the H3-H4 template as shown in (iii). The last step includes the dissociation of the H3-H4 tetramer from the DNA template resulting in naked DNA (iv).

(c) Chromatin remodelers contain multiple functions which results in either changes in the nucleosome position or composition. These four functions are depicted as reversible processes that can be achieved independently of one another. Chromatin remodelers are capable of sliding nucleosomes along a DNA template to change nucleosome positions (i), ejecting individual histones (ii), exchanging new histones into the nucleosome (H2A.Z is shown to be exchanged as an example in pink) (iii), or completely ejecting a full histone octamer (iv).

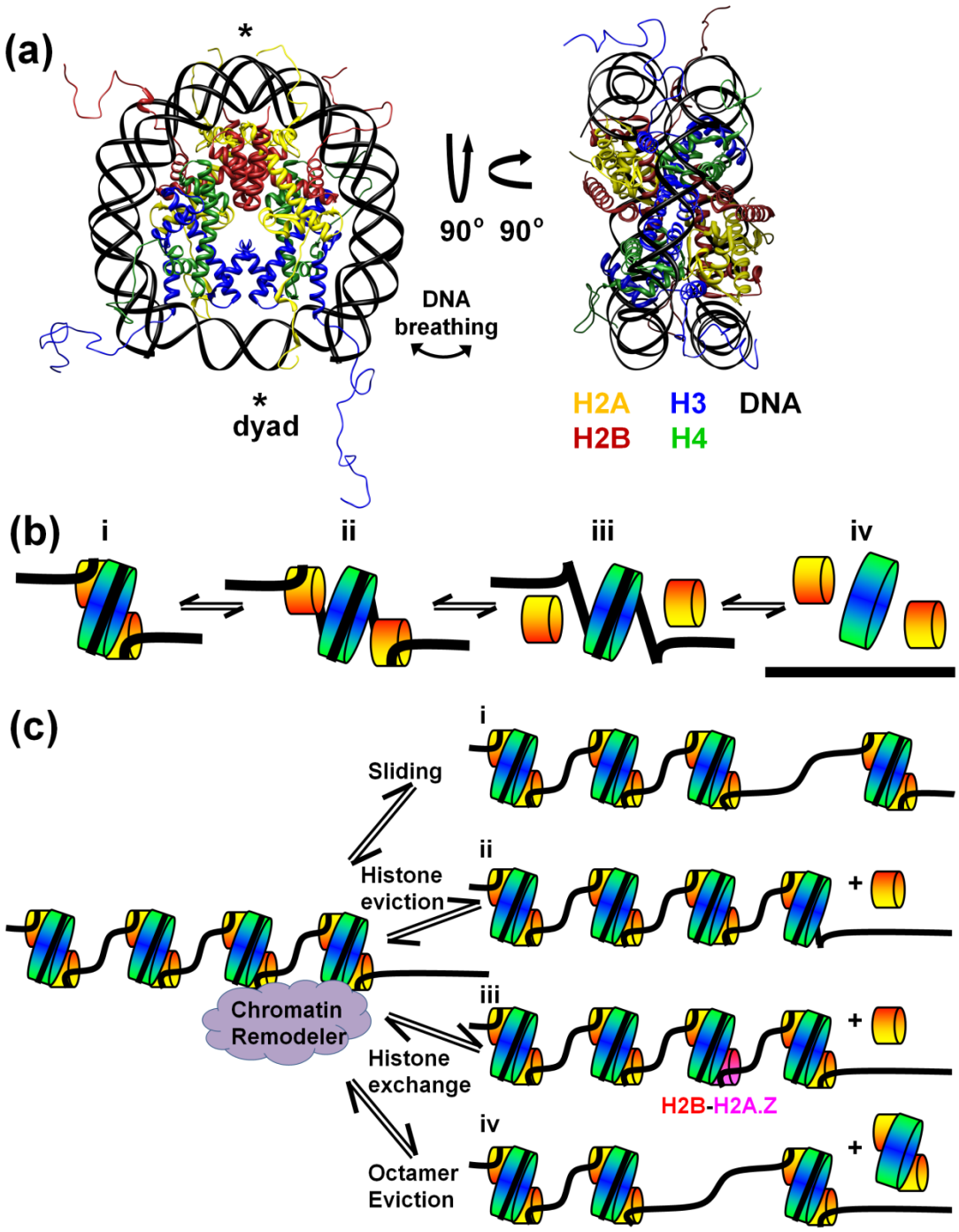
(a)
*
90° 90°
DNA
breathing
*
dyad
H2A
H3
DNA
H2B
H4
(b)
i
ii
iii
iv
(c)
i
Sliding
ii
Histone
eviction
+
Chromatin
Remodeler
iii
Histone
exchange
+
H2B-H2A.Z
iv
Octamer
Eviction
+

arrest (Hodges et al., 2009). The nucleosome increases Pol II's pause duration as it enters the first ~30 bp of the nucleosomal DNA and decreases Pol II's pause-free transcript elongation rates. These results also support additional biochemical data whereby a transient loop is formed from the upstream, transcribed DNA rewrapping around the histone, which consequently, returns histones back to the DNA in cis and maintains nucleosome positioning (Bintu et al., 2011; Hodges et al., 2009; Kulaeva et al., 2009). Both FRET and optical trap measurements demonstrate that under physiological conditions, the nucleosome provides a formidable barrier to Pol II transcription and that a significant barrier is first encountered after transcription of approximately the first 30 bp of nucleosomal DNA where contacts with the H2A-H2B dimer are strongest.

1.3 Chromatin Remodelers are ATP Driven Motors that Slide Nucleosomes and Evict Histones

Chromatin remodelers are enzymes, often a part of large macromolecular complexes, which hydrolyze ATP to translocate nucleosomes along a DNA template, evict or exchange histones, or in some cases completely evict the histone octamer (Figure 1c) (Clapier and Cairns, 2009; Hota and Bartholomew, 2011). Currently, there are four main families of chromatin remodelers that carry out these functions: *swi*tch/*s*ucrose *n*on*f*ermentable (SWI/SNF), *i*mitation *swi*tch (ISWI), *c*hromodomain-*h*elicase-*D*NA-binding protein (CHD), and *ino*sitol-requiring *80* (INO80). The combined

result of these family members' actions can provide access to underlying DNA elements or change the position, occupancy, or composition of an underlying nucleosome.

Although the SWI/SNF complex has been better studied for its role in nucleosome depletion near promoters (Brown et al., 2011; Tolkunov et al., 2011), it has also been implicated in remodeling nucleosomes in those genes that respond to rapid transcription activation. In yeast, SWI/SNF is present at both promoters and gene bodies and travels with elongating Pol II at many genes (Schwabish and Struhl, 2007; Shivaswamy and Iyer, 2008). These studies also show that SWI/SNF is needed for the loss of histones and full transcript elongation of activated methionine and heat shock genes (Schwabish and Struhl, 2007; Shivaswamy and Iyer, 2008). Just as with yeast, SWI/SNF can stimulate the loss of nucleosomes and transcription activation in humans following heat shock in vitro (Brown et al., 1996) as well as with Tat-activated transcription of the HIV-1 gene (Treand et al., 2006). It is likely that the ability of SWI/SNF to eject histones or full octamers (Bruno et al., 2003; Dechassa et al., 2010; Lorch et al., 1999) facilitates a robust transcriptional activation of many genes that respond to environmental stimuli.

Both the ISWI and CHD family of chromatin remodelers have been implicated in their ability to affect transcript elongation. The ISWI family of chromatin remodelers has been shown in vitro to possess histone exchange capabilities (Bruno et al., 2003) and to help overcome the nucleosomal barriers to transcription (Gaykalova et al., 2011). Although the ISWI complex

containing *b*romodomain *P*HD finger *t*ranscription *f*actor (BPTF or NURF-301) is able to bind to H3K4Me$_3$ and H4K16Ac (Ruthenburg et al., 2011), both marks of active transcription, ISWI is found only on the coding regions of highly transcribed genes (Gkikopoulos et al., 2011). CHD1 is also able to bind H3K4Me$_3$; but in contrast to ISWI, CHD family members all colocalize with Pol II and can participate in early steps in transcript elongation (Srinivasan et al., 2005). CHD1 is also likely to be important during transcript elongation, as it interacts with both the histone chaperone *fa*cilitates *c*hromatin *t*ranscription (FACT) and the Pol II elongation factor *D*RB *s*ensitivity *i*nducing *f*actor (DSIF) (Simic et al., 2003) and can facilitate replication-independent deposition of H3.3 (Konev et al., 2007). However, both ISWI and CHD's major reported function in vivo is to slide nucleosomes into ordered arrays throughout gene bodies and promote assembly of chromatin (Lusser et al., 2005). In yeast, ISWI helps position nucleosomes on the edge of the 5' and 3' nucleosome free regions (Whitehouse et al., 2007) and, even more strikingly, in combination with Chd1, ISWI directs the majority of nucleosome positions throughout the gene body into an ordered, repeating periodicity (Gkikopoulos et al., 2011). How or if the establishment of an ordered, periodic repeat of nucleosomes on gene bodies might be able to facilitate Pol II elongation has yet to be discovered.

The split family of ATPases which include the INO80 and *SW*I/SNF *r*elated protein *1* (SWR1) chromatin remodeling complexes facilitate transcript elongation by their ability to exchange histones. The SWR1 remodeling

complex is recruited to the 5' ends of many genes and is best characterized for its ability to deposit the variant H2A.Z-H2B dimer into nucleosomes containing canonical H2A-H2B dimers (Luk et al., 2010). Although INO80, like ISWI, slides nucleosomes into evenly spaced arrays (Udugama et al., 2011) it has also been recently shown that INO80 is able to carry out the reverse reaction of SWR1, the removal of H2A.Z-H2B variant dimers and reinsertion of canonical H2A-H2B dimers back into nucleosomes (Papamichos-Chronakis et al., 2011). It is not yet known though if the opposing actions of SWR1's deposition and INO80's removal of H2A.Z is an actively used mechanism to facilitate or hinder transcript elongation of Pol II.

1.4 Histone Chaperones Facilitate the Disassembly and Reassembly of the Nucleosome

The cell has provided the nucleus with specific safeguarding proteins that guide the proper incorporation of histones onto DNA and regulate the proper disassembly and reassembly of nucleosomes during passage of Pol II through the nucleosome. Unlike chromatin remodelers, histone chaperones do not use the energy of ATP hydrolysis, but instead have strong affinities for specific surfaces on either the H2A-H2B dimer or the H3-H4 tetramer to facilitate disruption of nucleosomes or deposition of histones (Das et al., 2010; Ray-Gallet and Almouzni, 2010). Many histone chaperones have been found to associate with specific histones, histone post-translational modifications, and elongation factors, which are listed in Table 1. I will focus on those

chaperones that have been implicated in their ability to facilitate transcription.

As Pol II approaches a nucleosome, the contacts of the nucleosome with the upstream H2A-H2B dimer are the first to be disrupted, and it is not surprising that the actions of the H2A-H2B chaperones, *n*ucleosome *a*ssembly *p*rotein *1* (Nap1) and FACT, contribute to this process. Both Nap1 and FACT have been used extensively in vitro for the assembly and disassembly of H2A-H2B within nucleosomes. Nap1 is able to cooperate with many other factors associated with transcriptionally active regions such as the *r*emodel the *s*tructure of *c*hromatin (RSC) (Lorch et al., 2006) or Chd1 (Walfridsson et al., 2007) chromatin remodelers to facilitate the disassembly of H2A-H2B dimers. Nap1 can also act directly on H3K14Ac modified nucleosomes (Luebben et al., 2010) to facilitate this disassembly. Nap1 could affect transcript elongation by managing the relative H2A-H2B density on genes by regulating the deposition of free H2A-H2B dimers onto DNA (Andrews et al., 2008). As opposed to Nap1, FACT has been shown to directly affect transcription coupled nucleosome disassembly. FACT was first identified by its ability to facilitate Pol II transcription through a nucleosome template in vitro (Orphanides et al., 1998). In vivo, FACT tracks with elongating Pol II (Mason and Struhl, 2003; Saunders et al., 2003) and also physically associates with many known factors that aid transcript elongation (Table 1). Ubiquitination of H2BK123, which is also associated with transcriptionally active regions (Figure 2), greatly stimulates FACT's ability to aid Pol II's transcription through chromatin assembled templates in vitro (Pavri et al., 2006). Recently, H2BK123

ubiquitination was shown to facilitate transcription elongation in vivo through its ability to promote nucleosome reassembly following Pol II transcription (Batta et al., 2011), perhaps through its association with FACT, or by directly altering chromatin structure (Fierz et al., 2011). It is not yet clear if Nap1 and FACT have separate or redundant functions, or if their major in vivo contribution to transcript elongation comes from aiding in disassembly of the H2A-H2B dimer or, as clearly shown in yeast (Del Rosario and Pemberton, 2008; Schwabish and Struhl, 2004), in the reassembly of the nucleosome in the wake of Pol II's passage or both.

Of the many histone chaperones that facilitate the disassembly and reassembly of the H3-H4 tetramer (Table 1), *a*nti *s*ilencing *f*actor *1* (Asf1) and *su*ppressor of *t*y homolog *6* (Spt6) facilitate transcript elongation. Asf1 interacts with promoters and gene bodies and mediates H3's eviction and deposition during Pol II transcription (Schwabish and Struhl, 2006). Asf1 also associates with the histone acetylase responsible for H3K56Ac and together can facilitate the replication-independent exchange of H3-H4 within coding regions (Rufiange et al., 2007). Spt6 also possesses H3-H4 chaperone activity and closely associates with elongating Pol II (Andrulis et al., 2000) and can positively affect the transcript elongation rate of Pol II in vivo (Ardehali et al., 2009). Loss of Spt6 function results in a genome-wide reduction in H3 density across many transcriptionally active genes implicating Spt6 in the reassembly of H3 back into nucleosomes after Pol II elongation (Ivanovska et al., 2011). It is unknown if Spt6's function in facilitating transcript elongation is

Table 1 Histone chaperones interact with specific histones, histone post-translational modifications, and additional factors that facilitate transcriptional elongation.

Histone Chaperone	Associated Histones[a]	Associated PTMs[b]	Associated Transcript elongation Factors[c]
Nap1	H2A-H2B (preferred) H2A.Z-H2B H3-H4		FACT, Chd1
FACT	H2A-H2B H2A.X-H2B	H2BK123Ub	Pol II, Chd1, PARP-1, CK2, PAF, Nap1, DSIF, Spt6, TopoI, TopoII, RPA
Chz1	H2A-H2B H2A.Z-H2B	H2BK123Ub	Swr1
Asf1	H3-H4	H3K56Ac, H3K9Ac, H4K5Ac, H4K12Ac, $H3K36Me_3$	HIRA, CAF-1, CK2, Set2, Bdf1, Spt15, TFIID, SWI/SNF
Spt6	H3-H4	$H3K36Me_{2/3}$	Pol II, CK2, Spn1, FACT, DSIF
HIRA	H3.3-H4		Asf1, TFIID, SWI/SNF, Rtt106, DSIF
Daxx	H3.3-H4		Atrx
CAF-1	H3-H4	H3K56Ac, H4K5Ac, H4K12Ac	Rtt106, Asf1,
Rtt106	H3-H4	H3K56Ac	HIRA, SWI/SNF, CAF-1
Vps75	H3-H4	H3K9Ac, H3K23/27Ac	R1109, Pol II, NuA4

[a]as reviewed in (Das et al., 2010)
[b]as reviewed in (Avvakumov et al., 2011)
[c]as reviewed in (Das et al., 2010) and mined from physical interaction data from http://www.thebiogrid.org and http://www.yeastgenome.org

a result of promoting nucleosome reassembly (Kaplan et al., 2003) or disassembly, or if Spt6 affects Pol II elongation through a completely separate mechanism.

Just as canonical histones have specific chaperones so too do histone variants. Whereas an H2A.Z specific histone chaperone, Chz1, has been identified in yeast (Luk et al., 2007) as a part of the Swr1 remodeling complex, other organisms may rely on Nap1 for this function or contain a yet to be determined H2A.Z chaperone. H3.3 variants have completely separate chaperones. Both the *hi*stone *r*egulator *A* protein (HIRA) (Tagami et al., 2004) and *d*eath domain-*a*ssociated protein (Daxx) (Goldberg et al., 2010) are able to aid in the assembly of the histone variant H3.3 into chromatin where it is deposited onto transcriptionally active gene bodies in a replication-independent manner (Deal et al., 2010). The Chd1 chromatin remodeler interacts with HIRA and aids in the deposition of H3.3 (Konev et al., 2007). Single-molecule experiments, with their ability to track individual transcribing complexes in real time, could provide valuable insights to the mechanisms by which histone chaperones actively destabilize or disassemble nucleosomes in the presence of elongating Pol II.

1.5 Histone Post-Translational Modifications Alter Nucleosome Composition and Chromatin Structure

Post-translational modifications (PTMs) of histones are able to regulate the specific composition and structure of nucleosomes at individual genes

(Bannister and Kouzarides, 2011; Taverna et al., 2007). These modifications alter the localized chromatin structure or composition by either directly changing the chromatin structure or by providing a specific binding surface that increases the affinity of particular effector proteins that are able to change chromatin. New modifications and related functions continue to be discovered (Tan et al., 2011). Here, I summarize those modifications associated with active transcription, along with the enzymes responsible for the modification, and the protein effectors that can bind to those modifications and further affect chromatin structure and function (Table 2). In this section, I will highlight modifications that specifically alter the structure of chromatin in a way that facilitates Pol II transcription.

There exists a plethora of data showing that nearly every imaginable post-translational modification within the cell can be found on histones. These include classical modifications such as acetylation, methylation, phosphorylation, ubiquitination, and sumoylation, but also less well studied modifications including ADP-ribosylation, citrullination, glycosylation, hydroxylation, formylation, and crotonylation. They occur at many residues, particularly on the N-terminal tails of histones, and can occur in specific combinations that can increase or decrease the affinity of other effector proteins important for transcript elongation. Although many of these modifications are known to positively correlate with the transcriptional activity of a gene, less causative information exists regarding their ability to facilitate Pol II's traversal of the nucleosome structure by either directly affecting the

Table 2 Elongating Pol II associates with specific PTMs of histones which a variety of effector proteins bind to and facilitate transcription.

Histone	PTM[a]	Modifying Enzyme[a]	Known Effector Domains and Proteins[b]
H2A	K5 Ac	Tip60/Esa1	
H2B	K5 Ac	P300, ATF2	
	K12 Ac	P300/CBP, ATF2	
	K15 Ac	P300/CBP, ATF2	
	K20 Ac	P300	
	S33/S36 PO_4	TAF1, AMPK	
	K120/123 Ub	UbcH6/Rad6	COMPASS (Cps35)
H3	R2 Me	CARM1	
	K4 $Me_{2/3}$	Set1, Set7/9, MLL, ALL-1, Ash1, ALR, ALR-1/2	Chromo (Chd1), PHD (BPTF, TAF3, RAG2, ING2,4, PHF2,8, YNG1) Tudor (JMJD2A,C, Sgf29), MBT, Zf-CW
	K4 Ac	Esa1	
	K9 Ac	Gcn5	
	S10 PO_4	Msk1, Msk2, IKK- ,Snf1, Jil-1	14-3-3, Gcn5, Bmh1, Bmh2
	K14 Ac	Gcn5/PCAF, P300, Tip60/Esa1, TAF1, Sas3	Tandem PHD (DPF3b), Tandem Bromo (Rsc4), Bromo 2 (Polybromo)
	R17 Me	CARM1	Tudor (TDRD3)
	K18 Ac	Gcn5, P300/CBP	
	K23 Ac	Gcn5, P300/CBP, Sas3	
	R26 Me	CARM1	
	S28 PO_4	Msk1, Msk2	
	K36 Me_3	Set2, HYPB, Smyd2, NSD1	Chromo (Eaf3, MSL3, MRG15), PWWP (Dnmt3A, Msh-6, BRPF1, NSD1,2,3, N-PAC)
	K56 Ac	Rtt109, P300	SWI/SNF (Snf5), Rtt106
	K79 Me_2	Dot1	Tudor (53BP1)
H4	R3 Me	PRMT1, PRMT5	P300, Tudor (TDRD3), Dnmt3a
	K5 Ac	P300, ATF2, Tip60/Esa1, HAT1	Bromo (Brdt)
	K8 Ac	P300, Gcn5/PCAF, ATF2, Tip60/Esa1, Elp3	Bromo (Brdt)
	K12 Ac	P300, HAT1, Tip60/Esa1	
	K16 Ac	Gcn5, MOF, Tip60/Esa1, ATF2, Sas2, NuA4	Bromodomain (Gcn5, NoRC)

[a]As reviewed in (Peterson and Laniel, 2004) [b]As reviewed in (Yun et al., 2011)

nucleosome structure or indirectly through facilitating the binding of a chromatin remodeler, histone chaperone, or transcriptional activator. Generally, the most commonly studied post-translational modifications of histones associated with elongating Pol II are the acetylation of the N-terminal tails of H3 and H4, the methylation of H3K4, H3K36, and H3K79, as well as the ubiquitination of H2B's C-terminus. Table 2 summarizes the factors that deposit and bind to the histone PTMs that are associated with active transcription.

The best studied example of how histone modifications can directly affect chromatin structure is through the acetylation of lysine residues within the histone tails. Generally, acetylation neutralizes the positive charge of lysine and thus weakens the ionic interaction with the negatively charged DNA backbone. In vitro, the acetylation of the H2A-H2B tails weakens the interactions that are present 40 bp on either side of the dyad, and acetylation of H3-H4 greatly reduces the formation of higher order structures and reduces the amount of DNA bound in the nucleosome (Brower-Toland et al., 2005). This effect caused by acetylation of H3-H4 agrees with predictions based on the nucleosome crystal structure that show the H4 tail mediating internucleosomal packing by contacting H2A-H2B dimers in an adjacent nucleosome (Luger et al., 1997). Acetylation of H4K16 was found to significantly hinder the ability of chromatin to form higher order structures by impeding internucleosomal interactions (Shogren-Knaak et al., 2006). A functional result of this modification is seen from dosage compensation in

Drosophila in which H4K16Ac is enriched on the male X chromosome and results in the twofold upregulation of X-linked genes by facilitating transcript elongation (Larschan et al., 2011).

Additional modifications have recently been discovered that also affect the intrinsic properties of chromatin structure to aid gene expression. These studies take advantage of new technologies in which site specific histone modifications can be made through chemical ligation (Allis and Muir, 2011). The ubiquitination of the C-terminal tail of H2B interferes with chromatin's ability to form higher order structures by creating an open, accessible fiber through a mechanism independent of and synergizes with the acetylation of the H4 tail (Fierz et al., 2011). Acetylation of H3K56, increases DNA breathing of the nucleosome ~40 bp away from the dyad by 7 fold, allowing DNA that is less tightly wound to gain easier access to proteins such as Pol II (Neumann et al., 2009). Lastly, phosphorylation of H3T118 was shown to be able to weaken histone-DNA interactions near the dyad thereby increasing accessibility at the dyad sixfold and increasing nucleosome mobility twenty-eightfold, making it easier to be remodeled by SWI/SNF (North et al., 2011). This power to create homogeneous samples with site-specific histone modifications will undoubtedly soon reveal how many of the histone modifications influence chromatin structure.

Histone modifications can also influence transcription through their ability to bind to and recruit specific effector proteins. For example, SWI/SNF and RSC chromatin remodelers both contain subunits that have a

bromodomain and can bind to acetylated H3 tails. In vitro, acetylation of H3 by the SAGA or NuA4 histone acetyltransferase complexes greatly stimulate RSC and SWI/SNF chromatin remodeling activities to facilitate Pol II transcript elongation (Carey et al., 2006; Chatterjee et al., 2011). Chd1, a chromodomain containing protein, is specifically targeted to the 5' ends of active genes through its ability to bind trimethylated H3K4 ($H3K4Me_3$) (Pray-Grant et al., 2005) (Figure 2). Another example is the PHD containing BPTF subunit of an ISWI remodeling complex that, like Chd1, can bind $H3K4Me_3$nucleosomes, but it binds more tightly to those nucleosomes containing both $H3K4Me_3$ and H4K16Ac, thus increasing the specificity of genomic locations where it will remodel nucleosomes (Ruthenburg et al., 2011). Another PTM associated with transcript elongation, H3K36 trimetylation (Figure 2), is important for the recruitment of a chromodomain-containing histone deacetylase that aids in nucleosome reassembly following transcription and is necessary for repression of cryptic initiation in gene bodies (Li et al., 2007b). The discovery of additional effectors of histone modifications will provide new insight as to how particular histone modifications are able to facilitate Pol II elongation by affecting chromatin structure and composition.

1.6 Histone Variants Affect Nucleosome Structure and Stability

In addition to histone PTMs, histone eviction, and chromatin remodeling, de novo deposition of specific histone variants can facilitate transcription through the nucleosome (Szenker et al., 2011). There are

numerous examples of different histone variants, whose families have expanded evolutionarily in higher eukaryotes (Talbert and Henikoff, 2010). Almost all eukaryotic organisms have variants of both H2A and H3, some contain H2B variants, but no variants of H4 appear to exist. As with PTMs, some of these variants are positively correlated with transcriptional activation including H2A.Z and H3.3, which I will highlight.

The deposition of H2A.Z into chromatin is an essential process for many organisms and is important for the proper transcription of many genes (Talbert and Henikoff, 2010). The Swr1 remodeling complex exchanges H2A-H2B dimers to create nucleosomes containing H2A.Z-H2B dimers near the 5' ends of genes (Luk et al., 2010) (Figure 2). Interestingly, homotypic H2A.Z-containing nucleosomes have been shown to be more stable than canonical H2A containing nucleosomes, creating a dichotomy as to why such a histone variant would facilitate transcript elongation (Ishibashi et al., 2009).
How H2A.Z facilitates transcript elongation might lie in the deposition of another histone variant H3.3. Deposition of histone H3.3 occurs mainly outside of the period of DNA replication and in a transcription-dependent manner (Tagami et al., 2004). H3.3 is deposited into promoters, gene bodies, and other gene regulatory elements by the HIRA and Daxx chaperones (Goldberg et al., 2010). Amazingly, H3.3 only differs from canonical H3.1 by 4 amino acids (Talbert and Henikoff, 2010). However, these small changes are enough to provide an in vivo mechanism whereby nucleosomes containing both H2A.Z and H3.3 are less stable than those containing canonical H3 or

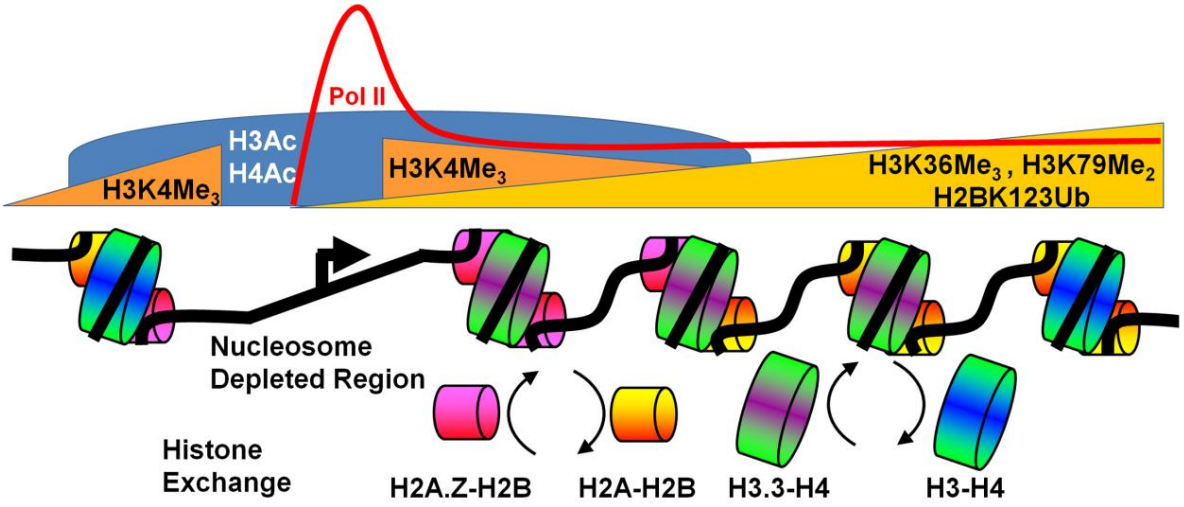

Figure 2 Transcriptionally Active Genes are Associated with Specific Histone PTMs and Histone Variants that Facilitate Transcript Elongation

A transcriptionally active gene is shown with the transcription start site of the gene indicated by the arrow, and a representative profile of Pol II density along the gene is shown above in a red line trace. The promoter region of most genes contain a nucleosome depleted region with flanking nucleosomes on either side that are enriched in the histone variants H2A.Z (pink) and H3.3 (purple) which have a higher rate of exchange than their canonical histones found further into the open reading frame. Nucleosomes are periodically spaced flanking the nucleosome-depleted region and may be the result of chromatin remodelers that evenly space the nucleosomes such as Chd1 and ISWI. Additionally, PTMs of histones that correlate positively with gene transcription are depicted above the gene. These include histone acetylation of the N-terminal tails of both H3 and H4, such as H3K9, H4K5, H4K8, H4K12, and H4K16, which are found near the promoters of genes (blue dome) and trimethylated at H3K4 (orange triangles), which are present on nucleosomes flanking the promoter in a monotonically decreasing fashion. Finally, the open reading frames of active genes are progressively modified by $H3K36Me_3$, $H3K79Me_2$, and H2BK123Ub (gold triangle).

H3.3 histones (Jin et al., 2009). Interestingly, H2A.Z and H3.3-containing nucleosomes occupy regions surrounding the promoter and also the 5' ends of transcribed genes (Figure 2). Taken together, these results imply less stable nucleosomes contribute to 5' nucleosome-depleted regions in vivo and allow Pol II and its regulators access to the underlying DNA to facilitate transcription. In support, both H2A.Z (Zhang et al., 2005) and H3.3 (Deal et al., 2010) are more rapidly incorporated into gene bodies and promoters (Figure 2) than their canonical counterparts. Of interest is how chaperones, modifications, or remodelers might synergize with the added instability and turnover of H2A.Z-H3.3 containing nucleosomes.

1.7 Activation of Poly(ADP-Ribose) Polymerase Promotes Chromatin Decondensation

*P*oly(*A*DP-*R*ibose) *P*olymerase (PARP) provides yet another way to alleviate the repressive nature of the chromatin fiber to facilitate transcription. PARP is a chromatin associated factor without any known remodeling or chaperoning activity that can facilitate transcription by altering chromatin structure at many genes. When activated, it uses NAD^+ as a substrate to synthesize *P*oly(*A*DP-*R*ibose) (PAR) onto target proteins as a PTM. The enzymatic activity of PARP is stimulated by many things including broken DNA, aberrant DNA structures, individual histones, and polynucleosomes. PARP binds to both DNA and to nucleosomes in vivo in a manner similar to that of the linker histone H1 (Kim et al., 2004). In vitro and in vivo the primary

target of PARP's enzymatic activity is itself, however other proteins have been identified as targets of PARylation including DNA repair factors, transcription factors, and histones.

PAR is chemically akin to a nucleic acid with the following key exceptions: PAR contains two negatively charged phosphates per nucleic acid and PAR can form either linear or branched structures of up to 200 units (Krishnakumar and Kraus, 2010a). One function of PAR's chemical likeness to a nucleic acid is that it is capable of competing or interfering with the functions of factors that bind nucleic acids. The ability of PARP to affect a wide-variety of cellular processes is likely a result of the generality of PAR to interact, compete, and interfere with many factors whose function is reliant on their affinity for nucleic acids.

PARP has been long studied for its role in DNA repair, but it has recently been investigated for its ability to affect chromatin structure and aid transcriptional activation. The activation of PARP's enzymatic activity has been long known to bring about relaxation of chromatin structure (Krishnakumar and Kraus, 2010a). Recently, PARP was shown to contribute to the formation of chromosomal puffs that occur at the loci of active transcript elongation in *Drosophila* polytene chromosomes (Tulin and Spradling, 2003). After heat shock, the loosening of chromatin structure is a result of the activation of PARP's enzymatic activity. How and to what extent PARP is able to bring about decondensation of chromatin structure upon transcriptional activation will be a major focus of this dissertation.

1.8 *Drosophila Hsp70* Provides a Model Gene to Determine How Pol II Overcomes the Nucleosome Barrier upon Transcriptional Activation

One of the most dramatic visual demonstrations of the decondensation event that occurs during transcriptional activation is with heat shock genes in *Drosophila melanogaster*. *Drosophila* polytene chromosomes have nine inducible heat shock puffs that form reproducibly and synchronously and are maximal in size by 20 minutes (Ashburner, 1967; Lewis et al., 1975). One of the most highly upregulated heat shock gene that undergoes one of the most dramatic decondensation events out of the nine inducible heat shock puffs is the *Hsp70* gene. The rapid and robust activation of *Hsp70* is ideal for studying not only how the chromatin structure changes in response to transcriptional activation of the gene but also factors that are responsible for bringing about these changes.

Before heat shock, *Hsp70* is primed in multiple ways to facilitate a rapid response to a heat stimulus. Notably, *Hsp70* was shown to contain a promoter that is relatively devoid of nucleosomes as it is highly sensitive to digestion by both DNaseI and MNase (Wu et al., 1979; Wu, 1980). The promoter has also been shown to contain a sequence specific DNA binding factor called GAGA Factor (GAF) already bound to it that is able to interact with the chromatin remodeler ISWI that is presumably able to affect the chromatin structure before heat shock (O'Brien et al., 1995; Sala et al., 2008; Tsukiyama et al., 1994). Just downstream of the promoter exists both the *Drosophila* H2A.Z variant, H2Av, and H3.3 (Leach et al., 2000; Mito et al.,

2007). The open chromatin structure near the promoter before heat shock (Shopland et al., 1995) extends beyond the transcription start site where Pol II has initiated, transcribed, and paused approximately 20-40 nucleotides into the gene (Rasmussen and Lis, 1993; Rougvie and Lis, 1988). The paused Pol II can be rapidly induced to undergo transcript elongation upon receiving correct activation signals. However, this elongating Pol II, like any other, still needs to overcome the nucleosome barrier during transcription elongation to achieve a robust activation.

Many factors that either directly affect chromatin structure or indirectly affect it through activating transcription are recruited to the *Hsp70* gene following heat shock. The first factor that is recruited to *Hsp70* is the master transcriptional activator heat shock factor (HSF). Upon heat shock, HSF trimerizes and binds within seconds to its cognate DNA elements (three 5-mer sites of AGAAN repeated head-to-tail), of which there are 4 found within the promoter of *Hsp70* (Boehm et al., 2003; Perisic et al., 1989; Westwood et al., 1991; Zobeck et al., 2010). HSF is necessary for both the gene activation and the chromatin decondensation at *Hsp70* following heat shock (Jedlicka et al., 1997; Wu, 1980). HSF is thought to do this through direct or indirect recruitment of coactivators and general transcription factors, specifically the mediator and SAGA complexes (Lebedeva et al., 2005; Park et al., 2001), elongation factors, including P-TEFb, the PAF complex, and Spt6 (Ardehali et al., 2009; Lis et al., 2000; Ni et al., 2007), histone modifying enzymes such as those mediating H3 K4, K36, and K79 methylation as well as histone

acetylation by CBP and Gcn5 (Adelman et al., 2006; Ardehali et al., 2011; Lebedeva et al., 2005; Smith et al., 2004), histone chaperones, such as FACT (Saunders et al., 2003), and chromatin remodelers including those from the CHD and ISWI families (Badenhorst et al., 2002; Simic et al., 2003; Srinivasan et al., 2005), but curiously not SWI/SNF(Armstrong et al., 2002). It is therefore imaginable that any of these factors, or combinations thereof, are able to alleviate the nucleosome barrier to Pol II upon heat shock. *Hsp70* therefore provides an excellent model gene with which to observe changes in nucleosomes upon transcriptional activation and to what extent different factors help alleviate the nucleosome barrier during transcript elongation.

1.9 Summary of Dissertation and Concluding Remarks about the Future of Understanding how Pol II Overcomes the Nucleosome Barrier

To better understand individual changes that happen to nucleosomes along the gene body of *Hsp70* throughout the time course of heat shock, I developed a sensitive method to be able to measure quantitatively the changes that occur in these nucleosomes. My results demonstrate that there is a rapid change in nucleosome structure by 30-60 seconds of HS that continues throughout the gene and is independent of active transcription of the gene (Petesch and Lis, 2008). The immediate and widespread change in chromatin structure at *Hsp70* following HS are critically dependent on HSF, GAF, and PARP. Both RNAi knockdown of HSF and PARP, as well as catalytic inhibition of PARP, results in the failure of *Hsp70* to undergo rapid,

transcription-independent loss of the chromatin structure upon HS. The activation of PARP and formation of PAR at *Hsp70* results in the depletion of histone density on the body of heat shock genes that in turn facilitates Pol II transcription (Petesch and Lis, 2008). This is achieved initially through recruitment of HSF, which in turn recruits the *Drosophila* Tip60 complex to acetylate H2AK5 and ignites PARP's enzymatic activity, the rapid spread of PAR throughout the region, and correspondingly rapid nucleosome loss (Petesch and Lis, 2012a) (Figure 3). Together, these results provide additional insight into a new method through which the nucleosome barrier can be overcome rapidly, and even before Pol II transcript elongation occurs.

Additionally, it has been found from the Tulin lab that the activation of PARP in vivo is also dependent on the C-terminal phosphorylation of H2A (Kotova et al., 2011), which is a known prerequisite for H2AK5Ac in *Drosophila* (Kusch et al., 2004). The *Drosophila* Tip60 complex also contains a known homolog of Swr1, whose ability to exchange out H2A is stimulated by H2AK5 acetylation (Kusch et al., 2004). It will be of interest to know how or if the disruption of nucleosomes through Swr1's exchange can activate PARP's enzymatic activity in vivo, how the activation and localized spread of PAR can lead to such dramatic histone depletion and relaxation of chromatin structure, and to what extent this mechanism of chromatin disruption is used at other genes.

Figure 3 Heat Shock Factor Triggers the Enzymatic Activity of Poly(ADP-Ribose) Polymerase to Facilitate the Rapid Disruption of Nucleosomes

Model of PARP activation at heat shock loci summarizing (Petesch and Lis, 2008; Petesch and Lis, 2012a).

(a) Before heat shock, the *Drosophila Hsp70* gene contains a transcriptionally engaged, paused Pol II (red) and inactive PARP (gray) present near the first well-positioned nucleosomes after the transcription start site, indicated by the arrow. *Hsp70* is known to contain the *Drosophila* H2A.Z variant, H2Av (pink), at the 5' end of the gene before heat shock. It is not known if the C-terminal S137 of H2Av is already in a phosphorylated state.

(b) After heat shock, the master transcriptional activator, *h*eat *s*hock *f*actor (HSF, orange), is recruited to the promoter of *Hsp70* as a trimer. HSF in turn is responsible for recruiting the dTip60 complex (purple cloud), which is part of a chromatin remodeling complex containing a protein homologous to Swr1. dTip60 is responsible for acetylating H2AK5 near the 5' end of the gene.

(c) Following acetylation of H2AK5, the dTip60 complex is likely to exchange out the H2Av variant as it is known to do in vitro with H2Av that is acetylated at K5 and phosphorylated at S137. The combination of the acetylation of H2AK5 and the exchange of H2A triggers activation of PARP's enzymatic activity (now shown in blue).

(d) The activation of PARP (blue) results in the formation of PAR (blue lines) and the redistribution of PARP throughout the coding region, and beyond, but halts at nearby natural chromatin insulating elements (not shown). This rapid and domain wide process leads to a buildup of PAR throughout the region which is able to locally disrupt and strip histones from the gene allowing for efficient transcript elongation and robust gene activation.

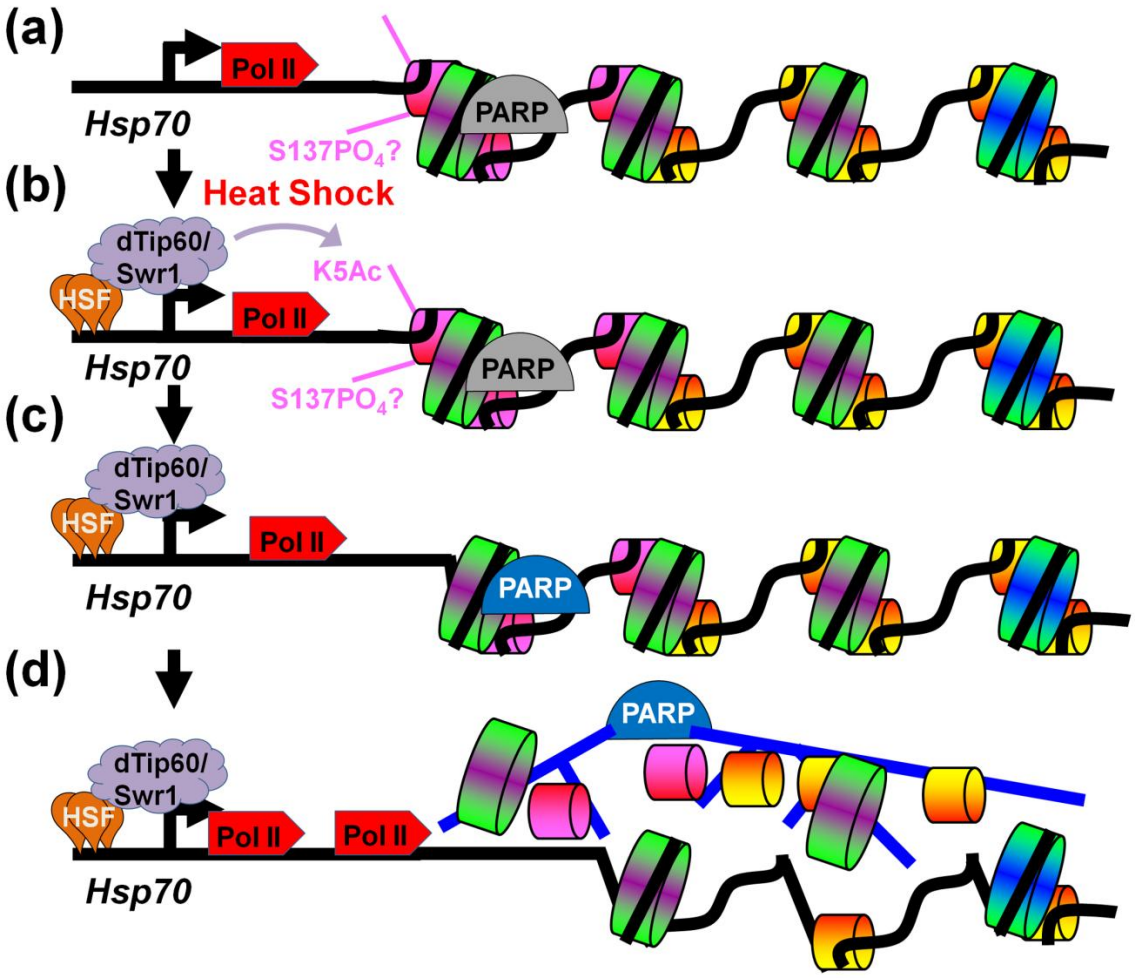
(a)
Pol II
Hsp70
PARP
S137PO4?
(b)
Heat Shock
dTip60/
Swr1
HSF
K5Ac
Pol II
Hsp70
PARP
S137PO4?
(c)
dTip60/
Swr1
HSF
Pol II
Hsp70
PARP
(d)
PARP
dTip60/
Swr1
HSF
Pol II
Pol II
Hsp70

The exploration of mechanisms by which cells overcome the nucleosome barrier to allow for efficient transcript elongation has resulted in the discovery of an entire subfield of eukaryotic gene expression. The discovery of a new mechanism of nucleosome displacement by PARP activation has generated numerous intriguing questions that can be addressed with existing and new technologies (Petesch and Lis, 2008; Petesch and Lis, 2012a). The advent of new technologies such as single molecule experiments (Killian et al., 2011) and protein chemical ligations (Allis and Muir, 2011; Fierz et al., 2011; North et al., 2011; Shimko et al., 2011) are just beginning to provide mechanistic details as to how chromatin remodelers, chaperones, modifications, and variants are able to destabilize, disassemble, or reassemble nucleosomes and should prove useful for dissecting PARP-based mechanisms. In addition, these technologies are being used to answer fundamental questions about what happens when Pol II engages a nucleosome and how specifications including Pol II density on genes (Jin et al., 2010), transcription rates (Bintu et al., 2011), and processivity affect the process of transcript elongation through nucleosomes. These views should be augmented with real time and high-resolution imaging approaches (Leung and Chou, 2011; Yao et al., 2008). Finally, genome-wide studies of Pol II, the composition of histones, and the presence of particular chromatin associated factors will be useful in evaluating the generality of particular mechanisms in regulating transcript elongation and alleviating nucleosomal barriers.

CHAPTER 2 RAPID, TRANSCRIPTION-INDEPENDENT LOSS OF NUCLEOSOMES OVER A LARGE CHROMATIN DOMAIN AT *HSP70* LOCI[2]

To efficiently transcribe genes, RNA Polymerase II (Pol II) must overcome barriers imposed by nucleosomes and higher order chromatin structure. Many genes, including *Drosophila melanogaster Hsp70*, undergo changes in chromatin structure upon activation. To characterize these changes, I mapped the nucleosome landscape of *Hsp70* following an instantaneous heat shock at high spatial and unprecedented temporal resolution. Surprisingly, I find an initial disruption of nucleosomes across the entire gene within 30 seconds following activation, faster than the rate of Pol II transcription, followed by a second further disruption within 2 minutes. This initial change occurs independently of Pol II transcription. Furthermore, the rapid loss of nucleosomes extends beyond *Hsp70* and halts at the scs and scs' insulating elements. An RNAi screen of 28 transcription and chromatin-related factors reveal that depletion of heat shock factor, GAGA Factor, or Poly(ADP-Ribose) Polymerase or its activity abolishes the loss of nucleosomes upon *Hsp70* activation.

2.1 INTRODUCTION

In eukaryotic cells, DNA is packaged into chromatin providing a natural barrier to factors requiring access to DNA (Rando and Ahmad, 2007). Many essential cellular processes, including gene expression, rely on the ability of

[2] Taken from (Petesch and Lis, 2008)

the cell to regulate and alleviate the restrictive properties of chromatin. *In vitro* studies have shown that the transcriptional rate and processivity of RNA Polymerase II (Pol II), which is responsible for expressing all mRNA-encoding genes, is severely inhibited by nucleosomes (Knezetic and Luse, 1986; Lorch et al., 1987). However, *in vivo* studies show that Pol II, and even the first 'pioneer' Pol II to transcribe an induced gene, is able to transcribe at rates (~1.5 kb/min) that suggest it is not inhibited by the presence of nucleosomes (O'Brien and Lis, 1993; Thummel et al., 1990). These results indicate that eukaryotic cells have mechanisms that modulate nucleosome position and structure at active genes.

The diversity of factors that act on chromatin indicate that eukaryotic cells use multiple general mechanisms to alter the position or composition of the nucleosome, allowing critical factors such as Pol II access to DNA (Li et al., 2007a). Chromatin remodeling complexes, such as SWI/SNF and ISWI, provide the cell with the ability to remove, transfer, or slide a nucleosome along a DNA template (Saha et al., 2006). Additionally, many transcription elongation factors and histone chaperones, such as FACT, Spt6, and Asf1 aid in the disassembly of nucleosomes and their reassembly in the wake of transcribing Pol II (Bortvin and Winston, 1996; Orphanides et al., 1998; Schwabish and Struhl, 2006). Finally, histone modifying enzymes can acetylate, methylate, phosphorylate, monoubiquitinate, sumoylate, or ADP-ribosylate histones, or carry out the reverse of each reaction (Li et al., 2007a). Many of these modifications can modulate inter and intranucleosomal

interactions (Reinke and Horz, 2003; Shogren-Knaak et al., 2006) and most are likely to serve as specific targets for effectors (Jenuwein and Allis, 2001; Wysocka et al., 2006), which can act locally to alleviate or reinforce the repressive structure of chromatin.

Understanding where nucleosomes are positioned and how these positions change during transcription is critical in deciphering how the changes occur. Early studies with micrococcal nuclease (MNase) or DNase1 on chromatin isolated from cells produced the first views of the chromatin structure of *Drosophila melanogaster* heat shock (HS) genes *in vivo*. These analyses showed that both the promoter and the 3' end of the *Hsp70* gene contained large hypersensitive regions and that nucleosomes on the coding regions before HS were disrupted after an extended HS (Wu et al., 1979; Wu, 1980). Recently, whole genome ChIP-chip and ChIP-seq studies have shown that many genes exhibit similar patterns of nucleosome occupancy (Johnson et al., 2006; Lee et al., 2007; Schones et al., 2008). In particular, nucleosomes are often absent in promoter regions just upstream of the transcriptional start site, allowing the transcriptional machinery easy access to DNA elements (Crawford et al., 2006; Mito et al., 2005; Yuan et al., 2005). Moreover, genes in *Saccharomyces cerevisiae* on average contain 1 well-positioned nucleosome on each side of the promoter region and nucleosomes become progressively less positioned beyond this point (Albert et al., 2007; Lee et al., 2007; Yuan et al., 2005). Thus, while many promoters are open and

accessible, and even occupied by Pol II (Lis, 2007), Pol II still must overcome nucleosomes occluding its downstream path into the gene.

D. melanogaster Hsp70 is a model gene used to study general mechanisms by which Pol II is able to transcribe through chromatin. *Hsp70* is rapidly activated within seconds after HS, and concomitantly its chromatin structure decondenses, evident by the formation of large puffs on polytene chromosomes (Boehm et al., 2003). Not surprisingly, an entire battery of transcription factors is recruited to *Hsp70* upon activation, under the direction of the master heat shock factor (HSF) activator (Saunders et al., 2006). Curiously, although puff size at HS induced genes increases with transcript length and promoter strength (Simon et al., 1985), previous studies also show that puffing of HS loci can be decoupled from active transcription of the gene using a chemical stimulus (Winegarden et al., 1996). Although informative, these studies do not demonstrate at the molecular level in living cells that changes are indeed happening to the nucleosomes occupying *Hsp70*.

The dramatic change in the chromatin structure upon gene activation begs several questions. Does this puffing entirely represent changes in nucleosomes? Are the nucleosomes evicted, or are their positions or configuration altered? How rapidly can changes in the chromatin structure be detected at the molecular level? And finally, which factors are responsible? Previous studies have shown that deletion of either Heat Shock Elements (HSEs) or GAGA factor (GAF) binding sites in the *Hsp70* promoter region result in reduced HSF binding and a loss in puff formation upon HS (Shopland

et al., 1995). GAF, encoded by the *Trithorax-like* gene, binds to repeating $(GA)_n$ sequences and is present at the *Hsp70* promoter before HS (O'Brien et al., 1995). GAF itself has been shown to play important roles in gene activation presumably by regulating chromatin structure by itself or through its interactions with the NURF remodeling complex (Tsukiyama et al., 1994; Tsukiyama and Wu, 1995).

In addition to HSF and GAF, recent evidence indicates that Poly(ADP-Ribose) Polymerase (PARP) is important in puff formation at many loci including *Hsp70* (Tulin and Spradling, 2003). PARP is an enzyme that catalyzes the polymerization of ADP ribose units from NAD^+ onto target proteins (primarily itself) and interacts with DNA and nucleosomes (Kim et al., 2004; Pinnola et al., 2007). PARP proteins have roles in several nuclear processes, including DNA damage responses (D'Amours et al., 1999), but have only recently been examined with respect to transcription (Kraus and Lis, 2003). A P-element insertion that disrupts PARP expression, or inhibition of PARP's catalytic activity, displays decreased puff sizes in polytene chromosomes and reduced Hsp70 protein levels upon HS (Tulin and Spradling, 2003). To understand puff formation and the roles of HSF, GAF, and PARP, examination of chromatin at the nucleosomal level is required. Moreover, the potential role of other factors needs to be evaluated.

In this paper, I map the nucleosome architecture of the *D. melanogaster Hsp70* gene at a 30 bp resolution and track its changes seconds after an instantaneous HS. I find that before HS, the chromatin structure of *Hsp70* has

characteristics similar to general genome-wide features at most genes. After HS, I find that the chromatin architecture at *Hsp70* has an initial dramatic change throughout the gene that is so rapid that it occurs even before the first wave of transcribing polymerase reaches the corresponding regions of the gene. Furthermore, I find this initial loss of nucleosomes is independent of transcription and extends to natural insulating elements flanking the HS genes. Through an RNAi screen of known coactivators, chromatin remodeling enzymes, histone modifiers, nucleosome assembly and disassembly factors, modifiers of DNA topology, and elongation factors, I indentify HSF, GAF, and PARP as each necessary for the rapid loss of nucleosomes at the *Hsp70* gene following HS. The effect of PARP requires its activity and a specific inhibitor added only 10 minutes before HS is sufficient to block the nucleosome loss.

2.2 RESULTS

2.2.1 The Chromatin Structure at *Hsp70* is Rapidly and Dramatically Altered Following Heat Shock

I employed a previously developed method (Sekinger et al., 2005) to track *in vivo* changes in the chromatin structure of the *Hsp70* gene at the mononucleosome level following activation. In my assay, *Hsp70* is induced in *Drosophila* S2 cells by an instantaneous HS for various times. The cells are cross-linked with formaldehyde and chromatin is then isolated and split into mock and MNase treated samples (Figure 4A). The DNA is then probed with

Figure 4 Rapid Loss of Chromatin Structure at *Hsp70* upon Heat Shock Detected by a High Resolution MNase Scanning Assay

(A) Diagram depicting the procedure followed for the high resolution MNase assay. S2 cells are heat shocked for 0 (dark blue), 5 (light blue), 30 (green), 60 (orange), or 120 seconds (red) (colors refer to 1C), immediately cooled to room temperature and crosslinked, and their chromatin is isolated. Purified DNA products from samples are treated with 0 or 500 U of MNase and used for qPCR.

(B) Diagram showing the PCR amplicons used at the *Hsp70Ab* gene. PCR products are 100±5 bp in size and are spaced 30±6 bp apart. The mRNA-encoding unit is shown in black. The gene nucleotide location, corresponding to panel C, is numbered below with the HSEs, TSS, and PolyA site (at +2343) indicated.

(C) The HS time course chromatin profile of *Hsp70* is determined by normalizing the amount of the MNase digested PCR product to that of the undigested product using the ΔC(t) method (y-axis), which is plotted against the gene nucleotide location (x-axis). Values from overlapping primer sets are averaged. The x-axis represents base pair units with 0 being the TSS. Lines represent the average of 3 separate experiments with error bars omitted for clarity.

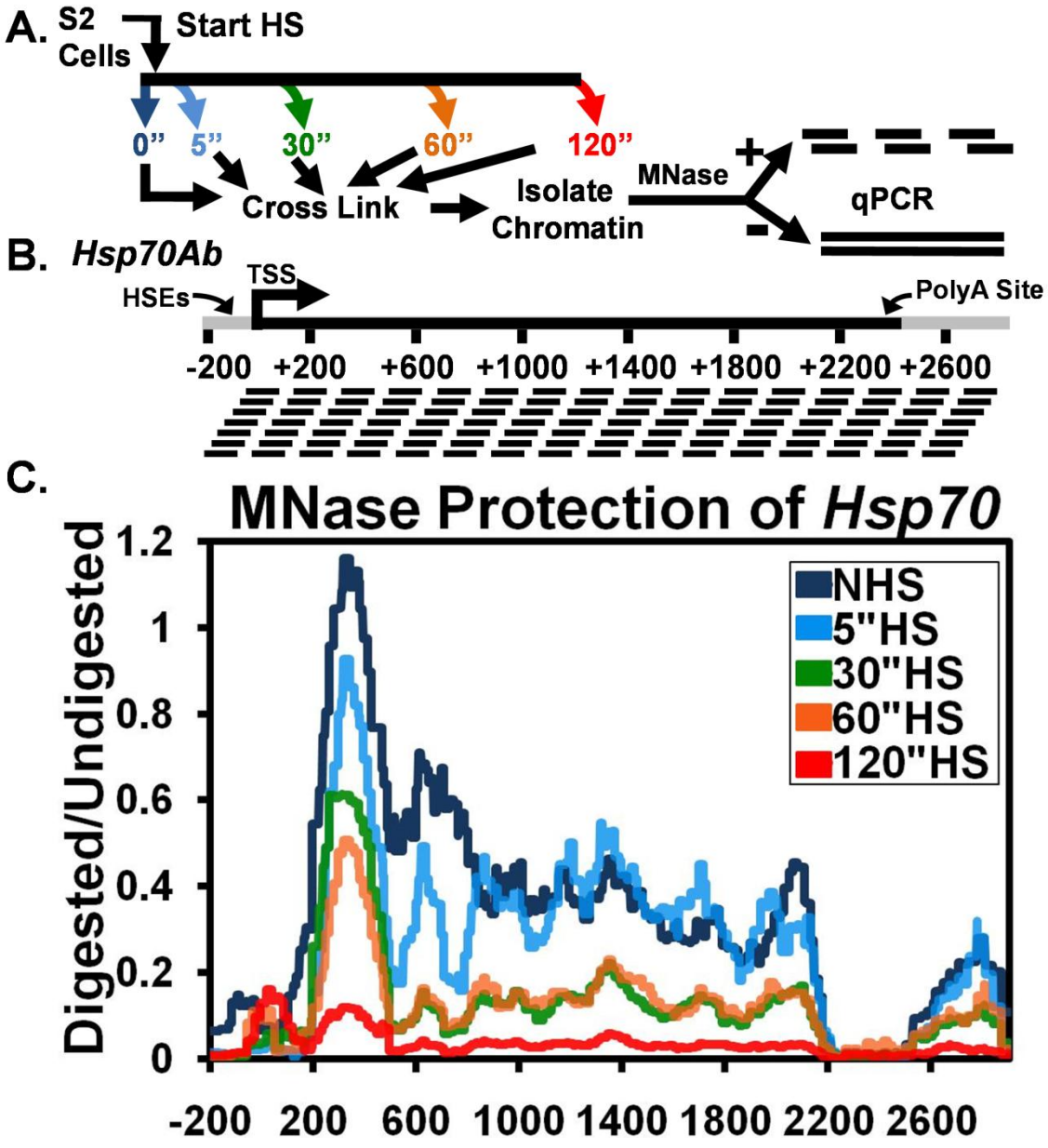
A.
S2 Cells
Start HS
0”
5”
30”
60”
120”
Cross Link
Isolate Chromatin
MNase
+
-
qPCR
B.
Hsp70Ab
HSEs
TSS
PolyA Site
-200 +200 +600 +1000 +1400 +1800 +2200 +2600
C.
MNase Protection of Hsp70
Digested/Undigested
1.2
1
0.8
0.6
0.4
0.2
0
NHS
5"HS
30"HS
60"HS
120"HS
-200 200 600 1000 1400 1800 2200 2600

over 100 separate primer sets that on average are spaced 30 bp apart and amplify 100 bp regions along the *Hsp70Ab* copy (Figure 4B and Table 4). The ability of a primer pair to amplify depends on the amount of contiguous DNA between the primers that remains after MNase digest; MNase cleaves linker DNA between nucleosomes and cleaves nucleosome-free DNA. To determine the amount of digestion in a particular region at the *Hsp70* gene, I calculated the relative ratio of the amount of digested DNA to the undigested control using quantitative PCR (qPCR). Efficient amplification of 100 bp regions ensures that amplifiable DNA in the digested sample is mononucleosome or subnucleosome in size but larger than tetrameric or hexameric structures. The amount of MNase was titrated to produce mononucleosomes from the bulk chromatin of nuclei (Figure 5A), and to observe protection under uninduced conditions at *Hsp70* with amplification of 100 bp sized fragments but not with 190 bp sized fragments (Figure 5B). This ensures that my assay has mononucleosome resolution, and provides a precise way to measure and track the positions of nucleosomes along *Hsp70* following a HS.

Under non heat shock (NHS) conditions, *Hsp70* contains 4 distinct chromatin regions: a nucleosome free promoter region, a well-positioned nucleosome centered approximately 330 nucleotides after the transcription start site (TSS), poorly positioned nucleosomes in the body of the gene, and a second nucleosome free region at the 3' end of the gene (Figure 4C, dark blue). (Each individual time point can be seen as a separate graph with error bars in Figures 6A-E.) The nucleosome free region at the 5' end of *Hsp70*

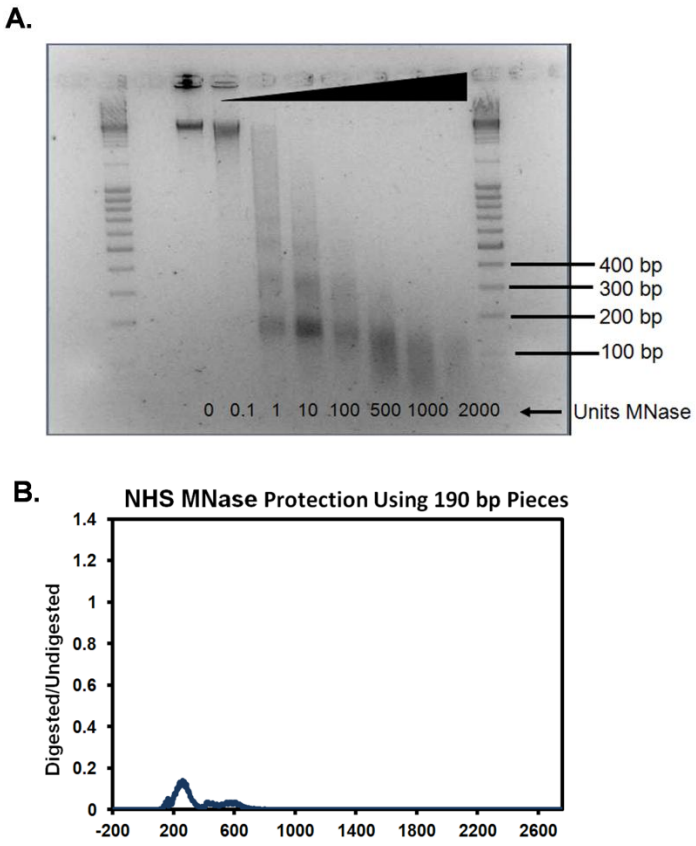

Figure 5 Titration of MNase to Produce Mononucleosome Size DNA Fragments

(A) The amount of MNase used to produce mononucleosome size pieces of DNA was titrated from 0 to 2000 U of MNase on cross-linked purified chromatin. Purified DNA inputs from $2.5x10^6$ cells, equal to what was used for the high resolution MNase mapping, was loaded onto a 1.3% agarose gel and stained with ethidium bromide. Digestion to dinucleosome size pieces is achieved by 100 U and by 500 U the chromatin is largely digested to mononucleosomes.

(B) The diagram shows the same NHS MNase profile for the NHS profile observed in Figure 1C, except PCR products are 190±7 bp to probe pieces of DNA that are larger than mononucleosome in size.

agree with earlier studies that show these regions are hypersensitive to

nucleases (Wu, 1980). The 5' hypersensitive region extends further into the

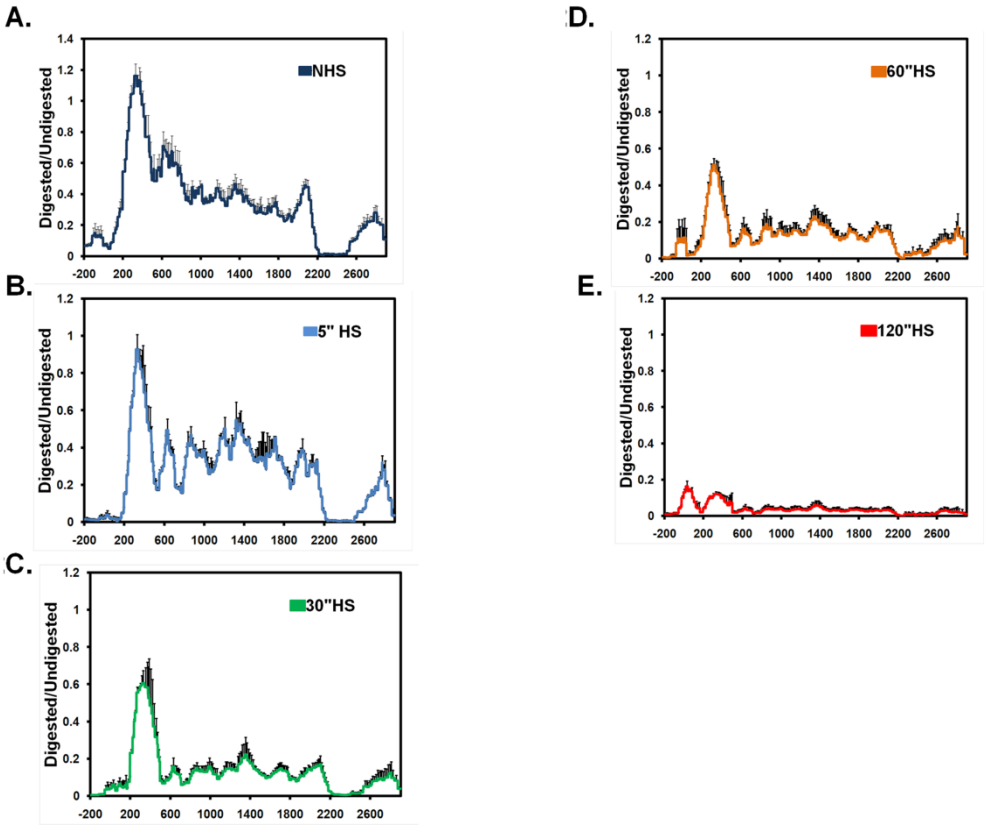

Figure 6 Individual Time Course MNase Profiles with Error Bars

(A-E) Each individual time course displayed in Figure 4C is plotted separately for NHS (A), 5”HS (B), 30”HS (C), 60”HS (D), and 120” HS (E) with error bars corresponding to the SEM for 3 independent measurements.

transcription unit than where Pol II is known to be transcriptionally engaged and paused 20 to 40 base pairs downstream of its initiation site (Giardina et al., 1992; Rasmussen and Lis, 1993; Rougvie and Lis, 1990). Beyond the first nucleosome, centered at +330 and well downstream of the paused Pol II, the body of the gene contains nucleosomes that gradually lose their positioning. This is seen from the relatively even distribution of protection along the gene.

A nucleosome just upstream of the polyadenylation (PolyA) site of *Hsp70* bookends the nucleosomes on the 3' end of the gene. Overall, under NHS conditions, the chromatin structure of the *Hsp70* gene accommodates paused polymerase but still provides an impending barrier to transcription elongation.

To determine how the chromatin structure of *Hsp70* changes upon an instantaneous HS, I used the high-resolution MNase assay following 5, 30, 60, and 120 seconds of HS. Within 5 seconds of HS, the protection of DNA in the immediate 5' region of the gene decreases (Figure 4C, light blue). By 30 seconds (Figure 4C, green), further loss in the 5' region is observed, but now losses are also observed extending past the 3' region of the gene. Surprisingly, these initial changes in the 3' end of the gene occur before RNA polymerase reaches the 3' end, which takes approximately 2 minutes (Boehm et al., 2003; O'Brien and Lis, 1993). No significant changes in nucleosome protection are seen between 30 and 60 seconds (Figure 4C, orange). However, by 120 seconds of HS (Figure 4C, red) another broad loss in the protection of nucleosomes occurs along the entire gene. In contrast to NHS conditions, the nucleosome protection pattern of a 120 second HS is decimated. This 2 minute protection pattern remains even after 20 minutes of HS (data not shown). Similar changes in nucleosomes were also observed on the same time scale for the shorter, HS inducible *Hsp26* gene (Figures 7A and 7B). During HS, the positions of nucleosomes neither move into nucleosome free regions nor do they increase in their relative level of protection.

To address whether or not these changes in the chromatin landscape

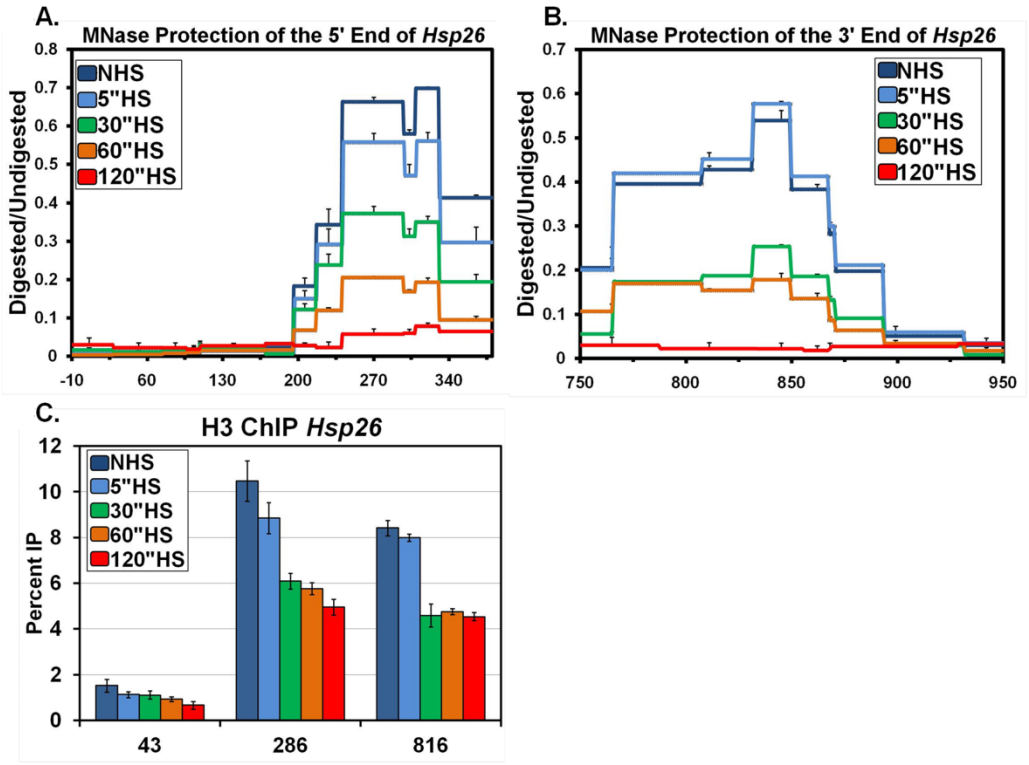

Figure 7 Rapid Loss of Chromatin Structure at *Hsp26* upon Heat Shock Detected by a High Resolution MNase Scanning Assay

The HS time course chromatin profile is determined at the 5' end (A) and 3' end (B) for the 1010 bp long *Hsp26* transcript following a 0 (dark blue), 5 (light blue), 30 (green), 60 (orange), or 120 seconds (red) HS just as in Figure 1 by normalizing the amount of the MNase digested PCR product to that of the undigested product using the ΔC(t) method (y-axis), which is plotted against the gene nucleotide location (x-axis). Values from overlapping primer sets are averaged. The x-axis represents base pair units with 0 being the transcription start site. Lines represent the average of 3 separate experiments with error bars representing the SEM. Primers used can be found in Table S1.

(C) Histone density across the *Hsp26* gene detected by ChIP using an H3 antibody just as in Figure 2. S2 cells are heat shocked for 0 (dark blue), 5 (light blue), 30 (green), 60 (orange), or 120 seconds (red). The y-axis represents the percent of input material immunoprecipitated. Error bars represent the SEM of 3 independent experiments. The x-axis represents base pair units along the *Hsp26* gene with 0 as the transcription start site; each number represents the center of the PCR amplicon. The intergenic region represents a region 32 kb downstream of *Hsp70Bc* that does not change upon HS.

are due to either a loss of histones or just an increased accessibility of the DNA at this locus, I performed traditional sonication ChIP with an antibody that recognizes histone H3 and its variants. The histone NHS landscape determined by ChIP matches that of the MNase protection assay (Figure 8, dark blue). Additionally, the same changes in the MNase protection pattern are seen with a histone H3 ChIP at 5, 30, and 60 seconds of HS (Figure 8, light blue, green, orange). The combination of increased MNase accessibility and decreased histone density indicate disruption of nucleosome structure on the gene, or a loss in nucleosomes. The only significant difference observed between the 2 methods is that there is not a change in histone levels between 60 and 120 seconds of HS. One likely explanation for these differences is that

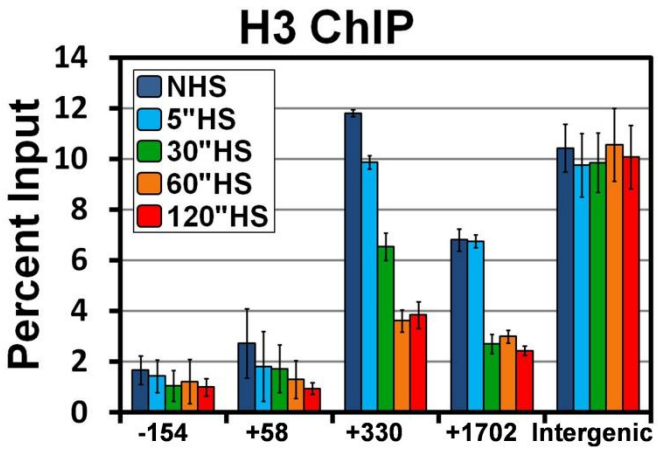

Figure 8 Rapid loss of Histone H3 from *Hsp70* upon Heat Shock

Histone density across the *Hsp70* gene detected by ChIP using an H3 antibody. S2 cells are heat shocked for 0 (dark blue), 5 (light blue), 30 (green), 60 (orange), or 120 seconds (red). The y-axis represents the percent of input material immunoprecipitated. Error bars represent the SEM of 3 independent experiments. The x-axis represents base pair units along the *Hsp70* gene with 0 as the TSS; each number represents the center of the PCR amplicon. The intergenic region represents a region 32 kb downstream of *Hsp70Bc* that does not change upon HS.

Pol II accumulates across the body of the gene by this point, resulting in further disruption of canonical nucleosomal structures. This could lead to an increased accessibility of this DNA to the MNase without a further decrease in the amount of histone H3 present. Again, similar results were found for *Hsp26* (Figure 7C). Figures 4 and 7 indicate that changes in nucleosomal structures at *Hsp70* start at the 5' end of the gene and move more rapidly than Pol II towards the 3' end.

2.2.2 Nucleosomes at *Hsp70* can be Lost Independently of Transcription

The loss of nucleosomes at *Hsp70* occurring prior to Pol II's occupancy of these regions suggests that the rapid changes in chromatin, which occur well before maximal puff formation at 20 min HS (Lewis et al., 1975), might also occur independently of transcription. To catalogue at high-resolution what chromatin changes occur independently of transcription, I used sodium salicylate or the nucleotide analog 5,6-dichloro-1-β-D-ribofuranosylbenzimidazole (DRB). Both of these chemicals reduce the level of HS induced *Hsp70* transcription (Giardina and Lis, 1993; Winegarden et al., 1996). Treatment of S2 cells with DRB followed by a 2 minute HS resulted in normal recruitment of HSF to the promoter (-154) (Figure 9A). Pol II was also normally recruited to the pause site (+58); however, it was not detected in regions further downstream (+1702) (Figure 9A), indicative of transcription elongation being inhibited. The nucleosome protection profile of a 2 minute (or 30 second) HS with DRB revealed that the initial loss of nucleosome structure

Figure 9 Initial Loss of Nucleosomes at *Hsp70* is Independent of Transcription

(A) ChIP at *Hsp70* for HSF and Rpb3 (Pol II) with and without 125 µM of the transcription inhibitor DRB before (NHS, black bars and NHS+DRB, dark gray bars) and during HS (2'HS, white bars and 2'HS+DRB, light gray bars). The y-axis represents the percent of input material immunoprecipitated. x-axis values represent base pair units centered on the HSEs (-154), the Pol II pause site (+58), a downstream region (+1702), and an intergenic region outside the scs and scs' regions. Error bars represent the SEM of 3 independent experiments.

(B) MNase protection profile of NHS with DRB (dark gray), 2'HS with DRB (light gray), and 2'HS (medium gray) as in Figure 4C. Lines represent the average of 3 separate experiments. Error bars representing the SEM are plotted just for the 2'HS+DRB line for clarity.

(C) ChIP as described in (A) except with and without 10 mM of sodium salicylate before (NHS, black bars and NHS+salicylate, dark gray bars) and during HS (20'HS, white bars and 20'HS+salicylate, light gray bars). Error bars represent the SEM of 3 independent experiments.

(D) MNase protection profile as in (B) with NHS (black), NHS+salicylate (dark gray), and 1'HS (light gray). Lines represent the average of 3 separate experiments. Error bars representing the SEM are plotted just for the NHS+salicylate line for clarity.

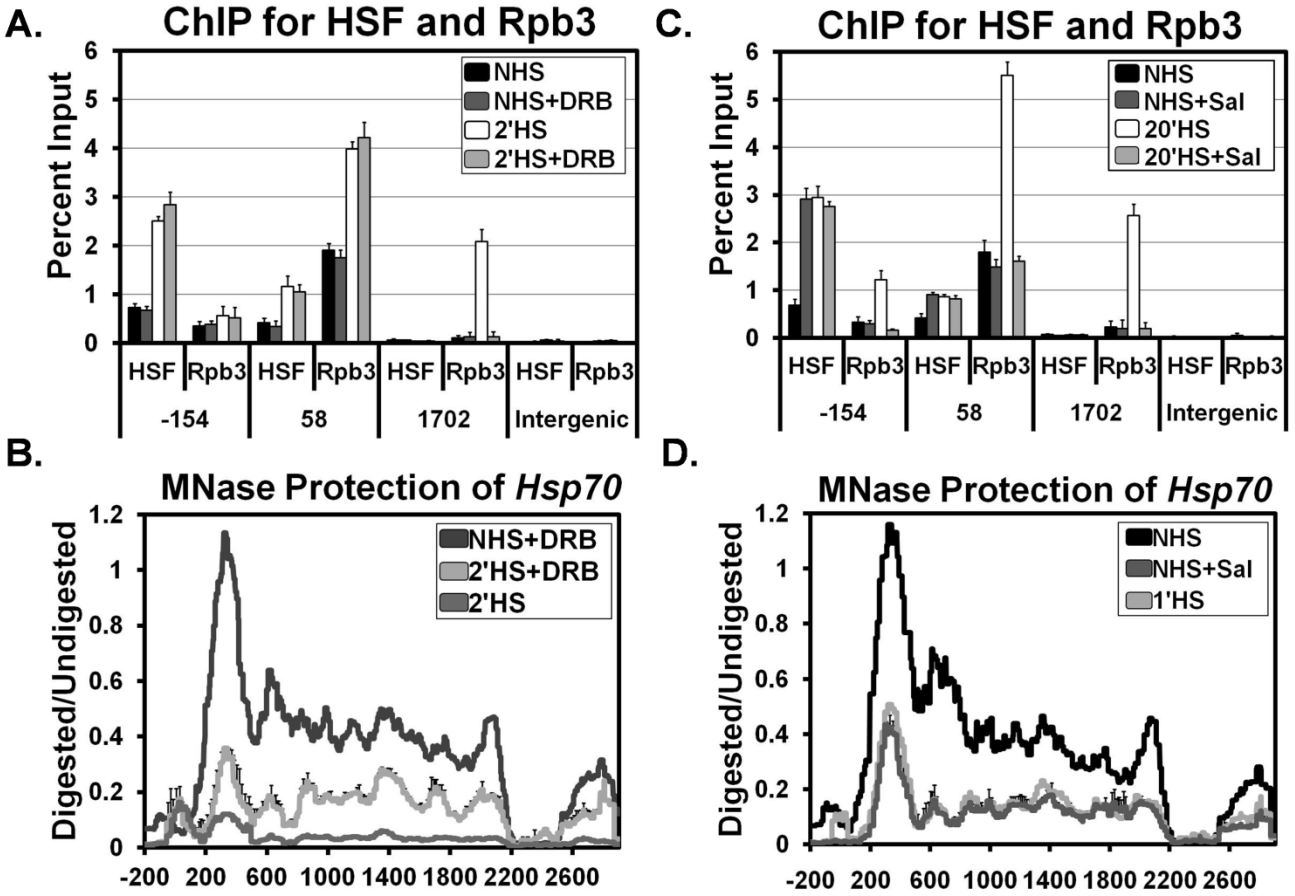
A.
ChIP for HSF and Rpb3
Percent Input
NHS
NHS+DRB
2'HS
2'HS+DRB
HSF
Rpb3
-154
58
1702
Intergenic
C.
ChIP for HSF and Rpb3
NHS
NHS+Sal
20'HS
20'HS+Sal
B.
MNase Protection of Hsp70
Digested/Undigested
NHS+DRB
2'HS+DRB
2'HS
-200 200 600 1000 1400 1800 2200 2600
D.
MNase Protection of Hsp70
NHS
NHS+Sal
1'HS

occurred even though Pol II never moved into the body of the gene (Figures 9B and 14A).

Treatment of cells with sodium salicylate under NHS conditions resulted in a level of HSF recruitment equivalent to that of a 20 minute HS (Figure 9C). The amount of Pol II at the pause site or in downstream regions, however, did not change from NHS levels (Figure 9C). These results are consistent with previous studies showing that sodium salicylate induces HSF binding to its HSEs, but does not result in additional promoter melting by the paused Pol II (Giardina and Lis, 1995). This NHS treatment with sodium salicylate, like HS in the presence of DRB, resulted in the loss of nucleosomes throughout the gene similar to the initial loss found by 30 or 60 seconds of HS (Figure 9D). Similar results for both experiments were found for *Hsp26* as well (Figures 10A-D). These experiments demonstrate that the initial loss of nucleosomes is due to a mechanism that is independent of transcription and the subsequent loss in protection is due to a transcription-dependent mechanism.

2.2.3 The Loss of Nucleosomes at *Hsp70* Halts at the *Drosophila* scs and scs' Boundary Elements

In my initial assay, I observed chromatin changes across the entire *Hsp70* region that I surveyed (Figure 4C). Next, I chose to determine where the loss in nucleosomal protection ceases. Decondensed polytene chromosome puffs do not spread indefinitely, suggesting that a relatively

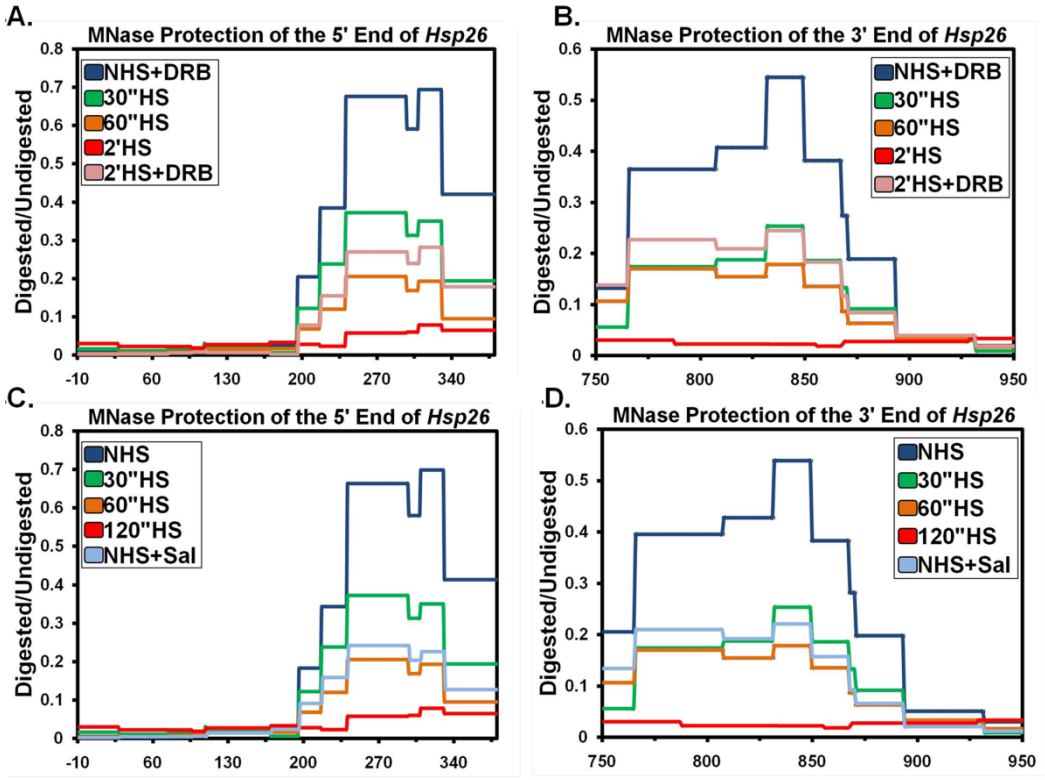

Figure 10 Initial Loss of Nucleosomes at *Hsp26* is Independent of Transcription

MNase protection profile of the 5' (A) and 3' (B) end of *Hsp26* as in Figure S3 of a 2 minute HS with DRB (pink) in comparison to a 0 (dark blue), 30 (green), 60 (orange), or 120 seconds (red) of HS. Lines represent the average of 3 separate experiments. Error bars representing the SEM are omitted for clarity. All primer sets are found in Table 5.

MNase protection profile of the 5' (C) and 3' (D) end of *Hsp26* as in Figure S3 of NHS with salicylate (light blue) in comparison to a 0 (dark blue), 30 (green), 60 (orange), or 120 seconds (red) of HS. Lines represent the average of 3 separate experiments. Error bars representing the SEM are omitted for clarity.

defined border of nucleosome loss might exist. To identify where this border occurs, I progressively walked downstream of the *Hsp70* genes at 87A to the scs and scs' boundary elements (Figure 11) (Udvardy et al., 1985). As insulators, the scs and scs' regions protect against positive and negative

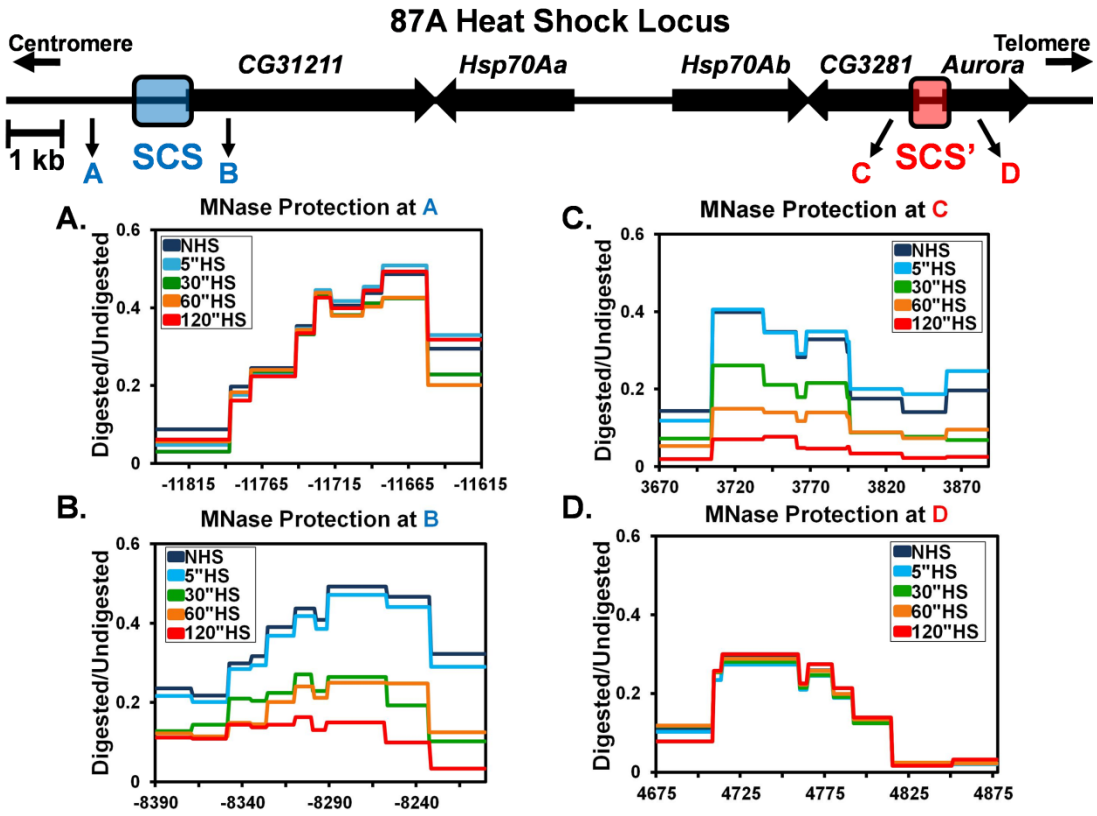

Figure 11 The scs and scs´ Regions Insulate the Heat Shock Locus from the Spread of Nucleosome Loss

(A -D) MNase HS time course protection as in Figure 4C flanking the scs and scs' insulators. The 87A HS locus shown above depicts the 4 sites analyzed flanking scs and scs'. Regions A and D are outside and B and C are inside of the scs and scs' insulators respectively. Regions A-D also correspond to A-D in the graphs. The x-axis of all 4 graphs uses the TSS of the *Hsp70Ab* copy as the 0 point. Each line represented is the average of 3 independent experiments. Error bars are omitted for clarity but the SEM from 3 independent experiments is less than ±0.06.

chromatin position effects, and can block cis-acting, promoter-enhancer interactions (Kellum and Schedl, 1991; Kuhn et al., 2004). The scs and scs' regions are known to contain nuclease hypersensitive regions as well as DNA binding elements for the zeste-white 5 (Zw5) and boundary element

associated factor 32 (BEAF-32) DNA binding proteins, respectively (Gaszner et al., 1999; Vazquez and Schedl, 1994; Zhao et al., 1995). Surprisingly, protection of nucleosomes anywhere between the *Hsp70* copies and either the scs or scs' regions was lost upon HS activation with similar kinetics to the loss observed at *Hsp70* (Figures 11B, 11C, and data not shown). However, nucleosomes outside the region enclosed by the scs and scs' elements were unaffected (Figures 11A and 11D). These results indicate that the scs and scs' regions also act as barriers to the spread of severely decondensed chromatin and that rapid nucleosome loss upon transcription activation is not confined to the transcription unit, but can extend several kb upstream and downstream of the activated gene. Interestingly, even though changes in nucleosomes occur over multiple genes within the region, only the *Hsp70* genes are induced following a HS (Figure 12A). Moreover, the loss of nucleosomes across this broad domain, corresponding to the 87A polytene puff, occurs well before maximal puff formation; therefore, puffing does not merely represent nucleosomal changes, but must also denote higher order structural changes at the locus.

2.2.4 HSF and GAF are Necessary for Nucleosome Loss at *Drosophila Hsp70*

The above results defined the location and rate of nucleosome loss at *Hsp70* but did not identify what factors are required for the nucleosome loss. To address this question I coupled the high resolution MNase assay to

transient depletions of candidate factors by RNAi. Given that a mutation in HSF or deletion or mutation of the HS or GAGA elements greatly inhibits the formation of HS puffs (Jedlicka et al., 1997; Shopland et al., 1995), I first targeted HSF and GAF for depletion. Depletion of HSF or GAF to less than

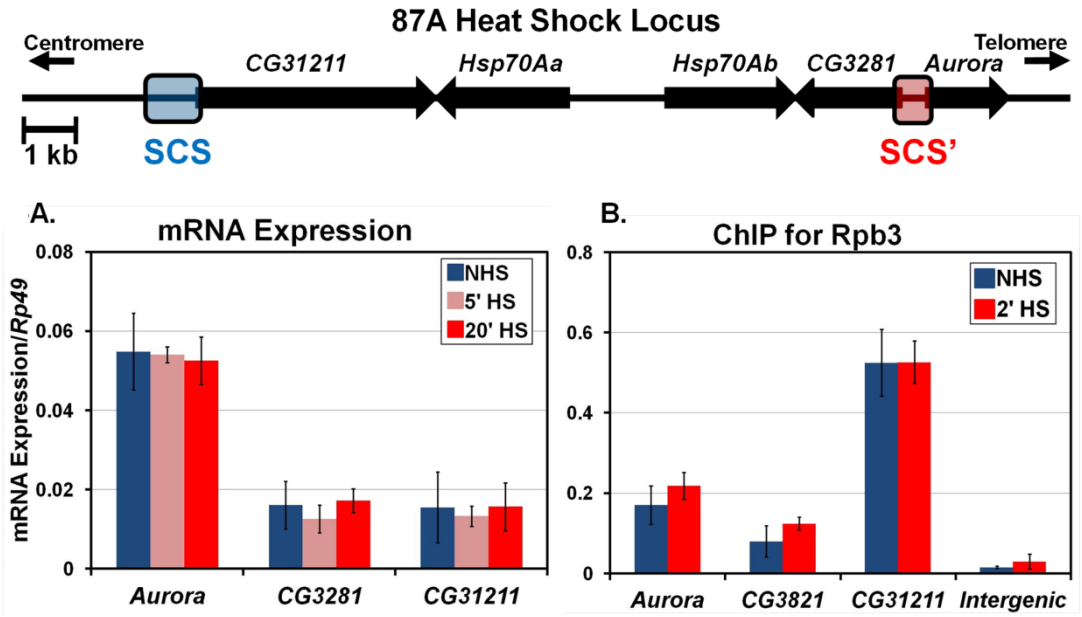

Figure 12 Expression and Pol II occupancy of Genes within the 87A Heat Shock Locus do not change after Heat Shock

The 87A HS locus shown above depicts the region enclosed by the scs and scs' regions.

(A) mRNA levels from *Aurora*, *CG3281*, and *CG31211*, *CG3281* under NHS conditions (blue) and following a 5 (pink) and 20 minute HS (red) were measured for S2 cells. Expression levels were measured by oligo dT primed reverse transcription followed by qPCR using specific *Hsp70Ab* primers. *Hsp70* mRNA levels are normalized to the *Rp49* gene with error bars representing the SEM of 3 replicates. PCR primer sets are found in Table 6.

(B) Pol II occupancy at the TSS of the *Aurora*, *CG3281*, and *CG31211* genes detected by ChIP using an Rpb3 antibody just as in Figure 3. S2 cells under NHS (blue) or 2 minutes of HS (red) conditions were analyzed. The y-axis represents the percent of input material immunoprecipitated. Error bars represent the SEM of 3 independent experiments. The x-axis represents the TSS of the respective gene analyzed. The intergenic region represents a region 32 kb downstream of *Hsp70Bc*. Primer sets can be found in Table 7.

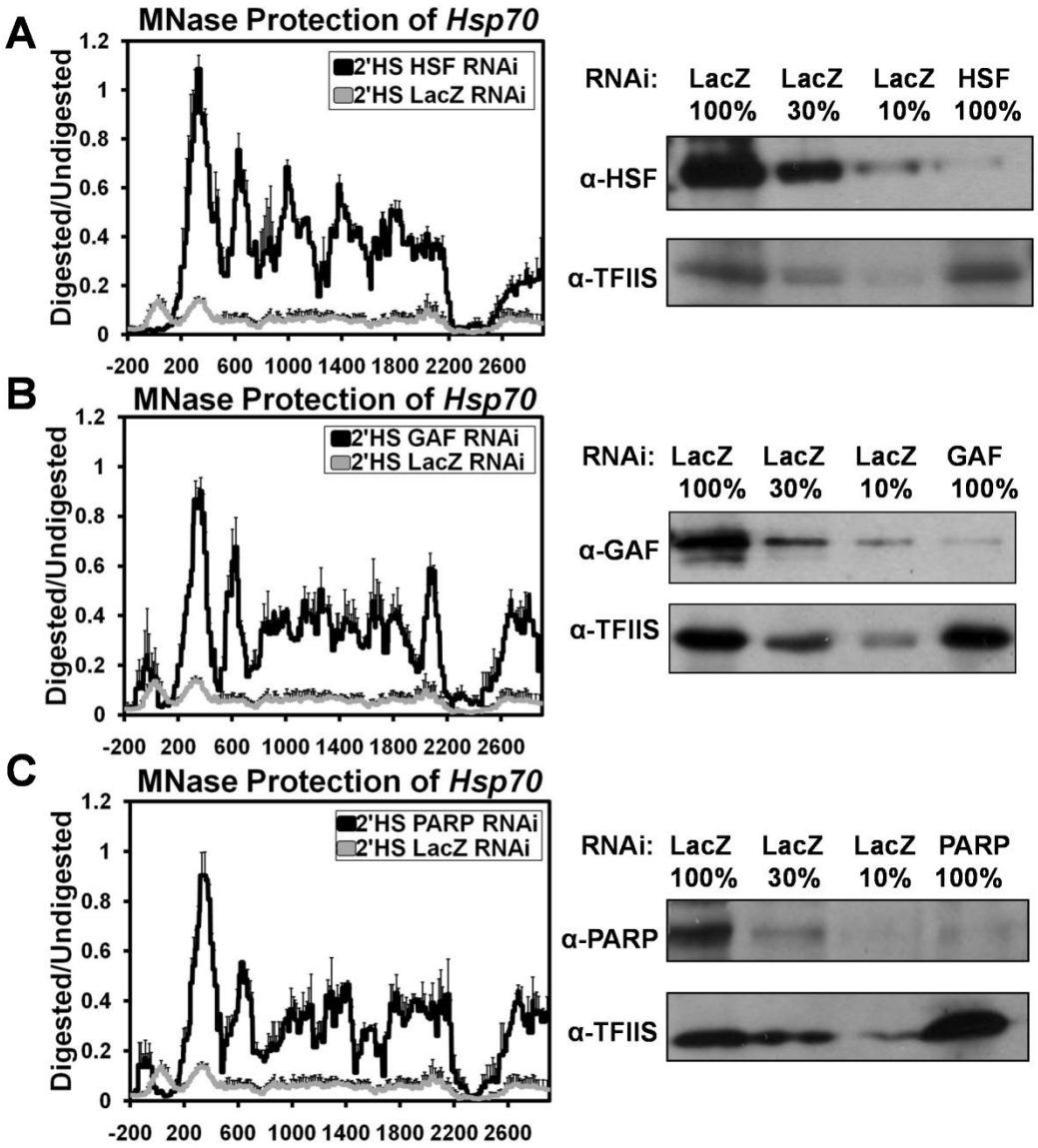

Figure 13 HSF, GAF, and PARP are Essential for the Loss of Nucleosomes at *Hsp70*

MNase protection profile as in Figure 4C comparing the chromatin architecture following an RNAi depletion of either (A) HSF, (B) GAF, or (C) PARP (black lines) in comparison to a control RNAi depletion of LacZ (gray lines) after a 2'HS at *Hsp70*. Each line represents the average of 3 independent experiments with error bars representing the SEM. Western blots showing corresponding knockdown of HSF, GAF, or PARP are shown to the right of each figure with TFIIS used as a loading control and a serial dilution of LacZ RNAi to quantify each knockdown.

10% of LacZ control cells (Figures 13A and 13B), abolished the changes in the chromatin structure of *Hsp70* after a 2 minute HS (Figures 13A and 13B) and with a shorter 30 second HS (Figures 14B and 14C). Therefore, both HSF and GAF are critical for bringing about the loss of nucleosomes upon HS.

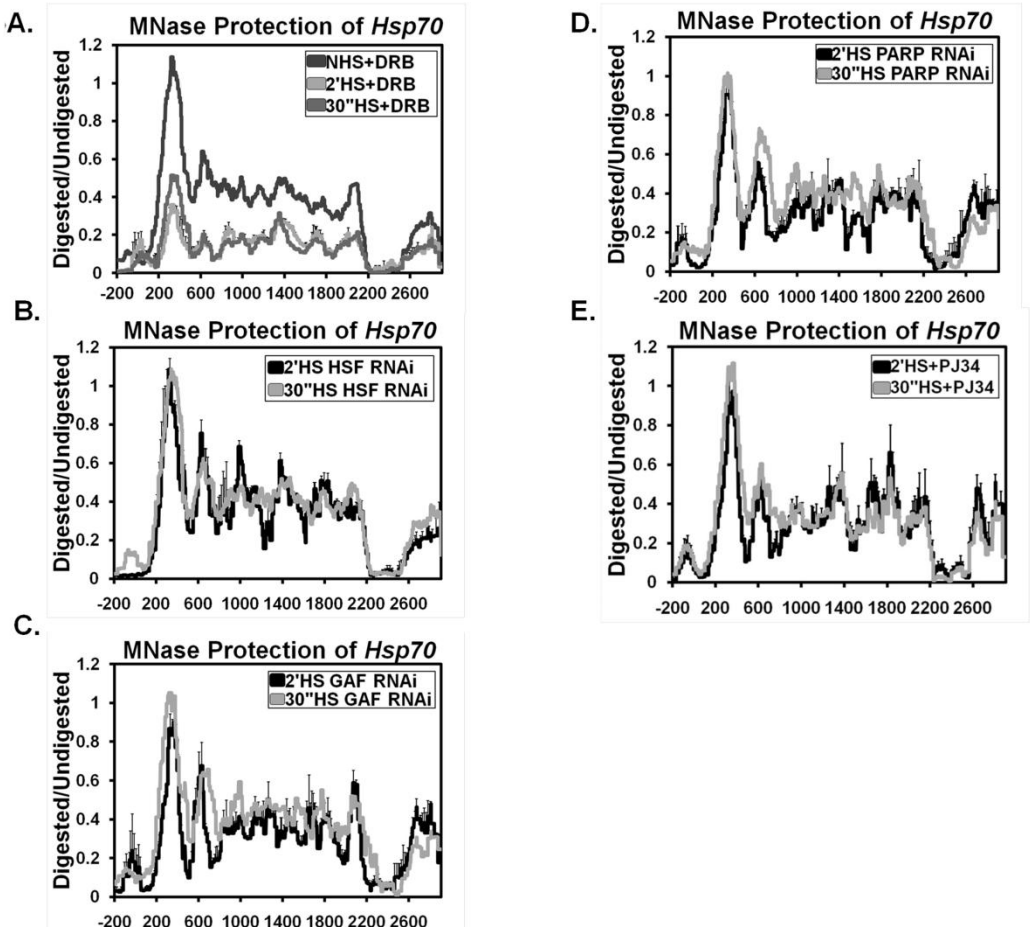

Figure 14 RNAi and Chemical Treatments do not Significantly Change between 30 Seconds and 2 Minutes of Heat Shock

(A) The MNase profiles for *Hsp70* are shown for NHS with DRB (black), 30 seconds of HS with DRB (dark gray), and 2 minutes of heat shock with DRB (light gray).
The MNase profiles for *Hsp70* are also shown for 30 seconds of HS (gray) and 2 minutes of heat shock (black) for HSF RNAi (B), GAF RNAi (C), PARP RNAi (D), or PJ34 treatment (E). Error bars representing the SEM from 3 independent experiments are shown for the 2 minute heat shock condition.

2.2.5 Poly(ADP-Ribose) Polymerase is Necessary for Nucleosomal Loss at *Hsp70*

To determine if other factors are required for the rapid changes in nucleosome structure upon HS, I targeted many additional factors by RNAi depletion: known players in the HS response, nucleosome remodelers, histone-interacting proteins, elongation factors, factors affecting DNA topology, and known boundary element factors. The results of these experiments are summarized in Table 3 and in Figures 15-21. Although not all knock-downs were confirmed, due to the unavailability of antibodies, those that were checked had protein levels decreased to 5-20% of control cells (Figure 22). Under NHS conditions, the ISWI remodeling complex containing Nurf301 and Chd1 had the largest effects, as nucleosomes on the body of the gene were better positioned in ISWI, Nurf301, and Chd1 RNAi treated cells (Figures 18B, 18C, and 18E). Additionally, RNAi depletion of HDAC3 reduced the protection of DNA corresponding to the positions of the first 2 nucleosomes (Figure 19D). After HS, some transcription related factors including Med15, P-TEFb, Spt6, and ERCC3 (Figures 15D, 17A, 17D, and 20C respectively) showed nucleosome profiles more closely resembling a 1 minute rather than a 2 minute HS, which may be a consequence of a transcription defect at *Hsp70* (Ni et al., 2007) or possibly a direct role in the disassembly of nucleosomes associated with elongating Pol II. Regardless, depletion of these 4 factors reinforces the finding that the second loss in MNase protection

Table 3 Affect of RNAi Depletion of Different Factors on the Chromatin Architecture at *Hsp70*

	Factor	Change from NHS	Change from 2'HS
Upstream Activators	HSF[1]	None	NHS[4]
	GAF[1]	None	NHS[4]
	CBP	None	None
	Med15	None	1'HS[5]
	Med23	None	None
SAGA Subunits	Gcn5	None	None
	Tra1	None	None
	Spt3	None	None
	Ubp8	None	NMP[6]
Elongation Factors	PTEF-b (Cyclin T[1])	None	1'HS[5]
	Paf1[1]	None	NMP[6]
	FACT (Spt16[1])	None	NMP[6]
	Spt6[1]	None	1'HS[5]
Chromatin Remodelers	Swi/Snf (Brm)	None	None
	ISWI	NWP[2]	None
	Nurf301	NWP[2]	None
	MI-2	None	None
	Chd1	NWP[2]	NMP[6]
	Kismet	None	None
Nucleosome Interacting Proteins	HIRA	None	None
	Asf1	None	None
	PARP[1]	None	NHS[4]
	HDAC3	NLP[3]	NMP[6]
DNA Topology	Topo1[1]	None	None
	Topo2	None	NMP[6]
	TFIIH (ERCC3[1])	None	1'HS[5]
Boundary Elements	BEAF-32	None	NMP[6]
	Zw5	None	NMP[6]

[1]Knockdown confirmed by Western to be 5-20% of LacZ RNAi levels.
[2]Nucleosomes on the body of the gene are better positioned.
[3]DNA at the 1st and 2nd nucleosomes after the TSS is less protected.
[4]Resembles a NHS profile.
[5]Resembles a 1' HS profile.
[6]DNA at the 1st nucleosome after the TSS is more protected.

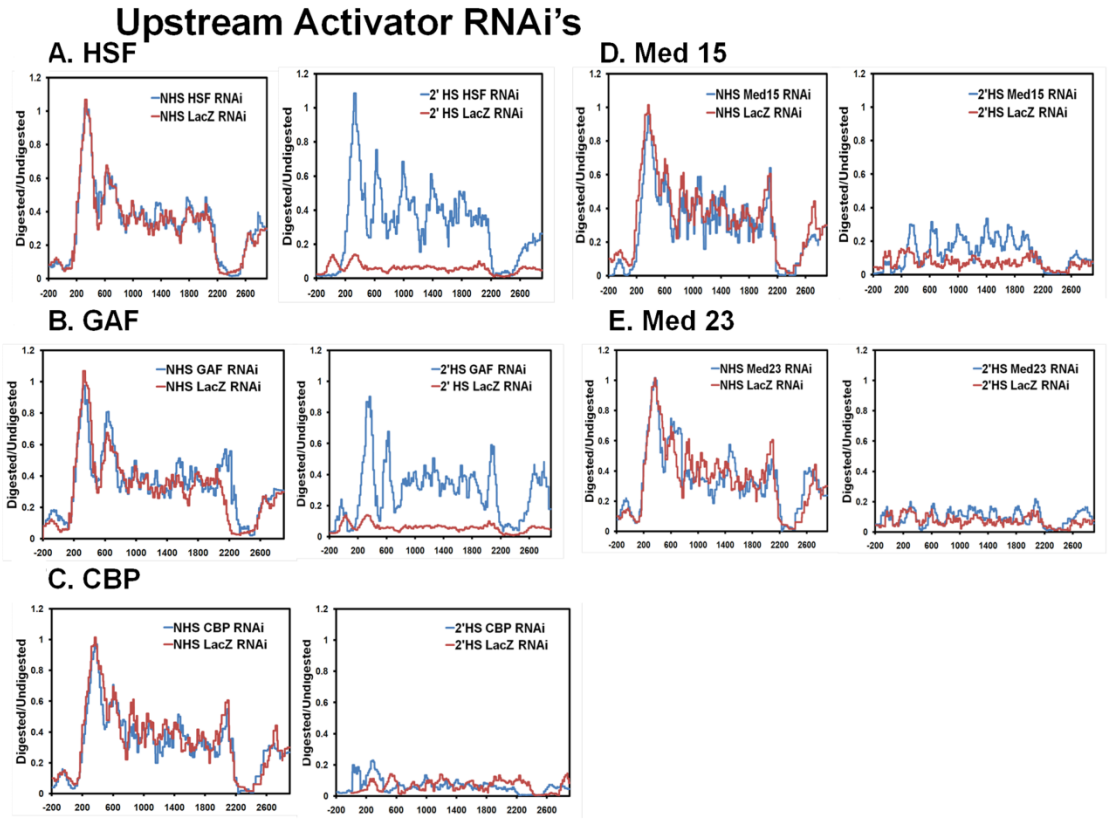

Figure 15 Upstream Activator RNAi MNase Profiles

The RNAi MNase profiles of both NHS (left) and a 2'HS (right) are shown for HSF (A), GAF (B), CBP (C), Med15 (D), and Med23 (E).

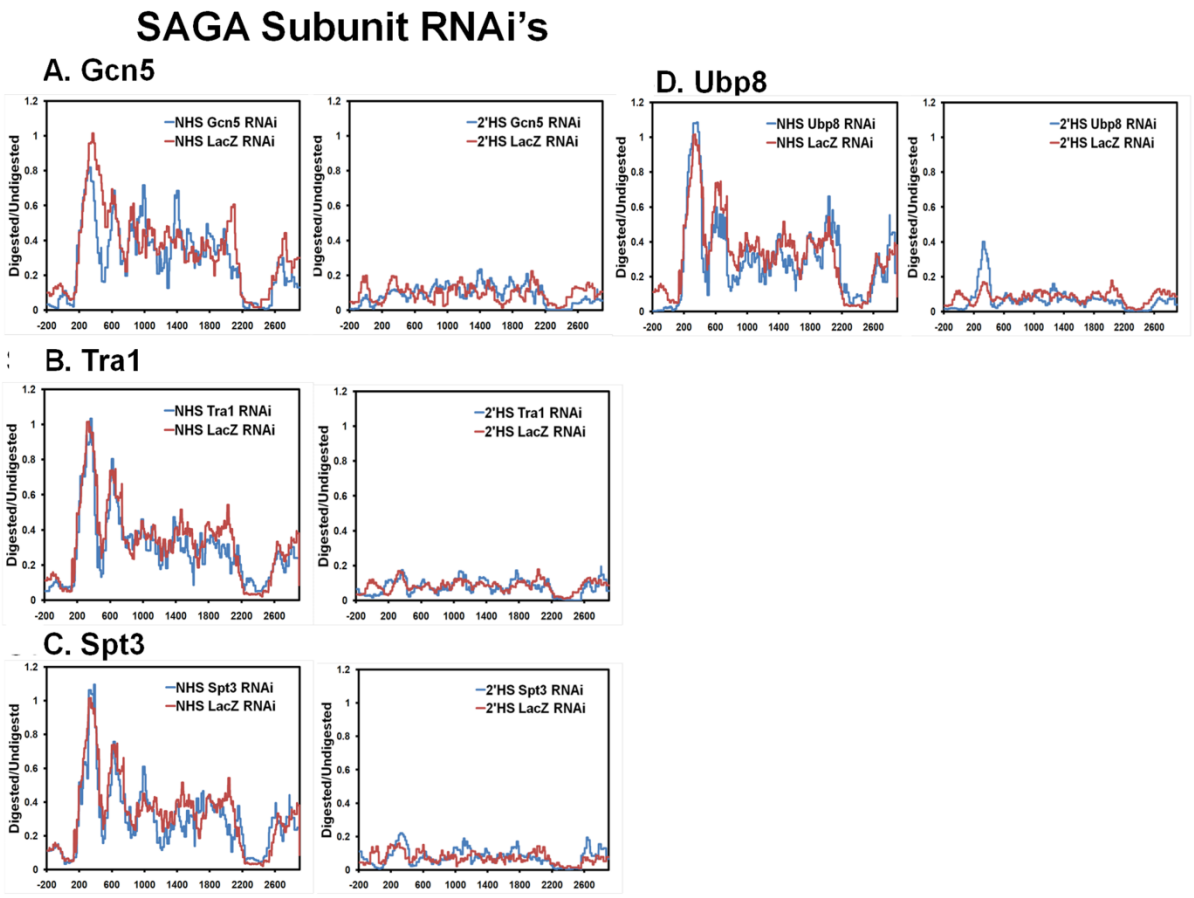

Figure 16 SAGA Subunit RNAi MNase Profiles

The RNAi MNase profiles of both NHS (left) and a 2'HS (right) are shown for Gcn5 (A), Tra1 (B), Spt3 (C), and Ubp8 (D).

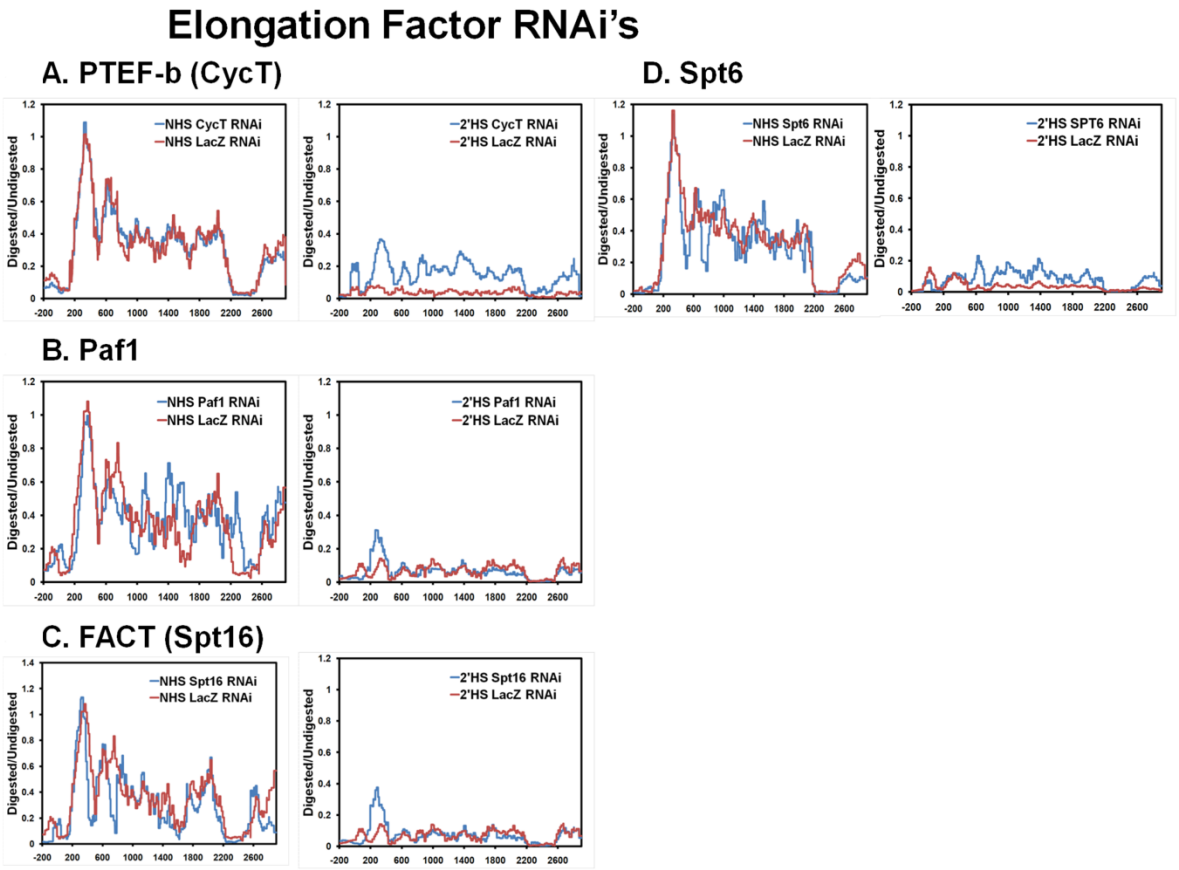

Figure 17 Elongation Factor RNAi MNase Profiles

The RNAi MNase profiles of both NHS (left) and a 2'HS (right) are shown for P-TEFb (Cyclin T) (A), Paf1 (B), FACT (Spt16) (C), and Spt6 (D).

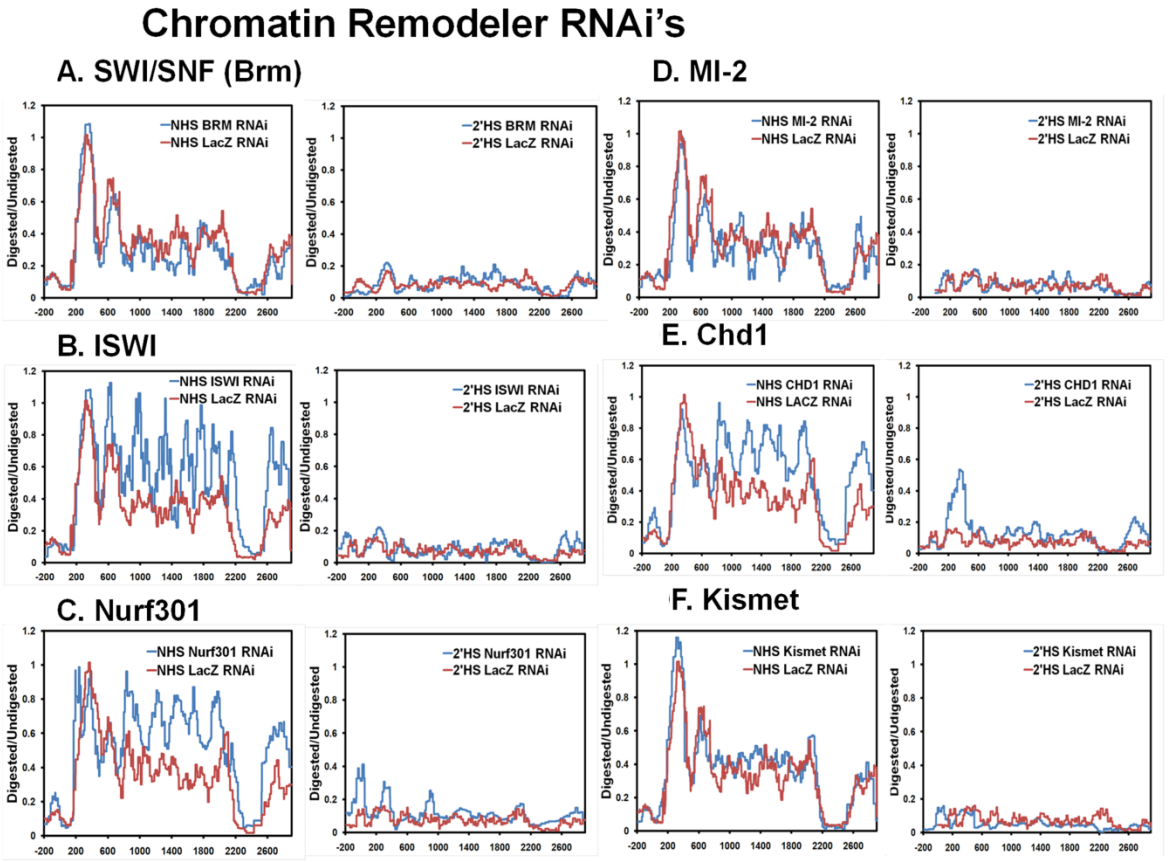

Figure 18 Chromatin Remodeler RNAi MNase Profiles

The RNAi MNase profiles of both NHS (left) and a 2'HS (right) are shown for SWI/SNF (Brm) (A), ISWI (B), Nurf301 (C), MI-2 (D), Chd1 (E), and Kismet (F).

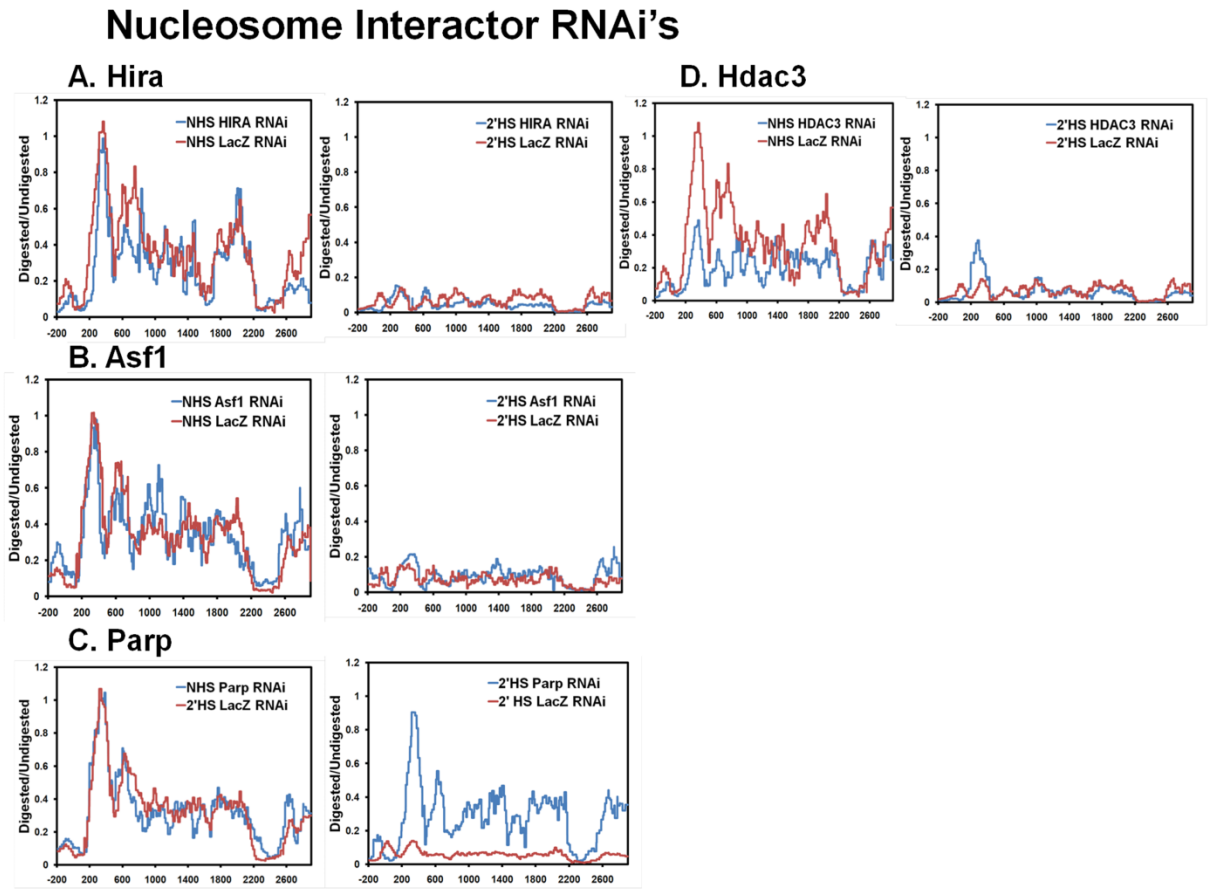

Figure 19 Nucleosome Interactor RNAi MNase Profiles

The RNAi MNase profiles of both NHS (left) and a 2'HS (right) are shown for HIRA (A), Asf1 (B), PARP (C), and HDAC3 (D).

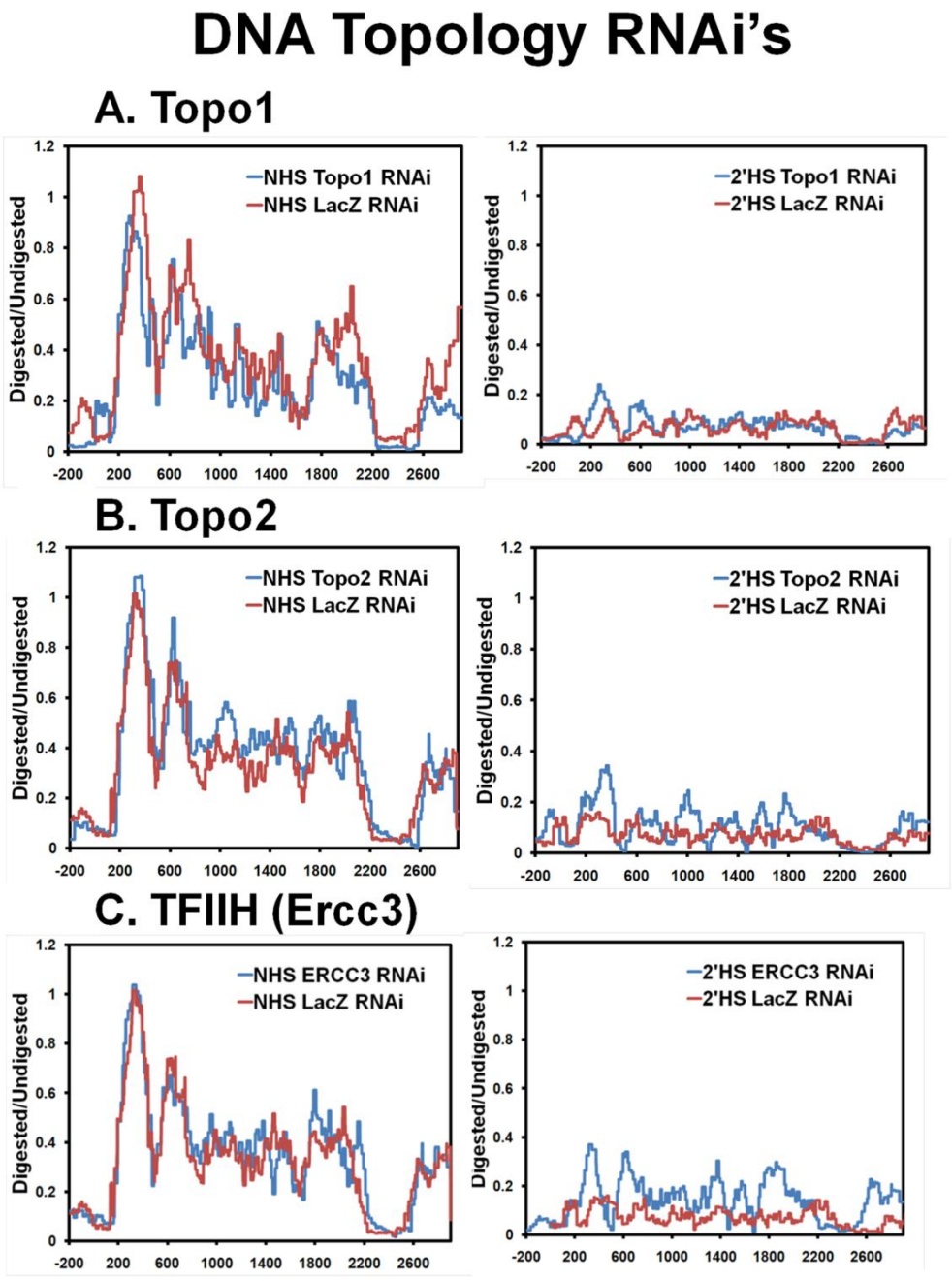

Figure 20 DNA Topology RNAi MNase Profiles

The RNAi MNase profiles of both NHS (left) and a 2'HS (right) are shown for Topo1 (A), Topo2 (B), and TFIIH (ERCC3) (C).

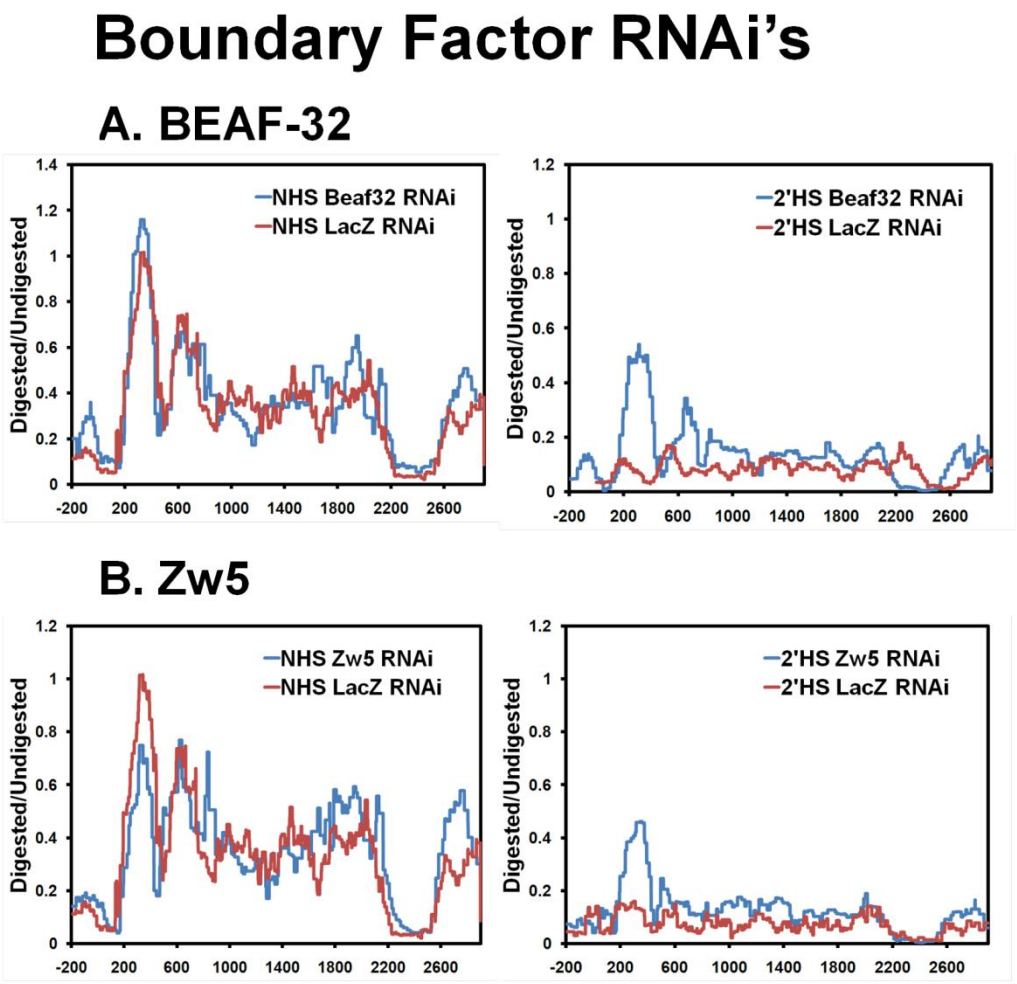

Figure 21 Boundary Factor RNAi MNase Profiles

The RNAi MNase profiles of both NHS (left) and a 2'HS (right) are shown for Beaf-32 (A), Zw5 (B).

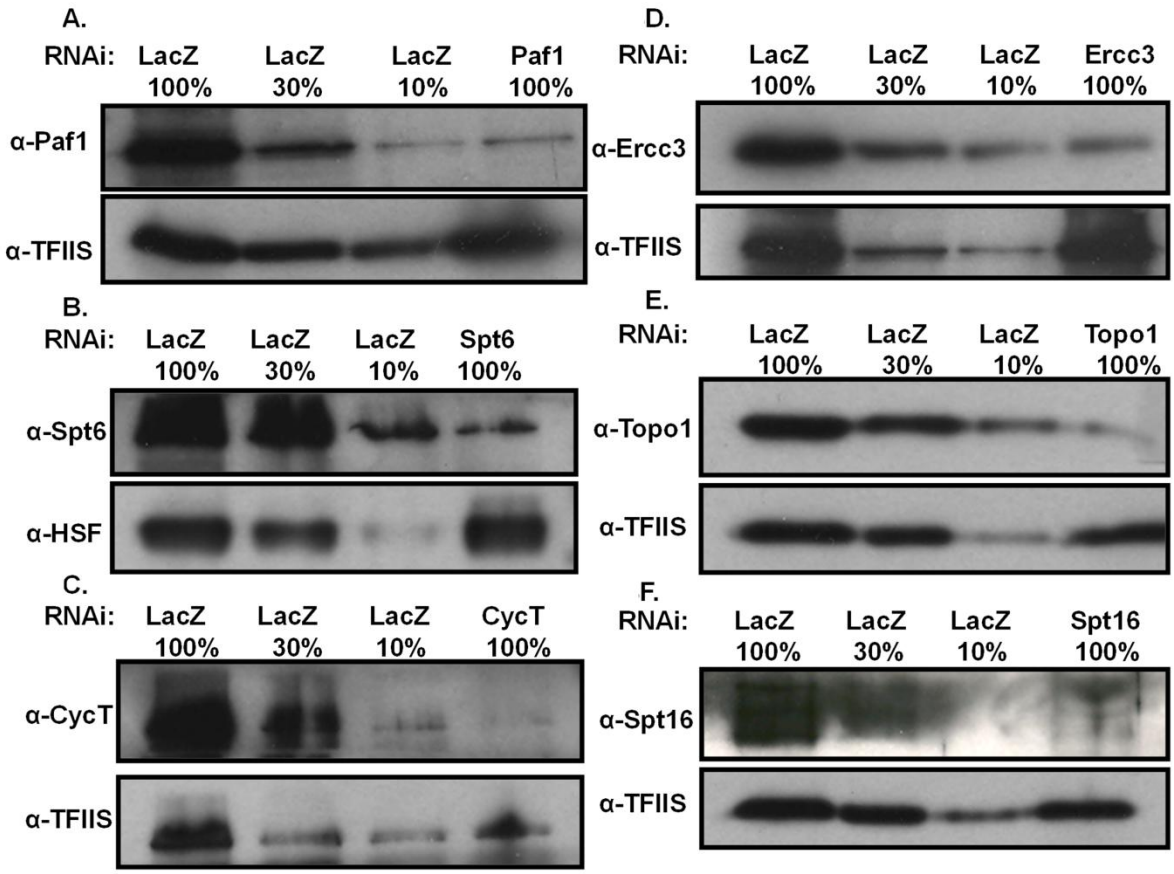

Figure 22 Western Blots of Confirmed RNAi Knockdowns

Western blots for the knockdown of Paf1 (A), Spt6 (B), Cyclin T (C), ERCC3 (D), Topo1 (E), and Spt16 (F) are shown followed by a Western blot of TFIIS or HSF used as a loading control. The percent of knockdown was confirmed through loading 10, 30, and 100% dilutions of the LacZ RNAi extracts in the first three lanes followed by extract from the knockdown cells corresponding to 100% of LacZ loaded.

(occurring between 1 to 2 minutes of HS) is a transcription-dependent event. Depletion of other factors resulted in slightly more protection at the site of the first nucleosome after the TSS upon HS (e.g. Figures 16D, 17B, 17C, etc). Additionally, a subset of factors, including Zw5 and BEAF-32, were chosen to determine if RNAi depletion of any factor allowed disruption of nucleosomes outside scs and scs', and none were found (Figure 23). Overall, most factors targeted for depletion did not show any difference in the nucleosome profile in comparison to control LacZ RNAi treatments before or after a 2 minute HS (e.g. Figures 15C, 15E, 16A, etc).

Beyond HSF and GAF only one additional factor, Poly(ADP-Ribose) Polymerase (PARP), was found to be essential for the dramatic changes in chromatin structure upon HS. In comparison to LacZ depleted cells which were heat shocked for 2 minutes, depletion of PARP to ~10% of control levels, resulted in a nucleosome profile more closely resembling NHS (Figure 13C), indicating PARP's importance in bringing about changes in chromatin structure upon HS. Similar results were found using a shorter 30 second HS (Figure 14D).

To determine if PARP's ability to mediate changes in chromatin structure were dependent on its catalytic activity, I used a specific PARP catalytic inhibitor, PJ34 (Virag and Szabo, 2002). Treatment of S2 cells with 300 nM PJ34 for 10 minutes did not affect the NHS chromatin profile (data not shown). However, treatment of cells with 300 nM PJ34 followed by 2 minutes of HS (Figure 24A) or 30 seconds of HS (Figure 14E) resulted in retention of

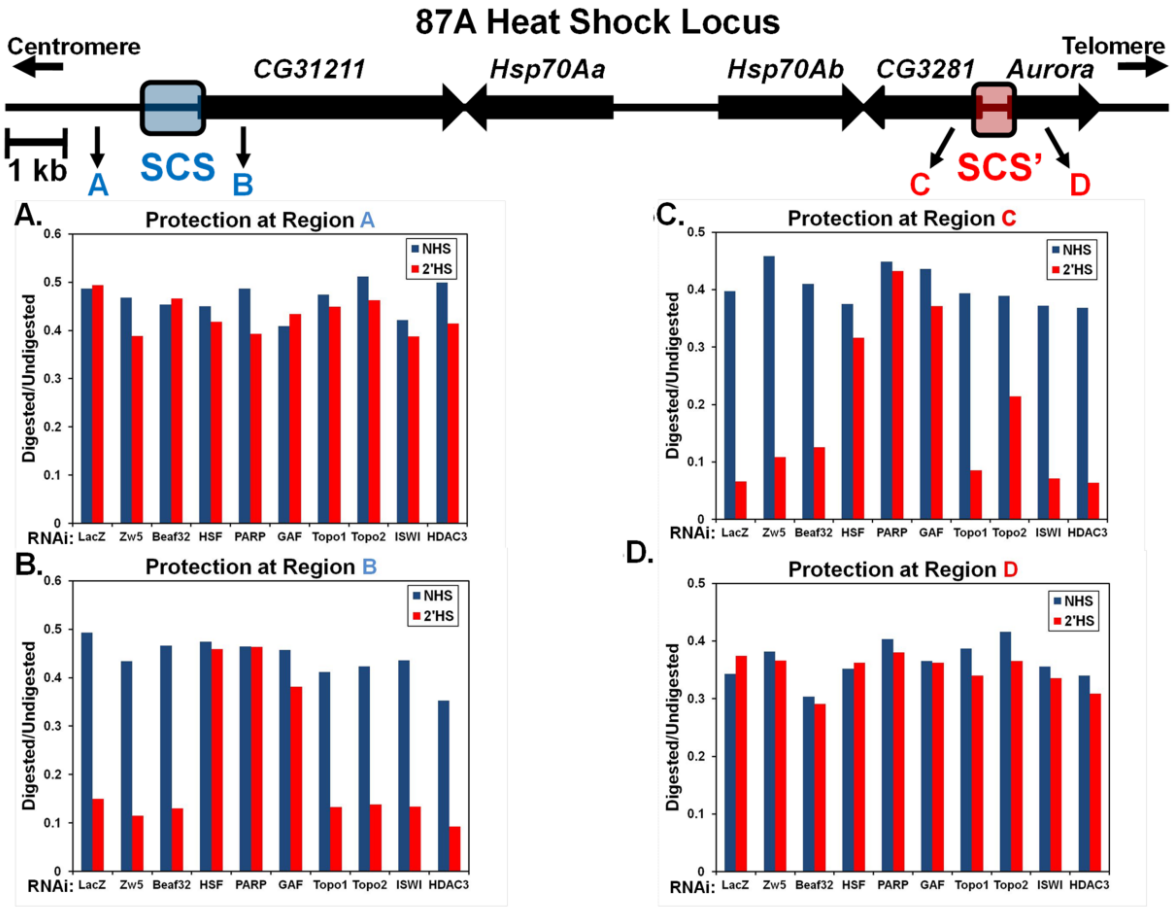

Figure 23 MNase Protection outside the 87A Heat Shock Locus Enclosed by scs and scs' are not Affected by RNAi Knockdown of Several Factors

The 87A HS locus shown above depicts the 4 sites analyzed flanking scs and scs'. Regions A and C are outside and B and D are inside of the scs and scs' insulators respectively. Regions A-D also correspond to A-D in the graphs. To compress data for each individual graph generated at a particular region for each RNAi knockdown (10 at each region, 40 in total) the highest level of protection for each region (found by the peaks seen in Figure 4) for each RNAi is plotted as a bar for either NHS (blue) or 2'HS (red). All knockdowns can be compared to control LacZ RNAi treated cells on the left. Note that the protection levels from Zw5 and Beaf32 RNAi did not change significantly from LacZ RNAi levels at regions A and D.

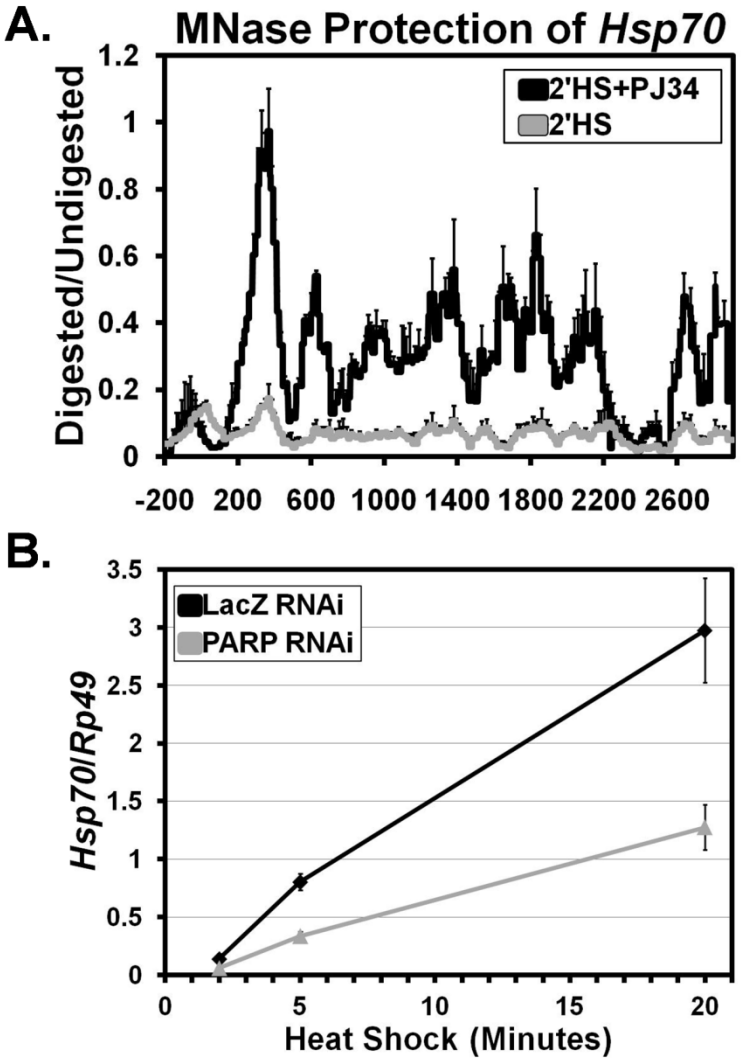

Figure 24 The Enzymatic Activity of PARP is Needed for Nucleosome Loss at *Hsp70* and PARP is Required for full *Hsp70* Expression

(A) MNase protection profile of *Hsp70* as in Figure 4C comparing the chromatin architecture of S2 cells treated (black line) or not treated (gray line) with the PARP enzymatic inhibitor PJ34 after a 2'HS. Each line represents the average of 3 independent experiments with error bars representing the SEM.

(B) *Hsp70* mRNA levels following a 2, 5, and 20 minute HS were measured for S2 cells RNAi depleted of LacZ (black) or PARP (gray). *Hsp70* expression levels were measured by oligo dT primed reverse transcription followed by qPCR using specific *Hsp70Ab* primers. *Hsp70* mRNA levels are normalized to the *Rp49* gene with error bars representing the SEM of 3 replicates.

the NHS nucleosome profile in comparison to untreated cells. These results confirm the RNAi knockdown data, arguing against an off target effect of the transient knockdown, and also show that PARP's enzymatic activity is required for the loss of nucleosomes at *Hsp70* following HS.

I then sought to determine if depletion of PARP has a functional consequence beyond retention of chromatin structure following HS. To address this, I measured *Hsp70* mRNA levels following 2, 5, and 20 minutes of HS. The result was almost a 3-fold reduction in the amount of transcript following each of the time points (Figure 24B), comparable to a previously estimated 5-fold reduction in Hsp70 protein levels (Tulin and Spradling, 2003). Collectively, my results show that upon HS, PARP is necessary for rapid nucleosome loss at *Hsp70* and consequently, full transcriptional activation of the gene.

2.3 DISCUSSION

Using a high resolution *in vivo* approach to map changes in the chromatin structure of the rapidly induced *Hsp70* gene, I observed a broad disruption of nucleosome structure that occurred at a rate faster than transcribing Pol II and broader than a single transcription unit, ceasing at the natural insulating elements. Furthermore, I found that the initial changes in chromatin architecture at *Hsp70* can be decoupled from transcription of the gene, whereas the second disruption by 2 minutes is transcription-dependent. A selective RNAi screen identified HSF, GAF, and PARP as each being

necessary for the changes in chromatin landscape at *Hsp70*.

Before HS, the *Hsp70* gene contains a chromatin landscape that has many general, as well as some distinct features. Like many other TATA containing genes (Albert et al., 2007), a highly positioned nucleosome exists downstream of the promoter region and the adjacent nucleosomes on the body of *Hsp70* gradually lose their positioning. Likewise, as seen with many genome-wide studies, the promoter, and a region at the 3' end of the gene, is relatively nucleosome free (Mito et al., 2005; Trinklein et al., 2007; Yuan et al., 2005). It is yet to be determined why 3' ends of genes are hypersensitive to nucleases. However, while many genes in yeast contain a positioned nucleosome starting within the first 100 bp of the transcription unit, *Hsp70* contains a nucleosome free region that extends further, with the first nucleosome centered 330 bp following the TSS. This extended nucleosome-free region may be a more general feature of genes containing a paused polymerase.

My HS time course shows that within 2 minutes following HS, the chromatin landscape of *Hsp70* drastically changes. By my assay, following 2 minutes of HS, there no longer exists appreciable protection of a contiguous 100 bp piece of DNA that would normally be provided from a histone octamer. However, there are still detectable levels of histone H3 on the body of the gene, albeit three-fold less than NHS levels. Although these results differ from early observations that histone levels on *Hsp70* do not change following HS (Nacheva et al., 1989; Solomon et al., 1988), my 3-fold decrease measured by

qPCR agrees with more recent quantifications of histone levels following HS (Adelman et al., 2006) and may have gone undetected in the qualitative analysis of these early experiments. Early electron microscopy spreads of native transcribing Pol II complexes with a growing RNA chain from *D. melanogaster* indicate that the bulk of transcribing Pol II *in vivo* appears to have nucleosomes flanking its path (McKnight and Miller, 1979). My results, however, suggest that at least for the rapidly induced *Hsp70* gene, the nucleosomal structure present before HS no longer exists following activation of the gene.

I also found that changes in chromatin upon *Hsp70* induction extend well beyond the transcription unit of *Hsp70* and halt at the scs and scs' insulating elements. Previous studies of scs and scs' have shown that these insulators are capable of blocking enhancer functions and establishing chromatin domains that are resistant to position effects (Kellum and Schedl, 1991; Kuhn et al., 2004). However, the scs and scs' regions have been located by DNA FISH on squashed polytene chromosomes to be within a HS puff at the endogenous 87A HS locus (Kuhn et al., 2004). This indicates that the scs and scs' regions by themselves are not absolute boundaries to changes in chromosome architecture, and supports my observation that puffing is maximal at a time well after nucleosome disruption and therefore denotes additional structural alterations beyond those observed here. Although transcription of *CG31211*, *CG3281*, and *Aurora* did not change following HS, and no factor targeted for RNAi permitted the disruption of

nucleosomes beyond scs or scs', both of these regions include a TSS with detectable amounts of Pol II (Figure 12B), consistent with previous results (Muse et al., 2007). It is therefore possible that the promoter architecture with Pol II present at these genes may be responsible for establishing a barrier at these sites. Overall, my results show that scs and scs' provide a primary barrier to the spread of chromatin decondensation, at least at the nucleosomal level, and add to my limited knowledge of the chromatin architecture of a puff.

Previous results, combined with ours, indicate that transcription-independent chromatin decondensation may prove more general. Changes in chromatin structure independent of transcription have been implicated at *Hsp70* in humans (Brown and Kingston, 1997) and also at developmentally regulated puffs in *Drosophila* (Crowley et al., 1984). Furthermore, my results indicate that the changes in chromatin at *D. melanogaster Hsp70* do not depend on many different transcription factors. In *Saccharomyces cerevisiae*, many HS genes also lose histone density within the body of the gene by 2 minutes of HS (Zhao et al., 2005), and as in my study, these changes are independent of SWI/SNF, Gcn5, and Paf1. Overall, transcription-independent chromatin decondensation might allow cells to rapidly activate genes by clearing the obstacles in the path of Pol II prior to its movement, together with its entourage of elongation factors, through the gene.

My results show that in addition to HSF and GAF, which have previously been implicated in the decondensation at *Hsp70* loci (Shopland et al., 1995), PARP is also necessary for rapid changes in the nucleosome

architecture of *Hsp70*. This is consistent with the finding that reduction of PARP expression results in decreased HS puff sizes (Tulin and Spradling, 2003). My results go further in demonstrating that PARP aids the rapid removal of nucleosomes within 2 minutes of HS. Poly(ADP-Ribose) (PAR) polymers are the enzymatic product of PARP and have similar chemical and structural features as a nucleic acid (D'Amours et al., 1999). Upon activation, PARP polyribosylates itself, which results in PARP's release from chromatin (Wacker et al., 2007). The result of this could be two fold. First, since PARP binds to nucleosomes in a similarly repressive manner as linker histone H1 (Kim et al., 2004), the activation of PARP could result in its release from chromatin to reverse any repressive effects on the chromatin structure at *Hsp70*. Second, the ADP-ribosylation of histones may destabilize the nucleosome, and the creation of these PAR polymers could act locally as a nucleic acid that attracts and removes histones from the body of the *Hsp70* gene. Alternatively, PARP could covalently modify another protein to activate its role in removal of nucleosomes.

In addition to histones, PAR could also attract transcription factors that bind nucleic acids. This could explain the rapid recruitment of Pol II and other important transcription factors to the site of active HS transcription (Boehm et al., 2003). Likewise, PAR could also provide a means through which transcription factors recruited to the gene are then retained locally (Yao et al., 2007). The activation of PARP could thus provide a rapid, transcription-independent method to deplete histones and promote transcription of the

Hsp70 gene.

2.4 EXPERIMENTAL PROCEDURES

2.4.1 ChIP

D. melanogaster S2 cells were grown in M3+BPYE media + 10% FBS (Invitrogen) to 5-7 x 10^6 cells/mL. Heat shocks were performed as in (Boehm et al., 2003). Briefly, an equal volume of M3+BPYE media that was preheated to 48 ˚C was added to an Erlenmeyer flask containing the S2 cells while under constant, slow swirling. The flask was then placed into a preheated incubator at 37 ˚C for the indicated time, except for the 5 second treatment in which cooling directly follows addition of the preheated media. After heat shock, the S2 cells were taken out of the 37 ˚C incubator and an equal volume of M3+BPYE media prechilled on ice is added to the flask while being swirled slowly and constantly. The cells were then immediately crosslinked at a final concentration of 1% formaldehyde for 1 minute at room temperature by the addition of 16% paraformaldehyde (Electron Microscopy Sciences). Cross linking was quenched by the addition of 2.5M glycine to the final concentration of 125 mM for 6-10' at room temperature, while being constantly swirled. Cross linked cells were resuspended to 1 x 10^8 cells/mL in sonication buffer (0.5% SDS, 20mM Tris pH 8.0, 2mM EDTA, 0.5 mM EGTA, 0.5 mM PMSF, and 1 complete protease inhibitor tablet/10mL) and incubated on ice for 10' prior to sonication. Extracts were sonicated at 4˚C on the high sonication

setting of the Bioruptor (Diagenode) using one 15 minute followed by three 5 minute intervals of 20" bursts followed by 1' of inactivity (corresponding to 24 total bursts) to receive average fragment sizes of 400bp. Sonicated material was then centrifuged at 20,800 rcf for 10' at 4˚C to remove debris. Extract corresponding to 2.5 x 10^6 cells was diluted 20 fold in ChIP dilution buffer (0.5 % Triton X-100, 2 mM EDTA, 20 mM Tris pH8.0, 150 mM NaCl, 10% glycerol) for all IP's excluding H3 in which only 0.5 x 10^6 cells were used. An input of 2.5 x 10^6 cells was saved at -20˚C and processed with the IP samples at the point of reversing cross links. Each IP was precleared with 30 µL of Protein-A conjugated agarose beads (Upstate), equilibrated in IP buffer, for 1-2 hours at 4˚C. The precleared extract was collected by centrifugation for 1' at 1,000 rcf and to the supernatant the following amount of antibody per IP was used: 4 µL rabbit anti-Rpb3 (Adelman et al., 2006), 2 µL rabbit anti-HSF (Boehm et al., 2003), and 2 µL rabbit anti-Histone H3-ChIP grade (Abcam ab1791). 60 µL of Protein-A conjugated agarose beads, equilibrated in IP buffer, were added and was allowed to IP overnight at 4˚C in 1.7 mL tubes on a rotating epindorf tube holder at 8 rpm. The beads were then washed with three 1 mL low salt washes (0.1% SDS, 1% Triton X-100, 2 mM EDTA, 20 mM Tris pH 8.0, 150 mM NaCl), three 1 mL high salt washes (same as low salt except 500 mM NaCl), two 1 mL LiCl washes (1 mM EDTA, 10 mM Tris pH 8.0, 0.25M LiCl, 1% NP-40, 1% NaDeoxycholate), and two 1 mL TE washes at 4˚C. Each wash was minimally 1' in length and after centrifugation at 1000 rcf for 1' the supernatant was discarded, always leaving 250 uL of supernatant above the

beads. The material was eluted sequentially with two 250 µL 15 minute washes with elution buffer (1% SDS and 100 mM $NaHCO_3$). 500 uL of elution buffer was then added to the frozen input material from the day before. 20 uL of 5 M NaCl was added to each elution and cross links were reversed for, minimally, 4 hours at 65˚C, followed by a 30' proteinase K digestion (2 µL of 20 mg/mL proteinase-K (Invitrogen) and 7.5 µL of 2 M Tris pH 8.0) at 37˚C. The material was extracted with an equal volume of phenol/chloroform and 1 mL of 100% ethanol and 1 µL of GlycoBlue (Ambion) were added to the aqueous layer. The sample was allowed to precipitate at room temperature for 10' before centrifugation at 20,800 rcf at 4˚C for 20'. IP pellets were resuspended in 100 µL of 10 mM Tris pH 8.0 to be used for quantitative PCR analysis. Inputs were resuspended in 30 uL of 10 mM Tris pH 8.0 and split into two. One sample was digested with 1 µL RNase Cocktail (Ambion) at 37 ˚C for 30' and visualized on a 1.3% agarose gel for fragment sizes. The other was brought up to a volume of 500 µL to be used for inputs to the quantitative PCR analysis, which was the equivalent of 10% of the input material.

2.4.2 High-resolution MNase Mapping

The same procedure for ChIP was used up until resuspension in sonication buffer. At this point, cross-linked cells were resuspended in hypertonic buffer A (300 mM sucrose, 2 mM Mg Acetate, 3 mM $CaCl_2$, 10 mM Tris pH 8.0, 0.1% Triton X-100, and 0.5 mM DTT) to 1 x 10^8 cells/mL, incubated on ice for 5', and dounced 20 times with a 2 mL dounce homogenizer (tight pestle,

Wheaton). Nuclei were collected by centrifuging at 4 ˚C for 5' at 720 g. The pellets were washed twice in buffer A, and then resuspended in buffer D (25% glycerol, 5 mM Mg Acetate, 50 mM Tris pH 8.0, 0.1 mM EDTA, 5 mM DTT) at 1 x 10^8 nuclei/mL. Chromatin was collected by centrifuging at 4 ˚C for 5' at 720 g. The pellets were washed twice in buffer D and then resuspended in buffer MN (60 mM KCl, 15 mM NaCl, 15 mM Tris pH 7.4, 0.5 mM DTT, 0.25 M sucrose, 1.0 mM $CaCl_2$) at 1 x 10^8 nuclei/mL. The equivalent of 2 x 10^7 nuclei was used per MNase reaction. MNase (USB), diluted in buffer MN, was added so that 0, 0.5, 5, 50, and 500 total units were used per reaction and timed for 30' at room temperature. Reactions were stopped with the addition of EDTA and SDS to final concentrations of 12.5 mM and 0.5% respectively. The equivalent of 5 x 10^6 nuclei was removed and processed like ChIP samples from the point of elution from the beads.

2.4.3 Quantitative Real-Time PCR Analysis

ChIP and RT-qPCR primer sets have previously been characterized as in (Adelman et al., 2006). Real-Time PCR was performed as in (Ni et al., 2007). For ChIP samples, a standard curve was generated by serially diluting input samples tenfold to quantify IP samples with a 10%, 1%, 0.1%, and 0.01% input. For MNase digests, a fold difference was calculated (Schmittgen et al., 2000) between MNase treated and untreated samples. All values used were collected from the linear range of amplification. Each qPCR well contained the following mix: 4 µL of DNA sample, 1.33 µL of the 5 µM forward qPCR primer,

1.33 µL of the 5 µM reverse qPCR primer, 3.34 µL ddH_2O, and 10 µL of 2x Sybr Green Mix. 2x Sybr Green mix consists of 950 µL of (1.7% glycerol, 12 mM Tris pH 8.0, 50 mM KCl, 5 mM $MgCl_2$, 165 mM (+)-Trehalose, 200 µg/mL ultrapure nonacetylated BSA (Ambion), 0.14x Sybr Green (Invitrogen)), 40 µL of lab prepared qPCR hot-start-TAQ polymerase, and 10 µL of 25 mM dNTP mix (Roche) containing equimolar amounts of dATP, dTTP, dCTP, and dGTP.

2.4.4 Chemical Treatments

All chemicals were added to S2 cells in media, at final concentrations of 125 µM DRB (Sigma), 10 mM Sodium Salicylate, and 300 nM PJ34 (Alex Biochemicals) and allowed to mix for 10' at room temperature. Cells were then collected following NHS or 2' HS conditions outlined in the ChIP section.

2.4.5 dsRNA Generation

To generate the dsRNA used for the RNAi treatment of S2 cells, the T7 RNA polymerase recognition sequence was added to the 5' ends of primers that were used to amplify >200 bp of the corresponding cDNA of the targeted mRNA that limited off-target effects. Genomic or cDNA from S2 cells was used to amplify the corresponding region targeted for RNAi. RNAi primers and RefSeq DNA Identifiers for all knockdowns are provided in Table 8. For 1 T7 reaction the following was added together: 8.75 uL DEPC treated water, 6 uL of 25 mM rNTPs (all 4 in equimolar amounts, Roche), 2 uL of 10x T7 reaction buffer (400 mM Tris-Cl pH8.0, 100 mM DTT, 20 mM spermidine-HCl, 200 mM

$MgCl_2$), 0.25 uL of PCR purified DNA template (100 ng/ uL), 0.5 uL SUPERaseIN (Ambion), 0.5 uL PPiase (100 U/mL, NEB), and 2 uL of a 1:20 dilution in DEPC water of lab stock T7 enzyme. Incubate the reaction at 37 ˚C for 16 hours. 1ul of DNaseI (RNase free, Ambion) is then added and incubated for 15-30' at 37 ˚C. 20ul NH_4Ac and 155 ul sterile ddH_2O (DEPC treated) are added for a single reaction or 50 ul NH_4Ac and sterile ddH_2O (DEPC treated) up to 500 ul for up to 5 reactions are added to aid precipitation. The solution is extracted twice with acid phenol:chloroform and precipitated by adding 2 volumes of 100% ethanol and incubated at room temperature for 10'. The solution is centrifuged at 20,000 rcf for 20' at 4 C and the dried pellet is resuspended in 30-100 uL of ddH_2O (DEPC treated). The dsRNA is annealed by incubating at 90 ˚C for 3', transferred to 75 ˚C for 3', and then allowed to cool to room temperature in water taken out from the 75 ˚C water bath.

2.4.6 RNAi Treatments

All RNAi treatments were preformed as in (Adelman et al., 2005) except knockdown was allowed to proceed for 96 hours. Briefly, S2 cells were grown to ~$6x10^6$ cells/mL and split to $2x10^6$ cells/mL in M3+BPYE media without FBS. 2.5 mL of the corresponding $2x10_6$ cells/mL were added to a T-25 cm2 flask containing 50 ug of the corresponding dsRNA. S2 cells were treated with double stranded RNA targeting either the coding sequence of the listed factor or β-galactosidase (LacZ, as a negative control). The flask was allowed to rest in the cell culture incubator for 1 hour before addition of an equal amount

of volume, 2.5 mL, of M3+BPYE media + 20%FBS. After 96 hours, cells were collected and split into NHS and 2' HS samples to be processed using the high resolution MNase assay.

2.4.7 mRNA Expression Analysis

All mRNA expression analyses were as performed in (Adelman et al., 2006). Briefly, total RNA was isolated (following the protocol set out by Qiagen RNeasy kits) from PARP RNAi and LacZ RNAi S2 cells following 2, 5, and 20 minutes of HS. *Hsp70* levels were determined from oligo dT mediated quantitative real-time reverse transcription-PCR. 25.2 ul of 20 uM oligo(dT) primer was mixed with 720ng RNA in 18ul (for 3 RT reactions, for 2 duplicates, and 1 no RT reaction). The samples were incubated at 80 ˚C for 5 minutes and then chilled on ice. To 12 uL of the primer/RNA mix 8 uL of the RT mix was added (4 uL 5x first strand buffer, 1 uL 0.1 M DTT, 1 uL 10 mM dNTPs, 1.7 uL DEPC-treated sterile ddH_2O, and 0.3 uL SuperscriptIII reverse transcriptase (Invitrogen) (or 0.3 uL of DEPC-treated sterile ddH2O for the no RT control). The mixture was incubated at 42 ˚C for 15' and then at 50 ˚C for 45 additional minutes. To each sample 5 uL of the corresponding mix was added to degrade the RNA (4.7 uL sterile ddH_2O, 0.15 uL of RNaseH (Ambion), and 0.15 uL RNase cocktail (Ambion)) and incubated at 37 ˚C for 30'. Each sample was brought up to a final volume of 200 uL in ddH_2O. Three serial tenfold dilutions of the control were used to quantify each experimental sample using qPCR and the corresponding primer sets to

measure the gene in question along with the stable ribosomal protein RpL32 gene (*Rp49*) to internally standardize for the amount of RNA.

2.4.8 Western Blots

Western blots were performed using standard conditions, and input dilutions were used as a quantitative indication of signal linearity. Antibody lab stocks were used at the following dilutions: HSF 1:2000 (Shopland et al., 1995), 1:1000 GAF (O'Brien et al., 1995), 1:3000 TFIIS (Adelman et al., 2005), 1:2000 Paf1 (Adelman et al., 2006),1:1000 Spt6 (Andrulis et al., 2000), 1:2000 Cyclin T (Lis et al., 2000), 1:5000 ERCC3, an antibody raised in guinea pig to full length Ercc3 by Pocono Rabbit Farms and Laboratory Inc., 1:1000 Topo1 (Fleischmann et al., 1984), and 1:2000 Spt16 (Saunders et al., 2003). Rabbit anti-Parp serum raised to recognize the C-terminus (Kim et al., 2004) was a gift of W. Lee Kraus and used at a 1:1000 dilution.

2.5 PRIMER SETS USED

Table 4. Primer Sets Used for MNase Scanning Assay with Respect to the Transcription Start Site of *Hsp70Ab*

5' Start location	Forward
-190	TCTCTGGCCGTTATTCTCTATTCG
-163	TTGTGACTCTCCCTCTTTGT
-140	TTGCTCTCTCACTCTGTCACAC
-116	TAAACGGCGCACTGTTCTCGTTG
-85	AGAGCGCGCCTCGAATGTT
-56	GCGCCGGAGTATAAATAGAGGA
-25	CGGAGAGTCAATTCTATTCAAACA
15	CGCTAAGCGAAAGCTAAGCAA
40	ACAAGCGCAGCTGAACAAGCTA

71	GCAATAAAGTGCAAGTTAAAGTGA
103	AAAGTAACCAACAACCAAGTAA
135	ACTGCAACTACTGAAATCAACCAAG
171	TGAAGACAAGAAGAGAACTCTGAA
197	CTTTCAACAAGTCGTTACCGAGG
223	AGAACTCACACACAATGCCTGC
247	ATTGGAATCGATCTGGGCAC
280	TGGGTGTCTACCAACATGGCAA
310	ATTATCGCCAACGACCAGGGCAA
344	CGTCCTACGTGGCTTTCACAGATT
377	TCATCGGCGATCCGGCTAAGAA
393	TAAGAACCAGGTGGCCATGA
427	TGTTTGACGCCAAGCGACTGAT
469	CCAAGATCGCAGAGGACATGAA
490	AGCACTGGCCTTTCAAGGTTGT
517	ACGGCGGAAAGCCCAAGAT
550	AGGGTGAGTCCAAGAGATTTGC
583	TCAGCTCGATGGTACTGACCAA
609	AAGGAGACGGCGGAGGCATATCT
639	AGCATCACAGACGCAGTCATCA
668	AGCCTACTTCAACGACTCCCA
698	TACCAAAGACGCCGGTCACAT
728	GAATGTGCTCCGCATCATCAA
763	CAGCACTGGCCTACGGACT
789	AACCTCAAGGGTGAGCGCAAT
814	TTATCTTCGACTTGGGCGGCG
844	ATGTCTCCATCCTGACCATCGAC
872	ATCACTGTTCGAGGTGCGCT
908	ACACTTGGGCGGCGAGGACTTT
933	AACCGGCTAGTCACTCATCT
970	GCAAGTACAAGAAGGATCTGCGCT
1004	CGCCCTACGACGCCTCAGAACA
1025	AGCAGCTGAACGGGCCAA
1062	ACGGAGGCCACCATCGAGATT
1093	TTGAGGGCCAAGACTTCTACACCA
1116	AAAGTGAGCCGCGCCAGGTTT
1152	GACCTCTTCCGCAACACCCT
1183	AGAAGGCCCTCAACGATGCCAA
1211	TAAGGGTCAGATCCACGACATC
1240	TCGGCGGATCCACTCGCATT
1275	CTGCTGCAGGACTTCTTCCACG
1301	GAACCTCAACCTATCCATCAACCC

1325 AGACGAGGCAGTTGCATACGGA
1362 GCTATCCTCAGCGGAGACCAGA
1389 AAGATCCAGGACGTGCTGCTG
1422 CCACTTTCATTGGGAATTGAGACCGC
1448 TGGAGGTGTAATGACCAAGCTG
1479 AACTGCCGCATTCCGTGCAA
1512 TTCTCCACATACGCGGACAACCA
1543 TCTCCATTCAGGTGTATGAGGGC
1570 GTGCGATGACGAAGGACAACAA
1602 ACCTTCGATCTGTCCGGCATT
1621 TTCCACCTGCACCAAGGG
1663 TCGACTTGGACGCCAATGGAAT
1687 TGAACGTCAGCGCCAAGGAGAT
1717 GCAAGGCCAAGAACATCACGATCA
1757 GCTCTCGCAGGCCGAGATTGAT
1780 GCATGGTGAACGAGGCTGAAA
1810 ACGAGGACGAGAAGCATCGCCA
1839 ACCTCTAGAAATGCCCTGGAGA
1867 TCTTCAATGTGAAGCAGGCCGT
1898 ACCTGCTGGCAAATTGGACGA
1929 AACTCCGTCTTGGACAAGTGC
1958 TATCCGGTGGCTGGACA
1990 AGAAGGAGGAGTTCGACCACAA
2017 AGGAGCTCACCCGCCACT
2049 ACCAAGATGCATCAGCAGGGTG
2081 AGCTGGTGGTCCGGGAGCAAA
2110 AGCAGGCGGGAGGATTT
2133 TACTCTGGACCCACGGTCGA
2165 AGGCCAAAGAGTCTAATTTT
2195 TGGGTTATAACATATGGGT
2242 AGACTGATAAGAATGTTTCG
2264 CGAATATTCCATAGAACAAC
2288 GTATTACCTAATTACCAAGTCT
2318 CAAAAATGTTATTGCTTATAG
2348 ATTATTTATTTGAAATTTAAAGT
2371 CAACTTGTCATTTAATGTTTT
2401 TGAAAGTCTTACGATACAATT
2432 ATACATGGGTTCATTCTACA
2461 AGTGATGATTTCTTTAGCTAG
2501 TCGGCTTTGATGATTTTCTG
2528 CCGAACGGATTTTCGTAGACCCTTT
2564 TGGCTCATTTTATTGCGATG

2586	CGGTCAGGAGAGCTCCACTTT
2617	TTCGCAGACACCGCATTTGTAGCA
2647	CGGGACATCCGGTTTGGG
2676	GTCTCTGTTGCAATTGGT
2707	TTGCAGGCGCATACGCTCTATATC
2741	CGCTGGTTGACCCTAGCATTTACA
2781	AATTTGCCTCTACTTCATTGCCCG
2810	AGCAGGCGGGAGGATTTGGA
3667	AGCTGAACAGTCTTGGTCTCCA
3702	TTTCCACGTGCTGTTCGGCAAA
3726	ACGTGGACAGGTATTGTGCCAT
3758	TCGTCTTGGTCTATAAGCTCCACG
3791	TGAACTTCATCCGGCTTGGCA
3821	TGTTGCTCGAAGAGATTCTGTAAAGT
4673	TCGGCTTTCATTGTTAACTGACC
4707	CTGTTCTGTTAGTTGTCGAGTGCC
4713	TGTTAGTTGTCGAGTGCCTGTG
4758	CATGTGCTGCGTCCCAAGGAAA
4778	AAATGCTCCGCACAGAATGCCA
-8480	ACGCTACTCCGGTGCCCAT
-8446	GCCGCCCATCATCAGCAATTT
-8427	TTGCGAGAATACCACCAGCAGA
-8402	TAGCAATGCCGGTGCCCAGTGT
-8368	ATTTCCGCAACTAGAGGAGCAC
-8330	ACATGGACGATGAGAATGATCGGG
-8284	ACCGCCAGCACCTTTGGTTA
-11840	CCAACCATGCAGCCGTATACCAAA
-11789	TAACATAATTGAGGCACCCGGC
-11775	CACCCGGCCGTTGAATGTTT
-11744	TGAGCAGAAAGCGAAGACCTGA
-11720	ATACGGGAGGTGAAACATGGAGCA

5' Start location	**Reverse**
-95	AACGAGAACAGTGCGCCGTTTA
-61	TTCGCGAACATTCGAGGCG
-37	CCTCTATTTATACTCCGGCGCTCT

-5	TGAATAGAATTGACTCTCCGTCG
18	GCGATGTGTTCACTTTGCTTG
50	GCTGCGCTTGTTTGTTTGCT
84	CTTGCACTTTATTGCAGATTGT
121	ACTTGGTTGTTGGTTACTTT
130	GTTTAATTACTTGGTTGTTGGTTAC
163	CTTCTTGGTTGATTTCAGTAGTTGC
193	TCAGAGTTCTCTTCTTGTCTTC
236	TGTGTGTGAGTTCTTCTTCCTCGG
261	CAGATCGATTCCAATAGCAGGC
296	ATGTTGGTAGACACCCACGCA
316	GCGATAATCTCCACCTTGCCAT
359	AAAGCCACGTAGGACGGC
379	ATGAGGCGTTCCGAATCTGTGA
412	TTCATGGCCACCTGGTTCTT
444	TCGCTTGGCGTCAAACACT
475	TCTTGGGGTCGTCGTATTTT
496	AGTGCTTCATGTCCTCTGCGAT
517	TCGCTTACAACCTTGAAAGGCCAG
561	TGGACTCACCCTTATACTCCAC
598	AGTACCATCGAGCTGATCTCC
618	CCGTCTCCTTCATCTTGGTCAGTA
648	CTGTGATGCTCTCGCCCAGATA
681	CGTTGAAGTAGGCTGGAACTGT
706	TCTTTGGTAGCCTGGCGCT
745	ATGATGCGGAGCACATTCAGGC
764	TGCCGCCGTGGGCTCATT
800	ACCCTTGAGGTTCTTGTCCAGT
830	GCCCAAGTCGAAGATAAGCACA
861	TGGTCAGGATGGAGACATCGAA
891	AGCGCACCTCGAACAGTGAT
916	CCCAAGTGTGTGTCTCCGGC
947	AGTGACTAGCCGGTTGTCAAAG
979	TTGTACTTGCGCTTGAACTCGTCC
1013	TCGTAGGGCGCGAGGGTT
1038	CCCGTTCAGCTGCTGTTCTGA
1066	TCCGTGCTGGAGGAGAGTGT
1103	TTGGCCCTCAAACAGTGCGTCAAT
1126	CGGCTCACTTTGGTGTAGAAGT
1154	GTCCGCGCACAGCTCCTCAAA
1195	TTGAGGGCCTTCTCCACAGGCT
1219	TGACCCTTATCCATCTTGGCATCG

1248 ATCCGCCGACGAGCACGATGT
1279 AGCAGACTTTGCACCTTGGGAA
1314 ATAGGTTGAGGTTCTTGCCGTG
1342 TATGCAACTGCCTCGTCTGGGTT
1370 GAGGATAGCGGCCTGCACAGCA
1396 TGGATCTTGCCGCTCTGGTCT
1432 AATGAAAGTGGGGCCACGTC
1458 TTACACCTCCAGCGGTCTCAAT
1490 AATGCGGCAGTTGCGCTCGAT
1520 TGTGGAGAACGTCTTAGTCTGC
1550 AATGGAGACTCCGGGCTGGTT
1578 TCATCGCACGTTCGCCCTCATA
1614 ACAGATCGAAGGTGCCCAATGC
1638 CCCTTGGTGCAGGTGGAAT
1667 GTCGAAGGTAACTTCTATCTGGG
1698 CGCTGACGTTCAGGATTCCATT
1725 TGGCCTTGCCCGTGCTCAT
1761 AGAGCCGTCCCTTGTCGTTCTT
1789 TTCACCATGCGATCAATCTCGG
1819 TCGTCCTCGTCGGCGTACTTT
1854 GGCATTTCTAGAGGTTATTCGCTGGC
1884 CCTGCTTCACATTGAAGACGTAGC
1910 TTTGCCAGCAGGTGCCTGTTCC
1939 AAGACGGAGTTCTTGTCAGCCT
1969 AGCCACCGGATAGTGTCGTT
2002 AACTCCTCCTTCTCGGCAGTGG
2028 GGGTGAGCTCCTCCAGCTT
2064 GCTGATGCATCTTGGTCAT
2090 ACCACCAGCTCCAGCTCC
2114 CTGCTGGCCGCAGTTTGCT
2145 TGGGTCCAGAGTAGCCTCCAAAT
2179 TAGACTCTTTGGCCTTAGTCGACCTC
2211 CCATATGTTATAACCCATTGATGAAC
2230 AACAAACTTATAATATAACCCA
2261 CGAAACATTCTTATCAGTCT
2297 TAGGTAATACTATTGTTGTTCTATGG
2336 ATAAGCAATAACATTTTTGC
2370 ACTTTAAATTTCAAATAAATAAT
2390 AAACATTAAATGACAAGTTGA
2415 ATCGTAAGACTTTCAAAAGT
2451 TGTAGAATGAACCCATGTAT
2471 AAATCATCACTAATATAGAATGTAG

2501	AATATAATTAAAATGTATTACTAGC
2531	TCGGAAAAAATCAGAAAATC
2562	AGTGATGATTTCTTTAGCTAG
2607	AAAAGTGGAGCTCTCCTGAC
2631	TGCGGTGTCTGCGAACAGAA
2670	AATCTCCCCAAACCGGATGT
2692	CCAATTGCAACAGAGACTGG
2718	ATGCGCCTGCAACGCATTCCCGAAA
2748	AACCAGCGCCGTTCGGAGGATATAGA
2778	GCTGCTGATCCTTATGTAAATGC
2807	TTCCGGGCAATGAAGTAGAGGCAA
2839	TCGTAACCGAAAGGGACATCTG
2874	GAGAGCTTTGTGTGCGGTTCG
2905	GTTATAACCCATTGATGAAC
3763	AGACGATGTGGTCAGTATGGCA
3792	TCATGTGGATGTCGTGGAGCTT
3827	AGCAACAGGAAGTTGCTGCCAA
3856	CGCCCATGAAACTTTACAGAATCTC
3884	CCTATGAGTTCATCGTCGAAGTGG
3920	CTGCCTATGCATCTGTGTCAAA
4762	ACATGGTCAGACGGATGGGACAT
4789	TGGCATTCTGTGCGGAGCATTT
4812	TTCTGGCATTCTGTGCGGAGCATT
4848	CGTACCTTCTTTCCCAATAGCAAG
4875	GCTGCACTCCAGAGATTTACCA
-8390	ACCGGCATTGCTAGCGTCT
-8348	TGCTCCTCTAGTTGCGGAAATC
-8320	ATCGTCCATGTCCATATCCGCCT
-8308	CCGATCATTCTCATCGTCCATGTCCA
-8265	TAACCAAAGGTGCTGGCGGT
-8222	ATCTGACCAGCCACTTCGGT
-8190	TCTACAAACCCGCTCCGTTGGA
-11732	CGCTTTCTGCTCATCAAAGCAC
-11699	CTCCATGTTTCACCTCCCGTAT
-11686	TCCCAACTCTCTGCTCCATGTT
-11655	TAGCCCTCCATCGCCATCTGCAT
-11618	TCCATCGTTGTTCTGCCAAGCG

Table 5. Primer Sets Used for MNase Scanning Assay with Respect to the Transcription Start Site of *Hsp26*

5' Start location	Forward
-13	TGTCACTTTCCGGACTCTTCT
29	AAAGCAGCGTCGCTTGACGAACA
75	CGAGCAGTGAACAACTCAAAGC
110	AGCAAAACTTCAAACGAGAA
151	GCTTACAAGTCAAACAAGTTCATTC
196	ATTTCAATCTCGCAAAAGGAAC
241	TGTCGCTATCTACTCTGCTTTCGC
298	TCTACGAGCTTGGACTGGGATT
746	CAAGTCCAAGGAGCGCATCATTCA
766	TTCAAATTCAGCAAGTGGGACCCG
808	CAAATGAAAGCGAGGTGAAGGGCA
850	ACGGCAAGGACAAGTAAAGGAG
871	GCCATCATCATCCAACATCATCCA

5' Start location	Reverse
96	GCTTTGAGTTGTTCACTGCTCG
108	TTGCGCAAAGTTGCTTTGAGTTGT
169	ACTTGTTTGACTTGTAAGCAAAGGT
216	TTCCTTTTGCGAGATTGAAA
260	AAGCAGAGTAGATAGCGACATTTT
308	AAGCTCGTAGATGGGGCTGC
330	AATGCGGATGCAATCCCAGTCCAA
389	GCAAGGGCATCCGTTGATGGAA
831	TGCCCTTCACCTCGCTTTCATTTG
867	TTTACTTGTCCTTGCCGTTGGGTG
893	GGATGATGTTGGATGATGATGGCTCC
931	GCAATAAATTAGGAACAATTAAGTAGGG
956	GTCTTTAGCTCATTACAAATACAATGC

Table 6. Primer Sets Used for RT-qPCR

Gene	Forward
Hsp70	TGGACGAGGCTGACAAGAACT
Aurora	AAACTGCCGGAGCACATTTCCA

CG3281	ATGTCCCGGCTATGTGCTACAA
CG31211	ATGATCATGGCAGCAACCGTAG

Gene	**Reverse**
Hsp70	ACCGGATAGTGTCGTTGCACTT
Aurora	ATCCAAGGATGCACCATCACCT
CG3281	TTATTGCGATGGACGGTCAGGA
CG31211	TATGCTTTCGAGCTGGAGTGGT

Table 7. Primer Sets Used for ChIP of scs/scs'

Gene	**Forward**
Aurora	GTCACGATATTCTTCAACCAACCG
CG3281	ATCGGGCATCTCTGAACATCAGGT
CG31211	TCATATGAGCGACCCGCTGTTAC

Gene	**Reverse**
Aurora	TTGAATTGTGAAGCGGGCGTGT
CG3281	TGGATCTCCGGTGTGTCCATGATT
CG31211	TTCGTCGCCTTCTACGCCATTT

Table 8. Primer Sets Used for RNAi

Gene Name	**Forward**
LacZ	GAATTAATACGACTCACTATAGGGAGAGATATCCTGCTGATGAAGC
HSF	GAATTAATACGACTCACTATAGGGAGAGCCTTCCAGGAGAATGCA
GAF	GAATTAATACGACTCACTATAGGGATGGTTATGTTGGCTGGCGTCAA
CBP	GAATTAATACGACTCACTATAGGGATGGCAACATTCCAGCACCACT
Med15	GAATTAATACGACTCACTATAGGGATGCCGGCGTTATGGAGAACC
Med23	GAATTAATACGACTCACTATAGGGATCATTCGCCTCCGTCATCTCCAT
Gcn5	GAATTAATACGACTCACTATAGGGATAGGGATCCAGTTCCA

	GCATGAACGAGCTA
Tra1	GAATTAATACGACTCACTATAGGGACTTCACCTCTGTTTGCCACTGTTC
Spt3	GAATTAATACGACTCACTATAGGGATCACTGCTCACAGAGATTGCGGAT
Ubp8	GAATTAATACGACTCACTATAGGGACATATGCGCGCGTGTGTATGTGTT
PTEF-b (Cyclin T)	GAATTAATACGACTCACTATAGGGAGACGTGGTGGATATCCAGGC
Paf1	GAATTAATACGACTCACTATAGGGACGTAACTTCAAGTATGACGTGCTGACGG
FACT (Spt16)	GAATTAATACGACTCACTATAGGGAGCTGCGAGGCTGCCATTGGCG
Spt6	GAATTAATACGACTCACTATAGGGACCGTAACCCCGGTGCCCGAGG
Swi/Snf (Brm)	GAATTAATACGACTCACTATAGGGACAGACGTACTACAGCATCGCTCATAC
ISWI	GAATTAATACGACTCACTATAGGGAGCTATGGATCGTGCTCATCGTATTGGTC
Nurf301	GAATTAATACGACTCACTATAGGGAACGCCATCTGTCCCATAAGTTCTC
MI-2	GAATTAATACGACTCACTATAGGGAAGAAGAAACCTCGTCGTAAGCGCA
Chd1	GAATTAATACGACTCACTATAGGGAAGTGCGAAACCATAGAGCGTATCC
Kismet	GAATTAATACGACTCACTATAGGGAACTGGCGCCTTTGTGTGATTGATG
HIRA	GAATTAATACGACTCACTATAGGGATAGCGATTGCTGTTGCCTCAA
Asf1	GAATTAATACGACTCACTATAGGGATTTGTGCGAAGACAAGCGGA
PARP	GAATTAATACGACTCACTATAGGGATGATGCCTACTTCAGGTTTCGC
HDAC3	GAATTAATACGACTCACTATAGGGATGACATCGTCATCGGCATTCTGGA
Topo1	GAATTAATACGACTCACTATAGGGAAAGAGCAGCAGTTCGTCGTCAA
Topo2	GAATTAATACGACTCACTATAGGGATCAGCCAAGTCATTGGCCGTAT
TFIIH (ERCC3)	GAATTAATACGACTCACTATAGGGAACTGGTGGACGACAATGATACTTTGGATG
Beaf-32	GAATTAATACGACTCACTATAGGGATATTACCAAGGCCAAGACGCTGA
Zw5	GAATTAATACGACTCACTATAGGGATACACAAATGTCAAGCCGCACCA

Gene Name	Reverse
LacZ	GAATTAATACGACTCACTATAGGGAGAGCAGGAGCTCGTTATCGC
HSF	GAATTAATACGACTCACTATAGGGAGAGCTCGTGGATAACCGGTC
GAF	GAATTAATACGACTCACTATAGGGATCTTTACGCGTGGTTTGCGT
CBP	GAATTAATACGACTCACTATAGGGATCTGGACTTGGCCATTTCGT
Med15	GAATTAATACGACTCACTATAGGGAGGCATTTACGTTCATTGGTC
Med23	GAATTAATACGACTCACTATAGGGACAAGGTGCTGATGTGCGAGAAAC
Gcn5	GAATTAATACGACTCACTATAGGGATCACCCACACTGGTCCTCTTGTTT
Tra1	GAATTAATACGACTCACTATAGGGATGACAAGCGGACCGGAACTGTAA
Spt3	GAATTAATACGACTCACTATAGGGAAATCTTACGGCTGCTCATTTGCCG
Ubp8	GAATTAATACGACTCACTATAGGGATTTGATAGTGCCGACAACCCGTCT
PTEF-b (Cyclin T)	GAATTAATACGACTCACTATAGGGAGAGGGCCCACTAGCCAAACTGG
Paf1	GAATTAATACGACTCACTATAGGGAGTTGTACTCTCGAGCGATCTTGTACTCG
FACT (Spt16)	GAATTAATACGACTCACTATAGGGACAGCTCGCGCTGTGCTCCTTGC
Spt6	GAATTAATACGACTCACTATAGGGAGGCTCTTGTGCCAGCTGTCGG
Swi/Snf (Brm)	GAATTAATACGACTCACTATAGGGAGACGACGAATGATAAGGATGCTCTCC
ISWI	GAATTAATACGACTCACTATAGGGAGATTCTCCTTCTCCTGGATCTCTTCCTC
Nurf301	GAATTAATACGACTCACTATAGGGAAGAAGCCATCTGCTCCTCGAC
MI-2	GAATTAATACGACTCACTATAGGGATGATCTTCTCAGCCTTGCCAGTGA
Chd1	GAATTAATACGACTCACTATAGGGAATCACCGAGTTCTCCTTGCACCAT
Kismet	GAATTAATACGACTCACTATAGGGACACCAGCTTTGGTGCAAAGGAGAA
HIRA	GAATTAATACGACTCACTATAGGGATAAAGGCGCAATGCAC

	TGCAGAA
Asf1	GAATTAATACGACTCACTATAGGGATAAAGAGGCTTTGTTG GCGGGTT
PARP	GAATTAATACGACTCACTATAGGGATTGGCACTATGCATGC CGATCT
HDAC3	GAATTAATACGACTCACTATAGGGAAATCGGGCTTGTCTTG GTCCTGAT
Topo1	GAATTAATACGACTCACTATAGGGATCGTCGTCATCGTCGTT ATCCA
Topo2	GAATTAATACGACTCACTATAGGGAATGGAGCGCTCATTGT CAGCAT
TFIIH (ERCC3)	GAATTAATACGACTCACTATAGGGACCCGAATTGAGTAATA GCCTTGCC
Beaf-32	GAATTAATACGACTCACTATAGGGATACGACACGCTGATTT GCCCATT
Zw5	GAATTAATACGACTCACTATAGGGATACAGCACCATCACCA CTTTGGA

CHAPTER 3 ACTIVATOR INDUCED SPREAD OF POLY(ADP-RIBOSE) POLYMERASE PROMOTES NUCLEOSOME LOSS AT *HSP70*[3]

Eukaryotic cells possess many transcriptionally regulated mechanisms to alleviate the nucleosome barrier. Dramatic changes to the chromatin structure of *Drosophila melanogaster Hsp70* gene loci are dependent on the transcriptional activator, Heat shock factor (HSF), and Poly(ADP-ribose) polymerase (PARP). Here I find that PARP is associated with the 5' end of *Hsp70*, and its enzymatic activity is rapidly induced by heat shock. This activation causes PARP to redistribute throughout *Hsp70* loci and Poly(ADP-ribose) to concurrently accumulate in the wake of PARP's spread. HSF is necessary for both the activation of PARP's enzymatic activity and its redistribution. Upon heat shock, HSF triggers these PARP activities mechanistically by directing Tip60 acetylation of histone H2A lysine 5 at the 5' end of *Hsp70* where inactive PARP resides before heat shock. This acetylation is critical for the activation and spread of PARP as well as for the rapid nucleosome loss over the *Hsp70* loci.

3.1 INTRODUCTION

Packaging of eukaryotic DNA into the nucleus relies on compaction of DNA into nucleosomes and higher order chromatin structures. Consequently, critical DNA sequences can be occluded from proteins that function by accessing particular DNA elements. Transcription is one such nuclear process

[3] Taken from (Petesch and Lis, 2012a)

that can be significantly inhibited by the barriers created by nucleosomes. In vitro studies demonstrate that nucleosomes are sufficient to block transcription initiation and also impair efficient transcription elongation by RNA Polymerase II (Pol II) (Knezetic and Luse, 1986; Lorch et al., 1987). Genome-wide, in vivo studies demonstrate that nucleosome disruption and turnover is greatest at the most highly transcribed mRNA encoding genes (Deal et al., 2010). These results indicate that eukaryotic cells possess mechanisms to alleviate the nucleosomal barrier to efficiently transcribe genes.

Addressing how Pol II traverses the nucleosome has resulted in the discovery of unique features of transcriptional regulation. Eukaryotes utilize five general mechanisms to change the occupancy, position, structure, or composition of nucleosomes. First, chromatin-remodeling complexes change the position and occupancy of nucleosomes through their ability to slide entire nucleosomes as well as remove or transfer individual histones (Saha et al., 2006). Second, histone chaperones facilitate transcription by the disassembly and reassembly of nucleosomes in the path of Pol II (Das et al., 2010). Third, the composition of individual histones are changed by the numerous post-translational modifications including acetylation, methylation, phosphorylation, ubiquitination, and sumoylation which can either directly affect chromatin structure or promote association of chromatin binding proteins (Taverna et al., 2007). Fourth, canonical core histones can be replaced by histone variants, like H2A.Z, which can change both the composition and structure of chromatin (Talbert and Henikoff, 2010). Lastly, many other non-histone proteins that bind

to nucleosomes or naked DNA can synergize or compete with nucleosomes to affect position, occupancy, structure, and composition (Gilchrist et al., 2010; Saunders et al., 2006).

Model inducible gene systems continue to elaborate the many ways in which these five methods are utilized to coordinate transcription-coupled nucleosome changes and thereby regulate changes in gene expression (Weake and Workman, 2010). The *D*. *melanogaster* heat shock (HS) inducible *Hsp70* genes employ these methods (Saunders et al., 2006) as well as an additional method that leads to rapid loss of nucleosomes extending beyond the *Hsp70* gene to the flanking scs and scs' insulator elements (Petesch and Lis, 2008). Interestingly, the nucleosome loss that occurs within the first minute of HS can be uncoupled from active transcription of *Hsp70*, whereas the additional changes in nucleosome structure by 2 minutes of HS are dependent on transcription. A directed RNAi screen identified both Heat shock factor (HSF) as well as Poly(ADP-ribose) polymerase (PARP) as factors necessary for both transcription-independent and dependent nucleosome loss during HS (Petesch and Lis, 2008). Although both HSF and PARP have been identified to bring about a rapid change in the entire HS locus independently of transcription, the mechanism through which these proteins accomplish this feat is still unknown.

HSF is the master regulatory protein of HS genes and acts as a traditional transcriptional activator of HS genes. Within seconds of HS, HSF trimerizes and binds to a specific HS DNA element (HSE) repeated multiple

times within the promoter of *Hsp70* (Boehm et al., 2003). Activated HSF is thought to increase transcription by recruiting transcriptional coactivators such as the mediator complex, P-TEFb, and histone acetyltransferases (HATs) (Lis et al., 2000; Park et al., 2001; Smith et al., 2004). These coactivators are thought to facilitate transcription by regulating additional recruitment and initiation of Pol II, releasing paused Pol II, or altering the structure and composition of nucleosomes to enhance Pol II elongation. It is yet to be determined if HSF-mediated, transcription-independent nucleosome loss is also achieved through a coactivator and what, if any, are the connections between HSF, coactivators, and PARP.

PARP is an enzyme well studied for its function in DNA repair, apoptosis, transcriptional regulation, as well as altering chromatin structure (Krishnakumar and Kraus, 2010a; Rouleau et al., 2010). PARP's enzymatic activity uses NAD^+ donor molecules to catalyze the polymerization of Poly(ADP-ribose) (PAR) onto acceptor proteins as a post-translational modification. The Zn fingers of PARP bind to many aberrant DNA structures, especially broken DNA, but also bind to nucleosomes (Kim et al., 2004; Krishnakumar and Kraus, 2010a). Damaged DNA, individual histones, and polynucleosomes can activate the enzymatic activity of PARP (Kim et al., 2004; Pinnola et al., 2007). In vivo, PARP primarily targets itself, although other proteins, including histones, are also known to be substrates of PARylation (D'Amours et al., 1999). Even though PARP is also able to affect transcription independently of its enzymatic activity at some genes (Hassa et

al., 2001; Pavri et al., 2005), the catalytic activity of PARP is known to be able to affect transcription at many genes, including *Hsp70* (Ju et al., 2006; Krishnakumar and Kraus, 2010b; Tulin and Spradling, 2003). PARP and its catalytic activity are necessary for decompaction of chromatin structure at HS loci as well as transcription-independent nucleosome loss at *Hsp70* (Petesch and Lis, 2008; Tulin and Spradling, 2003). Although formation of PAR is necessary to bring about changes in chromatin structure at HS loci, little is known about how PARP is activated at *Hsp70* and, more so, how this activation can lead to nucleosome loss over such a broad domain.

Here, I map the immediate kinetic changes that occur to PARP and its catalytic product, PAR, at *Hsp70* loci immediately following HS. I observe that PARP colocalizes with the first 2 nucleosomes at the beginning of the *Hsp70* transcription unit before HS. Upon HS, PARP spreads rapidly throughout the *Hsp70* gene and beyond, to the scs' insulator element, with kinetics similar to those previously measured to track changes in chromatin structure. The activation of PARP leads to accumulation of PAR throughout the locus in the wake of spreading PARP. Additionally, I find that HSF is necessary for both the activation and spread of PARP at *Hsp70* following HS and triggers these changes by altering the level of histone acetylation at the site where PARP is found prior to HS. Finally, I identify *Drosophila* Tip60 (dTip60) as the HAT responsible for increasing acetylation of histone H2A lysine 5 at *Hsp70* following HS. This increase in acetylation induces the activation and spread of PARP and a resulting nucleosome loss that is independent of transcription.

3.2 RESULTS

3.2.1 PARP Rapidly Redistributes along *Hsp70* upon Heat Shock

To investigate potential mechanisms by which PARP is able to bring about rapid and drastic changes in chromatin structure at the *Hsp70* gene loci upon heat shock (HS), I first examined PARP's location on *Hsp70* before and in the seconds following HS using chromatin immunoprecipitation (ChIP). In my assay, *Drosophila* S2 cells are instantaneously heat shocked, cooled, and immediately crosslinked with formaldehyde for durations previously used to characterize changes in nucleosomes (Petesch and Lis, 2008). The immunoprecipitated DNA was measured using quantitative PCR (qPCR) with 25 primer sets spaced, on average, 200 base pairs (bp) apart to canvas the *Hsp70* HS loci from the *Hsp70Ab* promoter to the scs' insulator element (Figure 25A).

Prior to HS, PARP is bound to the *Hsp70* gene downstream of the transcription start site (TSS) (Figure 25A, dark blue), and overlaps with the previously mapped position of the first 2 well-protected nucleosomes at *Hsp70* (Petesch and Lis, 2008). These results are consistent with those studies in *Drosophila* that detect PARP present at the *Hsp70* HS loci (Kotova et al., 2011; Tulin and Spradling, 2003; Zobeck et al., 2010) and studies in humans that show PARP concentrates on regions near the TSS (Krishnakumar et al., 2008). Within 5 seconds of HS (Figure 25A, light blue) PARP begins to be lost from its site occupied prior to HS, and decreases monotonically by 30, 60, and

Figure 25 PARP Rapidly Redistributes Across the *Hsp70* Heat Shock Locus upon Heat Shock

(A) Kinetic ChIP analysis of PARP at the *Hsp70Ab* HS locus. S2 cells are heat shocked for 0 (dark blue), 5 (light blue), 30 (green), 60 (orange), or 120 seconds (red). 25 primer sets, spaced approximately 200 bp apart provide high spatial resolution. The y-axis represents the percent of input material immunoprecipitated. The x-axis corresponds to base pair units with 0 being the TSS. Error bars represent the SEM of 3 independent experiments. The diagram below depicts the *Hsp70Ab* locus, noting the sites of the HSEs, its TSS, the PolyA site (+2343), the downstream gene, *CG3281*, and the site of the scs' insulator element. The diagram is on the same scale as the x-axis. Each subsequent figure labeled as ChIP will be for the *Hsp70Ab* HS locus and contains the same error bars, y-axis, and x-axis that corresponds to the diagram depicted.

(B) The amount of PARP detected by ChIP at the *Hsp70Ab* HS locus stays constant during the first 2 minutes of HS. The ChIP values for each of the 5 HS time points were integrated across the region depicted in (A) using the 25 percent input values as points to trapezoids. Each sum was normalized back to the NHS summation and plotted on the y-axis. The x-axis represents the elapsed time following HS in seconds. Error bars represent the propagated error associated with the summation of the SEM of each percent input.

(C) ChIP of PARP in the presence of PJ34, a catalytic inhibitor of PARP. Untreated NHS (dark blue) and 2' HS (red) S2 cells are compared to those NHS (light blue) and 2' HS (pink) cells pretreated with 300 nM PJ34 for 10 minutes. Error bars represent the SEM of 3 independent experiments.

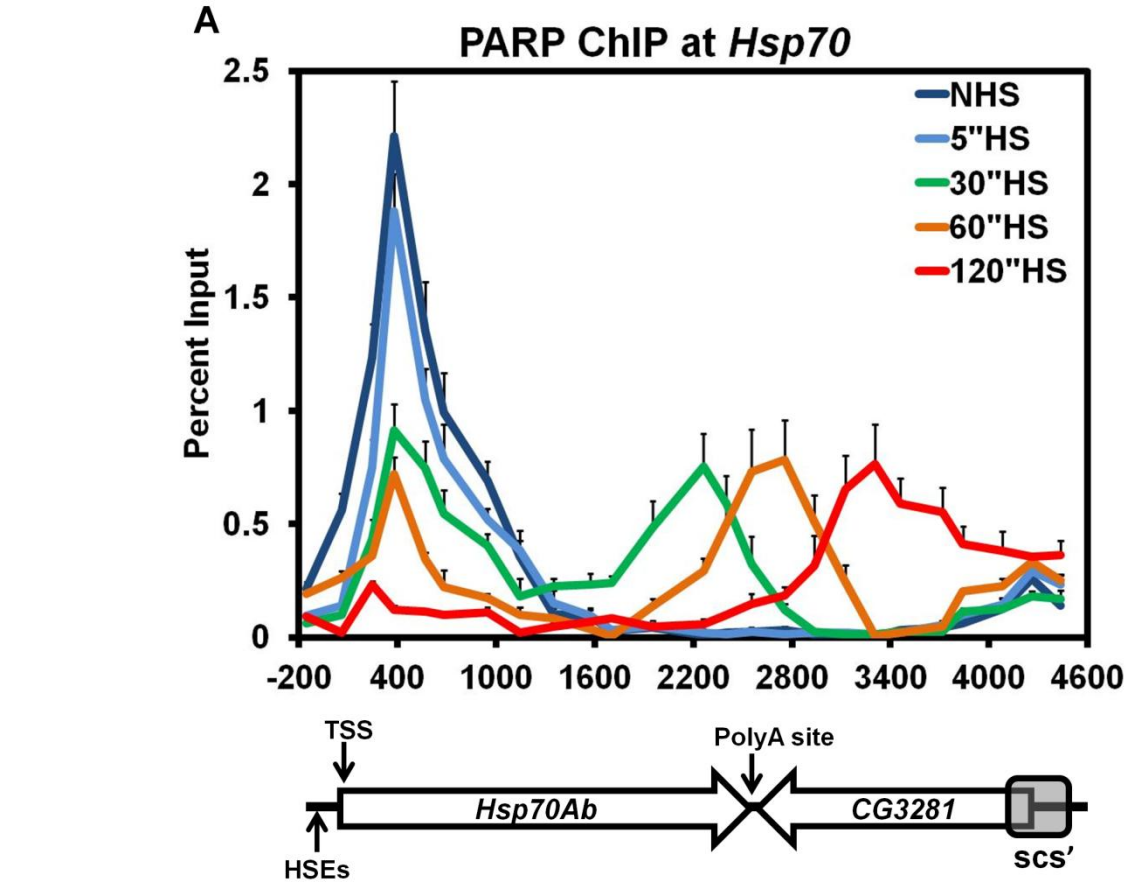
A
PARP ChIP at Hsp70
Percent Input
2.5
2
1.5
1
0.5
0
NHS
5"HS
30"HS
60"HS
120"HS
-200 400 1000 1600 2200 2800 3400 4000 4600
TSS
PolyA site
Hsp70Ab
CG3281
HSEs
SCS'

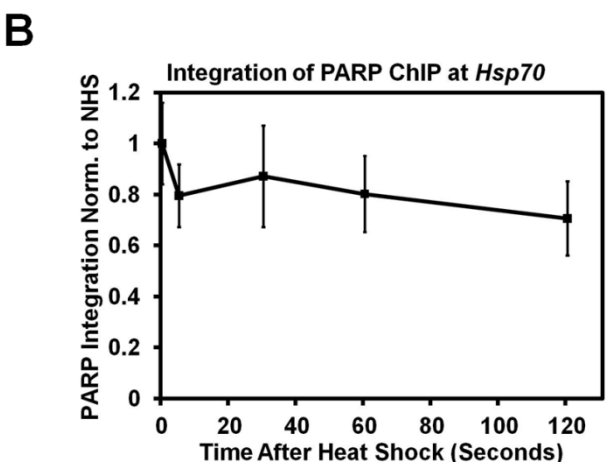
B
Integration of PARP ChIP at Hsp70
PARP Integration Norm. to NHS
1.2
1
0.8
0.6
0.4
0.2
0
0 20 40 60 80 100 120
Time After Heat Shock (Seconds)

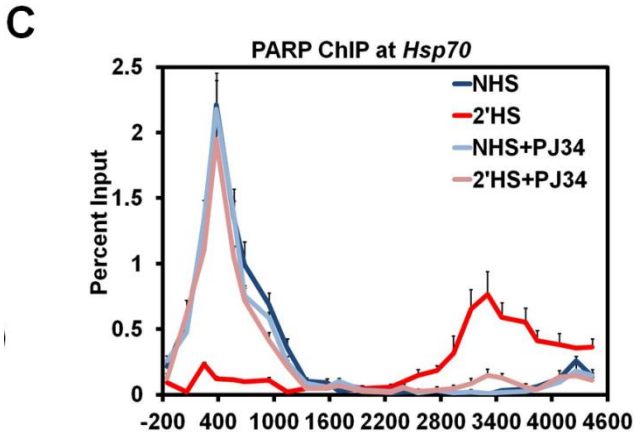
C
PARP ChIP at Hsp70
Percent Input
2.5
2
1.5
1
0.5
0
NHS
2'HS
NHS+PJ34
2'HS+PJ34
-200 400 1000 1600 2200 2800 3400 4000 4600

120 seconds of HS (Figure 25A, green, orange, and red respectively). Interestingly, the rate of PARP loss from this region mirrors the rate of nucleosome loss previously measured at this region. More surprising is the transient accumulation of detectable PARP ChIP signal progressively further downstream by 30, 60, and 120 seconds of HS, extending all the way to the scs' insulator element. These results can be explained by two simple models: 1) local PARP molecules are lost and new PARP is recruited to downstream sites after HS or 2) pre-bound PARP rapidly spreads across the *Hsp70* gene loci upon HS.

Previous live cell imaging experiments of PARP at *Hsp70* during HS show that the total amount of PARP at the loci, both unbound and bound to chromatin, remains unchanged from the non heat shock (NHS) state (Zobeck et al., 2010). To determine if the amount of PARP associated with the chromatin at the *Hsp70Ab* locus remains constant throughout the HS time course, I took the integral of each PARP ChIP time point curve (Figure 25B). The level of total PARP ChIP signals for 5, 30, 60, and 120 seconds of HS does not significantly change from the NHS time point. This is in contrast to most factors which progressively accumulate at *Hsp70* loci following the first few minutes of HS (Boehm et al., 2003). Together these experiments are consistent with a model in which PARP is pre-bound to the *Hsp70* loci before HS and this pre-bound PARP rapidly redistributes upon HS.

Since PARP's catalytic activity is necessary for the changes in chromatin structure that occur at *Hsp70* upon HS (Petesch and Lis, 2008), I

Figure 26 PARP is Not Necessary for HSF Recruitment to *Hsp70* Following Heat Shock and the PARP ChIP signal is Specific for dPARP

(A) Western blot confirming the RNAi knockdown of PARP. A serial dilution of the LacZ RNAi control cells were used to help measure the extent of PARP knockdown, shown in the last lane, with 100% equivalent to $5x10^6$ cells. The top panel shows the immunoblot of PARP and bottom panel shows the immunoblot of TFIIS as a loading control.

(B) Western blot showing the specificity of the N-terminal PARP antibody. Increasing amounts of full length, purified His-tagged *Drosophila* PARP (~115 kDa) was loaded in increasing amounts (10, 100, 1000 ng) from left to right and compared to a dilution of LacZ RNAi cells and PARP RNAi cells, with 100% equivalent to $5x10^6$ cells. The antibody is also capable of recognizing the first 43.6 kDa of a His-tagged recombinantly purified N-terminal truncation of *Drosophila* PARP shown in decreasing amounts in the final 3 lanes (1000, 100, 10 ng). The top panel shows the immunoblot of PARP and bottom panel shows the immunoblot of TFIIS as a loading control for the central 3 lanes.

(C) ChIP of PARP at the *Hsp70Ab* HS locus in PARP knockdown cells. S2 cells RNAi depleted of PARP are heat shocked for either 0 (light blue) or 2 minutes (pink) and compared to those LacZ RNAi NHS (dark blue) and 2' HS (red) cells. Error bars represent the SEM of 3 independent experiments.

(D) ChIP of HSF at *Hsp70* in PARP knockdown and PJ34 treated cells. S2 cells RNAi depleted of LacZ or PARP or treated with 300 nM PJ34 are heat shocked for either 0 (dark blue, medium blue, or light blue, respectively) or 2 minutes (red, pink, or dark pink, respectively). The y-axis represents the percent of input material immunoprecipitated. The x-axis represents the center of the PCR amplicons in base pair units with 0 being the TSS of *Hsp70* and -154 located at the promoter, 58 at the pause site, and 1702 in the body of the gene. Error bars represent the SEM of 3 independent experiments.

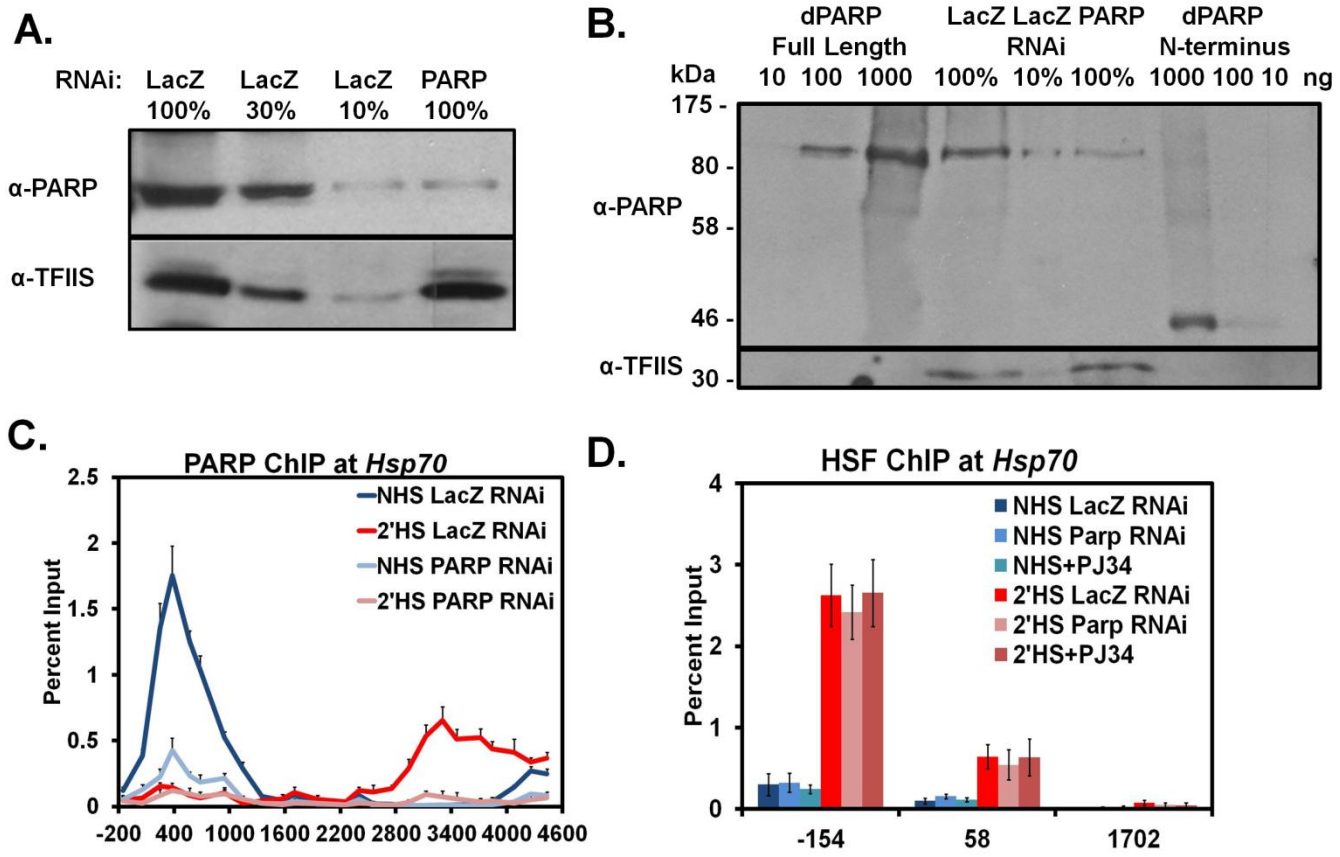
A.
RNAi: LacZ LacZ LacZ PARP
100% 30% 10% 100%
α-PARP
α-TFIIS
B.
dPARP Full Length
LacZ LacZ PARP RNAi
dPARP N-terminus
kDa
10 100 1000 100% 10% 100% 1000 100 10 ng
175 -
80 -
58 -
46 -
30 -
α-PARP
α-TFIIS
C.
PARP ChIP at Hsp70
Percent Input
NHS LacZ RNAi
2'HS LacZ RNAi
NHS PARP RNAi
2'HS PARP RNAi
2.5
2
1.5
1
0.5
0
-200 400 1000 1600 2200 2800 3400 4000 4600
D.
HSF ChIP at Hsp70
Percent Input
NHS LacZ RNAi
NHS Parp RNAi
NHS+PJ34
2'HS LacZ RNAi
2'HS Parp RNAi
2'HS+PJ34
4
3
2
1
0
-154
58
1702

tested whether PARP's enzymatic activity was also required for rapid loss and redistribution of PARP upon HS. S2 cells treated with PJ34, a catalytic inhibitor of PARP, did not alter the position or level of PARP present at the *Hsp70* gene before HS, indicating that PARP is bound to the *Hsp70* promoter independently of its catalytic activity (Figure 25C). Treatment with PJ34 for 10 minutes prior to a 2 minute HS prevented PARP redistribution. The loss of PARP from its NHS site upon HS is consistent with *in vitro* data showing that PARP binds to chromatin through its DNA binding domain and dissociates following activation of its catalytic domain (Kim et al., 2004; Poirier et al., 1982; Wacker et al., 2007).

3.2.2 PAR Rapidly Accumulates in the Wake of PARP and Tethers PARP to the Locus following Heat Shock

As the catalytic activation of PARP is necessary for the loss and redistribution of PARP along the *Hsp70Ab* locus, I employed the same kinetic ChIP assay outlined in Figure 25 to track the changes in PAR. Prior to HS, PAR is absent from *Hsp70* (Figure 27A, dark blue); immediately following 5 seconds of HS, PAR begins to accumulate at the 5' end of *Hsp70* (Figure 27A, light blue). Interestingly, the initial site of PAR polymerization overlaps with PARP's position before HS. By 30, 60, and 120 seconds of HS, PAR monotonically increases at the 5' end of *Hsp70* and, more surprisingly, accumulates further downstream until it reaches the scs' insulator element by120 seconds of HS (Figure 27A, green, orange, and red respectively). As

Figure 27 PAR Rapidly Accumulates Across the *Hsp70* Heat Shock Locus Upon Heat Shock

(A) Kinetic ChIP analysis of PAR at the *Hsp70Ab* HS locus as in Figure 25A. S2 cells are heat shocked for 0 (dark blue), 5 (light blue), 30 (green), 60 (orange), or 120 seconds (red). Error bars represent the SEM of 3 independent experiments for all 4 panels

(B) ChIP of PAR in the presence of the catalytic inhibitor of PARP, PJ34. Untreated NHS (dark blue) and 2' HS (red) S2 cells are compared to NHS (light blue) and 2' HS (pink) cells pretreated with 300 nM PJ34 for 10 minutes.

(C) ChIP of PAR at the *Hsp70Ab* HS locus with PARG digestion. ChIP extracts prepared for PAR IP were treated with 1200 nM of purified recombinant rat PARG (rPARG) prior to IP with either NHS (light blue) or 2' HS samples (pink). These values were compared to control NHS (medium blue) or 2' HS (dark red) samples that were mock treated at 37 °C for 30 minutes. The values of the mock treatment were not significantly different from those obtained without any additional treatment for NHS (dark blue) or 2' HS (red).

(D) ChIP for PARP with rPARG digestion as in (C).

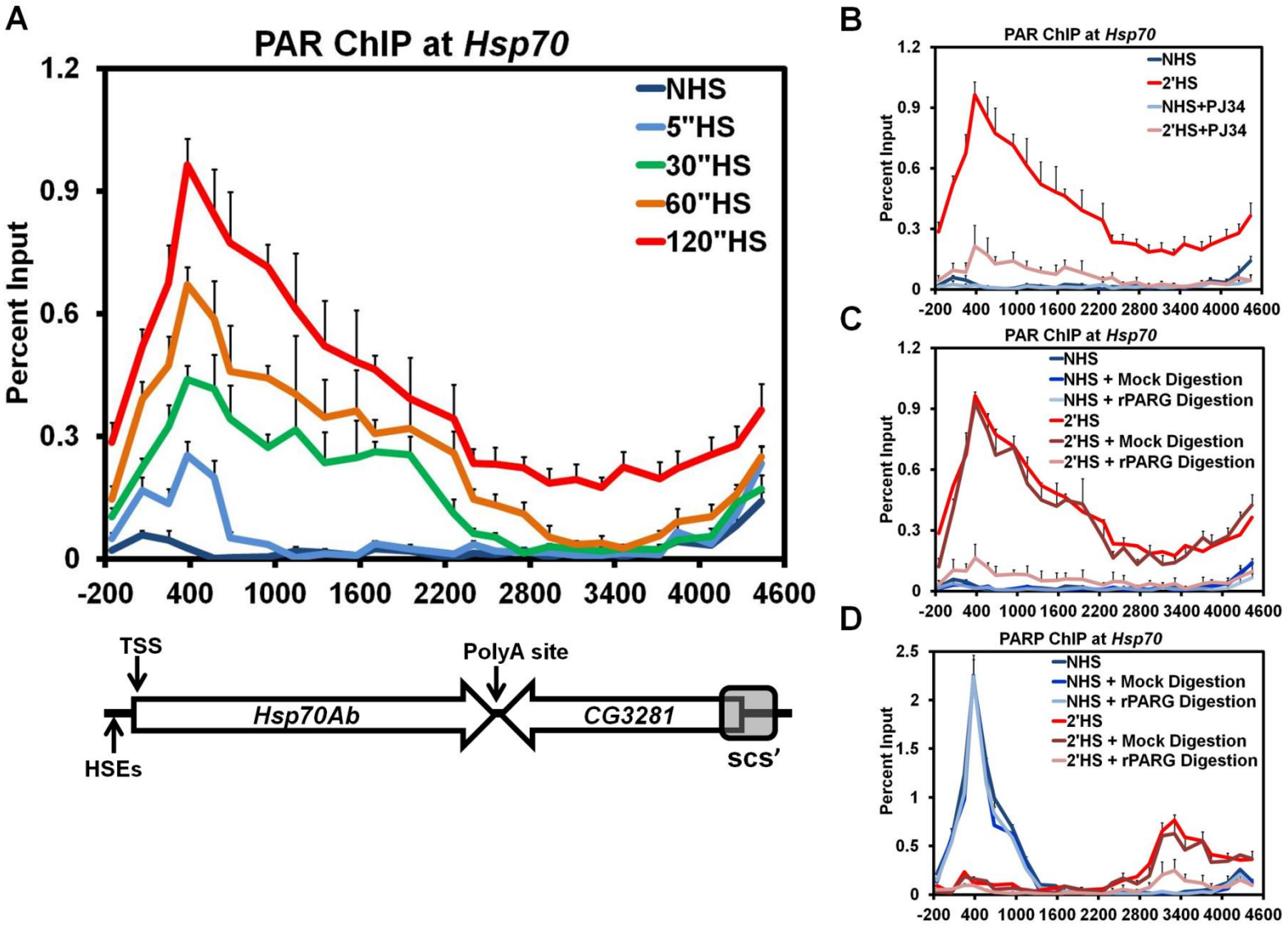
A
PAR ChIP at Hsp70
Percent Input
NHS
5"HS
30"HS
60"HS
120"HS
TSS
PolyA site
Hsp70Ab
CG3281
HSEs
SCS'
B
PAR ChIP at Hsp70
NHS
2'HS
NHS+PJ34
2'HS+PJ34
C
PAR ChIP at Hsp70
NHS
NHS + Mock Digestion
NHS + rPARG Digestion
2'HS
2'HS + Mock Digestion
2'HS + rPARG Digestion
D
PARP ChIP at Hsp70

expected, the accumulation of PAR at *Hsp70* after HS is dependent on both PARP and PARP's catalytic activity (Figures 28A and 27B). The position of PARP before HS and its downstream position by 30, 60, and 120 seconds of HS bookends the region of PAR accumulation at the corresponding time point of HS. These kinetic results demonstrate that PAR accumulates in the wake of PARP spreading along the *Hsp70Ab* locus.

Two non-mutually exclusive models can explain the results from the kinetic ChIP analysis of PARP and PAR. The first model asserts that PARP progressively modifies the underlying histones, or another component of chromatin, that fall within its path and cross-linking during ChIP captures PARP directly interacting with chromatin. The second model asserts that activated PARP modifies itself and the polymerization of PAR results in continuously further reaching contacts with distal chromatin and cross-linking captures PARP bridged indirectly to chromatin through PAR.

To test these two models, I purified recombinant Poly(ADP-ribose) glycohydrolase (PARG) and confirmed its ability to cleave PAR in ChIP extracts from cross-linked cells (Figure 28B). ChIP for PAR after PARG treatment of cross-linked material, in comparison to the mock treated samples, confirmed catabolism of PAR at *Hsp70* (Figure 27C). ChIP for PARP with PARG treated extracts resulted in no change in the ChIP signal under NHS conditions (Figure 27D), supporting the conclusion that PARP bound to the 5' end of *Hsp70* before HS is inactive and directly bound to chromatin. However, when 2 minute HS samples were treated with PARG the level of PARP ChIP

Figure 28 Accumulation of PAR at *Hsp70* is Dependent on PARP and rPARG is able to Metabolize PAR from ChIP Extracts

(A) ChIP of PAR at the *Hsp70Ab* HS locus in PARP knockdown cells. S2 cells RNAi depleted of PARP are heat shocked for either 0 (light blue) or 2 minutes (pink) and compared to those LacZ RNAi NHS (dark blue) and 2'HS (red) cells. Error bars represent the SEM of 3 independent experiments.

(B) Titration of the amount of purified recombinant, purified rat 6xHis-PARG (rPARG) using ChIP extracts. Western blots of sonicated ChIP extracts mock treated (first 3 lanes) or those treated with various amounts of rPARG (last 5 lanes) for 30 minutes at 37 °C to titrate the amount of rPARG needed to digest the bulk PAR. The first three panels are a serial dilution of the mock treated sample to help quantify the extent of digestion, with 100% of the input corresponding to $2.5x10^6$ S2 cells. The last five lanes contain the same amount of ChIP extracts as in lane 1 but varying amounts of rPARG, from 1200, 600, 300, 150, to 0 nM. Top panel: immunoblot of PAR showing the PAR signal associated with bands migrating at the molecular weight of PARP (~114 kDa). Middle panel: immunoblot for 6x-His to detect the amount of rPARG added to the ChIP extract. Bottom panel: immunoblot of TFIIS as a loading control.

(C) ChIP of PARP at the *Hsp70Ab* HS locus with PARG digestion. ChIP extracts prepared for PARP IP were treated with mock treatment or with 1200 nM of rPARG prior to IP with either NHS (light blue) or 30" HS samples (pale green-yellow). These values were compared to control NHS (medium blue) or 30" HS (dark green) samples that were mock treated at 37 °C for 30 minutes. The values of the mock treatment were not significantly different from those obtained without any additional treatment for NHS (dark blue) or 30" HS (bright green). Error bars for the mock and rPARG treated samples represent the SEM of 3 independent experiments. Error bars represent the SEM of 3 independent experiments.

(D) PARP's movement follows a constant rate of three-dimensional expansion at *Hsp70Ab*. The average distance of movement (from the center of the peak of PARP) was measured in base pairs for each time point and then subtracted from the NHS value. No significant difference was found between the 0 and 5 second time point. The distance between the 0 (+480) and the 30 (+2230), 60 (+2820), and 120 (+3400) second time points were used as a first order measure of linear distance. The base pair units were converted to nanometer distances by the fact that 1 base pair of DNA measures 0.34 nm. As the DNA is compacted into chromatin, the values were also divided by a compaction ratio of 10, typical of most 10-30 nm chromatin fibers. (Linear distances are plotted in Fig S2E, which shows a non-linear relationship versus time.) The

nanometer distances were then cubed and plotted on the y-axis to model the volume encompassed in μm^3. The x-axis represents the time elapsed following HS in seconds. The error bars represent the propagated error in volume from the SEM of each percent input used in measuring the average base pairs of movement.

(E) The average distance of movement in base pairs was measured for each time point and then subtracted from the NHS value. The distance between the 0 (+480) and the 30 (+2230), 60 (+2820), and 120 (+3400) second time points were first converted to nanometer distances by the fact that 1 base pair of DNA measures 0.34 nm. Since this DNA is compacted into chromatin, the value was also adjusted by a compaction ratio of 10, typical of most 10-30 nm chromatin fibers. The y-axis represents the linear distance traveled in μm. The x-axis represents the time following HS in seconds. The error bars represent the propagated error from the SEM of each percent input used in measuring the average base pairs of movement. The linear R^2 value is depicted on the graph.

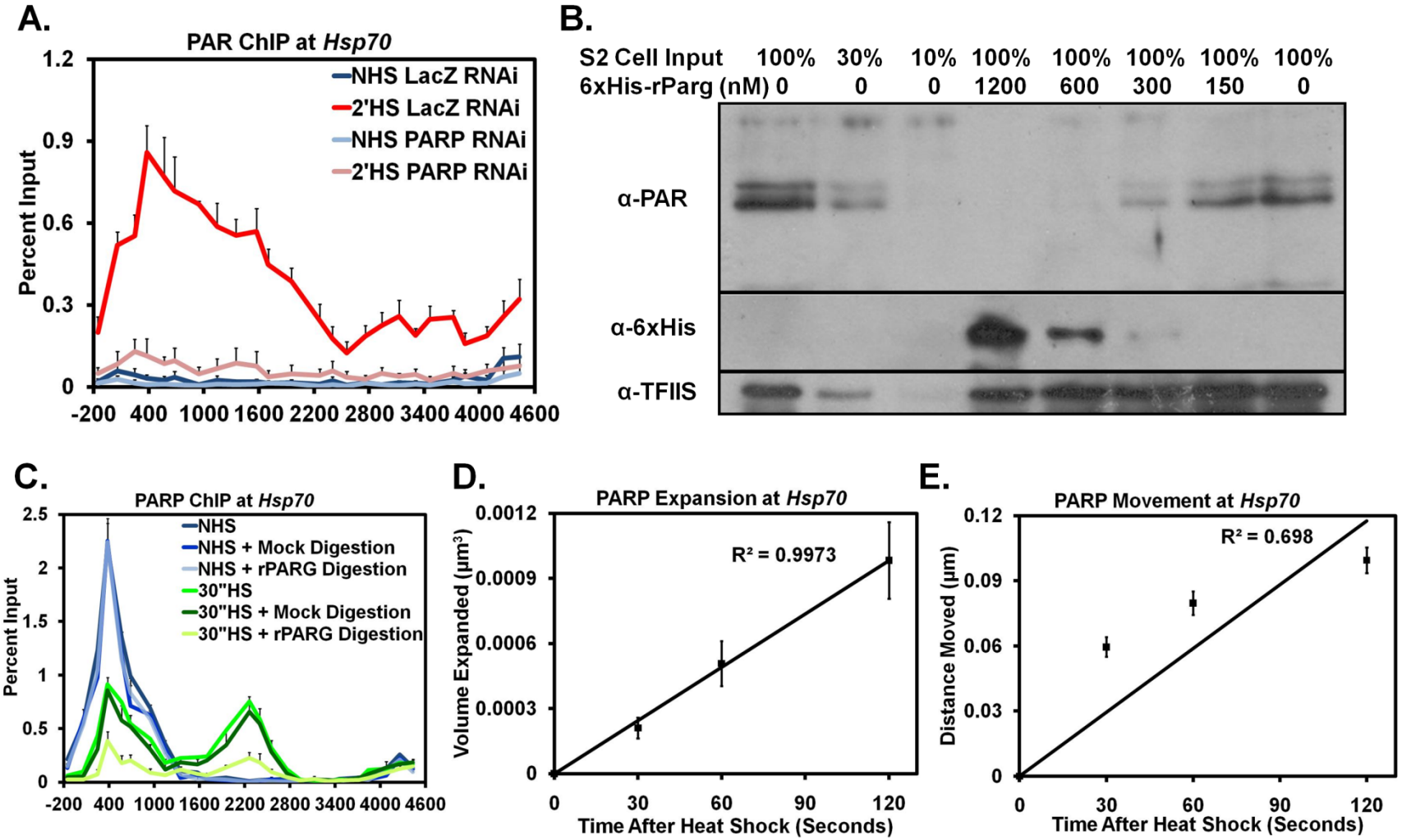
A.
PAR ChIP at Hsp70
Percent Input
1.2
0.9
0.6
0.3
0
-200 400 1000 1600 2200 2800 3400 4000 4600
NHS LacZ RNAi
2'HS LacZ RNAi
NHS PARP RNAi
2'HS PARP RNAi
B.
S2 Cell Input 100% 30% 10% 100% 100% 100% 100% 100%
6xHis-rParg (nM) 0 0 0 1200 600 300 150 0
α-PAR
α-6xHis
α-TFIIS
C.
PARP ChIP at Hsp70
Percent Input
2.5
2
1.5
1
0.5
0
-200 400 1000 1600 2200 2800 3400 4000 4600
NHS
NHS + Mock Digestion
NHS + rPARG Digestion
30"HS
30"HS + Mock Digestion
30"HS + rPARG Digestion
D.
PARP Expansion at Hsp70
Volume Expanded (μm³)
0.0012
0.0009
0.0006
0.0003
0
R² = 0.9973
0 30 60 90 120
Time After Heat Shock (Seconds)
E.
PARP Movement at Hsp70
Distance Moved (μm)
0.12
0.09
0.06
0.03
0
R² = 0.698
0 30 60 90 120
Time After Heat Shock (Seconds)

decreased in comparison to the mock treated sample (Figure 27D, pink compared to dark red). These results indicate that PARP detected by ChIP downstream during HS arises from cross-links that capture PAR bridging the interaction between PARP and chromatin and not from a direct interaction with the chromatin. Similar results are also found after 30 seconds of HS (Figure 28C). These results are additionally supported by the kinetics of PARP's redistribution more closely correlating with a constant rate of expansion in 3 dimensions (Figure 28D) rather than a 1-dimensional movement along the chromatin fiber (Figure 28E).

3.2.3 HSF is Necessary for Activation and Spread of PARP Following Heat Shock

My initial RNAi screen for factors that affected the loss of chromatin structure at *Hsp70* identified both PARP and HSF as critical components in both the transcription-dependent and independent changes that occurred following HS (Petesch and Lis, 2008). To determine if these two factors were working together in an ordered pathway, I RNAi depleted either HSF or PARP and used ChIP to assay if the other factor was affected. When PARP was either depleted or inhibited, the recruitment of HSF to the promoter of *Hsp70* following HS was not affected (Figures 26A-D). In contrast, HSF knockdown (Figures 29A and 30) prevented the redistribution (Figure 29B) and activation (Figure 29C) of PARP at *Hsp70* following HS, but not PARP deposition prior to HS. These results order a mechanism whereby HSF recruitment to *Hsp70*

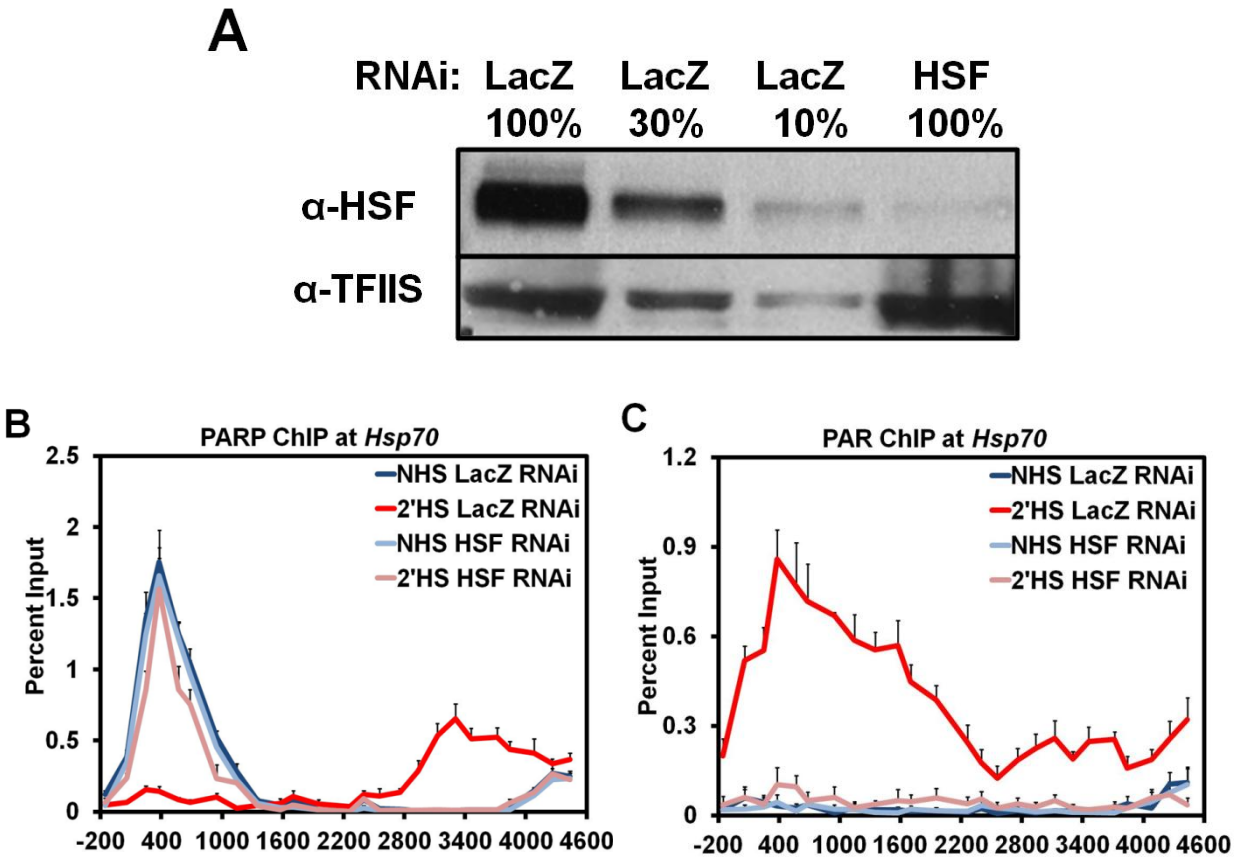

Figure 29 HSF is Necessary for the Activation and Redistribution of PARP at the *Hsp70* Heat Shock Locus Following Heat Shock

(A) Western blot confirming the RNAi knockdown of HSF. A serial dilution of the LacZ RNAi control cells were used to quantify the extent of HSF knockdown, shown in the last lane, with 100% equivalent to $5x10^6$ cells. The top panel shows the immunoblot of HSF and bottom panel shows the immunoblot of TFIIS as a loading control.

(B) ChIP of PARP at the *Hsp70Ab* HS locus in HSF RNAi cells. S2 cells RNAi depleted of HSF are heat shocked for either 0 (light blue) or 2 minutes (pink) and compared to those LacZ RNAi NHS (dark blue) and 2' HS (red) cells. Error bars represent the SEM of 3 independent experiments for (B) and (C).

(C) ChIP of PAR at the *Hsp70Ab* HS locus in HSF RNAi cells as in (B).

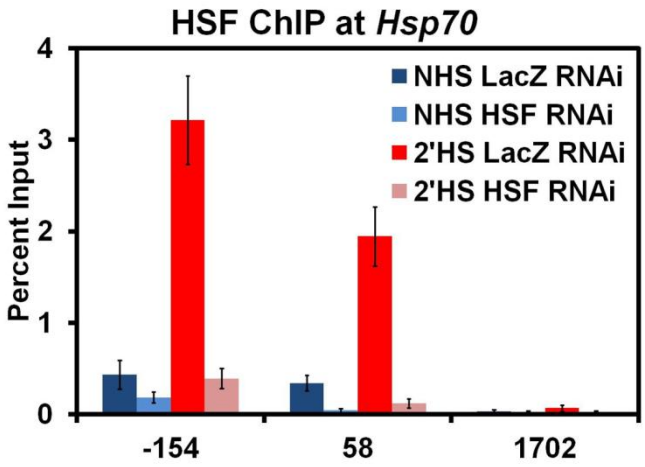

Figure 30 The HSF ChIP signal is Specific for HSF at *Hsp70* following Heat Shock

ChIP of HSF at *Hsp70*. S2 cells RNAi depleted of LacZ or HSF are heat shocked for either 0 (dark blue or light blue respectively) or 2 minutes (red or pink respectively). The y-axis represents the percent of input material immunoprecipitated. The x-axis represents the center of the PCR amplicons in base pair units with 0 being the TSS of *Hsp70* with -154 located at the promoter, 58 at the pause site, and 1702 in the body of the gene. Error bars represent the SEM of 3 independent experiments.

results in the rapid activation and spread of PARP.

3.2.4 The Activity of HDAC3 Maintains PARP Inactivity at *Hsp70* Prior to Heat Shock

Activated HSF binds to multiple HSEs at the promoter of *Hsp70* upon HS and directs changes in transcription by signaling to downstream, paused Pol II through multiple coactivators. I hypothesized that HSF recruitment to *Hsp70* also triggers a signaling mechanism through its coactivators that leads to activation of downstream PARP and the resulting transcription-independent

loss of nucleosomes.

To identify a potential coactivator responsible for activating PARP upon HS, I examined data from my previous RNAi screen looking for factors that affected the loss of chromatin structure at *Hsp70* before and after HS. Of the 28 factors tested, only one factor, HDAC3, had a significant effect on the loss of chromatin structure prior to HS (Petesch and Lis, 2008). Interestingly, RNAi depletion of HDAC3 in NHS cells results in a loss in chromatin structure to the level seen by 1 minute of HS when the initial, transcription-independent loss occurs. To determine if HDAC3 was responsible for the maintenance of PARP in an inactive state at *Hsp70* prior to HS, I RNAi depleted HDAC3 (Figure 31A) and looked by ChIP to determine if PARP or PAR was affected in NHS conditions. RNAi depletion of HDAC3 resulted in loss of PARP from its 5' binding site prior to HS and redistribution further downstream (Figure 31B, light blue). Strikingly, HDAC3 knockdown under NHS conditions also resulted in the accumulation of PAR across the *Hsp70Ab* locus, indicating HDAC3 is responsible for the maintenance of inactive PARP bound to *Hsp70* under NHS conditions (Figure 31C, light blue). HS and HDAC3 RNAi did not result in an additive effect as only a small increase in PAR accumulation was observed upon HS, comparable to normal HS levels. This increase in PAR upon HS is likely due to the activation and loss of the remaining PARP at the 5' end in HDAC3 RNAi NHS cells. Similar results were obtained by treating S2 cells with trichostatin A (TSA), an inhibitor of class I and II histone deacetylases, which includes HDAC3 (Figures 32A and 32B). Interestingly, the inhibition of

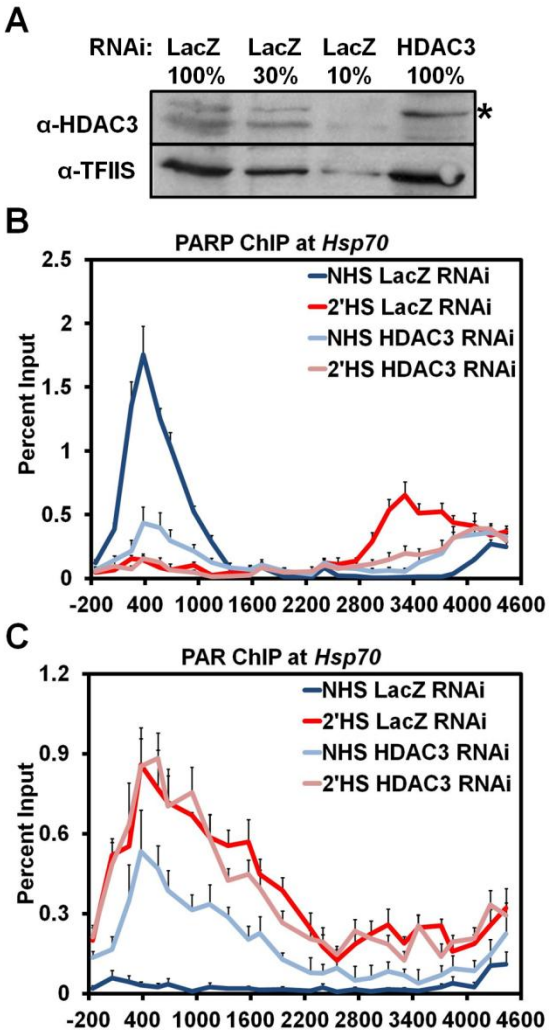

Figure 31 HDAC3 Knockdown Activates PARP at the *Hsp70* Heat Shock Locus under Non Heat Shock Conditions

(A) Western blot confirming the RNAi knockdown of HDAC3 as in Figure 29A with the top panel showing the immunoblot of HDAC3 and bottom panel shows the immunoblot of TFIIS as a loading control. * Indicates a slower-migrating, cytoplasmic, and cross-reactive protein to the HDAC3 antibody that is not affected by HDAC3 RNAi.

(B) ChIP of PARP at the *Hsp70Ab* HS locus in HDAC3 RNAi cells. S2 cells RNAi depleted of HDAC3 were heat shocked for either 0 (light blue) or 2 minutes (pink) and compared to those LacZ RNAi NHS (dark blue) and 2'HS (red) cells. Error bars represent the SEM of 3 independent experiments for (B) and (C)

(C) ChIP of PAR at the *Hsp70Ab* HS locus in HDAC3 RNAi cells as in (B).

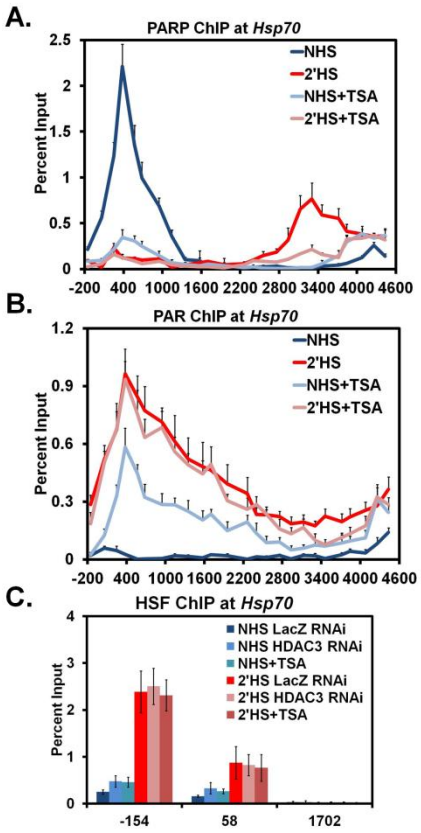

Figure 32 Inhibition of HDAC3's Catalytic Activity through treatment with the HDAC inhibitor. TSA, Recapitulates Results Found with an HDAC3 Knock Down

(A) ChIP of PARP at the *Hsp70Ab* HS locus in the presence of the HDAC inhibitor, TSA. Untreated NHS (dark blue) and 2' HS (red) S2 cells are compared to those NHS (light blue) and 2' HS (pink) cells pretreated with 3 μM TSA for 30 minutes. Error bars represent the SEM of 3 independent experiments.

(B) ChIP of PAR at the *Hsp70Ab* HS locus in the presence of TSA as in (A). Error bars represent the SEM of 3 independent experiments.

(C) ChIP of HSF at *Hsp70* in HDAC3 knockdown and TSA treated cells. S2 cells RNAi depleted of LacZ or HDAC3 dsRNA or treated with 3 μM TSA are heat shocked for either 0 (dark blue, medium blue, or light blue respectively) or 2 minutes (red, pink, or dark pink respectively). The y-axis represents the percent of input material immunoprecipitated. The x-axis represents the center of the PCR amplicons in base pair units with 0 being the TSS of *Hsp70* and -154 located at the promoter, 58 at the pause site, and 1702 in the body of the gene. Error bars represent the SEM of 3 independent experiments.

the enzymatic activity of HDAC3 is sufficient to bring about activation of PARP at *Hsp70* independent of HS-induced activated binding of HSF (Figure 32C).

3.2.5 Heat Shock Factor Facilitates Rapid Acetylation of Histone H2A at Lysine 5 upon Heat Shock

HDAC3 has multiple in vivo targets of deacetylation (Karagianni and Wong, 2007), but perhaps its best known targets are the N-terminal tails of histones H2A at lysine 5 (H2AK5) and H4 at lysines 5 and 12 (H4K5 and H4K12) (Johnson et al., 2002). I depleted cells of HDAC3 by RNAi knockdown and used ChIP assays to examine if either H2AK5Ac or H4K5Ac and H4K12Ac were affected using an antibody that specifically detects H2AK5Ac or an antibody recognizing 4 acetylation marks on H4 (K5, K8, K12, and K16) (Egelhofer et al., 2011). Under NHS conditions, HDAC3 knockdown results in an increase of H2AK5Ac as compared to control NHS LacZ RNAi cells (Figure 33A) and also moderate increases in the acetylation of H4 (Figure 34A). Again, similar results were found using TSA inhibition (Figures 34B and 34C).

To address if HS-induced loss of nucleosomes is accompanied by rapid histone acetylation, I performed a kinetic ChIP analysis. H2AK5Ac and H4Ac rapidly accumulate at *Hsp70* following HS (Figures 33B and 34D respectively) with kinetics similar to the extremely rapid recruitment of HSF (Boehm et al., 2003). Interestingly, the buildup of histone acetylation overlaps with the site occupied by PARP prior to HS. The rate of histone acetylation is also consistent with both the rates of loss of PARP and nucleosomes from the

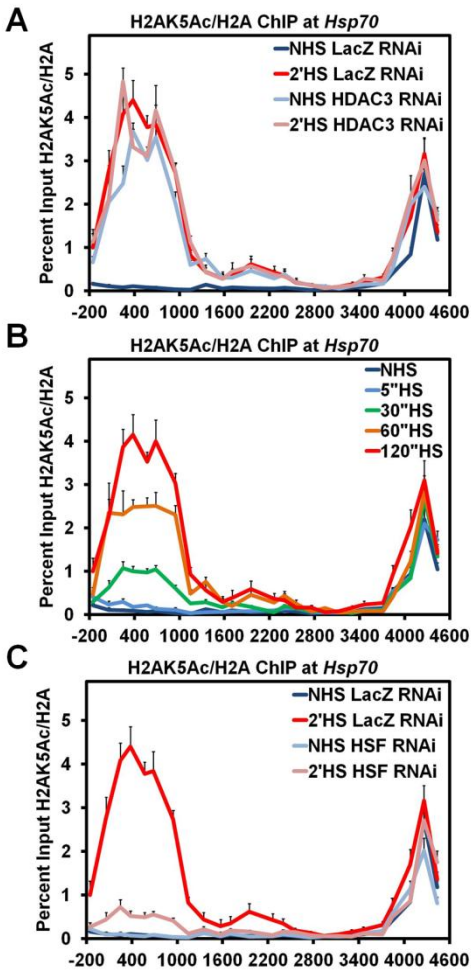

Figure 33 HSF Directs Acetylation of Histone H2A Lysine 5 upon Heat Shock at the *Hsp70* Heat Shock Locus

(A) ChIP of H2AK5 acetylation at the *Hsp70Ab* HS locus in HDAC3 knockdown cells. S2 cells RNAi depleted of HDAC3 and heat shocked for either 0 (light blue) or 2 minutes (pink) are compared to LacZ RNAi cells that were heat shocked for 0 (dark blue) or 2 minutes (red). The level of H2AK5 acetylation is normalized to ChIP values for histone H2A and plotted on the y-axis. Error bars represent the SEM of 3 independent experiments for all 3 panels.

(B) Kinetic ChIP analysis of H2AK5 acetylation normalized to histone H2A as in (A). S2 cells were heat shocked for 0 (dark blue), 5 (light blue), 30 (green), 60 (orange), or 120 seconds (red).

(C) ChIP of H2AK5 acetylation normalized to H2A as in (A) but with HSF RNAi depleted cells.

Figure 34 HSF, but not PARP, is necessary for both Tetra Acetylation of H4 and Acetylation of H2AK5 Following Heat Shock and is Maintained by HDAC3 Before Heat Shock

(A) ChIP of tetra acetylated H4 (antibody can recognize H4K5, K8, K12, and K16 acetylation) at the *Hsp70Ab* locus normalized to histone H3 and plotted on the y-axis. Cells RNAi depleted of HDAC3 and heat shocked for either 0 (light blue) or 2 minutes (pink) are compared to LacZ RNAi cells not heat shocked (dark blue) or heat shocked for 2 minutes (red). Error bars represent the SEM of 3 independent experiments.

(B) ChIP of H2AK5 acetylation at the *Hsp70Ab* locus in untreated NHS (dark blue) and 2' HS (red) S2 cells are compared to those NHS (light blue) and 2' HS (pink) cells pretreated with 3 μM TSA for 30 minutes. The level of H2AK5 acetylation is normalized to ChIP values for histone H2A and plotted on the y-axis. Error bars represent the SEM of 3 independent experiments.

(C) ChIP of tetra acetylated H4 as in (A) but untreated NHS (dark blue) and 2' HS (red) S2 cells are compared to those NHS (light blue) and 2' HS (pink) cells pretreated with 3 μM TSA for 30 minutes. Error bars represent the SEM of 3 independent experiments.

(D) Kinetic ChIP analysis of tetra acetylated H4 as in (A). S2 cells are heat shocked for 0 (dark blue), 5 (light blue), 30 (green), 60 (orange), or 120 seconds (red). Error bars represent the SEM of 3 independent experiments.

(E) ChIP of tetra acetylated H4 as in (A) but cells RNAi depleted of HSF and heat shocked for either 0 (light blue) or 2 minutes (pink) are compared to LacZ RNAi cells not heat shocked (dark blue) or heat shocked for 2 minutes (red). Error bars represent the SEM of 3 independent experiments.

(F) ChIP of H2AK5 acetylation as in (B) but untreated NHS (dark blue) and 2' HS (red) S2 cells are compared to those NHS (light blue) and 2' HS (pink) cells pretreated with 300 nM PJ34 for 10 minutes. Error bars represent the SEM of 3 independent experiments.

(G) ChIP of H2AK5 acetylation as in (B) but with S2 cells RNAi depleted of PARP and heat shocked for either 0 (light blue) or 2 minutes (pink) and compared to LacZ RNAi cells that were not heat shocked (dark blue) or heat shocked for 2 minutes (red). Error bars represent the SEM of 3 independent experiments.

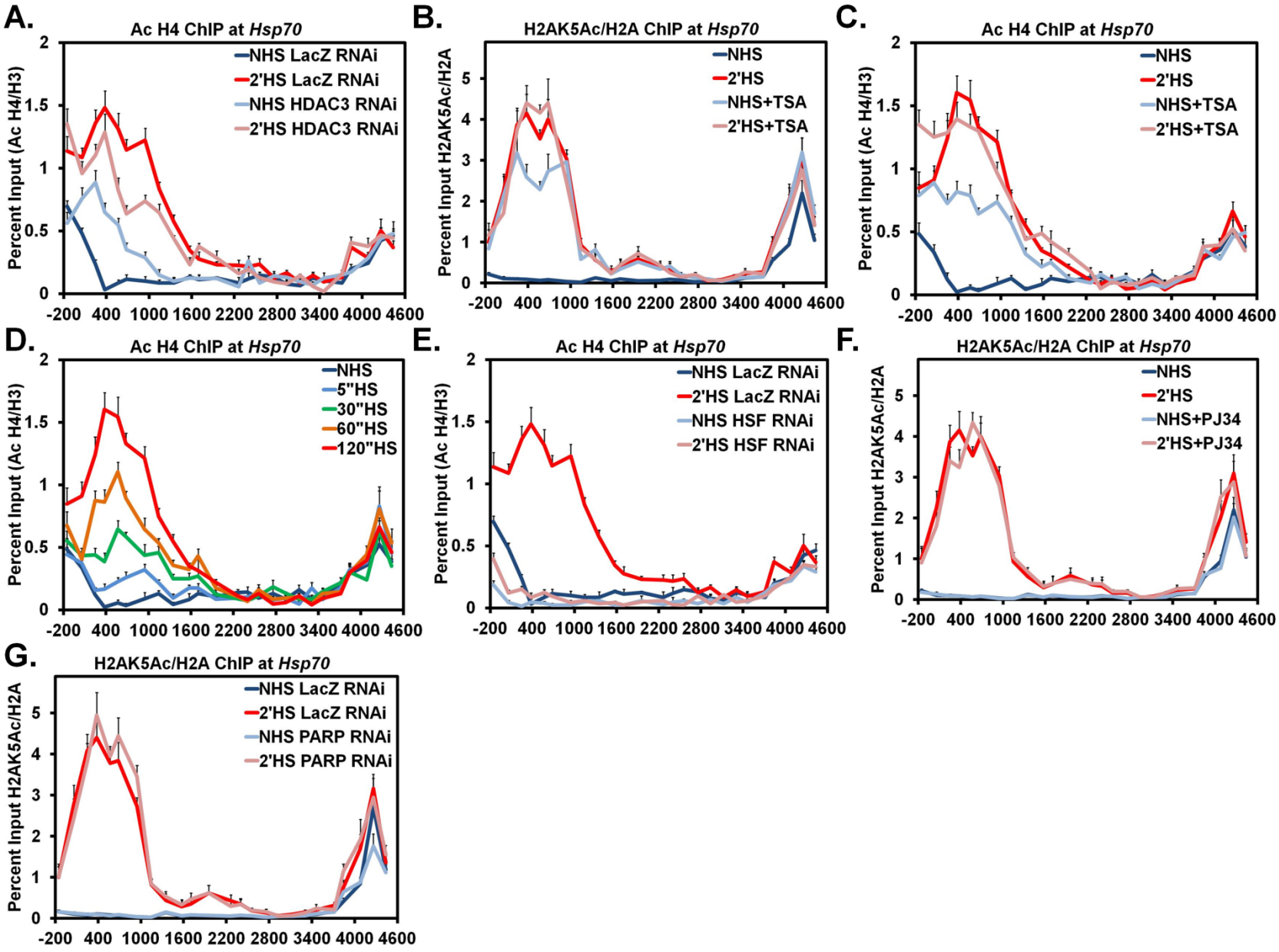
A.
Ac H4 ChIP at Hsp70
Percent Input (Ac H4/H3)
NHS LacZ RNAi
2'HS LacZ RNAi
NHS HDAC3 RNAi
2'HS HDAC3 RNAi
B.
H2AK5Ac/H2A ChIP at Hsp70
Percent Input H2AK5Ac/H2A
NHS
2'HS
NHS+TSA
2'HS+TSA
C.
Ac H4 ChIP at Hsp70
Percent Input (Ac H4/H3)
NHS
2'HS
NHS+TSA
2'HS+TSA
D.
Ac H4 ChIP at Hsp70
Percent Input (Ac H4/H3)
NHS
5"HS
30"HS
60"HS
120"HS
E.
Ac H4 ChIP at Hsp70
Percent Input (Ac H4/H3)
NHS LacZ RNAi
2'HS LacZ RNAi
NHS HSF RNAi
2'HS HSF RNAi
F.
H2AK5Ac/H2A ChIP at Hsp70
Percent Input H2AK5Ac/H2A
NHS
2'HS
NHS+PJ34
2'HS+PJ34
G.
H2AK5Ac/H2A ChIP at Hsp70
Percent Input H2AK5Ac/H2A
NHS LacZ RNAi
2'HS LacZ RNAi
NHS PARP RNAi
2'HS PARP RNAi
-200 400 1000 1600 2200 2800 3400 4000 4600

5’ end of *Hsp70*. Additionally, knockdown of HSF severely inhibits the acetylation of H2AK5 and H4 following HS (Figures 34C and 35E). However, inhibition or RNAi depletion of PARP did not affect acetylation following HS (Figures 35F and 35G). Together, these results demonstrate that HSF is necessary for acetylation of H2AK5 and H4 upon HS, and acetylation either under NHS conditions by HDAC3 knockdown or after HS by HSF recruitment both result in the activation of PARP and reduced nucleosome occupancy at *Hsp70*.

3.2.6 dTip60 is Responsible for Acetylation of Histone H2A Lysine 5 and Activation of PARP upon Heat Shock

To demonstrate that acetylation of histones H2A or H4 was necessary for the activation and spread of PARP following HS at *Hsp70*, I sought to identify the responsible histone acetyltransferase (HAT). Previously, knockdown of CBP or Gcn5, 2 major HATs recruited to *Drosophila Hsp70* following HS (Lebedeva et al., 2005; Smith et al., 2004), did not block nucleosomes loss upon HS (Petesch and Lis, 2008). Instead, I sought to target the dTip60 HAT, which was previously shown to acetylate H2AK5 as well as other sites on H4 (Kimura and Horikoshi, 1998; Kusch et al., 2004). Indeed, knockdown of dTip60 (Figure 36A) prevented the full acetylation of H2AK5Ac following a 2 minute HS (Figure 35A), but only mildly affected acetylation of H4 (Figure 36B), indicating that dTip60 specifically targets H2AK5 for acetylation at *Hsp70* following HS. Strikingly, depletion of dTip60

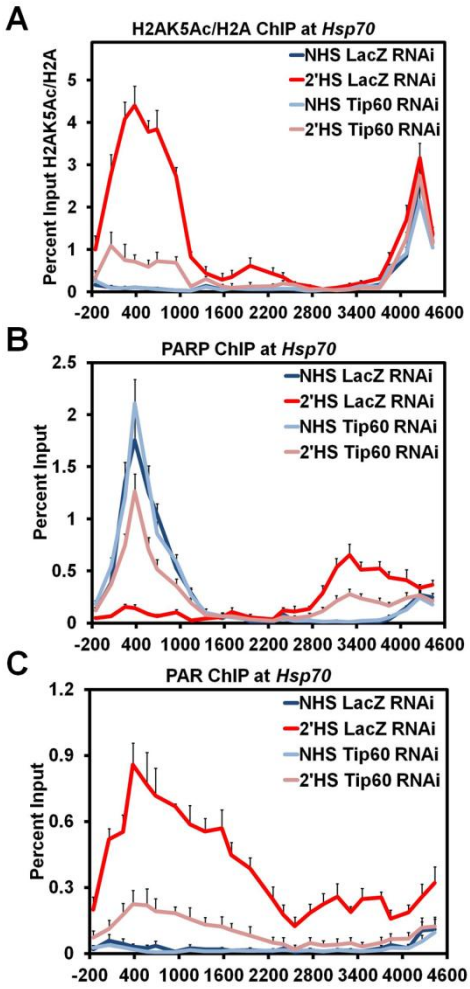

Figure 35 The dTip60 Histone Acetyltransferase is Necessary for Acetylation of Histone H2A Lysine 5 and Activation of PARP upon Heat Shock

(A) ChIP of H2AK5 acetylation at the *Hsp70Ab* HS locus in dTip60 knockdown cells. S2 cells RNAi depleted of dTip60 and heat shocked for either 0 (light blue) or 2 minutes (pink) are compared to LacZ RNAi cells heat shocked for 0 (dark blue) or 2 minutes (red). The level of H2AK5 acetylation is normalized to ChIP values for histone H2A and plotted on the y-axis. Error bars represent the SEM of 3 independent experiments for all 3 panels.

(B) ChIP of PARP in dTip60 knockdown cells. S2 cells RNAi depleted of dTip60 and heat shocked for either 0 (light blue) or 2 minutes (pink) are compared to LacZ RNAi treated cells heat shocked for 0 (dark blue) or 2 minutes (red).

(C) ChIP of PAR in dTip60 knockdown cells as in (B).

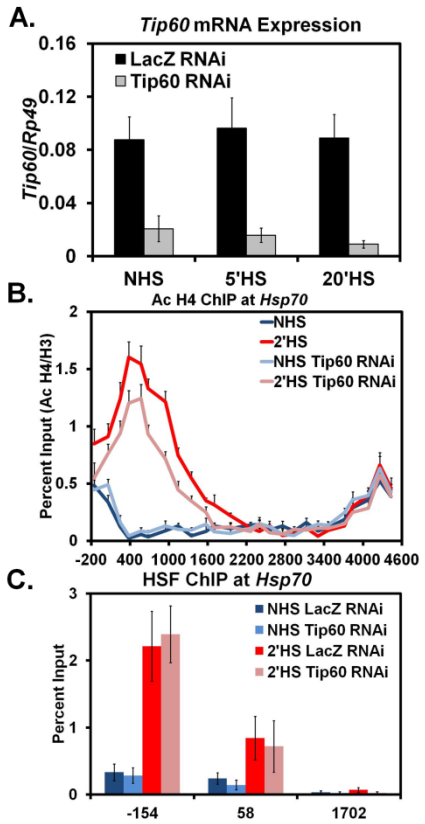

Figure 36 Knockdown of dTip60 is specific and does not Affect the Acetylation of H4 or the Recruitment of HSF Following Heat Shock

(A)*Tip60* mRNA levels following 0, 5, and 20 minutes of HS were measured for S2 cells RNAi depleted of LacZ (black) or Tip60 (gray). *Tip60* expression levels were measured by oligo dT primed reverse transcription followed by qPCR using*Tip60* specific primers. *Tip60* mRNA levels are normalized to the *Rp49* gene with error bars representing the SEM of 3 replicates.

(B) ChIP for tetra acetylated H4 (antibody can recognize H4 K5, K8, K12, and K16 acetylation) normalized to histone H3 was performed using S2 cells RNAi depleted of Tip60 and heat shocked for either 0 (light blue) or 2 minutes (pink) and compared to LacZ RNAi cells that were not heat shocked (dark blue) or heat shocked for 2 minutes (red).

(C) ChIP of HSF at *Hsp70*. S2 cells RNAi depleted of LacZ or Tip60 are heat shocked for either 0 (dark blue or light blue respectively) or 2 minutes (red or pink respectively). The y-axis represents the percent of input material immunoprecipitated. The x-axis represents the center of the PCR amplicons in base pair units with 0 being the TSS of *Hsp70* with -154 located at the promoter, 58 at the pause site, and 1702 in the body of the gene. Error bars represent the SEM of 3 independent experiments.

prevented the full loss of PARP from its 5' site and its spread further downstream (Figure 35B). Correspondingly, dTip60 RNAi inhibited full activation of PARP at *Hsp70* following HS (Figure 35C). Loss of dTip60, however, did not prevent recruitment of HSF to *Hsp70* (Figure 36C). These results demonstrate that upon HS, HSF stimulates dTip60 to specifically acetylate H2AK5 at *Hsp70* which results in activation of PARP.

3.2.7 dTip60 is Necessary for the Loss of Nucleosomes and Full Transcriptional Activation of *Hsp70* upon Heat Shock

As dTip60 is necessary for the activation of PARP upon HS, changes in chromatin structure at *Hsp70* should also be dependent on dTip60. I utilized my previously developed high-resolution MNase protection assay of mononucleosomes at *Hsp70* both before and after HS (Petesch and Lis, 2008). Briefly, S2 cells from NHS and 2 minute HS samples are cross-linked and their chromatin is isolated and split into mock and MNase treated samples. The DNAs from both matched samples are probed using qPCR to quantify the amount of protection for each of the 100 primer sets amplifying 100 bp regions of *Hsp70Ab* spaced 30 bp apart. The MNase protection assay of nucleosomes at *Hsp70* before HS does not show significant differences with dTip60 depletion. However, following a 2 minute HS, knockdown of dTip60 significantly inhibits the loss in chromatin structure of *Hsp70* that occurs both initially from PARP's activation as well as from Pol II's movement through the gene by 2 minutes of HS (Figure 37A, compare pink to red). This pattern of

Figure 37 The dTip60 Histone Acetyltransferase is Necessary for Nucleosomal Loss and Transcriptional Activation of the *Hsp70* Heat Shock Locus

(A) dTip60 affects the rapid loss of nucleosomes at the *Hsp70Ab* HS locus. Control S2 cells treated with RNAi targeting LacZ or dTip60 were heat shocked for 0 (dark blue and light blue respectively) or 2 minutes (red and pink respectively), immediately cooled to room temperature and crosslinked, and their chromatin was isolated. Purified DNA products from samples were treated with 0 or 500 U of MNase and assayed by qPCR. PCR products are 100±5 bp in size and are spaced 30±6 bp apart. The chromatin profile of *Hsp70* was determined by using approximately 100 PCR amplicons with an average size of 100±5 bp, spaced 30±6 bp apart. To assess relative levels of protection the amount of MNase digested PCR product was normalized to the undigested product using the ΔC(t) method (y-axis), which is plotted against the gene nucleotide location (x-axis). Values from overlapping primer sets are averaged. The x-axis represents base pair units with 0 being the TSS. Lines represent the average of 3 separate experiments with error bars representing the SEM of 3 independent experiments.

(B) *Hsp70* mRNA levels following 0, 5, and 20 minutes of HS were measured for S2 cells RNAi targeting of LacZ (black) or dTip60 (gray). *Hsp70* expression levels were measured by oligo dT primed reverse transcription followed by qPCR using *Hsp70* specific primers and normalized to the *Rp49* gene with error bars representing the SEM of 3 replicates.

(C) Model of HSF mediated actions at *Hsp70* to activate PARP and affect nucleosome loss. Top: Linear order of steps of the model depicted below. Bottom: Under NHS conditions, GAGA Factor (GAF) is bound to the promoter of *Hsp70*, Pol II is transcriptionally paused 20-40 base pairs downstream of the TSS, and inactive PARP is bound to the region occupied by the first well positioned nucleosome at *Hsp70*. Upon HS, by 30-60 seconds, HSF trimerizes and binds to multiple HSEs found at the promoter of *Hsp70*. The recruitment of HSF stimulates dTip60 mediated H2AK5 acetylation of nearby nucleosomes, which in turn activates PARP's catalytic activity, PAR chain formation, and release from the nucleosome it was bound prior to HS. The activation of PARP leads to the spread of active PARP and build up of PAR across the HS locus. The progressive and rapid buildup of PAR within the region ultimately leads to nucleosome loss contained within the HS locus.

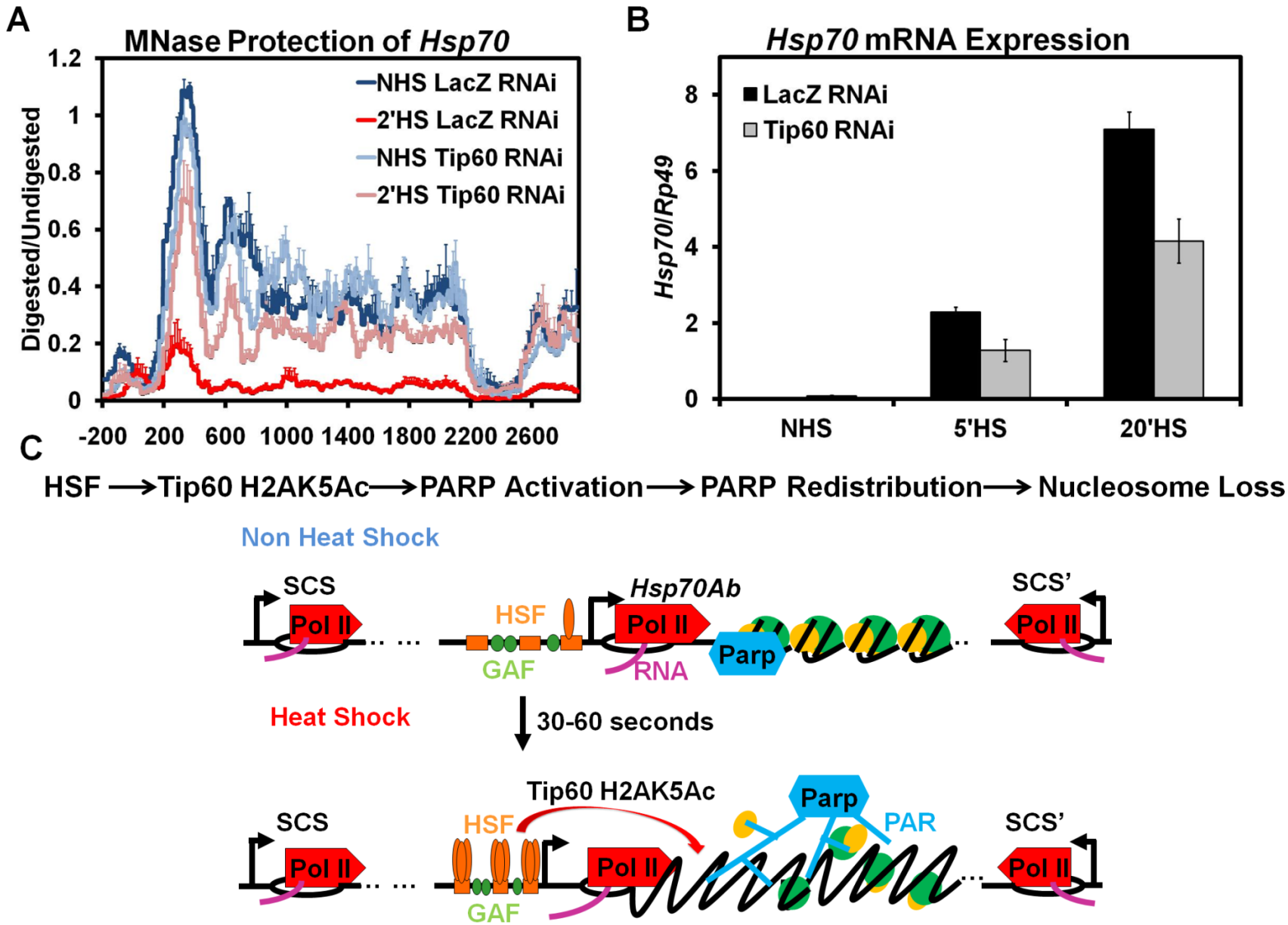
A
MNase Protection of Hsp70
Digested/Undigested
1.2
1
0.8
0.6
0.4
0.2
0
-200 200 600 1000 1400 1800 2200 2600
NHS LacZ RNAi
2'HS LacZ RNAi
NHS Tip60 RNAi
2'HS Tip60 RNAi
B
Hsp70 mRNA Expression
Hsp70/Rp49
8
6
4
2
0
LacZ RNAi
Tip60 RNAi
NHS
5'HS
20'HS
C
HSF ⟶ Tip60 H2AK5Ac ⟶ PARP Activation ⟶ PARP Redistribution ⟶ Nucleosome Loss
Non Heat Shock
SCS
Pol II
HSF
GAF
Hsp70Ab
Pol II
RNA
Parp
SCS'
Pol II
Heat Shock
30-60 seconds
Tip60 H2AK5Ac
Parp
PAR
SCS
HSF
Pol II
GAF
Pol II
SCS'
Pol II

nucleosome retention following HS in dTip60 depleted cells matches those found when PARP is inhibited or depleted (Petesch and Lis, 2008).

To test if retention of chromatin structure by 2 minutes of HS in dTip60 depleted cells has functional consequences on *Hsp70* transcription, I measured mRNA levels before HS and after a 5 and 20 minute HS. dTip60 depletion does not significantly affect *Hsp70* NHS mRNA levels but significantly reduces mRNA levels of *Hsp70* by 50% to that of control cells following both 5 and 20 minutes of HS (Figure 37B), mirroring those results obtained with PARP depletion (Petesch and Lis, 2008).

My previous results demonstrated that nucleosome loss upon HS could occur independently of *Hsp70* transcription. Treatment of S2 cells with sodium salicylate induces recruitment of HSF to the *Hsp70* promoter under NHS conditions, but it does not result in Pol II movement into the gene (Petesch and Lis, 2008; Winegarden et al., 1996). To both assess PARP and dTip60's role in this transcription-independent nucleosome loss and solidify an ordered mechanism whereby HSF recruitment results in nucleosome loss, I performed ChIP in S2 cells treated with sodium salicylate. Under NHS conditions, sodium salicylate causes the activation, loss, and spread of PARP at *Hsp70* (Figures 38A and 38B). Additionally, under NHS conditions, sodium salicylate also induces H2AK5Ac and H4Ac (Figures 38C and 38D). These results support a mechanism whereby HSF-induced histone acetylation triggers PARP activation and spread and nucleosome loss at *Hsp70* that can be decoupled from active transcription.

Figure 38 Sodium Salicylate Induces Histone Acetylation under Non Heat Shock Conditions and Activates PARP in a Transcription-Independent Manner

(A) ChIP of PARP at the *Hsp70Ab* HS locus in the presence of sodium salicylate. Untreated NHS (dark blue) and 2' HS (red) S2 cells are compared to those NHS (light blue) and 2' HS (pink) cells pretreated with 10 mM sodium salicylate for 30 minutes.

(B) ChIP of PAR at the *Hsp70Ab* HS locus in the presence of sodium salicylate as in (A). Error bars represent the SEM of 3 independent experiments.

(C) ChIP of H2AK5 acetylation normalized to H2A in the presence of sodium salicylate as in (A). Error bars represent the SEM of 3 independent experiments.

(D) ChIP of tetra acetylated H4 normalized to H3 in the presence of sodium salicylate as in (A). Error bars represent the SEM of 3 independent experiments.

(E) Model depicting how dTip60 activates PARP. A single nucleosome, representing the first nucleosomes at *Hsp70* before HS, is depicted with H2Av in yellow, H2B in red, H3 in blue, and H4 in green with inactive PARP bound depicted in gray. The N-and C-terminal tails of H2Av are shown as yellow protrusions from H2Av with K5 and S137 highlighted. An unknown kinase is responsible for phosphorylating the C-terminal domain of H2Av at S137. Upon HS, Tip60 is recruited to *Hsp70* and the acetyltransferase activity is stimulated by the presence of S137 phosphorylation, leading to H2AvK5Ac. The acetylation stimulates the dTip60 complex to exchange the modified H2Av-H2B dimer, thereby exposing the H4 within the nucleosome. The exposure of H4 within the nucleosome can provide an epitope that stimulates the activity of PARP leading to its activation, shown in purple.

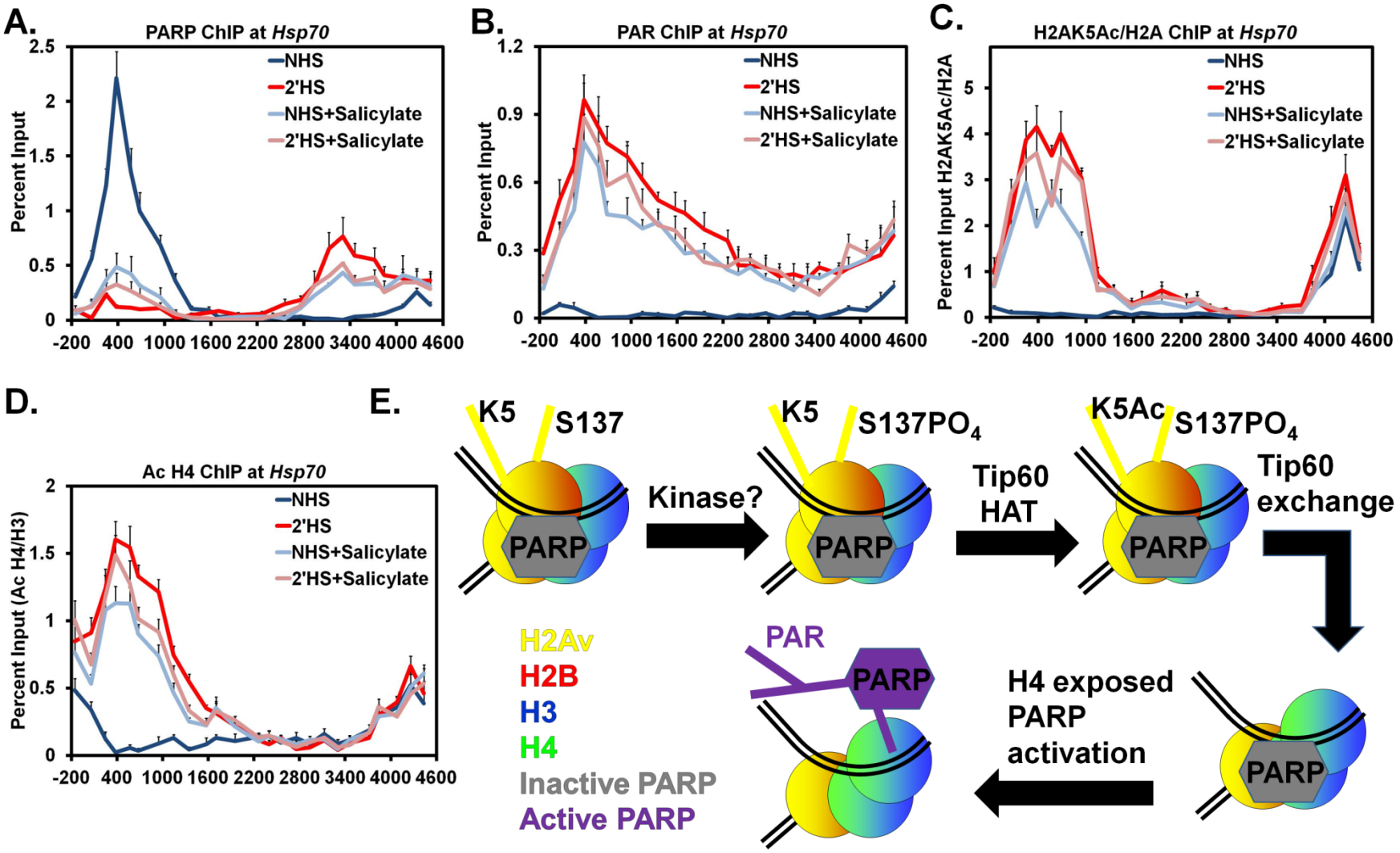
A.
PARP ChIP at Hsp70
Percent Input
NHS
2'HS
NHS+Salicylate
2'HS+Salicylate
-200 400 1000 1600 2200 2800 3400 4000 4600
B.
PAR ChIP at Hsp70
Percent Input
C.
H2AK5Ac/H2A ChIP at Hsp70
Percent Input H2AK5Ac/H2A
D.
Ac H4 ChIP at Hsp70
Percent Input (Ac H4/H3)
E.
K5
S137
PARP
Kinase?
K5
S137PO4
Tip60
HAT
K5Ac
S137PO4
Tip60
exchange
H4 exposed
PARP
activation
PAR
H2Av
H2B
H3
H4
Inactive PARP
Active PARP

3.3 DISCUSSION

This study establishes an ordered mechanism by which a transcription activator binding to a gene's regulatory region leads to rapid removal of nucleosomes throughout the gene locus. Specifically, the transcriptional activator, HSF, stimulates dTip60 acetylation of H2AK5 that in turn activates PARP, causing its redistribution along *Hsp70* and reduced nucleosome occupancy over the locus (Figure 37C). Moreover, all of these steps can be accomplished independently of transcription. This activation of PARP and its rapid spread throughout the *Hsp70* HS loci demonstrate an interesting mechanism by which the nucleosome barrier can be alleviated to facilitate efficient transcription by Pol II.

HSF and many other transcriptional activators have been classically studied for their ability to recruit or release Pol II into transcriptional elongation. My results speak to another function of HSF as an activator to direct changes in chromatin structure upon HS. HSF is able to achieve this function through physically interacting with the dTip60 complex and facilitating its recruitment to *Hsp70* following HS (personal communication by Thomas Kusch). Just as the presence of paused Pol II in NHS conditions primes the *Hsp70* gene for rapid transcriptional induction (Rougvie and Lis, 1988), inactive PARP bound in NHS conditions primes *Hsp70* for rapid changes in chromatin structure. Interestingly, trimerization and binding of HSF to the promoter of *Hsp70* precipitates the activation of both Pol II and PARP through distinct pathways that ultimately synergize to facilitate rapid and robust transcriptional activation.

In vitro studies have shown that the DNA binding and catalytic domains of PARP comprise the minimal structure sufficient for inactive PARP to bind and locally compact nucleosomes and, upon activation, release PARP from chromatin and decompact chromatin structure (Kim et al., 2004; Leduc et al., 1986; Poirier et al., 1982; Wacker et al., 2007). Activation of PARP is known to result in the formation of linear and branched anionic polymers with upwards of 200 units of ADP-ribose (D'Amours et al., 1999). Electron micrograph structures of branched PAR make it easy to visualize how creation of these voluminous, dendritic structures causes automodified PARP to expand 3-dimensionally throughout the *Hsp70* loci following HS (de Murcia et al., 1983). My results also indicate that PARP is cross-linked to *Hsp70* after HS through a PAR linkage to chromatin. Although PARylation of another target, such as histones, cannot be ruled out, my results fit the simplest model where PARP is its own target. In agreement with the aforementioned in vitro studies, PARP automodification would result in its release from nucleosomes bound prior to HS and the PAR created from this automodification could create a bridging interaction between PARP and chromatin formed during cross-linking as seen in Figure 27D. This also is consistent with in vivo studies showing the major target of PARylation is PARP itself (D'Amours et al., 1999; Kim et al., 2004). Antibodies specifically recognizing ADP-ribosylated target proteins, such as PARP or histones, are needed to identify the target of PARP following HS at *Hsp70*.

The accumulation of PAR throughout the *Hsp70* locus provides

additional functional consequences to how activation of PARP upon HS can affect chromatin structure and transcriptional activation. PAR has remarkable chemical similarity to other nucleic acids, such as DNA and RNA, but it has twice the charge per nucleic acid residue and the potential to form non-linear, branched structures. As such, in vitro reconstitution assays have shown that PAR has the ability to locally compete with DNA to bind histones and potentially disrupt native chromatin structure (Althaus et al., 1994). The transient formation of PAR to alter chromatin structure followed by catabolism of PAR to return histones to its DNA template has been referred to as histone shuttling (Althaus et al., 1994). While initially investigated to explain PARP's role in DNA damage repair, this phenomenon can be equally extended to PARP's role in facilitating transcription. Indeed, the formation of PAR at *Hsp70* loci after HS results in formation of a localized compartment that aids in the local retention of transcription factors, including Pol II, to sustain continued transcription activation of *Hsp70* (Zobeck et al., 2010). It is yet to be determined if PAR also aids in the local retention of histones that were previously measured to be lost from *Hsp70* after HS (Petesch and Lis, 2008).

The activation of PARP through the acetylation of H2AK5 also ascribes a unique function to dTip60. Like PARP, Tip60 has been studied for both its roles in DNA repair and also transcriptional activation (Sapountzi et al., 2006). In *Drosophila*, dTip60 is part of a complex containing Domino, an ATPase homologous to the mammalian p400 and SRCAP proteins, which, like Swr1p in *S. cerevisiae*, catalyzes the exchange of histone variant H2A.Z into H2A

containing nucleosomes (Kusch et al., 2004; Mizuguchi et al., 2004; Talbert and Henikoff, 2010). *Drosophila* contains only one H2A variant, which has properties of both H2A.Z and the C-terminal extension of H2A.X, and, when phosphorylated, marks sites of DNA damage (Madigan et al., 2002). Before HS, it is known that *Hsp70* contains nucleosomes harboring H2Av near the 5' end of the gene that is lost upon HS (Leach et al., 2000). Recently, the phosphorylation of H2AvS137 was shown to globally regulate PARP activation and is necessary for full transcriptional activation of *Hsp70* (Kotova et al., 2011). dTip60 acetylates K5 on H2Av that is already phosphorylated on its C-terminal domain at S137 (Kusch et al., 2004). This acetylation stimulates the dTip60 complex to exchange out the modified H2Av. Additionally, in vitro studies show that the ability of H4 to activate PARP is squelched in the context of a nucleosome due to H2A (Pinnola et al., 2007). Collectively, these studies suggest a model in which the phosphorylation of H2AvS137 stimulates dTip60 to acetylate H2AvK5 following its recruitment upon HS (Figure 38E). These modifications are sufficient to stimulate the dTip60 complex to remove the modified H2Av and expose PARP that is bound to these nucleosomes to H4 and activate its enzymatic activity. The importance of H2A variant exchange has also been documented in *Arabidopsis* where the Swr1 complex is also necessary for changes in chromatin structure at HS genes following HS (Kumar and Wigge, 2010).

This purposed model for the order of events that lead to the activation of PARP upon HS raises many questions for future exploration. First, is the

H2Av that is present before HS already phosphorylated and what is the kinase responsible for phosphorylation? Second, is phosphorylation of H2Av necessary for dTip60 acetylation of H2AvK5 upon HS? Third, is H2AvK5Ac or in combination with S137 phosphorylation sufficient for PARP activation in vitro? Fourth, is the ATPase activity of the dTip60 complex to exchange H2Av following HS necessary or sufficient for PARP activation? Finally, is the activity of PARP regulated on a genomic scale at sites with H2Av nucleosomes that are both acetylated at K5 and phosphorylated at S137?

The fact that transcription-independent nucleosome loss following HS at *Hsp70* is reliant on factors that respond to DNA damage provokes the question if changes in chromatin at *Hsp70* are the result of a response to DNA repair. Indeed, transcriptional activation can occur in response to PARP activation from a topoisomerase II break in DNA (Ju et al., 2006). However, in contrast to this study, I find that PARP is already present at *Hsp70* before HS and is not recruited upon HS. Although topoisomerase II mediated breaks have been mapped to sites near the TSS of *Hsp70* before HS (Udvardy and Schedl, 1991), these breaks are not sufficient to detect active PARP at *Hsp70* before HS and might be more important for the initial deposition of PARP before HS. I propose an alternative mechanism for PARP activation whereby a transcriptional activator hijacks DNA repair proteins to aid transcriptional activation. The fact that PARP is bound near the majority of human TSSs containing Pol II (Krishnakumar et al., 2008), like at *Drosophila Hsp70*, also hints at the generality for a mechanism whereby activation of pre-bound PARP

leads to changes in chromatin structure and ultimately contributes to gene expression.

3.4 EXPERIMENTAL PROCEDURES

All primer sets used are listed in Table 9. The experimental procedures follow those used in (Petesch and Lis, 2008) and in section 2.4 with the following exceptions.

3.4.1 ChIP

Heat shocks and ChIP were performed as in (Petesch and Lis, 2008) with the following exceptions. Following resuspension of the cross-linked pellet in sonication buffer, samples to be immunoprecipitated for PAR were TCA precipitated. 100% (w/v) TCA was added to a final concentration of 20% and incubated at 4 °C for 10 minutes. The sample was centrifuged at 4 °C for 5 minutes at 20,000 g and the resulting pellet was washed twice with 250 µL of acetone with the same centrifuging conditions. The final pellet was dried and resuspended in ChIP sonication buffer and the typical ChIP protocol was resumed from the point of sonication.

For ChIP with PARG treated extracts, chromatin from cross-linked cells was isolated as in the high-resolution MNase assay and resuspended in the sonication buffer not containing SDS. Samples were split and either treated with final concentrations of 0 or 1200 nM PARG for 30 minutes at 37 °C. The reaction was stopped by addition of SDS to a final concentration of 0.5% and

the ChIP protocol continued at the step of sonication. The amount of antibody per IP used was: 8 µL rabbit anti-PARP raised to the N-terminus (Kim et al., 2004) a gift of W. Lee Kraus, 4 µL mouse anti-PAR (Trevigen 4335), 2 µL rabbit anti-Histone H2A acetyl K5 (Abcam ab45152), 4 µL rabbit anti-Histone H2A-ChIP grade (Abcam ab13923), 2 µL of rabbit anti-HSF (Boehm et al., 2003), 2 µL of rabbit anti-tetra acetyl-Histone H4 (Millipore 06-598), and 2 µL of rabbit anti-Histone H3 ChIP grade (Abcam ab1791).

3.4.2 Quantitative Real-Time PCR Analysis

ChIP and RT-qPCR primer sets are provided in Table S1. Real-Time PCR was performed as in (Petesch and Lis, 2008). For ChIP samples, a standard curve was generated by serially diluting input samples to quantify IP samples. For MNase digests, a fold difference was calculated between MNase treated and untreated samples. All values used were collected from the linear range of amplification.

3.4.3 Chemical Treatments

PJ34 was added to S2 cells in media to a final concentration of 300 nM and allowed to mix for 10’ at room temperature. Cells were then collected following NHS or 2’ HS conditions outlined in the ChIP section. Additional chemical treatments included in supplementary figures not performed in the main document were performed by adding both final concentrations of 3 µM TSA or 10 mM sodium salicylate directly to the S2 cells while still in media

either 30 or 10 minutes respectively prior to HS for either 0 or 2 minutes.

3.4.4 RNAi Treatments

All RNAi treatments were performed as in (Petesch and Lis, 2008). RNAi primers and RefSeq DNA Identifiers for all knockdowns are provided in Table S1. Briefly, S2 cells were treated with double stranded RNA, designed using the Ambion MEGAscript manual, targeting either the coding sequence of the listed factor or β-galactosidase (LacZ, as a negative control). Cells were collected and split into NHS and 2' HS samples to be processed using the ChIP or high-resolution MNase assay.

3.4.5 mRNA Expression Analysis

All mRNA expression analyses were as performed in (Petesch and Lis, 2008). Briefly, total RNA was isolated (Qiagen RNeasy) from Tip60 and LacZ RNAi S2 cells following 0, 5, and 20 minutes of HS. *Hsp70*and *Tip60* levels were determined from oligo dT mediated quantitative real-time reverse transcription-PCR using primers targeting either *Hsp70* or *Tip60*. The stable ribosomal protein RpL32 gene (*Rp49*) was used to internally standardize for the amount of RNA.

3.4.6 High-resolution MNase Mapping

MNase mapping was preformed as in (Petesch and Lis, 2008). Briefly, nuclei isolation, followed by chromatin isolation was performed using cross-linked S2

cells. Samples were split into equal portions and treated with either 0 or 500 total units of MNase (USB) for 30 minutes at room temperature and their DNA recovered.

3.4.7 PARG and PARP Purification

Recombinant, rat, 6xHis-N-terminally tagged PARG was a gift of W. Lee Kraus and was purified as in (Kim et al., 2004). *Drosophila* full length and N-terminus (corresponding to the first 383 amino acids) PARP were cloned into pET-19b harboring a 6xHis-N-terminal tag. Briefly, transformed BL21-CodonPlus (DE3)-RIPL *E*. *coli* cells (Agilent Technologies) were induced with 1 mM IPTG for 3 hours at 30 °C. 6xHis tagged proteins were purified using conventional Ni-NTA Agarose (Qiagen) methods.

3.4.8 Western Blots

Western blots were performed using standard conditions, and input dilutions were used as a quantitative indication of signal linearity. Antibody lab stocks of HSF (Shopland et al., 1995) and TFIIS (Adelman et al., 2005) were used at dilutions of 1:2000 and 1:3000 respectively. Rabbit anti-HDAC3 antibody (Santa Cruz sc-11417) was used at a 1:500 dilution. Additional Western blots were performed using rabbit anti-Parp serum raised to recognize the N-terminus (Kim et al., 2004) was a gift of W. Lee Kraus, mouse anti-PAR (Trevigen 4335), and mouse anti-6xHis (Santa Cruz sc-8036) at 1:1000, 1:500, and 1:1000 dilutions respectively.

3.5 Primer Sets Used

Table 9 Primer Sets Used for ChIP of *Hsp70*

5' Start	Forward Primer
-200	TGCCAGAAAGAAAACTCGAGAAA
-13	CAATTCAAACAAGCAAAGTGAACAC
196	CTTTCAACAAGTCGTTACCGAGG
335	CACCACGCCGTCCTACGT
517	ACGGCGGAAAGCCCAAGAT
626	ATATCTGGGCGAGAGCATCACA
860	CATCGACGAGGGATCACTGTTC
1093	TTGAGGGCCAAGACTTCTACACCA
1301	GAACCTCAACCTATCCATCAACCC
1512	TTCTCCACATACGCGGACAACCA
1637	GGGTGTGCCCCAGATAGAAG
1912	TGGACGAGGCTGACAAGAACT
2185	TGTTCATCAATGGGTTATAACATATGGGTT
2371	CAACTTGTCATTTAATGTTTT
2501	TCGGCTTTGATGATTTTCTG
2707	TTGCAGGCGCATACGCTCTATATC
2882	ACTCCACACTGATATGGTCGCT
3077	GTGTGCTGACGCATGTGAAGACTA
3265	CGTTTCTTCGGGTTCCAATGCGAT
3419	CTGTCAGTTTGTGGGCTTGGGAAA
3667	AGCTGAACAGTCTTGGTCTCCA
3791	TGAACTTCATCCGGCTTGGCA
4013	TGGAAACTGCCTCCAACAACTG
4207	TTGTTAATAACACCTGATGTTCAGAGAT
4394	AGACGCTTTGATAGATGTATTTGTATAG

5' Start	Reverse Primer
-108	GACAGAGTGAGAGAGCAATAGTACAGAGA
97	TGATTCACTTTAACTTGCACTTTA
296	ATGTTGGTAGACACCCACGCA
414	GGTTCATGGCCACCTGGTT
618	CCGTCTCCTTCATCTTGGTCAGTA
700	GTAGCCTGGCGCTGGGAGTC
1007	GGCGCGAGGGTTGGA
1195	TTGAGGGCCTTCTCCACAGGCT
1396	TGGATCTTGCCGCTCTGGTCT
1614	ACAGATCGAAGGTGCCCAATGC

1749	TGTCGTTCTTGATCGTGATGTTC
1965	ACCGGATAGTGTCGTTGCACTT
2310	AAGACTTGGTAATTAGGTAATACTATTGTT
2471	AAATCATCACTAATATAGAATGTAG
2607	AAAAGTGGAGCTCTCCTGAC
2807	TTCCGGGCAATGAAGTAGAGGCAA
2989	TCAAAGGCCGTACTCCTGCAAA
3174	ATTCGGCGACATACGGGCGATAAT
3345	ACATTCAAGCGTCAGGACACACTC
3509	ACTTCATCTACAAGTGCGCCGTCT
3763	AGACGATGTGGTCAGTATGGCA
3884	CCTATGAGTTCATCGTCGAAGTGG
4102	AGACGCACGAGACCAATCTGTA
4315	ATCGTTAATTGTGTACATCTCAATTCCA
4476	TTGAATAGTGCTCTAAACTTTGGCATTT

Table 10 Tip60 Primer Sets Used

RT-qPCR

Tip60 Forward	CAATGGACAAGCGCAAGATC
Tip60 Reverse	ACTACAAGCTACAACGAAGCC

RNAi

Tip60 Forward	GAATTAATACGACTCACTATAGGGATCTGTACACGCGAAAGGTGCAA
Tip60 Reverse	GAATTAATACGACTCACTATAGGGATTGTGAGAATGCAGGCCACGTT

CHAPTER 4 A SURVEY OF ADDITIONAL SITES THAT BIND HSF FOLLOWING HEAT SHOCK TO DETERMINE THE GENERALITY OF THE HSP70 MECHANISM OF NUCLEOSOME LOSS

The mechanistic insight gained from a detailed analysis of changes in nucleosomes that occur after heat shock at *Hsp70* have provided a new mechanism to further study how Pol II is able to overcome the nucleosome barrier during transcription. One interesting and unanswered question from this work is how general this mechanism is to other sites that respond to heat shock. A survey of 12 additional genes throughout the *Drosophila* genome nearby an HSF binding site identified *Hsp22*, *Hsp27*, *Hsp68*, and *Hsrω* as genes that also have a reduced nucleosome protection upon heat shock. As with *Hsp70*, these four genes identified are also dependent on HSF, PARP, and dTip60 to bring about this loss. These results indicate that HSF binding alone is not sufficient to induce changes in nucleosome protection, but a similar mechanism like that identified at *Hsp70* is used at other sites where nucleosome loss does occur upon heat shock. The results from a PARP ChIP-seq experiment will likely provide insight into the proximity requirement between PARP deposition before heat shock and HSF binding after heat shock and those sites that exhibit a loss in nucleosomes.

4.1 Introduction

Nucleosomes pose a ubiquitous barrier to the ability of RNA Polymerase II (Pol II) to be able to efficiently transcribe mRNA enconding

genes. The cell has distinct methods with which to facilitate Pol II's traversal of the nucleosome (Petesch and Lis, 2012b). Recent studies have uncovered a novel mechanism of nucleosome loss whereby a transcription activator is able to activate the enzymatic activity of Poly(ADP-Ribose)Polymerase (PARP) through the histone acetyltransferase coactivator Tip60 (Petesch and Lis, 2008; Petesch and Lis, 2012a). These studies have extensively mapped the changes that occur to both nucleosomes and the formation of Poly(ADP-Ribose) (PAR) polymers upon heat shock stimulation at the major heat shock gene in *Drosophila melanogaster*, *Hsp70*. Although initial studies of *Drosophila* PARP indicate that its enzymatic activity is used to facilitate chromatin decondensation at many sites upon heat shock (Tulin and Spradling, 2003), as well as at sites that decondense upon hormone treatment and stimulation of the innate immune response, the generality of this phenomenon and what is sufficient to elicit the PARP-dependent loss of chromatin structure is unknown.

HSF is the master regulator of the heat shock response and orchestrates the cellular response to heat shock stimulation through the upregulation of heat shock genes. HSF achieves this through first a trimerization event (Rabindran et al., 1993) followed by its DNA binding domain recognizing and binding to its consensus DNA sequence of three tandem 5-mer repeats of AGAAN oriented in a head-to-tail fashion (Perisic et al., 1989). Initial studies of HSF binding in *Drosophila melanogaster* upon heat shock were able to map over 164 distinct cytological loci from polytene

chromosome staining (Westwood et al., 1991), however, only 9 of these sites were observed to undergo visible chromatin decondensation to various extents (Andrulis et al., 2000; Ashburner, 1967; Lis et al., 2000; Saunders et al., 2003). Although these sites are known to contain genes that are upregulated upon heat shock, as observed by the recruitment of active Pol II to these sites (Plagens et al., 1976; Saunders et al., 2003), HSF recruitment and chromatin decondensation can be uncoupled from active transcription of these genes (Winegarden et al., 1996). Together, these results indicate that, even though HSF is recruited to many sites throughout the genome, HSF recruitment is not sufficient to elicit either transcriptional activation or chromatin decondensation.

A recent study of *Drosophila* HSF has mapped all genomic locations of HSF binding both before and after heat shock through high-throughput ChIP sequencing. These ChIP seq results indicate that HSF binds to 20 locations before heat shock and 464 sites following a 20 minute heat shock (Guertin et al., 2010). Of these 464 sites, 442 contained an underlying consensus Heat Shock Element (HSE), and 422 of these were inducibly bound upon heat shock. Of these 422, 364 (82%) fall within the promoter or the gene body and make them prime candidate sites for being able to initiate changes in chromatin structure to facilitate transcript elongation upon heat shock.

With this data set, it is possible to probe the chromatin structure at different loci surrounding HSF binding sites to answer specific questions of how or if HSF binding is able to affect changes in chromatin structure. First, is HSF binding sufficient to bring about localized changes in chromatin structure

that was not detectable from polytene chromosome staining that lacks the resolution to resolve changes in individual nucleosomes? Second, are changes in nucleosomes only detected from those 9 major heat shock sites? Third, does the distance of HSF binding from the gene affect HSF's ability to bring about changes in nucleosomes at nearby genes upon heat shock? Fourth, do changes in nucleosomes occur only at those genes that are upregulated transcriptionally upon heat shock? Last, does the presence or amount of paused polymerase correlate with those sites that undergo changes in chromatin structure, as it does with *Hsp70*?

To begin to answer some of these questions, with the help of three separate rotation students, I designed primer sets to 12 additional sites to map changes in nucleosomes by my MNase protection assay on genes nearby a characterized HSF binding site. These sites were selected to represent a variety of different aspects from being both within and outside of known sites of chromatin decondensation, containing different strengths of HSF binding, having an HSF binding site at a variety of distances away from the gene, and also HSF binding nearby to genes containing different amounts of paused polymerase. In addition to characterizing these 12 additional sites, I tested those sites that did show changes in their MNase protection patterns upon heat shock for their dependence on HSF as well as PARP and Tip60 to determine if these sites additionally used a similar mechanism to nucleosome loss as determined with *Hsp70*.

4.2 Results

4.2.1 Major Heat Shock Sites Contain Genes that Exhibit Nucleosome Loss upon Heat Shock

To broaden the current understanding of what genes undergo changes in chromatin structure following heat shock at the resolution of individual nucleosomes, I identified genes within previously characterized major heat shock puff sites that contained an HSF binding site nearby. The major heat shock puff sites are found at the cytological loci indentified from polytene chromosome staining after heat shock, and these include 33B, 48E, 63B, 64EF, 67B, 87A, 87C, 93D, and 95D (Ashburner, 1967; Westwood et al., 1991). Although reported, no outright visible HSF binding site was observed near the annotated 33B locus. 87A and 87C contain multiple copies of the *Hsp70* gene, already extensively characterized, and 63B contains the constitutively active *Hsp83* (homologous to *Hsp90*) with HSF already bound before heat shock. To the additional 6 loci, we used previously genome-wide NHS H3 ChIP-chip (Mito et al., 2005) and MNase-seq profiles of mononucleosomes (Gilchrist et al., 2010) to choose a region at each gene that contained the first well-occupied nucleosome after the nucleosome free region near the transcription start site to design primer sets for my MNase protection assay.

The first genes tested were *Hsp22* and *Hsp27*, which are found within the 67B locus. This locus contains multiple HSF binding sites and multiple

Figure 39 Nucleosome Loss Occurs at *Hsp22* after Two Minutes of Heat Shock

(A) A UCSC genome browser shows a 6 kb region on chromosome 3L highlighting *Hsp22* with the black arrow at the bottom indicating the transcription start site and direction of transcription and surrounding RefSeq genes in blue. The top track shows a NHS Rpb3 ChIP seq experiment (from (Gilchrist et al., 2010)) that detects Pol II signal in the region (dark red). The middle two tracks show a NHS GRO-seq experiment (unpublished data) that maps the position, amount, and orientation of transcriptionally engaged polymerases across the region moving left to right (to track in red, +) or right to left (bottom track in blue, -). The site of HSF binding after 20 minutes of heat shock is shown below in green (from (Guertin et al., 2010)). The last track shows the NHS nucleosome landscape from an MNase-seq experiment (from (Gilchrist et al., 2010)). This track was used to design primer sets to the closest occupied nucleosome to the HSF binding site (highlighted in the orange box).

(B) A NHS (blue) and 2'HS (red) MNase protection assay as in Figure 4 plots the relative level of protection (y axis) versus the center of the amplified primer set's distance from the TSS of *Hsp22* (x axis). The error bars represent the SEM from 3 independent experiments.

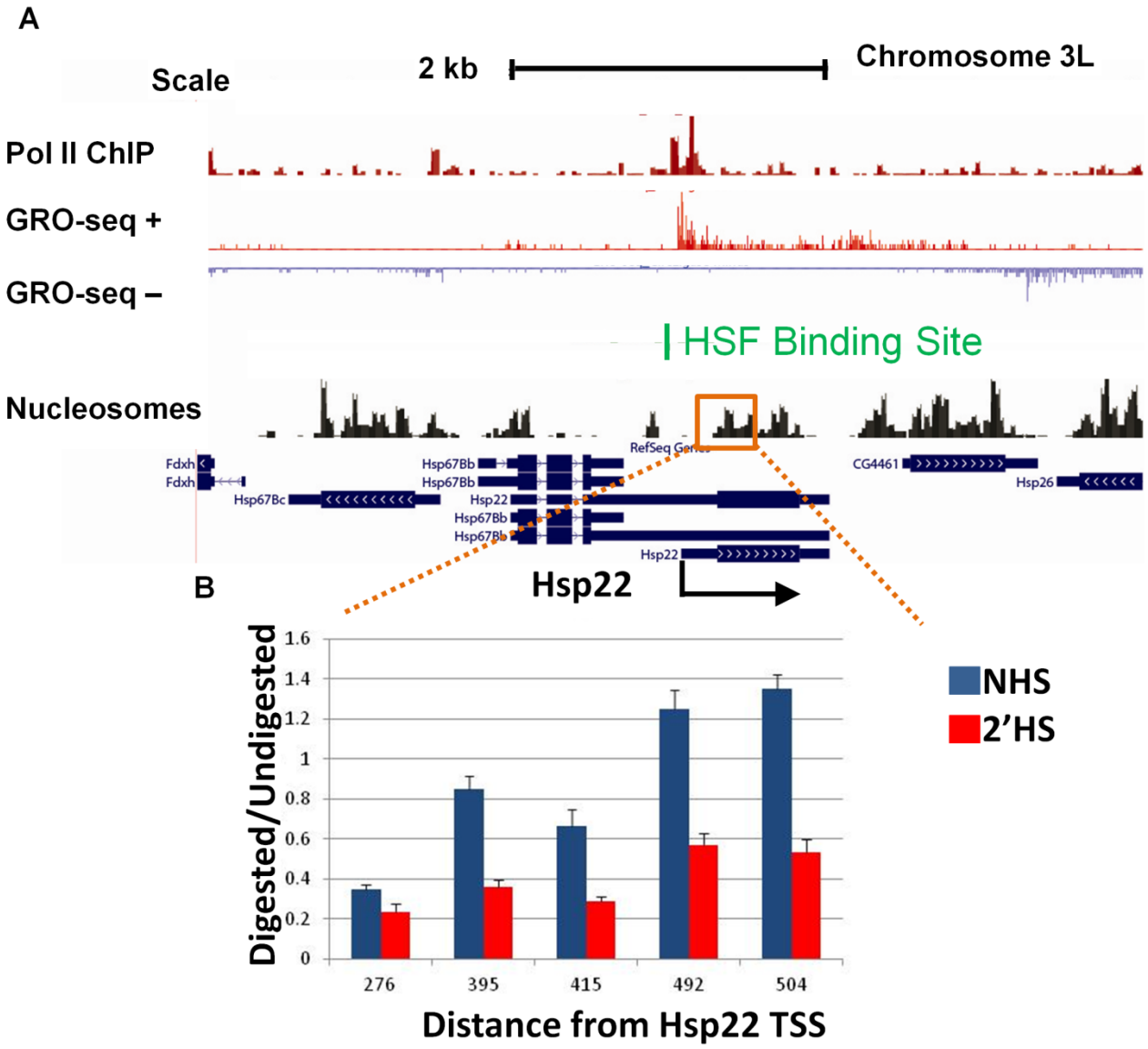
A
Scale
2 kb
Chromosome 3L
Pol II ChIP
GRO-seq +
GRO-seq –
HSF Binding Site
Nucleosomes
RefSeq Genes
Fdxh
Fdxh
Hsp67Bc
Hsp67Bb
Hsp67Bb
Hsp22
Hsp67Bb
Hsp67Bb
Hsp22
CG4461
Hsp26
B
Hsp22
Digested/Undigested
1.6
1.4
1.2
1
0.8
0.6
0.4
0.2
0
276
395
415
492
504
Distance from Hsp22 TSS
NHS
2'HS

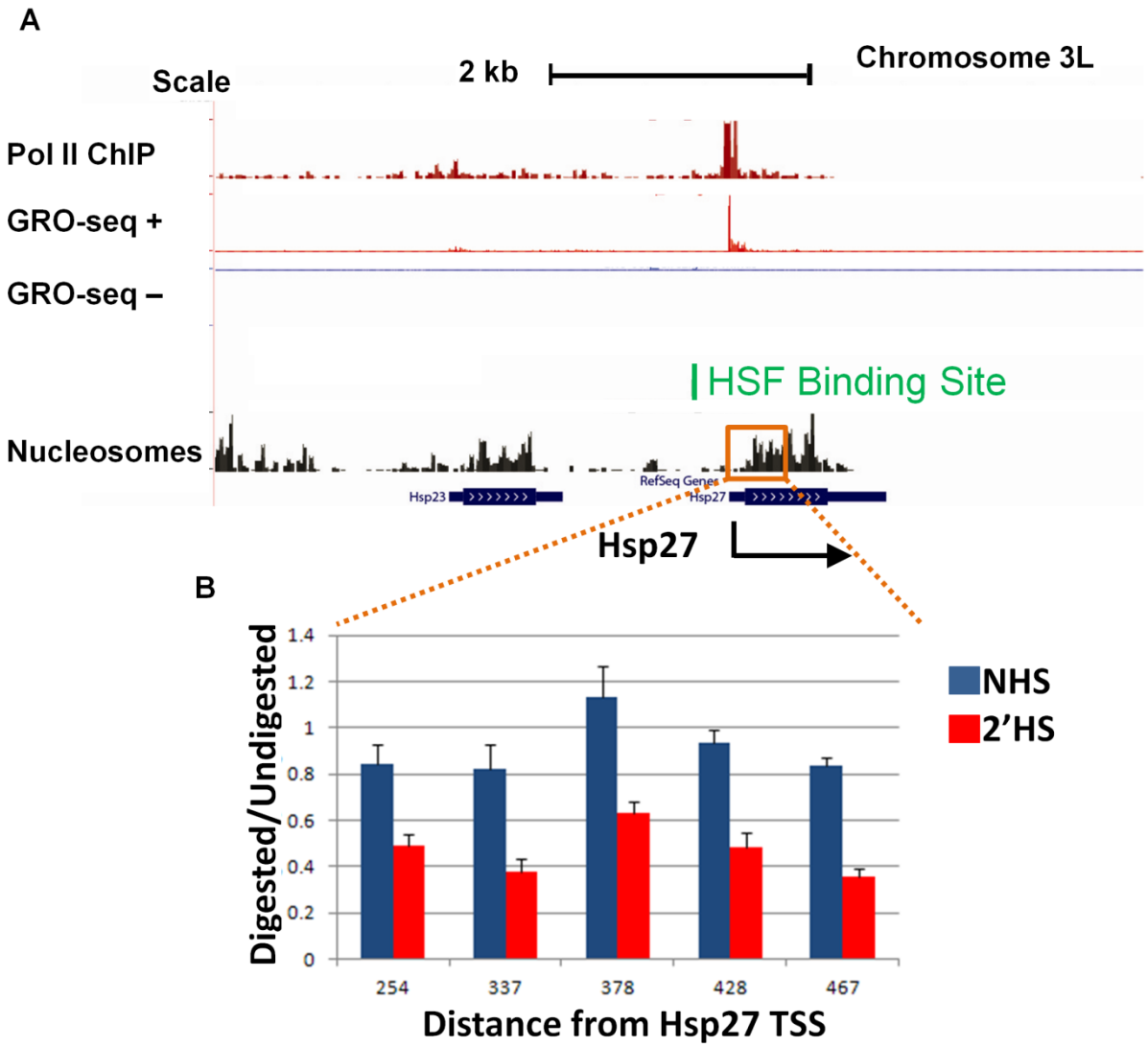

Figure 40 Nucleosome Loss Occurs at *Hsp27* after Two Minutes of Heat Shock

(A) A UCSC genome browser shows a 6 kb region on chromosome 3L highlighting *Hsp27* as in Figure 39.

(B) A NHS (blue) and 2'HS (red) MNase protection assay as in Figure 4 plots the relative level of protection (y axis) versus the center of the amplified primer set's distance from the TSS of *Hsp27*. The error bars represent the SEM from 3 independent experiments.

major heat shock genes, including the previously mapped *Hsp26* gene (Figures 7 and 10). These two genes both contain HSF binding to a promoter-proximal HSE following a 20 min heat shock (less than 500 bp upstream of the annotated TSS), and paused polymerases as detected by Rpb3 ChIP-seq and GRO-seq before heat shock (Figures 39A and 40A), but at mild and moderate levels. These two genes are also known to be highly transcriptionally activated after heat shock (Guertin et al., 2010). As seen by the MNase-seq profiles and from our MNase protection assay of these regions before heat shock, a nucleosome occupies the 5' end of these genes. As expected, these regions also show a hypersensitivity to MNase digestion following heat shock (Figures 39B and 40B), as observed with other major heat shock genes *Hsp70* and *Hsp26*. These results corroborate those results showing the 67B locus undergoes significant puffing after heat shock.

The next genes to be tested are found within the 95D and 93D loci which also show significant puffing following heat shock. *Hsp68* is at the 95D locus and contains an HSF that binds to a promoter-proximal HSE after heat shock and is transcriptionally upregulated following heat shock (Guertin et al., 2010). *Hsp68* contains a paused polymerase before heat shock (Figure 41A), although at moderate levels. Again, as expected, a nucleosome that occupies *Hsp68* before heat shock is lost following a two minute heat shock (Figure 41B). The 93D locus contained two separate genes, that each contained an HSF binding a promoter-proximal HSE, *Hsrω* and *mod(mdg4)*. *Hsrω* is a non coding RNA that is upregulated upon heat shock and contains multiple

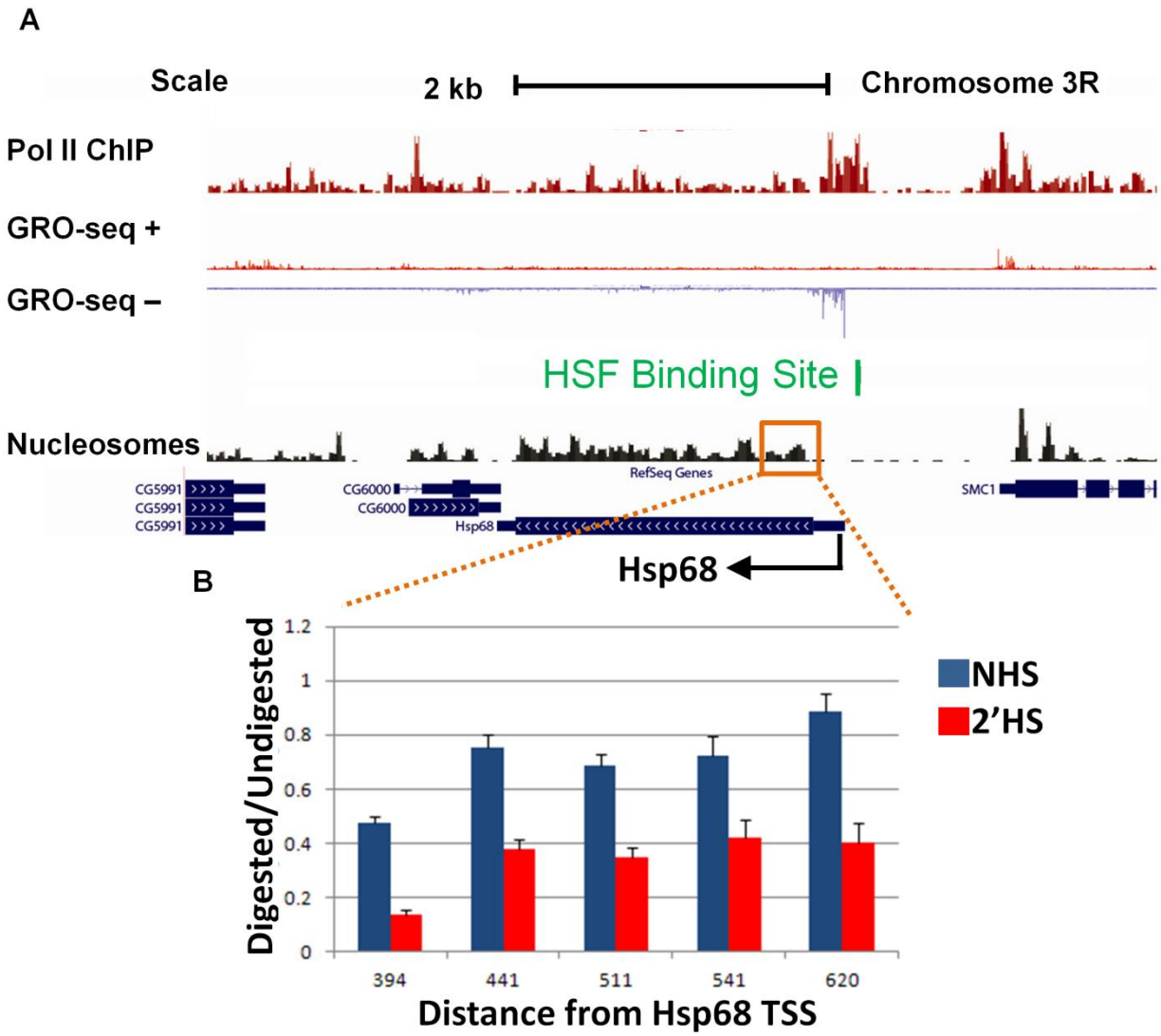

Figure 41 Nucleosome Loss Occurs at *Hsp68* after Two Minutes of Heat Shock

(A) A UCSC genome browser shows a 6 kb region on chromosome 3L highlighting *Hsp68* as in Figure 39.

(B) A NHS (blue) and 2'HS (red) MNase protection assay as in Figure 4 plots the relative level of protection (y axis) versus the center of the amplified primer set's distance from the TSS of *Hsp68*. The error bars represent the SEM from 3 independent experiments.

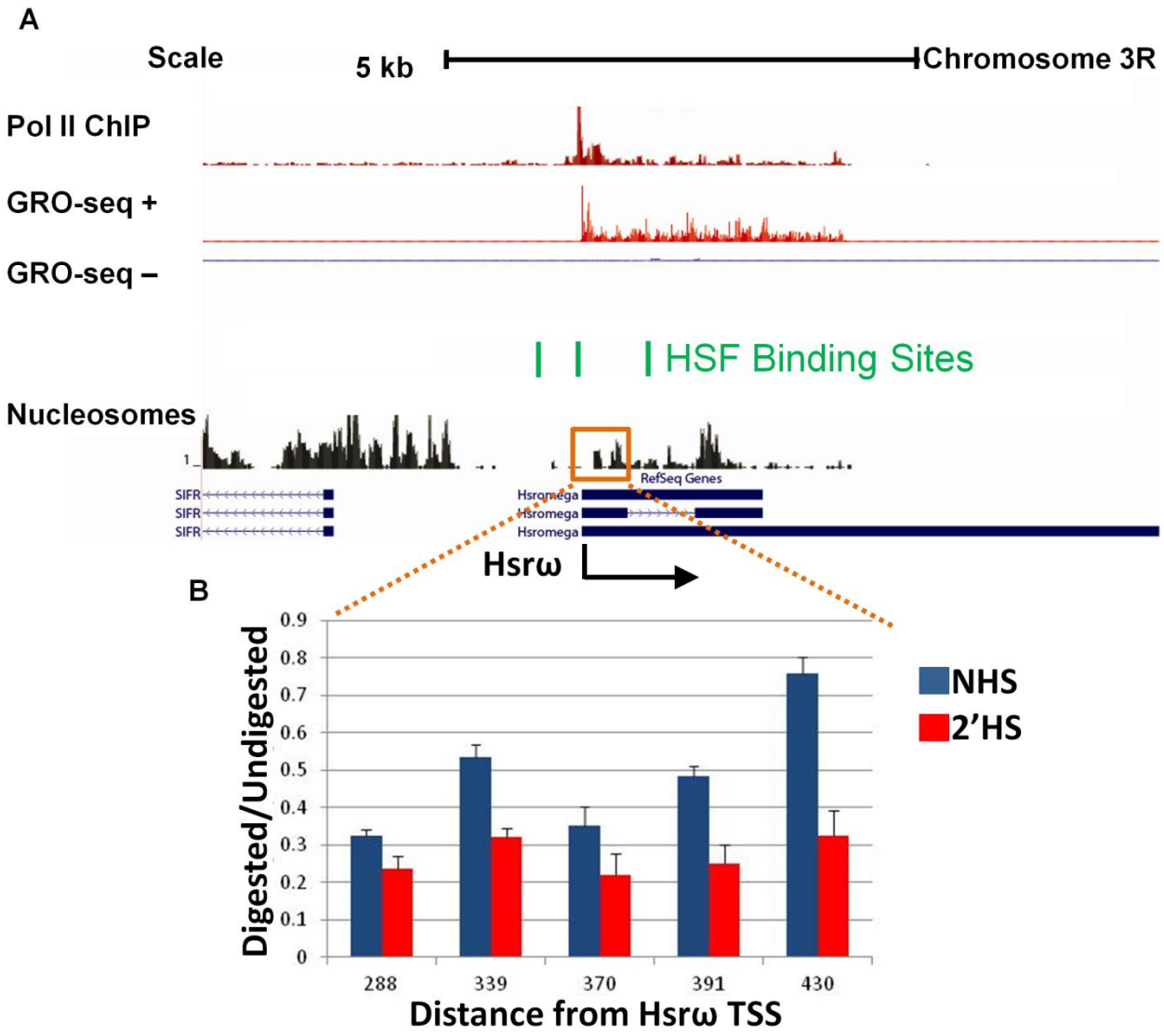

Figure 42 Nucleosome Loss Occurs at *Hsrω* after Two Minutes of Heat Shock

(A) A UCSC genome browser shows an 8 kb region on chromosome 3R highlighting *Hsrω* as in Figure 39. Note, there are 3 separate HSF binding sites both upstream and within the gene body of *Hsrω*.

(B) A NHS (blue) and 2'HS (red) MNase protection assay as in Figure 4 plots the relative level of protection (y axis) versus the center of the amplified primer set's distance from the TSS of *Hsrω*. The error bars represent the SEM from 3 independent experiments.

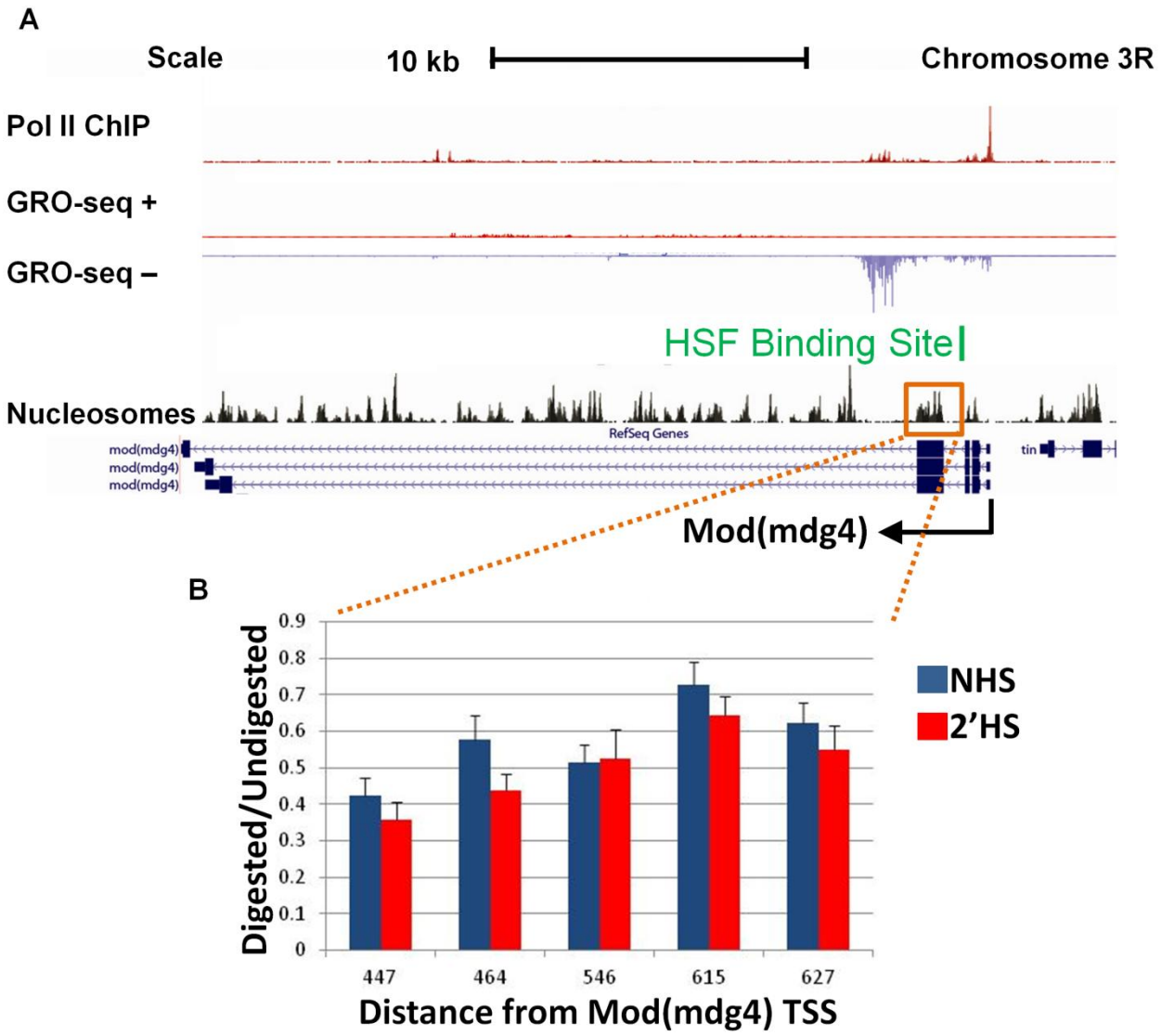

Figure 43 Nucleosome Loss Does Not Occur at *Mod(mdg4)* after Two Minutes of Heat Shock

(A) A UCSC genome browser shows a 20 kb region on chromosome 3R highlighting *Mod(mdg4)* as in Figure 39.

(B) A NHS (blue) and 2'HS (red) MNase protection assay as in Figure 4 plots the relative level of protection (y axis) versus the center of the amplified primer set's distance from the TSS of *Mod(mdg4)*. The error bars represent the SEM from 3 independent experiments.

promoter-proximal HSEs and one downstream of the gene that bind HSF after heat shock (Bendena et al., 1989). *mod(mdg4)* contains just one HSE that binds HSF but is located 200 bp downstream of the TSS and, unlike *Hsrω*, is not known to be upregulated after heat shock. Both genes have high levels of polymerase and show some transcriptional activity before heat shock; however, only *Hsrω* is considered to have a paused polymerase (Figure 42A versus 43A). Interestingly, although both genes are found to be within the same cytological locus, changes in nucleosomes are observed only at *Hsrω* after a heat shock and not at *mod(mdg4)* 80 kb away (Figure 42B versus 43B). These results are not surprising though as the changes observed at the 87A *Hsp70* locus were contained within the scs/scs´ region (~12.5 kb) and did not spread into other regions still contained within the 87A locus (Figure 11).

The final two regions that have been identified to be within regions identified to undergo heat shock puffing upon heat shock are at 64EF and 48E, although along with 33B, these are considered to be only minor heat shock puffs in comparison to the other 6 loci. At 64EF the best candidate gene identified was *DnaJ-1.* *DnaJ-1* is known to be upregulated following heat shock (Leemans et al., 2000), although not to the extent as the previously identified genes. *DnaJ-1* contains two HSEs, one promoter-proximal and another one downstream of its polyA site, that each binds HSF after a 20 minute heat shock. *DnaJ-1* contains a moderately paused polymerase (Figure 44A) at a moderate total level. Surprisingly, *DnaJ-1* does not show any change in chromatin structure by 2 minutes of heat shock (Figure 44B). At

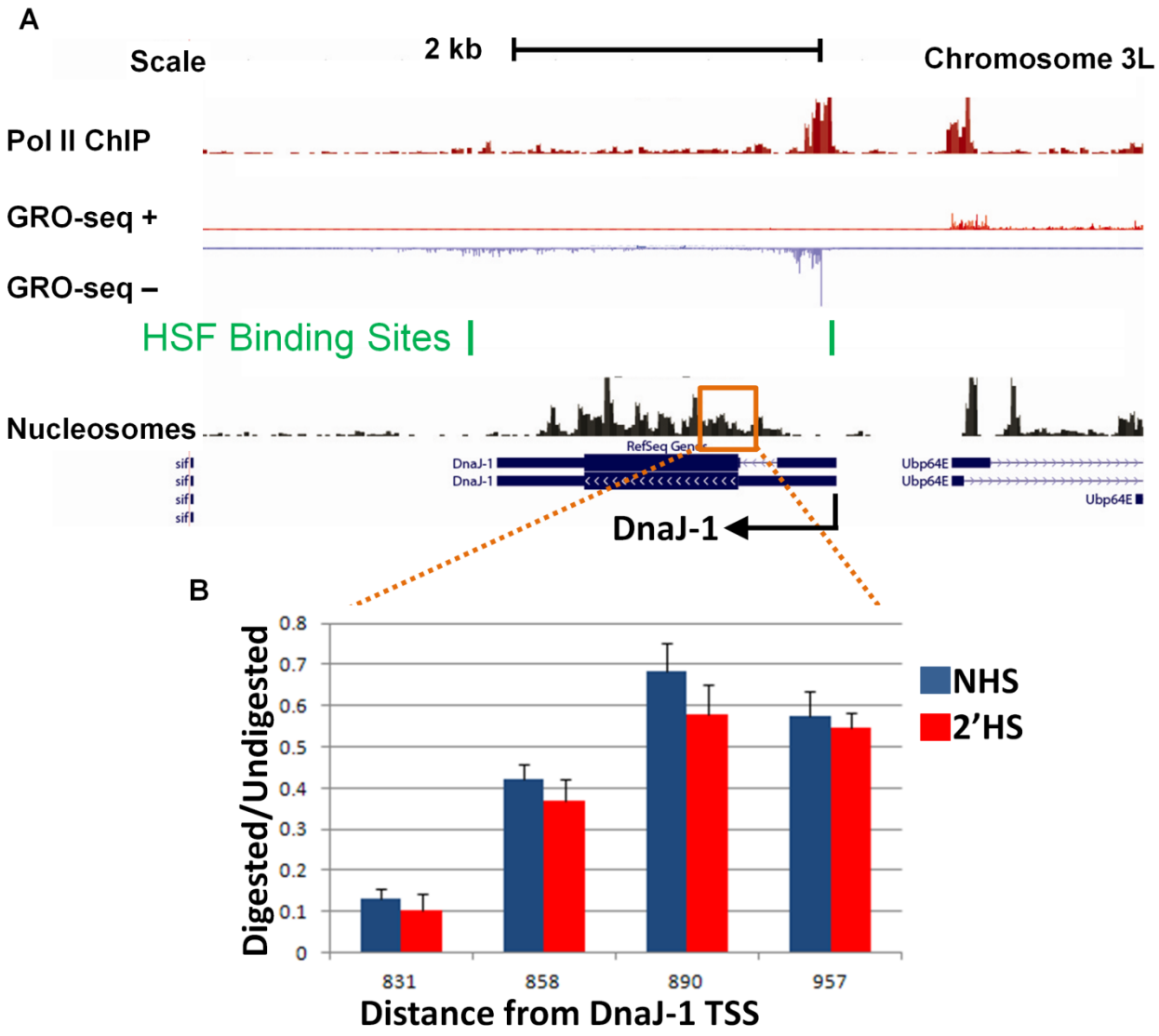

Figure 44 Nucleosome Loss Does Not Occur at *DnaJ-1* after Two Minutes of Heat Shock

(A) A UCSC genome browser shows a 7 kb region on chromosome 3L highlighting *Dm* as in Figure 39. Note, there are 2 HSF binding sites just upstream and downstream of *DnaJ-1*.

(B) A NHS (blue) and 2'HS (red) MNase protection assay as in Figure 4 plots the relative level of protection (y axis) versus the center of the amplified primer set's distance from the TSS of *DnaJ-1*. The error bars represent the SEM from 3 independent experiments.

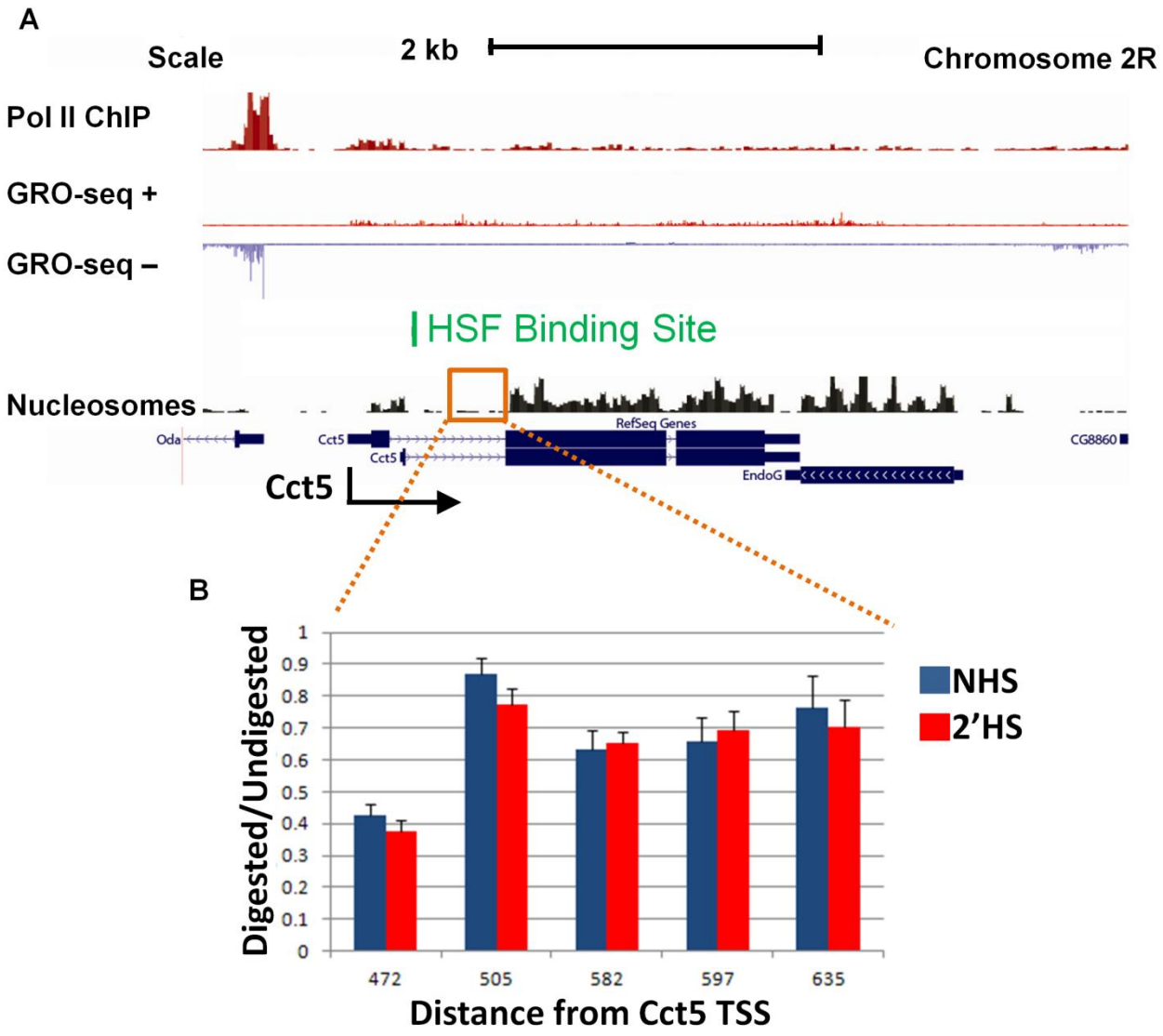

Figure 45 Nucleosome Loss Does Not Occur at *Cct5* after Two Minutes of Heat Shock

(A) A UCSC genome browser shows a 6 kb region on chromosome 2R highlighting *Cct5* as in Figure 39.

(B) A NHS (blue) and 2'HS (red) MNase protection assay as in Figure 4 plots the relative level of protection (y axis) versus the center of the amplified primer set's distance from the TSS of *Cct5*. The error bars represent the SEM from 3 independent experiments.

48E, the gene with the highest level of HSF binding after a 20 minute heat shock was *Cct5*, which contains an HSE 200 bp downstream of its annotated TSS. Unlike the previously analyzed genes, before heat shock, *Cct5* had only minimally detected polymerase and no observable signs of a paused polymerase (Figure 45A). Just like with *DnaJ-1*, *Cct5* did not have any observable change in the mapped nucleosome by two minutes of heat shock (Figure 45B). These results indicate that although HSF is locally recruited to promoter-proximal sites that are within minor sites of heat shock puffing, HSF is not sufficient to bring about changes in nucleosomes at these sites.

4.2.2 Additional Non Heat Shock Puff Sites that Recruit HSF Do Not Exhibit Nucleosome Loss upon Heat Shock

In addition to designing primer sets to the known major and minor heat shock sites, I also chose additional sites outside these regions that HSF bound. These HSF binding sites, as measured by ChIP-seq all showed similar binding strength to the variety displayed from the major heat shock genes (moderate to high levels). However, we were able to chose sites where, like the major heat shock genes, HSF bound in or near the promoter as well as greater the 500 bp, 5000 bp, and 15,000 bp from the nearest gene to determine if HSF could act at greater distances. Also, since HSF's ability to bring about changes in chromatin structure can be decoupled from transcriptional activation of the gene through PARP activation (Petesch and Lis, 2012a), we also chose additional sites that had varying degrees of the

amount of polymerase at the gene (from transcriptionally silent to active) and amount of paused polymerase (from low to extremely high) to determine if HSF could initiate changes in chromatin structure independent of the transcriptional level of the gene. The differences between the 12 sites chosen are summarized in Table 11.

Table 11 Summary of Analyzed Genes with Proximal HSF Binding After Heat Shock, their Pol II and Transcriptional Status, and if they Lose Nucleosomes

Gene	Region	HS Puff	NHS Pol II	NHS transcri-ption	HS upregulated	HSF distance (bp)	Nucleo-some loss
Hsp70	87A/C	+++	++	-	Yes	<500	Yes
Hsp26	67B	++	++	-	Yes	<500	Yes
Hsp22	67B	++	+	-	Yes	<500	Yes
Hsp27	67B	++	++	-	Yes	<500	Yes
Hsp68	95D	++	+	+	Yes	<500	Yes
Hsrω	93D	++	++	++	Yes	<500	Yes
Mod(mdg4)	93D	++	++	++	No	<200 down	No
DnaJ-1	64EF	+	++	+	Yes	<500	No
Cct5	48E	+	-	-	n.d.	<200 down	No
CG3884	49E	-	+	-	n.d.	<500	No
CG9705	73C	-	+	+	n.d.	<500	No
CG33111	95BC	-	++	+	n.d.	<500	No
CG9837	85B	-	-	-	n.d.	<5000	No
Dm	3D	-	+++	+	n.d.	<20000	No

The number of + indicates the relative measured level by GRO-seq or polytene staining heat shock puff size. n.d.= not determined by the literature

The first analyzed gene outside annotated heat shock puffs is *CG3884* located at 49E. HSF binds to a promoter-proximal HSE after heat shock at similar levels to many of the major heat shock puff loci genes, but unlike them, *CG3884* contains little polymerase before heat shock, mainly at its pause site

(Figure 46A). Although there is little polymerase present before heat shock, HSF binding proximally to this gene is unable to incite changes in a nucleosome that was mapped just downstream of its TSS following a two minute heat shock (Figure 46B).

The second analyzed region is similar to many sites in that HSF is recruited to the locus at moderate levels after heat shock, except it is betwixt two divergent genes, *CG9705* and *CG13025*. HSF binds proximally to *CG9705* and just outside the 500 bp promoter region of the upstream *CG13025* gene. The *CG9705* gene has a low level of transcription across its gene before heat shock, whereas *CG13025* is almost transcriptionally silent before heat shock as measured by GRO-seq (Figure 47A). HSF theoretically could potentially induces changes in chromatin structure in either a uni or bidirectional manner, and this was the rational for choosing a site that could be easily measured for this property. Unfortunately, no detectable changes in either nucleosome at *CG9705* or *CG13025* could be observed after a two minute heat shock (Figure 47B).

The next three analyzed regions were chosen for their differing distances in which HSF bound from the closest TSS. The three genes, *CG33111*, *CG9837*, and *Dm*, contain an HSE that binds HSF within the promoter-proximal region of the gene, within 5 kb, and within 15 kb of the gene respectively. There is no indication that the binding of HSF to these intergenic regions can actually affect a gene from such a distance, but these rare binding events so far from a nearby gene are interesting natural cases worth including.

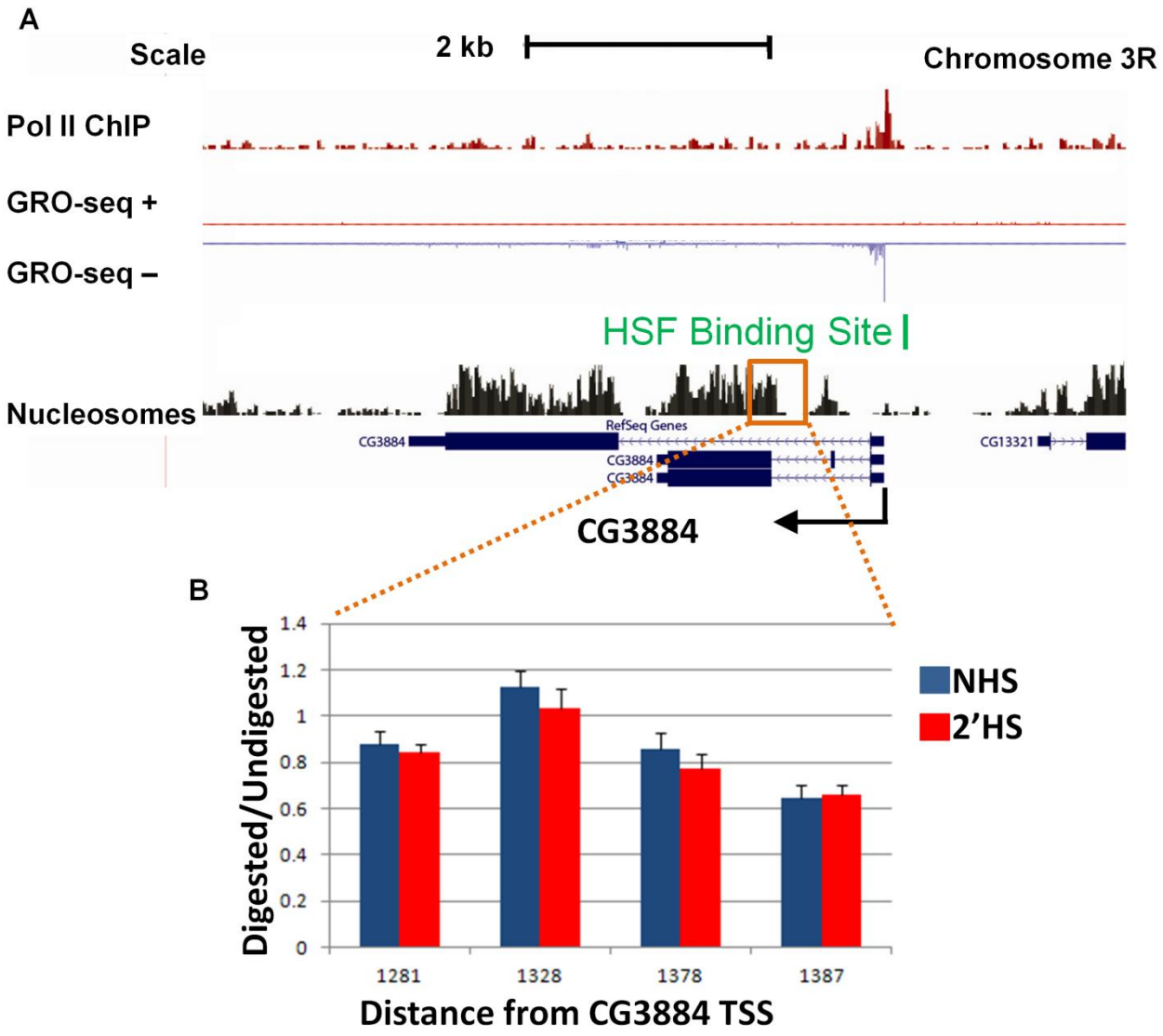

Figure 46 Nucleosome Loss Does Not Occur at *CG3884* after Two Minutes of Heat Shock

(A) A UCSC genome browser shows a 7 kb region on chromosome 3R highlighting *Cct5* as in Figure 39.

(B) A NHS (blue) and 2'HS (red) MNase protection assay as in Figure 4 plots the relative level of protection (y axis) versus the center of the amplified primer set's distance from the TSS of *Cct5*. The error bars represent the SEM from 3 independent experiments.

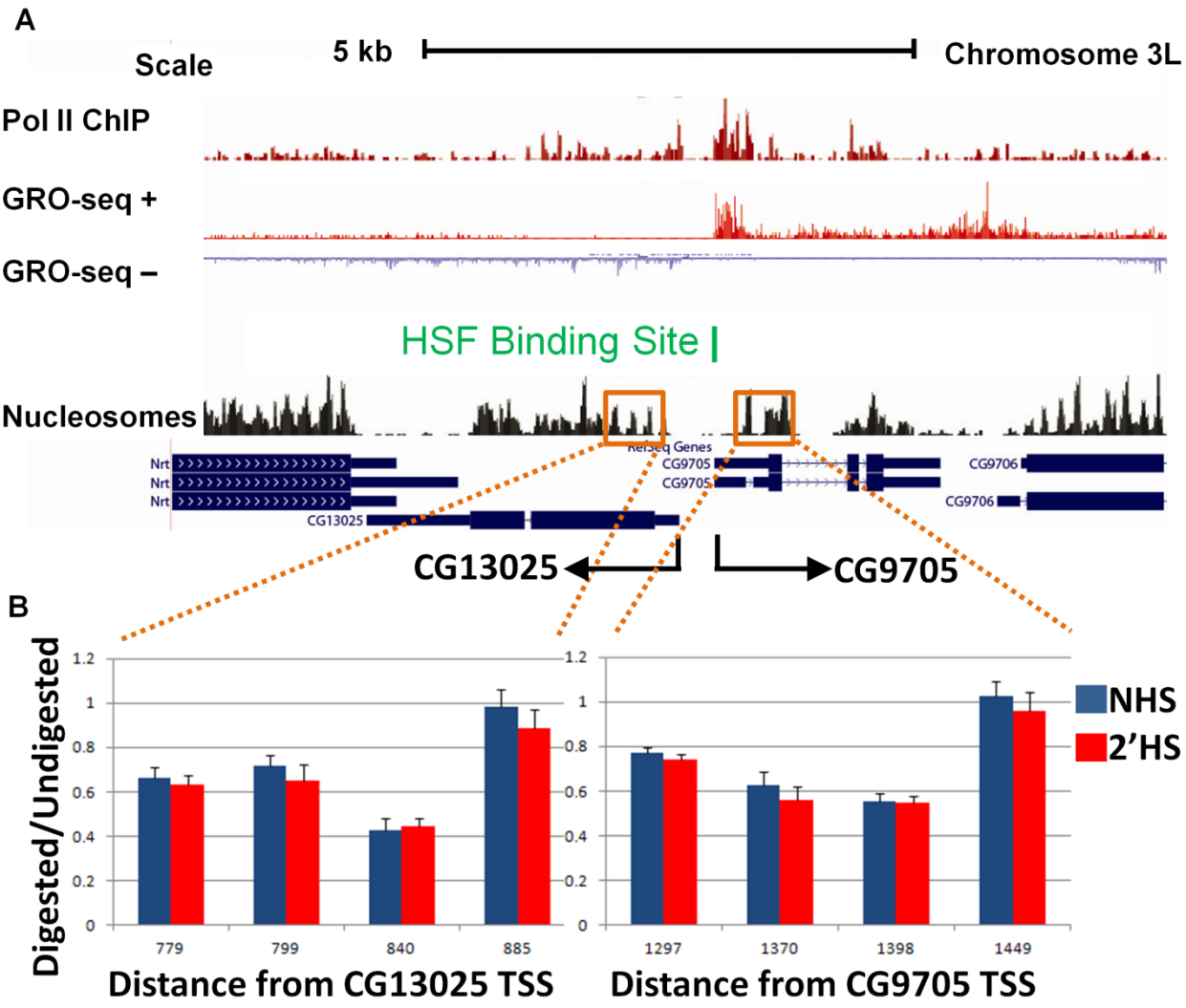

Figure 47 Nucleosome Loss Does Not Occur at *CG130125* or *CG9705* after Two Minutes of Heat Shock

(A) A UCSC genome browser shows an 8 kb region on chromosome 3L highlighting divergent *CG13025* and *CG9705* as in Figure 39.

(B) A NHS (blue) and 2'HS (red) MNase protection assay as in Figure 4 plots the relative level of protection (y axis) versus the center of the amplified primer set's distance from the TSS of either *CG13025* or *CG9705*. The error bars represent the SEM from 3 independent experiments.

The first gene, *CG33111*, has a moderate level of paused polymerase at the gene and mild transcription before heat shock (Figure 48A). Additionally, it has a fairly high level of HSF detected by ChIP-seq and appears a likely candidate for nucleosome loss upon heat shock; however, no detectable changes were observed at the mapped nucleosome following heat shock (Figure 48B). The second gene, *CG9837*, appears to have HSF that binds an HSE approximately 5 kb upstream of its gene at a moderate level, in the middle of what appears to be post polyA transcription from the nearest upstream gene, transcribed in the same orientation (Figure 49A). *CG9837*, like *CG3884*, contains very little polymerase at its gene before heat shock as detected by GRO-seq. After heat shock, HSF is unable to affect changes in the mapped nucleosome at *CG9837* from such a considerable distance (Figure 49B). The final gene, *Dm*, is a very unusual case in which HSF moderately binds to two separate HSEs, approximately 2 kb apart, after heat shock in a gene poor region that is not transcribed before heat shock (Figure 50A). The closest gene promoter, almost 20 kb away, is the *Dm* gene (the homolog of c-myc), which contains an extremely high level of paused polymerase. Heat shock does not induce significant changes in nucleosomes across the *Dm* 5' end of the gene after a two minute heat shock (Figure 50B), as this distance from the HSE is larger than the entire scs/scs´ region.

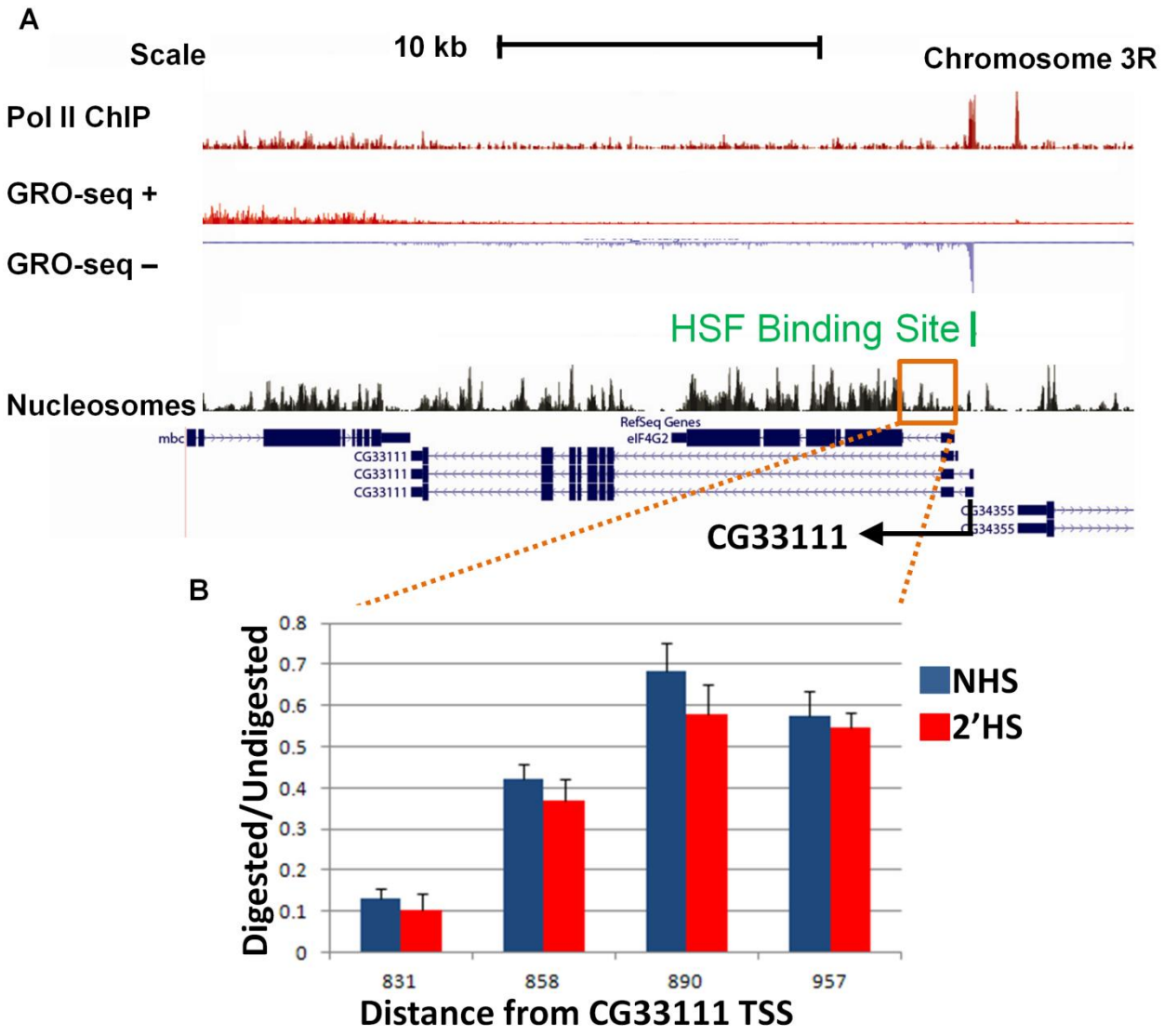

Figure 48 Nucleosome Loss Does Not Occur at *CG33111* after Two Minutes of Heat Shock

(A) A UCSC genome browser shows a 30 kb region on chromosome 3R highlighting *CG33111* as in Figure 39.

(B) A NHS (blue) and 2'HS (red) MNase protection assay as in Figure 4 plots the relative level of protection (y axis) versus the center of the amplified primer set's distance from the TSS of *CG33111*. The error bars represent the SEM from 3 independent experiments.

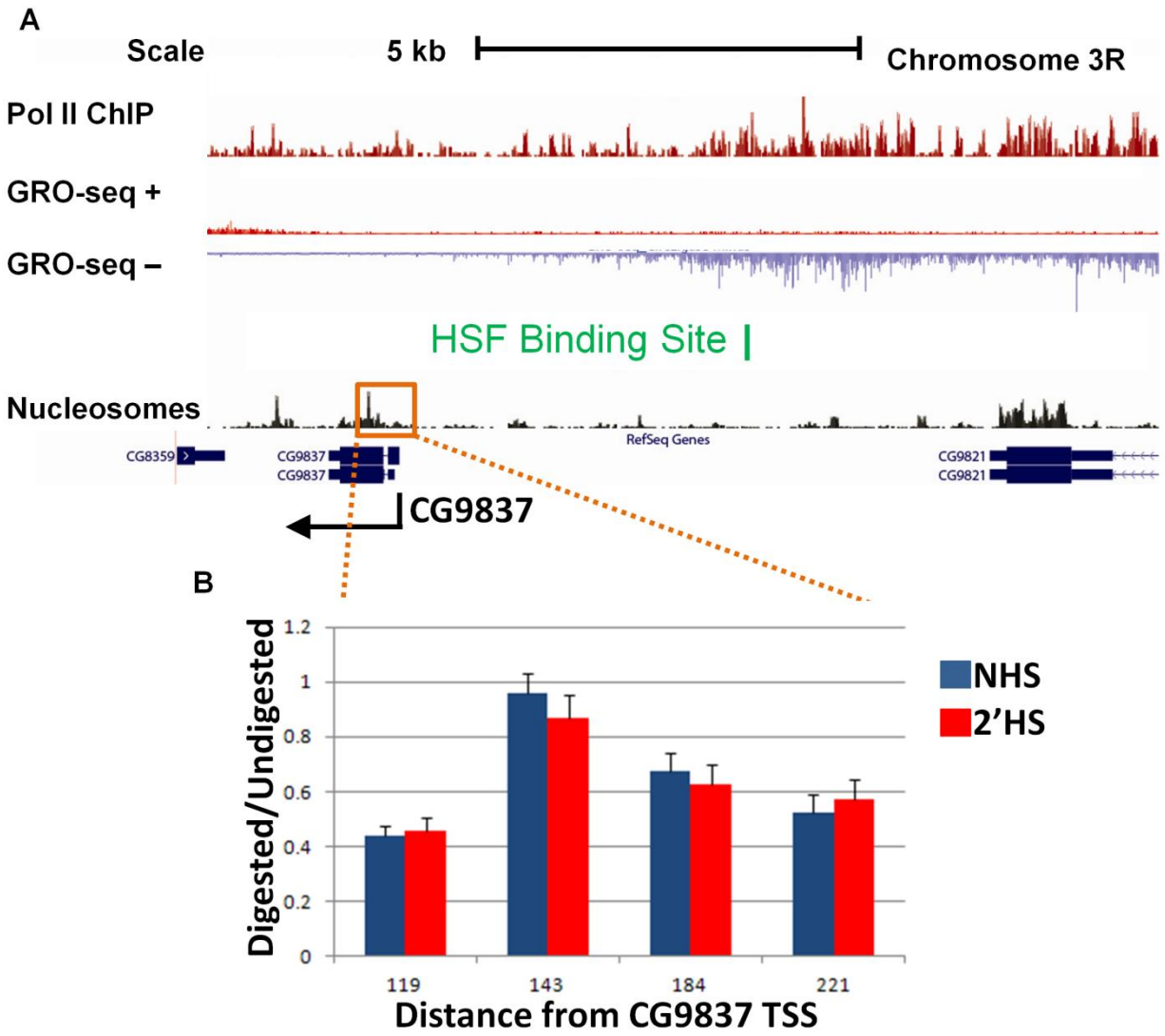

Figure 49 Nucleosome Loss Does Not Occur at *CG9837* after Two Minutes of Heat Shock

(A) A UCSC genome browser shows an 8 kb region on chromosome 3R highlighting CG*9837* as in Figure 39.

(B) A NHS (blue) and 2'HS (red) MNase protection assay as in Figure 4 plots the relative level of protection (y axis) versus the center of the amplified primer set's distance from the TSS of *CG9837*. The error bars represent the SEM from 3 independent experiments.

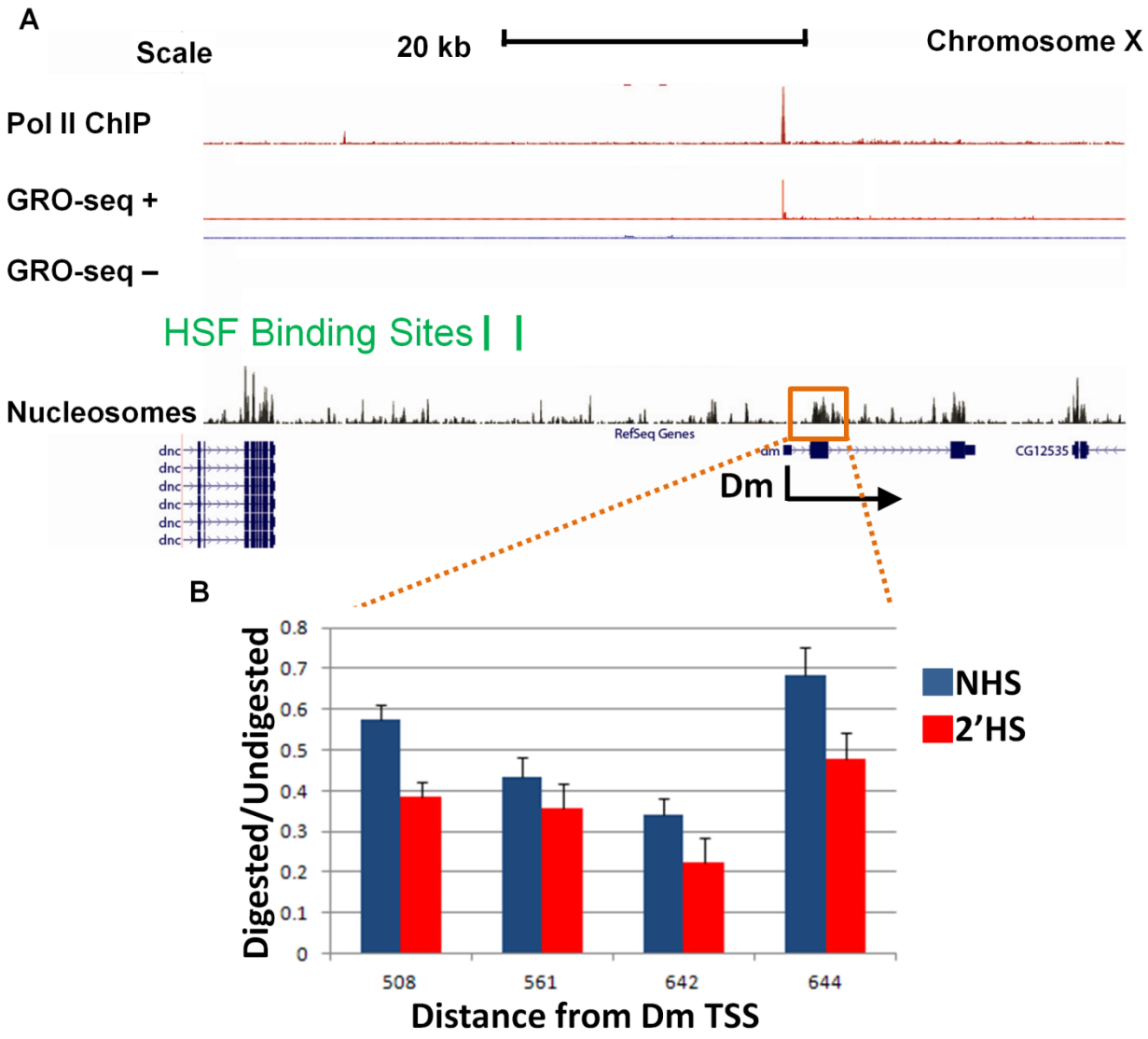

Figure 50 Nucleosome Loss Does Not Occur Across *Dm* after Two Minutes of Heat Shock

(A) A UCSC genome browser shows a 60 kb region on chromosome X highlighting *Dm* as in Figure 39. Note, there are 2 HSF binding sites almost 20 kb from upstream of the gene. The nearest upstream gene, is oriented in the same direction as *Dm*.

(B) A NHS (blue) and 2'HS (red) MNase protection assay as in Figure 4 plots the relative level of protection (y axis) versus the center of the amplified primer set's distance from the TSS of *Dm*. The error bars represent the SEM from 3 independent experiments. Only a significant difference was found from the first primer set (+508, $p<0.05$, student T-test).

4.2.3 Major Heat Shock Puff Sites Require HSF, PARP, and Tip60 to Lose Nucleosomes following Heat Shock

Although HSF is unable to bring about changes at every site that it binds to locally within the genome, regardless of the strength of HSF binding, its distance, or the relative amount of polymerase at the gene before heat shock, I did discover that nucleosomes are lost at four additional major heat shock sites following heat shock in a similar rapid manner to *Hsp70* and *Hsp26*. To determine if a similar mechanism that is utilized at *Hsp70* following heat shock, I preformed RNAi depleted HSF, PARP, and Tip60 as previously performed to determine if the same factors were utilized at these other sites that do lose chromatin structure following a short heat shock.

The results for all four genes that were found from this study to lose nucleosomes upon heat shock, *Hsp22*, *Hsp27*, *Hsp68*, and *Hsr*ω, are shown in comparison for each primer set with control LacZ RNAi samples in dark blue and dark red for NHS and heat shock samples and the corresponding RNAi NHS in light blue and heat shock in pink. As expected, all four genes were completely dependent on HSF for their ability to lose their chromatin structure following heat shock (Figures 51 A-D). Additionally, all these genes were dependent on the presence of PARP (Figures 52 A-D) and Tip60 (Figures 53 A-D) in order to undergo changes in nucleosomes near the 5' end of their genes after two minutes of heat shock.

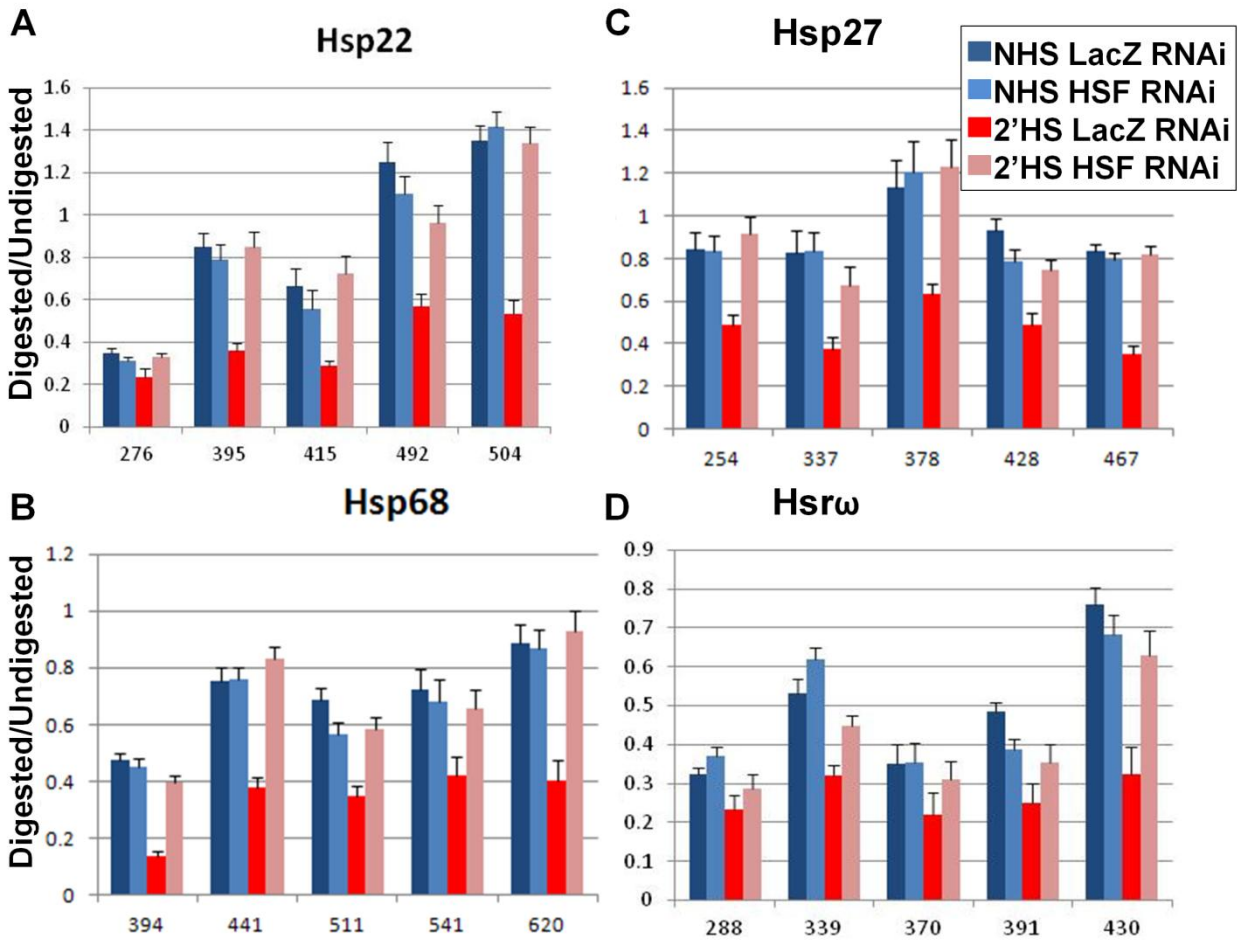

Figure 51 Nucleosome Loss at *Hsp22*, *Hsp27*, *Hsp68*, and *Hsrω* after Two Minutes of Heat Shock is Dependent on HSF

The nucleosome protection profile for LacZ control RNAi for NHS (dark blue) and 2' HS (dark red) is plotted along with HSF RNAi knockdown for NHS (light blue) and 2'HS (pink) as in Figures 39-42 with the relative level of protection (y axis) versus the center of the amplified primer set's distance from the TSS for *Hsp22* (A), *Hsp68* (B), *Hsp27* (C), and *Hsrω* (D). The error bars represent the SEM from 3 independent experiments.

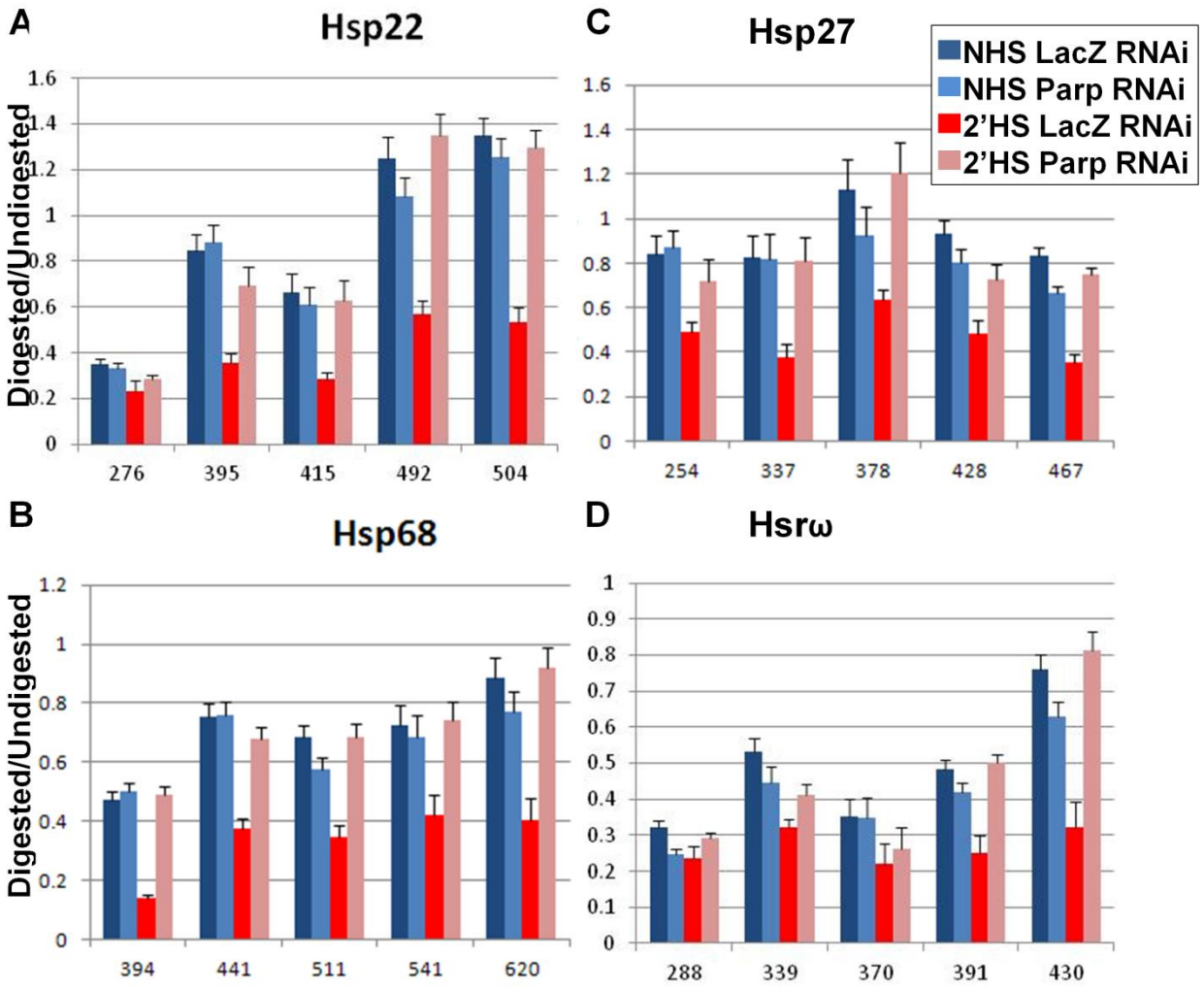

Figure 52 Figure 51 Nucleosome Loss at *Hsp22*, *Hsp27*, *Hsp68*, and *Hsrω* after Two Minutes of Heat Shock is Dependent on PARP

The nucleosome protection profile for LacZ control RNAi for NHS (dark blue) and 2' HS (dark red) is plotted along with HSF RNAi knockdown for NHS (light blue) and 2'HS (pink) as in Figures 39-42 with the relative level of protection (y axis) versus the center of the amplified primer set's distance from the TSS for *Hsp22* (A), *Hsp68* (B), *Hsp27* (C), and *Hsrω* (D). The error bars represent the SEM from 3 independent experiments.

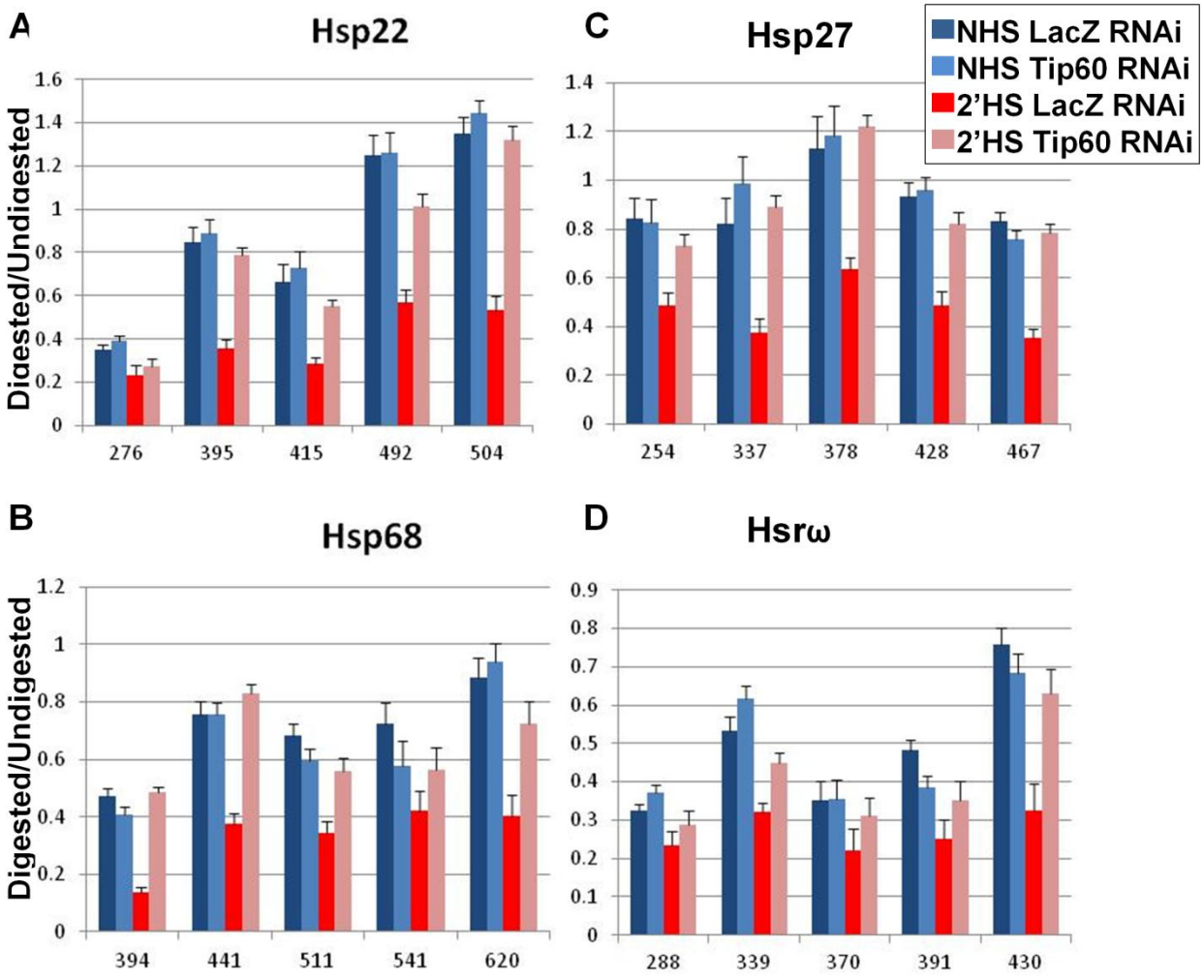

Figure 53 Figure 51 Nucleosome Loss at *Hsp22*, *Hsp27*, *Hsp68*, and *Hsrω* after Two Minutes of Heat Shock is Dependent on Tip60

The nucleosome protection profile for LacZ control RNAi for NHS (dark blue) and 2' HS (dark red) is plotted along with HSF RNAi knockdown for NHS (light blue) and 2'HS (pink) as in Figures 39-42 with the relative level of protection (y axis) versus the center of the amplified primer set's distance from the TSS for *Hsp22* (A), *Hsp68* (B), *Hsp27* (C), and *Hsrω* (D). The error bars represent the SEM from 3 independent experiments.

4.3 Conclusions

These results reinforce the generality of the findings from a detailed study of *Hsp70* whereby an ordered mechanism leads to changes in chromatin structure at many heat shock genes in *Drosophila* first through HSF recruitment to a promoter-proximal region, followed by Tip60 induced activation of PARP followed by PAR destabilization of the underlying chromatin structure of the locus. Although this survey of selected regions in the genome is by no means representative of the entirety of the genome it expands our current knowledge of what is likely to be sufficient to bring about the rapid changes in nucleosomes on gene bodies from a PARP-dependent mechanism.

The first general finding from these results confirms the many years of research into heat shock genes from polytene chromosomes. Whereas by both immunological staining of HSF on polytene chromosomes (Westwood et al., 1991) and more sophisticated ChIP-seq analysis (Guertin et al., 2010) demonstrates that HSF binds to hundreds of locations following heat shock, not every site that HSF binds to induces changes in the underlying chromatin structure. From my small survey of selected regions, the findings that the 6 major heat shock puff sites are also regions of the genome where HSF binds and induces local changes in the chromatin structure through a rapid mechanism by just two minutes of heat shock. Although the other three minor heat shock puff sites did not either have significant HSF ChIP-seq signal or changes in chromatin structure following a two minute heat shock, this does

not discount the fact that there might be other genes within this region that is undergoing some sort of chromatin decondensation or that the changes might occur later in heat shock. A longer heat shock might be needed for the kinetics of HSF or Tip60 recruitment or PARP activation. Additionally, these minor heat shock sites might rely on a separate method for chromatin decondensation after a longer heat shock when polymerase density has built up and transcription-dependent factors have remodeled the nucleosomes, which occurs at *Hsp70* following the first minute of heat shock when polymerase indeed builds up on the gene.

The second important finding from these results is that HSF recruitment to a gene promoter is not sufficient to elicit local changes in nucleosomes upon heat shock. The genes selected for these 12 additional sites all contained moderate to high levels of HSF binding, as observed at *Hsp70* and *Hsp26* after heat shock. The majority of the genes contain an HSE within 200 bp of the TSS, as with *Hsp70* and *Hsp26*, however, this proximity alone is not enough to bring about changes in nearby well-occupied nucleosomes following heat shock at all sites. Even though those genes with HSF binding at a distance did not have changes in their underlying chromatin structure after heat shock, it does not discount the fact that HSF could locally change the intergenic chromatin structure locally. It also does not discount the possibility that it may take more time to form a higher order chromatin structure in which HSF can reach over such large distances. It is just as likely, however, that HSF can only act over short distances through the limitations of Tip60's ability

to locally acetylate its targets.

The final finding from this survey is that although not predictive, the sites that did change its nucleosome protection pattern upon heat shock also contained paused polymerase before heat shock. These results might speak to another correlation that exists between the presence Pol II at the 5' of a gene and PARP occupancy at that gene (Krishnakumar et al., 2008). It is not clear at this point what is unique about the sites that do observe losses in nucleosome protection following heat shock as opposed to genes like *DnaJ-1* and *CG33111* which like the major heat shock genes also contain paused polymerase before heat shock and recruit HSF to its promoter. Results from a ChIP seq of PARP (Appendix B) are likely to draw more distinctions between the regions that are capable of undergoing changes in chromatin structure in a rapid fashion following heat shock and HSF recruitment.

4.4 Experimental Procedures

All of the experimental procedures for this chapter follow those outlined in sections 2.4.2, 2.4.3, 2.4.5, and 2.4.6. The following table lists the primer sets used in this chapter to the additional 12 sites that were designed.

Table 12 Primer Sets Used in Survey of Additional 12 Loci

Gene:	**Hsp22**
Center of Amplicon	Forward Primer
276	CTACAATGCGTTCCTTACCGATG
395	TACCGAGGAACTGGCAGCAGATT
415	TTTGGAGTGTGGCGCTACCGA
492	ACGTCAAGGACTACAGCGAGCTAA
504	TAAAGGTCAAGGTGCTGGACGAGA
Center of Amplicon	Reverse Primer

276	GCTCGTGGAAGAAGGCGTGAAA
395	TTGACGTCCAGGGTGAGTTTGT
415	TGTAGCCATCCTTGTTGACGGT
492	GGCTTCCTATTTCAATCTTTCAAAA
504	TGCCTGGAGCTATAGCCACCTT

Gene: Hsp27

Center of Amplicon	Forward Primer
254	TACTGCCCAACACCCTGGGACT
337	AGCCATGGCCACCACAATCAAA
378	CAAAGATGGCTTCCAGGTGTGCAT
428	ATGTGTCGCAGTTCAAGCCCAA
467	TGGACAACACCGTGGTGGTAGA
Center of Amplicon	Reverse Primer
254	ACGCGCGACGTGACATTTGATT
337	AACTGCGACACATCCATGCACA
378	TCTACCACCACGGTGTTGTCCA
428	TGGATCATTCCATGGCCGTCCT
467	AAAGCCCTTGGGCAGGGTATACTT

Gene: Hsp68

Center of Amplicon	Forward Primer
394	TACTTCTCCGCCTCACTGAGCAT
441	ACGACCCTTGTCGTTCTTGATGGT
511	TCCTTGGCGGTCACATTCAGGATA
541	AGTAACGTCGATCTTGGGCACT
620	ACATTGTTGTCCTTGGTCAGAGCC
Center of Amplicon	Reverse Primer
394	TACTTCTCCGCCTCACTGAGCAT
441	TTGGACGCAAACGGTATCCTGA
511	ATTCGATCTCACTGGCGTTCCA
541	AGGGCTCTGACCAAGGACAACAAT
620	TGCAAGCAGTCCAAGACCTTCA

Gene: Hsrω

Center of Amplicon	Forward Primer
288	GGAAACAATGAAACCATACGCAAACCC
339	TTTGCTGGTCAGCGTCGGG
370	TTCGCAATGCAGCAGGCAGTTT
391	TTGGCTAGAAAGTGACCCACTAGG

430	CCAGGATGTAAGGATGTGTGCAGT
Center of Amplicon	Reverse Primer
288	AAACTGCCTGCTGCATTGCGAA
339	TAACTGCCTCAGACTGCCTAGT
370	TCGACACAGAGAGTACTGCACA
391	GCCATCGCCATTCGACACAGA
430	GCTGTGTATGTATACCTGGCTTCC

Gene:	**mod(mdg4)**
Center of Amplicon	Forward Primer
447	GTGGCTGACGTTGTTCAGGAAT
464	ACTGCAAGATAGGCGAAGAGAG
546	GGCACAAACTCACCGATAGCGT
615	ATAACACCAATCGGTGGGCCTTCA
627	TTCACTATTTGGCCCTCGGCG
Center of Amplicon	Reverse Primer
447	ACGCTATCGGTGAGTTTGTGCC
464	ACCCACGCTATCGGTGAGTTTGT
546	AAGGCCCACCGATTGGTGTTAT
615	AACACGAATTTGTCGGCCGGCTT
627	GTGCTGGAACAACTTCAACACG

Gene:	**DnaJ-1**
Center of Amplicon	Forward Primer
868	AAACATATCGTCGCCGCCAATG
947	AAGATCTCGTTGGTATTGCCGC
982	TGTTATCGCCGCCGGTAAAGAA
1012	ATCGCCGTGGAACTGGTAAGTGTA
Center of Amplicon	Reverse Primer
868	ATCCGTTTGGCGCGTTCTTTAC
947	GGCCACATTTGCCCAGTTCTTT
982	TACACTTACCAGTTCCACGGCGAT
1012	AGAAGCGCGACATCTTCGACAA

Gene:	**Cct5**
Center of Amplicon	Forward Primer
472	ACCCGAAGAACAAGGAGCCACTTA
505	TGGGCAGCAAGATCGTGAACAA
582	TGGCCGACATTGAGAAGAAGGA
597	AGGACGTGAACTTCGAGCTCATCA

635	ATGGAGGACTCGATGCTGGTGAA
Center of Amplicon	Reverse Primer
472	AGCACAGCATCCACAGCCATTT
505	TCCTTCTTCTCAATGTCGGCCA
582	TCAACGATGACACCCTTCACCA
597	ATGGCTGAGGGTCTTGTCAACGAT
635	AATGGCCAGCTTGACGTTCCTT

Gene: CG3884

Center of Amplicon	Forward Primer
1281	TAAATGGGAGTACGGTCGGAGT
1328	ACTGCGCCCGGAGGAGTGTAA
1378	ACGTCGTGCTGCTGCTTGATGA
1387	CTGGCCGCCAAATGGAATGTAT
Center of Amplicon	Reverse Primer
1281	ACACCTACGAGGTGCTCATCAA
1328	TCAACACCTACGAGGTGCTCATCA
1378	AAAGTTCATCCATCGCACGGCT
1387	TCTATGTGGGACGCGGACATCA

Gene: CG9705

Center of Amplicon	Forward Primer
1297	CCATGCGCATCCTCCATTGATT
1370	AAACGCAAACACGCGCAAACTC
1398	AAACATAGCTCCGCTCGGGCCTT
1449	TGAAATCCTTCAGCCGCACCAA
Center of Amplicon	Reverse Primer
1297	GAGTTTGCGCGTGTTTGCGTTT
1370	TGCGGCTGAAGGATTTCACCAT
1398	AATGAAGCCGTGTCCTTTGGTG
1449	TCACTTACTCGGAAACGTGGCA

Gene: CG13025

Center of Amplicon	Forward Primer
779	TGGGGAAAGCTGCATTCGGCGGTG
799	CGGCGGTGGTTAAACGAAAGCCAT
840	CAGTGCAAGACGAAGGCCACATTTAG
885	TCATCTGTATGCGAAGCGCATTCAG
Center of Amplicon	Reverse Primer
779	CGGATATCTCTAAATGTGGCCTTC

799	TGAATGCGCTTCGCATACAGATGACG
840	CAGCTGCTCCCTAATATCCGTGTCC
885	GCTTCGCGGTAGCCAGCTCTGTTGTTAG

Gene:	**CG33111**
Center of Amplicon	Forward Primer
831	TACCGCTTCCTGTGCTTCGATT
858	AGGTAGACCTGCCTTTAAGCCT
890	TTCCCTTGACACCTGGTCAAGCTCTA
957	CTCCTCCTGCTGCTGCTTATTT
Center of Amplicon	Reverse Primer
831	AAGCCGGATAGGCTTAAAGGCA
858	ACGGAGGAGCAAATAAGCAGCA
890	AGACGAGGAGTTTCCACGAGAA
957	TTCCGGATAGAGCCAACAACCA

Gene:	**CG9837**
Center of Amplicon	Forward Primer
119	AGCCTTAGTAGTCGCTCCTTCGTT
143	AATGGTCTTGTCGATGGTGTCGGA
184	GCTGCTGTACGTGAAAGTCCAA
221	AAGTGAAACCGCATGCTACCCT
Center of Amplicon	Reverse Primer
119	AGCCTTAGTAGTCGCTCCTTCGTT
143	AGGGTAGCATGCGGTTTCACTT
184	TTGTGCAAGCCTGCTGGATGTT
221	TTTGGTCCAGGCATGTTTCCGA

Gene:	**Dm**
Center of Amplicon	Forward Primer
508	CTGGAAAGCAAAGGAAGCTAACTAA
561	ACGGAAACTATGTTCAGCGAGGTG
642	TCGGAACGCAACGACTTCAA
644	AAATCGCGCCACTACGGG
Center of Amplicon	Reverse Primer
508	TTTGCACTCACCTCGCTGAACA
561	TTGAAGTCGTTGCGTTCCGA
642	TGTGTGTGAGAGCACCGTTA
644	TCATTGTGTGTGAGAGCACCGT

CHAPTER 5 POTENTIAL FUTURE DIRECTIONS OF THE PROJECT

The purpose of this chapter is to provide any additional future member's of the Lis lab potential future areas to pursue given the results of this project.

5.1 Determining if the Components and Mechanism Used by *Hsp70* is General for Sites that Undergo Chromatin Decondensation Following Heat Shock

My preliminary results looking at various sites throughout the genome where HSF binds following heat shock have identified other sites that rely on HSF, Tip60, and PARP to disrupt a gene's nearby chromatin structure, just as with *Hsp70*. The most logical next step to extend these results in an unbiased genome-wide method is to follow up on the non heat shock PARP ChIP-seq results with an additional Tip60 ChIP-seq (or H2AK5Ac ChIP-seq) following heat shock. It is likely that an entire constellation of factors need to assemble locally, like at *Hsp70*, to bring about a rapid, transcription-independent loss of nucleosomes, and this is the limiting factor in determine which sites within the genome undergo changes in chromatin decondensation. If the purposed model in Figure 3 is correct, HSF needs to be able to bind locally to a site that already has PARP deposited before heat shock and then additionally recruit Tip60 to the same region. If the additional results obtained from the Tulin lab are correct there may be additional factors that need to be present at this locus, including the histone variant H2Av and the unknown kinase that

specifically phosphorylates S137 at this site (Kotova et al., 2011). As HSF limits the potential for a genome-wide decondensation event to just 464 sites scattered throughout the genome, it is not surprising that perhaps an overlap of many of these additional factors may provide an even limited set within this 464 sites to perhaps just the 9 first observed in polytene heat shock puffs.

One additional very interesting and largely outstanding question is what determines the sites of PARP deposition before heat shock. Although PARP binds to many different DNA structures as well as nucleosomes, it is likely that there is an additional factor that helps specify where PARP will bind throughout the genome. The non heat shock PARP ChIP-seq data will easily be correlated with ModEncode ChIP-chip data to help illuminate this point.

5.2 Determining How the Tip60 Complex is Capable of Activating PARP in vivo

My results indicate that the Tip60 complex is necessary for the activation of PARP at *Hsp70*, and likely other sites that lose their nucleosome structure upon heat shcok, but the exact method with which this occurs is unknown. The dTip60 complex is able to interact directly with HSF (personal communication with Tom Kusch) but there is no evidence that it interacts with PARP. It is unclear if the acetylation activity is actually required for this process. Although mammalian PARP-1 is activated by acetylation by other histone acetyltransferases (Hassa et al., 2005), there is no indication that it can be acetylated by Tip60, and those sites that are acetylated in the

mammalian PARP-1 are poorly conserved in dPARP. There also is not a well defined and specific inhibitor of the MYST family of acetylases, which would be helpful to determine if the acetylation activity of Tip60 is necessary or if some additional method is used.

The most likely working hypothesis is that the Tip60 complex contains the homolog of the SWR1 remodeler, and is capable of exchanging H2Av-H2B dimers into nucleosomes that have H2A-H2B or H2AvK5AcS137P-H2B dimers. The most logical test of this hypothesis is to in vitro assemble chromatin with PARP and see if PARP activity is stimulated by addition of the dTip60 complex, or just a SWR1 chromatin remodeler. These experiments would speak to a general method with which to regulate PARP activity while it is still bound to nucleosomes genome-wide. It does not seem to be a coincidence that different variants of H2A, H2Av in *Drosophila* (Kotova et al., 2011) and macroH2A (Nusinow et al., 2007; Ouararhni et al., 2006) in mammals, each seem to be able to regulate PARP activity.

5.3 Determining the Target of PARP Activation that Facilitates Chromatin Decondensation

One of the most troublesome and interesting question that still has yet to be definitively answered is what the target of PARP's catalytic activity upon heat shock is and how does that bring about changes in chromatin structure. The biggest hurdle to being able to answer this question is that there are no specific reagents available yet to identify specific PARylated targets as there is

with other PTMs. An antibody, or even an RNA aptamer, recognizing automodified PARP or even PARylated histones would prove to be an invaluable reagent to be able to specifically detect the target of PARP's activity at *Hsp70* following heat shock. Additionally, a targeted mutational approach could be used to try and re-express mutant forms of potential targets of PARP's activity that are not able to be PARylated. Although there is some indication of potential sites on both PARP and histones that might be sites that can be PARylated it is less clear that mutations in these sites actually ablate the ability of PARP to PARylate the target. A more unbiased method would potentially be to identify which proteins are PARylated following heat shock by mass spec and further characterize which residues on those proteins that are sites of PARylation.

One tangential question that this also brings up would be to be able to show that perhaps just PARylated PARP, as speculated from my results, is the likely target upon heat shock and this alone is sufficient to bring about chromatin decondensation. To try and address this question I have entertained the idea of trying to deliver an in vitro PARylated PARP back into the cell to try and observe if chromatin now decondenses near regions where PARylated PARP was reintroduced. The biggest hurdle to this process is that methods such as electroporation or transfection are only able to deliver a protein that is the size of PARylated PARP (114 kDa) to the cytoplasm but not the nucleus. It is likely that another sophisticated method needs to be developed to be able to reintroduce PARylated PARP into the nucleus of cells.

5.4 Establishing the Generality of Transcription Independent Nucleosome Loss

One of the most shocking observations from my initial study is that the nucleosome loss that occurs at *Hsp70* following heat shock can be decoupled from transcription. My results also speak to a method whereby this process is dependent upon PARP's catalytic activation. Thus far, this transcription-independent nucleosome loss has only been observed at *Hsp70* and *Hsp26*. To better understand how general this process is on a more genome-wide scale, the most logical first step would be to define regions of the genome that undergo chromatin decondensation upon a stimulus like heat shock. This could be done with the increased depth and length of high throughput sequencing today with MNase-seq experiments. In addition to being able to provide a large array of data, these results could also be coupled with conditions in which transcription was halted genome-wide with such inhibitors as DRB or flavorpiridol. These results would provide data about not only those regions with the ability to undergo transcription-independent changes in chromatin, but also be able to identify other regions whose nucleosome assembly or disassembly is dependent on actively transcribing polymerase. Finally, these results would provide a large data set to determine more boundaries of nucleosome loss that occurs at other regions beyond just the scs/scs´ region.

5.5 Determining what Constitutes a Chromatin Insulator and Blocks the Progression of Nucleosome Loss from Occurring

Another exciting finding from my initial results is that traditional chromatin insulators that have been studied for their ability to block enhancer-promoter interactions as well as block position effect variegation is also able to block the spread of nucleosome loss upon heat shock. A single factor has yet to be identified as providing an insulator function as knockdown of either insulator protein, Zw5 or BEAF-32, did not result in an increase locus of nucleosome loss. Although other insulator proteins in *Drosophila* exist or could provide redundancy, such as CTCF, CP190, Chriz, Su(Hw), etc., it appears unlikely from the literature that just one factor is sufficient to establish full chromatin insulator activity.

One attractive hypothesis is that gene promoters, or those that contain paused polymerases like at scs/scs´, and the many associated factors are able to produce the insulating function. This hypothesis is also consistent with other genome-wide chromatin confirmation capture assays that identify active promoters as boundary sites that segregate different classes of chromatin structure, such as active and inactive. The structure of active promoters might also be in some way able to stop the spread of expanding PAR. In addition to information from MNase-seq data to identify potentially new sites of chromatin insulators, one could also make use of the many *Hsp70* transgenic constructs that have been inserted across the genome. These insertions could be used to identify new sites of chromatin insulation that are typically not used at

endogenous heat shock genes. It is possible that genes flanking this insertion site that contain paused polymerase could provide the insulator activity from nucleosome loss spreading after heat shock. Furthermore, this theory could be tested by altering a genes activity by knocking down a critical factor in its transcriptional regulation or by utilizing different cell types in which a nearby gene is differentially expressed.

5.6 Concluding Remarks

The ideas and issues presented as potential avenues for further pursuit are by no means comprehensive. Nor do they begin to address many other key unanswered points as to my original, simple question of how Pol II is able to overcome the nucleosome barrier during transcription. What is the fate of individual remodeled nucleosomes either from Pol II's traversal or through a Pol II independent method that is able to disassemble the nucleosome? Have we identified all the methods that facilitate Pol II's ability to overcome the nucleosome barrier during transcription elongation? What dictates the extent of nucleosome loss at any given transcribed gene? The answers to these and many other questions still need to be addressed to completely understand how Pol II is able to achieve efficient transcript elongation.

APPENDIX A ADDITIONAL FACTORS SCREENED FOR THEIR ABILITY TO FACILITATE TRANSCRIPTIONAL ACTIVATION OF *HSP70* AFTER A 20 MINUTE HEAT SHOCK

The purpose of this appendix is to document the additional factors that I designed RNAi primer sets for to test if they had positive or negative effects on the ability to activate *Hsp70* following a heat shock. The additional RNAi screen performed beyond that initiated by Karen Adelman, Behfar Ardehali, and Nick Fuda grew out of an initial project looking at the effects upstream kinases might have on the heat shock transcriptional response.

A.1 Introduction

Cell viability is critically dependent on the ability of cells to adapt to external stresses created by their environment. One prominent stress that cells must adjust to is external temperatures elevated above the normal physiological level. Cells have adapted over time to develop a heat shock response that produces proteins integral to responding to this immediate threat. This response begins by rapidly transcribing heat shock genes within minutes of a heat shock. One well studied example of this phenomena is the transcription of heat shock protein 70 (Hsp70) in the organism *Drosophila melanogaster*. Upon heat shock, the protein heat shock factor (HSF), usually found in a monomeric state prior to heat shock, trimerizes and binds to regulatory elements upstream of the *Hsp70* gene called heat shock elements

(HSEs). The binding of HSF to HSEs is the key regulatory event that drives the transcription of the *Hsp70* gene.

Many of the ensuing events in the transcription of the *Hsp70* gene in *D. melanogaster* have been well characterized. However, the question remains as to how the external stress of heat propagates itself through the cell and stimulates these well characterized events in the transcription of *D. melanogaster* heat shock genes, including the trimerization of HSF. The mitogen activated kinase (MAPK) signaling cascade has previously been shown to be activated in response to environmental stresses in eukaryotic cells. The MAPK signaling pathways also is conserved from yeast to mammals. Three distinct, major MAPK signaling pathways have been identified: extracellular signal-reuglated kinase (ERK), stress-activated protein kinase/C-Jun N-terminal kinase (JNK), and p38/MK2 kinase. It has been shown that upon heat shock in *D. melanogaster* specific MAP2K and MAP3Ks upstream of the p38 kinase pathway phosphorylate p38 (Zhuang et al., 2006). p38 has been shown to phosphorylate many various transcription factors and/or other downstream kinases that can affect transcription. Likewise, a knockout of p38a, a specific isoform of p38 in *D. melanogaster*, has been linked to its ability to tolerate heat shock conditions (Craig et al., 2004). These two pieces of information indicate that the p38 MAPK signaling pathway may have either a direct or indirect impact role in the transcription of the *Hsp70* gene in *D. melanogaster*.

A.2 Results from Selected RNAi Screens

To answer whether or not the p38 MAPK signaling pathway has an effect on the transcription of the H*sp70* gene RNAi was used to knockdown p38 and potential upstream kinases to try and disrupt the transcript levels of *hsp70*. Primers with a 5' T7 RNA polymerase binding site were designed to produce PCR products that could be used for a transient knockdown of a specific protein. These PCR products were transcribed into ssRNA and reannealed to produce dsRNA. Ten micrograms of the dsRNA was added to 3 mL of $1x10^6$ to *D. melanogaster* S2-S cells. The cells were allowed to grow 3-4 days at room temperature and at which point were split into 4 groups for final cell counts, Western blots, non-heat shock control, and heat shock for 30 minutes at 37 °C. All experiments included a knockdown of LacZ, which S2-S cells do not express, to serve as a negative control. Total RNA from each of the fractions was collected using the QIAgen RNAeasy kit and analyzed using gel electrophoresis. Reverse transcription reactions were performed using oligo dT followed by an RNase treatment. The cDNA products were then analyzed and quantified using real time PCR with primers specifically targeted for the far 3' end of *Hsp70* and *Rp49*, a control gene unaffected by heat shock. Each sample was run in duplicate to quantify *Hsp70* and *rp49* transcript levels. The *hsp70* transcript levels was first normalized to *rp49* to control for the amount loaded in each PCR reaction and then again normalized to either LacZ or untreated cell levels to quantify the decrease in *Hsp70* transcript levels.

Initial experiments knocked down LacZ and HSF as controls along with

p38. Following the initial knockdown of p38 a broader knockdown of other kinases potentially involved in the pathway of p38 were then targeted and knocked down in the same process to screen for other kinases linked in a pathway to p38. The results from this experiment are seen in Figure 54. Knockdown of p38 produced approximately a 30% reduction in *Hsp70* transcript levels, which was consistently obtained in experiments following the first. Other factors that produced significant decreases in *hsp70* transcript levels consistent with a knockdown of p38 alone were the MAP2K lic and the MAP3Ks pk92B and Mekk1. These results are consistent with those upstream kinases previously identified by (Zhuang et al., 2006) as contributing to the phosphorylation of p38 upon heat shock. Double and triple knockdowns must be repeated to optimize the amount of total dsRNA to add in order to authenticate these preliminary results. Also, knockdown of MKK4, a MAP2K known to be a key stimulator of the JNK pathway in *D. melanogaster*, produced the same amount of *hsp70* transcript levels as untreated cells. This indicates that the p38 MAPK and not the JNK MAPK signaling pathway have an effect on the transcription of *Hsp70*.

In addition to these upstream MapK related kinases, I designed additional primer sets to numerous other factors that were used to compile a comprehensive list of additional factors published in (Ardehali et al., 2009). The list of complete RNAi primer sets designed is found in Table 13.

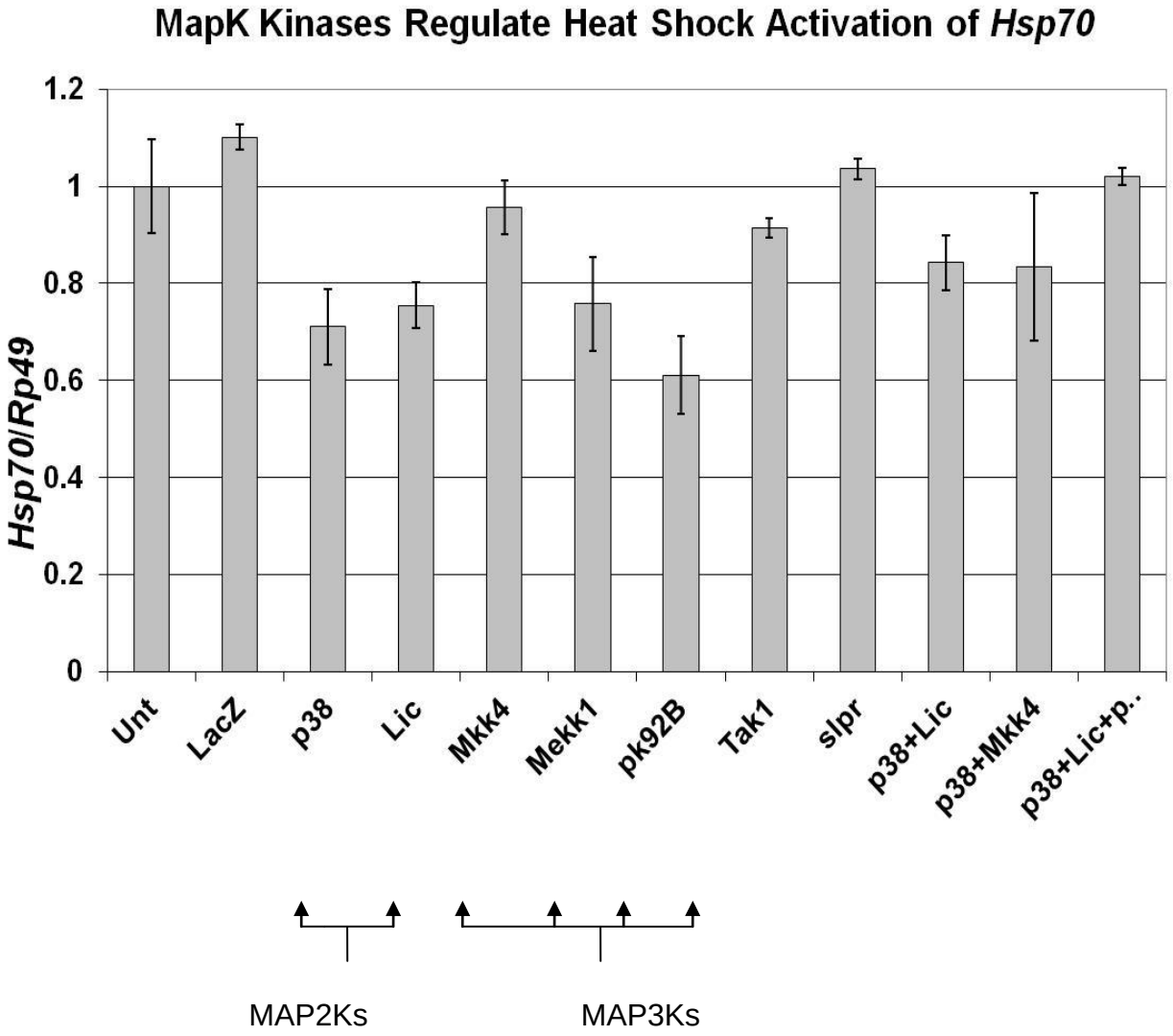

Figure 54 RNAi Screen of Kinases Upstream of p38. Knockdown of p38 and its known upstream kinases (Lic, pk92B, and Mekk1) all resulted in a 30% reduction in *Hsp70* transcript levels. Knockdown of MKK4, a known kinase in the JNK pathway did not reduce HSP70 levels.

A.3 Conclusions

The results from these experiments show that p38 has a significant effect on *Hsp70* transcript levels, but these effects appear to be mild at best. The data indicate that the propagation of the heat shock signal to the nucleus

perhaps is not through a linear p38 signaling pathway but may be a result of a more sophisticated pathway. To further study whether a signaling pathway is responsible for activation of transcription of *Hsp70* in *D. melanogaster* many additional factors can be investigated. First of which would include looking at the basal levels of transcription of each of the factors knocked down. Additionally, RT-q-PCR could be used to quantify the knockdown of each of these factors to confirm that knockdown is occurring at the RNA level since commercial antibodies are not available. Secondly, an antibody against *D. melanogaster* could be raised to determine if p38 actually localizes itself to H*sp70* loci upon heat shock. This could be determined by both ChIP and also by immunofluorescence. Third, the knockdown of factors could be expanded to include the ERK signaling pathway. Finally, Western blots of HSF both before and after heat shock could be used to determine whether or not the knockdown of these factors has an effect on the phosphorylation levels of HSF as found previously with yeast (Sorger and Pelham, 1988). Phosphorylation of HSF after heat shock could be determined by band migration and also by treating whole cell extract with calf intestinal phosphotase both before and after heat shock. This technique if applicable to *D. melanogaster* HSF could identify potential kinases upstream of HSF itself.

Table 13 RNAi Primer Sets Designed and Incorporated into the RNAi Screen Presented in (Ardehali et al., 2009)

Gene Targeted	**Forward Primer Sequence**
p38a	GAATTAATACGACTCACTATAGGGATCCACCGTGATCTTAAGCCCT
p38b	GAATTAATACGACTCACTATAGGGACCATCGTGATCTAAAGCCATCG
DSOR1	GAATTAATACGACTCACTATAGGGATGCATGGAGTATATGGACGGTGGA

LIC	GAATTAATACGACTCACTATAGGGAAATTGGCGACCGGACCTTT
MKK4	GAATTAATACGACTCACTATAGGGACAACCATGTGACCCGCTGTTT
HEP	GAATTAATACGACTCACTATAGGGAGGAGCGTTGTGAATAACGGCA
MEKK1	GAATTAATACGACTCACTATAGGGAAATCAGCCGCGAACAGGTTGT
Pk92B	GAATTAATACGACTCACTATAGGGATGCTTGAACGGCGAAATTCCCA
Tak1	GAATTAATACGACTCACTATAGGGATGATGACCAACAATCGCGGCA
Slpr	GAATTAATACGACTCACTATAGGGATAGCTTTGCACTGCCCAACCA
Dak1	GAATTAATACGACTCACTATAGGGATTTGGCACGAACGACGTTGA
CG8979	GAATTAATACGACTCACTATAGGGACATTTGGTCGTACGGTGTGGT
GAGA Factor	GAATTAATACGACTCACTATAGGGATGGTTATGTTGGCTGGCGTCAA
TBP	GAATTAATACGACTCACTATAGGGATGGCGCACAAACAAATGCAG
Daxx	GAATTAATACGACTCACTATAGGGATAATCGTGATGCAACCGCAGCTT
Med31	GAATTAATACGACTCACTATAGGGATCCTTGCACAGCGTGGATTT
Cdk8	GAATTAATACGACTCACTATAGGGATTGCTGCGCGAACTGAAGCAT
CG3773	GAATTAATACGACTCACTATAGGGATTTGCACCAACTGCCGGACAA
Elp1	GAATTAATACGACTCACTATAGGGATAACATTGAACGCGGTGCGAAGA
Elp2	GAATTAATACGACTCACTATAGGGATCAAAGGACACACAAGTGGCGT
Elp4	GAATTAATACGACTCACTATAGGGATAACAATAGCAGCAGCGTGACCA
Ell	GAATTAATACGACTCACTATAGGGATAACATGTGGCGTCCAACAGCAA
ElonginA	GAATTAATACGACTCACTATAGGGATGCACTGCATCACCAAGCTGTT
ElonginC	GAATTAATACGACTCACTATAGGGATAGGTCTGCATGTACTTCACCT
Pitslre	GAATTAATACGACTCACTATAGGGATTTACCGAGTATCCCGTCTCGCAA
Eaf3	GAATTAATACGACTCACTATAGGGATACTAACAGCACCGCCAACTCTACA
Elf1	GAATTAATACGACTCACTATAGGGATGTAGGGTGTGCTTGGAGGATT
Spt2	GAATTAATACGACTCACTATAGGGATTTTGTTGTCGGCCCGTGAGAAA
Leo1	GAATTAATACGACTCACTATAGGGATAAGAGCCGCAGTCAAAGCAAGT
Ctr9 F	GAATTAATACGACTCACTATAGGGATAAGGCCACCAACTTGTACACCA
NelfA F	GAATTAATACGACTCACTATAGGGATAAGCAATGCTGGTGACAGCTCA
NelfD F	GAATTAATACGACTCACTATAGGGATTGTGGTGGGAGTTGGTGTCATT
Acf F	GAATTAATACGACTCACTATAGGGATGGAGCAAACAGCAAAGGCCA
Dom/Swr1	GAATTAATACGACTCACTATAGGGATAATTAATGCTCCAACGCCCGCT
Nurf38	GAATTAATACGACTCACTATAGGGATACTCAACTCAGGGCTGAAGA
Nurf55	GAATTAATACGACTCACTATAGGGATGCTTGTGGGACATCAATGCCA
Osa	GAATTAATACGACTCACTATAGGGATATGGATCGCAGTGGCAAGGA
Bap111	GAATTAATACGACTCACTATAGGGATCGGTGCCATGTGGAAGTT
Bap45	GAATTAATACGACTCACTATAGGGATTTGTGCCGGCTATTGCACA
Bap60	GAATTAATACGACTCACTATAGGGATGAATCCCGCAGTTTGGGT
Bap55	GAATTAATACGACTCACTATAGGGATCGTGGAATGTCCGCAACAA
Nap1	GAATTAATACGACTCACTATAGGGATAGCAAATGGTCAAGATGCTGCC
Hira	GAATTAATACGACTCACTATAGGGATAGCGATTGCTGTTGCCTCAA

Asf1	GAATTAATACGACTCACTATAGGGATTTGTGCGAAGACAAGCGGA
CBP	GAATTAATACGACTCACTATAGGGATGGCAACATTCCAGCACCACT
PR-Set7	GAATTAATACGACTCACTATAGGGATAGCCACAGCGAACAGCAACAAA
Ash2	GAATTAATACGACTCACTATAGGGATGGTACTTTGAGGTCACCATCG
Art1	GAATTAATACGACTCACTATAGGGATGCATCAAGCGCAACGACTT
Art4	GAATTAATACGACTCACTATAGGGATCCCTGGAGTTTCACATTCTGC
Art5	GAATTAATACGACTCACTATAGGGATCAAAGGACATGCGGGACTT
Rpd3	GAATTAATACGACTCACTATAGGGATAGGCTGCTTCAATCTCACCGT
BCH110	GAATTAATACGACTCACTATAGGGATCCAATCTCGCCTGCCATTT
JMJD2A	GAATTAATACGACTCACTATAGGGATACGTGCAGCCAAATCCGAAGAA
UbcD2	GAATTAATACGACTCACTATAGGGATACCTCCAGTGCCACCTCAAAT
RNF40	GAATTAATACGACTCACTATAGGGATACCCGAAACCAGCTTCAAACGA
Dsp1	GAATTAATACGACTCACTATAGGGATCAGGTTGGCCAATGTGTGT
HMG20A	GAATTAATACGACTCACTATAGGGATGCTTACGAACCACATACCTGTGA
HMGD	GAATTAATACGACTCACTATAGGGATAACCACCCGCAAGCAAACAA
HMGZ	GAATTAATACGACTCACTATAGGGATAGCCAAGAAGGCCAAGAAGA
Rl	GAATTAATACGACTCACTATAGGGATCGCTGAAGTGCCATTTCGGATT
MAPKAPK1	GAATTAATACGACTCACTATAGGGATAGCGATGACATGCCCAAACA
MAPKAPK3	GAATTAATACGACTCACTATAGGGATTGGCTTCGCCAAGGAGACATT
PpD3	GAATTAATACGACTCACTATAGGGATGTATGGATTCACTGGCGAGGT
Wdb	GAATTAATACGACTCACTATAGGGATAGCCGTTGCAGTTGCAGATT
Rai1	GAATTAATACGACTCACTATAGGGATGCATCGGTGTGTGCAGCATAA
B52	GAATTAATACGACTCACTATAGGGATGGTTGAGTTCGCCTCGTTGT
CstF64	GAATTAATACGACTCACTATAGGGATGGATCCCAGGTTAAGGGCA
CstF77	GAATTAATACGACTCACTATAGGGATGGTGCGAGCTCAGCAAGT
Cspf30	GAATTAATACGACTCACTATAGGGATAGCAAGGTGAAGGATTGTCCGT
Cspf160	GAATTAATACGACTCACTATAGGGATAGTGGTTGCCATTTCGGCAT
Sus1	GAATTAATACGACTCACTATAGGGATAGACGCTGCGAAATCGACAA
Magoh	GAATTAATACGACTCACTATAGGGATAACTGGAGATCGTCATCGGA
SSRP1	GAATTAATACGACTCACTATAGGGATAAGAACACCAAGACCGGCAA

Gene Targeted	**Reverse Primer Sequence**
p38a	GAATTAATACGACTCACTATAGGGATAGCCTGTCATCTCGTTCTCCGTT
p38b	GAATTAATACGACTCACTATAGGGATCCGGTCATCTCGCTTTCT
DSOR1	GAATTAATACGACTCACTATAGGGATTGTCGCGCAGATAGCTCAA
LIC	GAATTAATACGACTCACTATAGGGATCGGTTTGCTTATGGCGCA
MKK4	GAATTAATACGACTCACTATAGGGAAATGCACCGCGTCCAATTTCG
HEP	GAATTAATACGACTCACTATAGGGATTCTTGCGCAGCAATAGCGGT
MEKK1	GAATTAATACGACTCACTATAGGGAGACGCATGCGCAAGAACTCAT
Pk92B	GAATTAATACGACTCACTATAGGGATTCGTCTAGTGCCAGCACCTT
Tak1	GAATTAATACGACTCACTATAGGGATTAAAGGGCTGCTTCCTGGACA

Slpr	GAATTAATACGACTCACTATAGGGAAGAAGCAGTGCCGTGGAAACT
Dak1	GAATTAATACGACTCACTATAGGGATGGCCTTGGAATGTCGCAAT
CG8979	GAATTAATACGACTCACTATAGGGAGCTTGAGAGAGTTGTTGCCCA
GAGA Factor	GAATTAATACGACTCACTATAGGGATCTTTACGCGTGGTTTGCGT
TBP	GAATTAATACGACTCACTATAGGGATAATCACAGCCGCAAATCGCT
Daxx	GAATTAATACGACTCACTATAGGGATGCGTCGAAGTCATTGGTGCTT
Med31	GAATTAATACGACTCACTATAGGGATGCTGAAGCTGCTGTTGTTGCT
Cdk8	GAATTAATACGACTCACTATAGGGATGCGGAAAGCCCATCACATT
CG3773	GAATTAATACGACTCACTATAGGGATGTGGACATTGGACTTGGTGGT
Elp1	GAATTAATACGACTCACTATAGGGATGGCGTTGTCCAGTTTGGCAAT
Elp2	GAATTAATACGACTCACTATAGGGATACCGATTCCAAGCTCACTGCAT
Elp4	GAATTAATACGACTCACTATAGGGATAGGCTGTGGCATTGGAATTGCT
Ell	GAATTAATACGACTCACTATAGGGATAGCTTGGCGTGCAGGTAATCAA
ElonginA	GAATTAATACGACTCACTATAGGGATACTGCTGCTGGATTTGCTGGAA
ElonginC	GAATTAATACGACTCACTATAGGGATTCTCGCAGGGACAATCTTCTCGT
Pitslre	GAATTAATACGACTCACTATAGGGATGCGTTATTCCAGCGTTCAGGA
Eaf3	GAATTAATACGACTCACTATAGGGATCCAACGCAGAGTAGCTGAGCAT
Elf1	GAATTAATACGACTCACTATAGGGATCACTCTACGAATCTCCTTTGCG
Spt2	GAATTAATACGACTCACTATAGGGATGTCTTTGCAGCTGCCGGAATTT
Leo1	GAATTAATACGACTCACTATAGGGATAATGCCACTGGTCTTGCTGGAT
Ctr9	GAATTAATACGACTCACTATAGGGATGATTGGCCAGGTGATTGAGCA
NelfA	GAATTAATACGACTCACTATAGGGATTGCCCACAGTGGTTGTGGTT
NelfD	GAATTAATACGACTCACTATAGGGATAATTCGGACACGGGATCGTTGT
Acf	GAATTAATACGACTCACTATAGGGATAATATATGCCCAACGCTGCCGT
Dom/Swr1	GAATTAATACGACTCACTATAGGGATGATTGGATGCAGCAACGCCA
Nurf38	GAATTAATACGACTCACTATAGGGATTAGCGCCCTTCTCAACGGTTT
Nurf55	GAATTAATACGACTCACTATAGGGATAAACATTCTCGGCCATCTGCCA
Osa	GAATTAATACGACTCACTATAGGGATGAGGAAGCCAACTCCGTT
Bap111	GAATTAATACGACTCACTATAGGGATTCGCTGCGCTATTCGCATT
Bap45	GAATTAATACGACTCACTATAGGGATATTGGCCAGTCGTCGCATT
Bap60	GAATTAATACGACTCACTATAGGGATAACTTCATCCGCTGGCAACT
Bap55	GAATTAATACGACTCACTATAGGGATTTGAGCAGCAACCCGTTCGT
Nap1	GAATTAATACGACTCACTATAGGGATATCGATTAGCTTGCGGATGGCG
Hira	GAATTAATACGACTCACTATAGGGATAAAGGCGCAATGCACTGCAGAA
Asf1	GAATTAATACGACTCACTATAGGGATAAAGAGGCTTTGTTGGCGGGTT
CBP	GAATTAATACGACTCACTATAGGGATCTGGACTTGGCCATTTCGT
PR-Set7	GAATTAATACGACTCACTATAGGGATGCGGCCGCTGTTTGATAA
Ash2	GAATTAATACGACTCACTATAGGGATAGCACCTCGGGATACTTGAA
Art1	GAATTAATACGACTCACTATAGGGATACGTGCTGCTGTACAACTTGCT
Art4	GAATTAATACGACTCACTATAGGGATTGCGTGATCCTTGCGTGT
Art5	GAATTAATACGACTCACTATAGGGATAGGCGTATGGGTCAGAGGATTGAT

Rpd3	GAATTAATACGACTCACTATAGGGATGCGCAGGTTCTCGAACAGA
BCH110	GAATTAATACGACTCACTATAGGGATTGCTCCCACATCGGCAAT
JMJD2A	GAATTAATACGACTCACTATAGGGATACGGACAAATTCAGTCTGCCCT
UbcD2	GAATTAATACGACTCACTATAGGGATAGCAGGGAGCAAATTGACAGCA
RNF40	GAATTAATACGACTCACTATAGGGATCGCGCACCGTTTCACTTT
Dsp1	GAATTAATACGACTCACTATAGGGATAGGTTCGCAGACAGTTGAGT
HMG20A	GAATTAATACGACTCACTATAGGGATGCCTCGATGTAGGGCAACTT
HMGD	GAATTAATACGACTCACTATAGGGATTTGCCACCCGATCTTCGATCA
HMGZ	GAATTAATACGACTCACTATAGGGATGACGCGATCGAAAGTTGCT
Rl	GAATTAATACGACTCACTATAGGGATCACGTTTCTTACATCAGGTAGCC
MAPKAPK1	GAATTAATACGACTCACTATAGGGATACAAAGCGTAATGCTGCAGGGA
MAPKAPK3	GAATTAATACGACTCACTATAGGGATGTCCAGCGCCTTGATTTGCAT
PpD3	GAATTAATACGACTCACTATAGGGATAGTTCGGAGCAGAGAAGACTGT
Wdb	GAATTAATACGACTCACTATAGGGATTTCTGTAGCGCGAGGAACCTTGA
Rai1	GAATTAATACGACTCACTATAGGGATTCGGCGCCGTATAGCATCAAA
B52	GAATTAATACGACTCACTATAGGGATAGCGGGAGCGAGAACGAGACTTGA
CstF64	GAATTAATACGACTCACTATAGGGATAGTTTCAGCGCTGGGTACTCTT
CstF77	GAATTAATACGACTCACTATAGGGATAGACCCGACTTGGTTTCCTTCA
Cspf30	GAATTAATACGACTCACTATAGGGATGCAGACCGCTTTCGACCTTT
Cspf160	GAATTAATACGACTCACTATAGGGATAAAGCAAGGATTGACGCCGCAT
Sus1	GAATTAATACGACTCACTATAGGGATACAAATCCAATGACGCTGAG
Magoh	GAATTAATACGACTCACTATAGGGATGTTGTCTGCTACTACATCG
SSRP1	GAATTAATACGACTCACTATAGGGATAGCACCTTCATCACTTTGCCCA

APPENDIX B: CHIP-SEQ ANALYSIS OF PARP IN *DROSOPHILA* S2 CELLS UNDER NON HEAT SHOCK CONDITIONS

At the time of the submission of this thesis, PARP non heat shock ChIP-seq samples have been prepared and sent to be sequenced to determine the overlap of sites where HSF binds inducibly after heat shock and where PARP is present before heat shock. This data set will determine if HSF binding near a site containing PARP deposited before heat shock is sufficient to predict sites where rapid changes in nucleosomes will occur following heat shock, like that observed at *Hsp70*. The following appendix is to document the experimental procedure used to generate the PARP ChIP-seq samples.

Two separate dPARP antibodies raised to separate epitopes, one containing the central and C-terminal domain to dPARP as well as one raised just to the C-terminal domain of dPARP from Alexei Tulin's lab (unpublished data), were both used to provide a list of high-confidence binding sites through the overlap of the two antibody ChIP peaks observed. In addition to further verify a peak detected by ChIP-seq is indeed specific to dPARP and not from a common off-target signal shared between the two antibodies, untreated PARP ChIP-seq samples will be compared to PARP RNAi PARP ChIP-seq samples. A replicate of each untreated and PARP RNAi PARP ChIP-seq sample was used to verify the reproducibility of the experiment for each

antibody.

The original ChIP-seq libraries inputs were verified using a 1.3% agarose gel to image the size of the input DNA to the IPs (Figure 55). 5 separate IPs using 25 µL of each antibody was used for each replicate and each sample (untreated or PARP RNAi) and combined. The resulting PARP ChIP-seq library used ChIP-seq barcodes, with the following 3 bp barcode for the following conditions: Untreated #1: ACT, Untreated #2: GGA, PARP RNAi #1: TTG, PARP RNAi #2: CAC. The same barcodes were used for each antibody and pooled to be sequenced using two separate lanes. At the stage

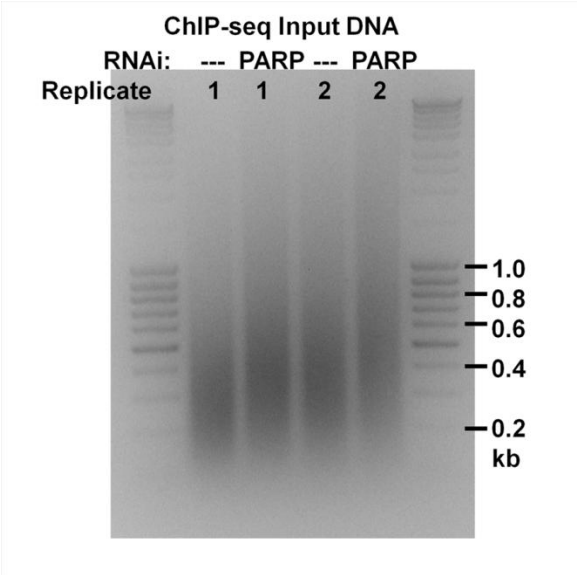

Figure 55 PARP Non Heat Shock ChIP seq Input DNAs

A 1.3% agarose gel was used to visualize the ChIP input DNA from the Untreated #1, PARP RNAi #1, Untreated #2, and PARP RNAi #2 samples (shown from left to right). DNA ladder from Fermentas DNA MassRuler was used to verify the average size of the input DNA size, and flank the 4 samples with a molecular weight marker's sizes labeled on the right in kilobases. The average library size was measured using ImageJ and is as follows: Untreated #1: 320 bp, PARP RNAi #1: 380 bp, Untreated #2: 360 bp, and PARP RNAi #2: 410 bp.

of gel extraction, the amplified library was dissected such that only fragments from the sizes of 100-300 bp were saved to form the final ChIP-seq libraries. The first antibody had a pooled ChIP-seq library with a concentration of 3.1 ng/μL and the second antibody had a pooled ChIP-seq library with a concentration of 4.8 ng/μL.

The following is a record of the material and methods used to generate the ChIP-seq libraries. The general ChIP method outlined in section 2.4.1 was followed with the following exceptions. Cells were cross-linked at 2% final concentration of formaldehyde for 2 minutes and quenched with 0.25 M glycine.

ChIP IP

Protein-A-agarose beads were pre-cleared before the IP step in ChIP IP buffer for 1 hour at 4 C and then blocked with 1 mg/mL of PVP and 1 mg/mL ultrapure BSA (Ambion) in ChIP IP buffer for 1 hour at 4 C. Samples were pre-cleared for each condition (5 IPs worth) for each antibody in 1 15 mL conical with 4x55 uL of blocked beads for 1 hour at 4 C. 1 sample was saved to check the input size of as usual. The pre-cleared beads were spun down at 1,000 rcf for 1 minute and split into 5 IPs (5 epi 1.7 mL tubes) with 55 uL of blocked beads with 25 μL of corresponding antibody for each IP for every condition and replicate and IPed overnight at 4 °C. The subsequent washes, elutions, reversal of cross-links, phenol:chloroform extraction, and ethanol purification the following day was as usual with the ChIP protocol. At this stage 1 IP from 1 condition was resuspended with 34 uL of water and was

then used to resuspend each of the other 4 IPs worth from the same condition with the same 34 uL of water. Samples were quantified using the Qubit using the high sensitive dsDNA standards.

End Repair

To the 34μl of DNA in water the following was added: 5μl 10x END Repair Buffer (Epicentre Biotechnologies, #ER0720), 5μl 2.5mM dNTPs, 5μl 10mM ATP, 1μl END-IT enzyme mix (Epicentre Biotechnologies, #ER0720). This was incubated at RT for 45′. This step was stopped using Qiagen's MinElute protocol to purify (minelute kit: Qiagen, #28004) using the manufacturer's protocol but eluted twice, the first time in 20μl EB, and then 13μl EB.

Klenow Reaction

To the ~32 μl of eluted material with blunt DNA ends the following was added: 5 μl 10xNEB2, 10μl 1mM dATP (Invirogen), and 3μl Klenow (3′-5′ exo-) 5U/ml (from New England BioLabs). This was incubated for 30' at 37°C and stopped using Qiagen's MinElute protocol and eluted with two elutions of 10μl and 12μl of buffer EB.

Ligation:

To the eluted material 0.5μl of ligated 1μM DNA adapter, 25μl of 2x ligase buffer, and 5 μl of UltraPure Ligase (Enzymatics T4 DNA Ligase L603-HC-L 600,000 U/mL) was added an incubated at RT for 1 hour. The reaction was stopped using Qiagen's MinEluted protocol using two elutions of 15μl and 23μl of EB buffer.

PCR Amplification

To the ~37 µl of eluted DNA template 10 µl of 5x Phusion HF buffer, 1.5 µl of 10 mM dNTP, 0.5 µl of both the 25µM long and short PCR primers, and 0.5 µl of Phusion polymerase from NEB was added. The following amplification conditions were used: 30 seconds at 98°C followed by 13 total cycles of 10 seconds at 98°C, 30 seconds at 65°C, 30 seconds at 72°C, 5 minutes at 72°C, and hold at 4°C.

The following are the PCR primer sequences:

5' AATGATACGGCGACCACCGAGATCTACACTCTTTCCCTACACGACGCT CTTCCGATCT 3' (long, PAGE purified by IDT)

5' CAAGCAGAAGACGGCATACGAGCTCTTCCGATCT 3' (short, standard desalting IDT)

PCR Purification

Use AMPure beads (Agencourt BioSciences Corporation). Transfer the PCR reaction to a new 1.7 ml Epi tube and add 90µl of the mixed beads to the PCR solution and mix by pipetting up and down about 10 times, followed by brief vortexing. The samples incubated at RT for 5′ and were harvested using a magnetic stand to pull the beads to the side of the tube for 10 minutes at RT. When the solution is clear the solution's supernatant was removed and the beads were washed with 70% EtOH to the beads to cover the beads (500µl), incubated for 30′′ at RT, and pipetted off the EtOH. Repeat for a total of two washes and the beads air dried for 20′ at RT. The DNA was eluted from the beads by resuspending them in 20 uL of Qiagen's EB and then placed back

on the magnetic rack and after 5' the supernatant was pipetted off.

Gel Purification

All 20 uL of the eluted DNA product was resolved on an 8% Native PAGE gel, made with fresh 10x TBE, by first prerunning the gel for 20 minutes at 50 V at RT, and the samples loaded with loading buffer containing bromophenol blue and xylene cyanol and run at 75 V for 5 hours.

Gel Extraction

As the gel is running puncture the bottom of a sterile, nuclease-free, 0.5 ml microtube 4–5 times with a 21-gauge needle (heat under flame and then pierce tube) so that there are 4-5 separate holes at the bottom of the tube. Do this for as many gel slices that you'll have. Place the 0.5 ml microtube into a sterile, round-bottom, nuclease-free, 2 ml microtube. Pry apart the cassette and stain the gel with the ethidium bromide in a clean container for 2–3 minutes. View the gel on a Dark Reader transilluminator and using a clean scalpel, cut out the smear in the sample lanes (the gel slice can be wider than the smear but make sure the cut is well above the primer dimer around 92 bp, so that the bottom cut is just at the base of the visible smear, and upwards to about 300 bp in size. If the smear has smiled while running in the gel, make the cut so that it smiles as well and is not just a rectangle). Place the band into the 0.5 ml microtube. Centrifuge the stacked tubes at 10,000 rpm for 2 minutes at room temperature to shred the gel through the holes into the 2 ml tube. Elute from the gel once overnight, and once for four hours at RT or 37°C (I prefer 37C). Use 500 ul of elution buffer (TE, 150mM NaCl, 0.1% tween).

Transfer the eluates and the gel debris to the top of a Spin-X filter (do this as soon as the eluates are collected for each step but save the Spin-X filter and reuse for the same sample but seprate eluates.) Centrifuge the filter for 2 minutes at 10,000 rpm. After removing the eluates and spinning through the Spin-X coumns, add 500ul water to the gel pieces with a wide-bore pipet, so that you can move the gel pieces to the Spin-x column, and spin the remaining eluate through. Pool the elutions and lyophilize the sample from 1500μl, to bring the volume to 500ul (2 hours on the low setting). Add an equal volume of phenol/chloroform and extract the eluates, after spinning the eluate through the spin-X columns. Precipitate DNA with 2ul Glycogen (or glyco-blue), 300mM NaCl (final), and 2.5 volumes ethanol. Wash pellet with 70% ethanol. Resuspended samples in 20 μl of water. Use 1ul for Qubit quantification of DNA with the high sensitivity dsDNA standards. Finally, the barcoded libraries were combined in equimolar amounts in a total volume of 10 uL and sent to be sequenced.

REFERENCES

Adelman, K., Marr, M.T., Werner, J., Saunders, A., Ni, Z., Andrulis, E.D., and Lis, J.T. (2005). Efficient release from promoter-proximal stall sites requires transcript cleavage factor TFIIS. Mol. Cell *17,* 103-112.

Adelman, K., Wei, W., Ardehali, M.B., Werner, J., Zhu, B., Reinberg, D., and Lis, J.T. (2006). Drosophila Paf1 modulates chromatin structure at actively transcribed genes. Mol. Cell. Biol. *26,* 250-260.

Albert, I., Mavrich, T.N., Tomsho, L.P., Qi, J., Zanton, S.J., Schuster, S.C., and Pugh, B.F. (2007). Translational and rotational settings of H2A.Z nucleosomes across the Saccharomyces cerevisiae genome. Nature *446,* 572-576.

Allis, C.D., and Muir, T.W. (2011). Spreading chromatin into chemical biology. Chembiochem *12,* 264-279.

Althaus, F.R., Hofferer, L., Kleczkowska, H.E., Malanga, M., Naegeli, H., Panzeter, P.L., and Realini, C.A. (1994). Histone shuttling by poly ADP-ribosylation. Mol. Cell. Biochem. *138,* 53-59.

Andrews, A.J., Downing, G., Brown, K., Park, Y.J., and Luger, K. (2008). A thermodynamic model for Nap1-histone interactions. J. Biol. Chem. *283,* 32412-32418.

Andrulis, E.D., Guzman, E., Doring, P., Werner, J., and Lis, J.T. (2000). High-resolution localization of Drosophila Spt5 and Spt6 at heat shock genes in vivo: roles in promoter proximal pausing and transcription elongation. Genes Dev. *14,* 2635-2649.

Ardehali, M.B., and Lis, J.T. (2009). Tracking rates of transcription and splicing in vivo. Nat. Struct. Mol. Biol. *16,* 1123-1124.

Ardehali, M.B., Mei, A., Zobeck, K.L., Caron, M., Lis, J.T., and Kusch, T. (2011). Drosophila Set1 is the major histone H3 lysine 4 trimethyltransferase with role in transcription. EMBO J. *30,* 2817-2828.

Ardehali, M.B., Yao, J., Adelman, K., Fuda, N.J., Petesch, S.J., Webb, W.W., and Lis, J.T. (2009). Spt6 enhances the elongation rate of RNA polymerase II in vivo. EMBO J. *28,* 1067-1077.

Armstrong, J.A., Papoulas, O., Daubresse, G., Sperling, A.S., Lis, J.T., Scott, M.P., and Tamkun, J.W. (2002). The Drosophila BRM complex facilitates global transcription by RNA polymerase II. EMBO J. *21,* 5245-5254.

Ashburner, M. (1967). Patterns of puffing activity in the salivary gland chromosomes of Drosophila. I. Autosomal puffing patterns in a laboratory stock of Drosophila melanogaster. Chromosoma *21,* 398-428.

Avvakumov, N., Nourani, A., and Cote, J. (2011). Histone chaperones: modulators of chromatin marks. Mol. Cell *41,* 502-514.

Badenhorst, P., Voas, M., Rebay, I., and Wu, C. (2002). Biological functions of the ISWI chromatin remodeling complex NURF. Genes Dev. *16,* 3186-3198.

Bannister, A.J., and Kouzarides, T. (2011). Regulation of chromatin by histone modifications. Cell Res. *21,* 381-395.

Batta, K., Zhang, Z., Yen, K., Goffman, D.B., and Pugh, B.F. (2011). Genome-wide function of H2B ubiquitylation in promoter and genic regions. Genes Dev. *25,* 2254-2265.

Bendena, W.G., Garbe, J.C., Traverse, K.L., Lakhotia, S.C., and Pardue, M.L. (1989). Multiple inducers of the Drosophila heat shock locus 93D (hsr omega): inducer-specific patterns of the three transcripts. J. Cell Biol. *108,* 2017-2028.

Bintu, L., Kopaczynska, M., Hodges, C., Lubkowska, L., Kashlev, M., and Bustamante, C. (2011). The elongation rate of RNA polymerase determines the fate of transcribed nucleosomes. Nat. Struct. Mol. Biol. *18,* 1394-1399.

Boehm, A.K., Saunders, A., Werner, J., and Lis, J.T. (2003). Transcription factor and polymerase recruitment, modification, and movement on dhsp70 in vivo in the minutes following heat shock. Mol. Cell. Biol. *23,* 7628-7637.

Bohm, V., Hieb, A.R., Andrews, A.J., Gansen, A., Rocker, A., Toth, K., Luger, K., and Langowski, J. (2011). Nucleosome accessibility governed by the dimer/tetramer interface. Nucleic Acids Res. *39,* 3093-3102.

Bondarenko, V.A., Steele, L.M., Ujvari, A., Gaykalova, D.A., Kulaeva, O.I., Polikanov, Y.S., Luse, D.S., and Studitsky, V.M. (2006). Nucleosomes can form a polar barrier to transcript elongation by RNA polymerase II. Mol. Cell *24,* 469-479.

Bortvin, A., and Winston, F. (1996). Evidence that Spt6p controls chromatin structure by a direct interaction with histones. Science *272,* 1473-1476.

Brower-Toland, B., Wacker, D.A., Fulbright, R.M., Lis, J.T., Kraus, W.L., and Wang, M.D. (2005). Specific contributions of histone tails and their acetylation to the mechanical stability of nucleosomes. J. Mol. Biol. *346,* 135-146.

Brown, C.R., Mao, C., Falkovskaia, E., Law, J.K., and Boeger, H. (2011). In vivo role for the chromatin-remodeling enzyme SWI/SNF in the removal of promoter nucleosomes by disassembly rather than sliding. J. Biol. Chem. *286,* 40556-40565.

Brown, S.A., Imbalzano, A.N., and Kingston, R.E. (1996). Activator-dependent regulation of transcriptional pausing on nucleosomal templates. Genes Dev. *10,* 1479-1490.

Brown, S.A., and Kingston, R.E. (1997). Disruption of downstream chromatin directed by a transcriptional activator. Genes Dev. *11,* 3116-3121.

Bruno, M., Flaus, A., Stockdale, C., Rencurel, C., Ferreira, H., and Owen-Hughes, T. (2003). Histone H2A/H2B dimer exchange by ATP-dependent chromatin remodeling activities. Mol. Cell *12,* 1599-1606.

Carey, M., Li, B., and Workman, J.L. (2006). RSC exploits histone acetylation to abrogate the nucleosomal block to RNA polymerase II elongation. Mol. Cell *24,* 481-487.

Chatterjee, N., Sinha, D., Lemma-Dechassa, M., Tan, S., Shogren-Knaak, M.A., and Bartholomew, B. (2011). Histone H3 tail acetylation modulates ATP-

dependent remodeling through multiple mechanisms. Nucleic Acids Res. *39,* 8378-8391.

Clapier, C.R., and Cairns, B.R. (2009). The biology of chromatin remodeling complexes. Annu. Rev. Biochem. *78,* 273-304.

Craig, C.R., Fink, J.L., Yagi, Y., Ip, Y.T., and Cagan, R.L. (2004). A Drosophila p38 orthologue is required for environmental stress responses. EMBO Rep. *5,* 1058-1063.

Crawford, G.E., Holt, I.E., Whittle, J., Webb, B.D., Tai, D., Davis, S., Margulies, E.H., Chen, Y., Bernat, J.A., Ginsburg, D.*, et al.* (2006). Genome-wide mapping of DNase hypersensitive sites using massively parallel signature sequencing (MPSS). Genome Res. *16,* 123-131.

Crowley, T.E., Mathers, P.H., and Meyerowitz, E.M. (1984). A trans-acting regulatory product necessary for expression of the Drosophila melanogaster 68C glue gene cluster. Cell *39,* 149-156.

D'Amours, D., Desnoyers, S., D'Silva, I., and Poirier, G.G. (1999). Poly(ADP-ribosyl)ation reactions in the regulation of nuclear functions. Biochem. J. *342 (Pt 2),* 249-268.

Das, C., Tyler, J.K., and Churchill, M.E. (2010). The histone shuffle: histone chaperones in an energetic dance. Trends Biochem. Sci. *35,* 476-489.

de Murcia, G., Jongstra-Bilen, J., Ittel, M.E., Mandel, P., and Delain, E. (1983). Poly(ADP-ribose) polymerase auto-modification and interaction with DNA: electron microscopic visualization. EMBO J. *2,* 543-548.

Deal, R.B., Henikoff, J.G., and Henikoff, S. (2010). Genome-wide kinetics of nucleosome turnover determined by metabolic labeling of histones. Science *328,* 1161-1164.

Dechassa, M.L., Sabri, A., Pondugula, S., Kassabov, S.R., Chatterjee, N., Kladde, M.P., and Bartholomew, B. (2010). SWI/SNF has intrinsic nucleosome disassembly activity that is dependent on adjacent nucleosomes. Mol. Cell *38,* 590-602.

Del Rosario, B.C., and Pemberton, L.F. (2008). Nap1 links transcription elongation, chromatin assembly, and messenger RNP complex biogenesis. Mol. Cell. Biol. *28,* 2113-2124.

Egelhofer, T.A., Minoda, A., Klugman, S., Lee, K., Kolasinska-Zwierz, P., Alekseyenko, A.A., Cheung, M.S., Day, D.S., Gadel, S., Gorchakov, A.A.*, et al.* (2011). An assessment of histone-modification antibody quality. Nat. Struct. Mol. Biol. *18,* 91-93.

Fierz, B., Chatterjee, C., McGinty, R.K., Bar-Dagan, M., Raleigh, D.P., and Muir, T.W. (2011). Histone H2B ubiquitylation disrupts local and higher-order chromatin compaction. Nat. Chem. Biol. *7,* 113-119.

Fleischmann, G., Pflugfelder, G., Steiner, E.K., Javaherian, K., Howard, G.C., Wang, J.C., and Elgin, S.C. (1984). Drosophila DNA topoisomerase I is associated with transcriptionally active regions of the genome. Proc. Natl. Acad. Sci. U. S. A. *81,* 6958-6962.

Fuda, N.J., Ardehali, M.B., and Lis, J.T. (2009). Defining mechanisms that regulate RNA polymerase II transcription in vivo. Nature *461,* 186-192.

Gansen, A., Valeri, A., Hauger, F., Felekyan, S., Kalinin, S., Toth, K., Langowski, J., and Seidel, C.A. (2009). Nucleosome disassembly intermediates characterized by single-molecule FRET. Proc. Natl. Acad. Sci. U. S. A. *106,* 15308-15313.

Gaszner, M., Vazquez, J., and Schedl, P. (1999). The Zw5 protein, a component of the scs chromatin domain boundary, is able to block enhancer-promoter interaction. Genes Dev. *13,* 2098-2107.

Gaykalova, D.A., Nagarajavel, V., Bondarenko, V.A., Bartholomew, B., Clark, D.J., and Studitsky, V.M. (2011). A polar barrier to transcription can be circumvented by remodeler-induced nucleosome translocation. Nucleic Acids Res. *39,* 3520-3528.

Giardina, C., and Lis, J.T. (1995). Sodium salicylate and yeast heat shock gene transcription. J. Biol. Chem. *270,* 10369-10372.

Giardina, C., and Lis, J.T. (1993). Polymerase processivity and termination on Drosophila heat shock genes. J. Biol. Chem. *268,* 23806-23811.

Giardina, C., Perez-Riba, M., and Lis, J.T. (1992). Promoter melting and TFIID complexes on Drosophila genes in vivo. Genes Dev. *6,* 2190-2200.

Gilchrist, D.A., Dos Santos, G., Fargo, D.C., Xie, B., Gao, Y., Li, L., and Adelman, K. (2010). Pausing of RNA polymerase II disrupts DNA-specified nucleosome organization to enable precise gene regulation. Cell *143,* 540-551.

Gkikopoulos, T., Schofield, P., Singh, V., Pinskaya, M., Mellor, J., Smolle, M., Workman, J.L., Barton, G.J., and Owen-Hughes, T. (2011). A role for Snf2-related nucleosome-spacing enzymes in genome-wide nucleosome organization. Science *333,* 1758-1760.

Goldberg, A.D., Banaszynski, L.A., Noh, K.M., Lewis, P.W., Elsaesser, S.J., Stadler, S., Dewell, S., Law, M., Guo, X., Li, X.*, et al.* (2010). Distinct factors control histone variant H3.3 localization at specific genomic regions. Cell *140,* 678-691.

Guertin, M.J., Petesch, S.J., Zobeck, K.L., Min, I.M., and Lis, J.T. (2010). Drosophila heat shock system as a general model to investigate transcriptional regulation. Cold Spring Harb. Symp. Quant. Biol. *75,* 1-9.

Hall, M.A., Shundrovsky, A., Bai, L., Fulbright, R.M., Lis, J.T., and Wang, M.D. (2009). High-resolution dynamic mapping of histone-DNA interactions in a nucleosome. Nat. Struct. Mol. Biol. *16,* 124-129.

Hassa, P.O., Covic, M., Hasan, S., Imhof, R., and Hottiger, M.O. (2001). The enzymatic and DNA binding activity of PARP-1 are not required for NF-kappa B coactivator function. J. Biol. Chem. *276,* 45588-45597.

Hassa, P.O., Haenni, S.S., Buerki, C., Meier, N.I., Lane, W.S., Owen, H., Gersbach, M., Imhof, R., and Hottiger, M.O. (2005). Acetylation of poly(ADP-ribose) polymerase-1 by p300/CREB-binding protein regulates coactivation of NF-kappaB-dependent transcription. J. Biol. Chem. *280,* 40450-40464.

Hodges, C., Bintu, L., Lubkowska, L., Kashlev, M., and Bustamante, C. (2009). Nucleosomal fluctuations govern the transcription dynamics of RNA polymerase II. Science *325,* 626-628.

Hota, S.K., and Bartholomew, B. (2011). Diversity of operation in ATP-dependent chromatin remodelers. Biochim. Biophys. Acta *1809,* 476-487.

Ishibashi, T., Dryhurst, D., Rose, K.L., Shabanowitz, J., Hunt, D.F., and Ausio, J. (2009). Acetylation of vertebrate H2A.Z and its effect on the structure of the nucleosome. Biochemistry *48,* 5007-5017.

Ivanovska, I., Jacques, P.E., Rando, O.J., Robert, F., and Winston, F. (2011). Control of chromatin structure by spt6: different consequences in coding and regulatory regions. Mol. Cell. Biol. *31,* 531-541.

Izban, M.G., and Luse, D.S. (1991). Transcription on nucleosomal templates by RNA polymerase II in vitro: inhibition of elongation with enhancement of sequence-specific pausing. Genes Dev. *5,* 683-696.

Jedlicka, P., Mortin, M.A., and Wu, C. (1997). Multiple functions of Drosophila heat shock transcription factor in vivo. EMBO J. *16,* 2452-2462.

Jenuwein, T., and Allis, C.D. (2001). Translating the histone code. Science *293,* 1074-1080.

Jiang, C., and Pugh, B.F. (2009). Nucleosome positioning and gene regulation: advances through genomics. Nat. Rev. Genet. *10,* 161-172.

Jin, C., Zang, C., Wei, G., Cui, K., Peng, W., Zhao, K., and Felsenfeld, G. (2009). H3.3/H2A.Z double variant-containing nucleosomes mark 'nucleosome-free regions' of active promoters and other regulatory regions. Nat. Genet. *41,* 941-945.

Jin, J., Bai, L., Johnson, D.S., Fulbright, R.M., Kireeva, M.L., Kashlev, M., and Wang, M.D. (2010). Synergistic action of RNA polymerases in overcoming the nucleosomal barrier. Nat. Struct. Mol. Biol. *17,* 745-752.

Johnson, C.A., White, D.A., Lavender, J.S., O'Neill, L.P., and Turner, B.M. (2002). Human class I histone deacetylase complexes show enhanced catalytic activity in the presence of ATP and co-immunoprecipitate with the ATP-dependent chaperone protein Hsp70. J. Biol. Chem. *277,* 9590-9597.

Johnson, S.M., Tan, F.J., McCullough, H.L., Riordan, D.P., and Fire, A.Z. (2006). Flexibility and constraint in the nucleosome core landscape of Caenorhabditis elegans chromatin. Genome Res. *16,* 1505-1516.

Ju, B.G., Lunyak, V.V., Perissi, V., Garcia-Bassets, I., Rose, D.W., Glass, C.K., and Rosenfeld, M.G. (2006). A topoisomerase IIbeta-mediated dsDNA break required for regulated transcription. Science *312,* 1798-1802.

Kaplan, C.D., Laprade, L., and Winston, F. (2003). Transcription elongation factors repress transcription initiation from cryptic sites. Science *301,* 1096-1099.

Karagianni, P., and Wong, J. (2007). HDAC3: taking the SMRT-N-CoRrect road to repression. Oncogene *26,* 5439-5449.

Kellum, R., and Schedl, P. (1991). A position-effect assay for boundaries of higher order chromosomal domains. Cell *64,* 941-950.

Killian, J.L., Li, M., Sheinin, M.Y., and Wang, M.D. (2011). Recent advances in single molecule studies of nucleosomes. Curr. Opin. Struct. Biol.

Kim, M.Y., Mauro, S., Gevry, N., Lis, J.T., and Kraus, W.L. (2004). NAD+-dependent modulation of chromatin structure and transcription by nucleosome binding properties of PARP-1. Cell *119,* 803-814.

Kimura, A., and Horikoshi, M. (1998). Tip60 acetylates six lysines of a specific class in core histones in vitro. Genes Cells *3,* 789-800.

Kireeva, M.L., Walter, W., Tchernajenko, V., Bondarenko, V., Kashlev, M., and Studitsky, V.M. (2002). Nucleosome remodeling induced by RNA polymerase II: loss of the H2A/H2B dimer during transcription. Mol. Cell *9,* 541-552.

Knezetic, J.A., and Luse, D.S. (1986). The presence of nucleosomes on a DNA template prevents initiation by RNA polymerase II in vitro. Cell *45,* 95-104.

Konev, A.Y., Tribus, M., Park, S.Y., Podhraski, V., Lim, C.Y., Emelyanov, A.V., Vershilova, E., Pirrotta, V., Kadonaga, J.T., Lusser, A., and Fyodorov, D.V. (2007). CHD1 motor protein is required for deposition of histone variant H3.3 into chromatin in vivo. Science *317,* 1087-1090.

Kotova, E., Lodhi, N., Jarnik, M., Pinnola, A.D., Ji, Y., and Tulin, A.V. (2011). Drosophila histone H2A variant (H2Av) controls poly(ADP-ribose) polymerase 1 (PARP1) activation in chromatin. Proc. Natl. Acad. Sci. U. S. A. *108,* 6205-6210.

Kraus, W.L., and Lis, J.T. (2003). PARP goes transcription. Cell *113,* 677-683.

Krishnakumar, R., Gamble, M.J., Frizzell, K.M., Berrocal, J.G., Kininis, M., and Kraus, W.L. (2008). Reciprocal binding of PARP-1 and histone H1 at promoters specifies transcriptional outcomes. Science *319,* 819-821.

Krishnakumar, R., and Kraus, W.L. (2010a). The PARP side of the nucleus: molecular actions, physiological outcomes, and clinical targets. Mol. Cell *39,* 8-24.

Krishnakumar, R., and Kraus, W.L. (2010b). PARP-1 regulates chromatin structure and transcription through a KDM5B-dependent pathway. Mol. Cell *39,* 736-749.

Kuhn, E.J., Hart, C.M., and Geyer, P.K. (2004). Studies of the role of the Drosophila scs and scs' insulators in defining boundaries of a chromosome puff. Mol. Cell. Biol. *24,* 1470-1480.

Kulaeva, O.I., Gaykalova, D.A., Pestov, N.A., Golovastov, V.V., Vassylyev, D.G., Artsimovitch, I., and Studitsky, V.M. (2009). Mechanism of chromatin remodeling and recovery during passage of RNA polymerase II. Nat. Struct. Mol. Biol. *16,* 1272-1278.

Kulaeva, O.I., Gaykalova, D.A., and Studitsky, V.M. (2007). Transcription through chromatin by RNA polymerase II: histone displacement and exchange. Mutat. Res. *618,* 116-129.

Kumar, S.V., and Wigge, P.A. (2010). H2A.Z-containing nucleosomes mediate the thermosensory response in Arabidopsis. Cell *140,* 136-147.

Kusch, T., Florens, L., Macdonald, W.H., Swanson, S.K., Glaser, R.L., Yates, J.R.,3rd, Abmayr, S.M., Washburn, M.P., and Workman, J.L. (2004). Acetylation by Tip60 is required for selective histone variant exchange at DNA lesions. Science *306,* 2084-2087.

Larschan, E., Bishop, E.P., Kharchenko, P.V., Core, L.J., Lis, J.T., Park, P.J., and Kuroda, M.I. (2011). X chromosome dosage compensation via enhanced transcriptional elongation in Drosophila. Nature *471,* 115-118.

Leach, T.J., Mazzeo, M., Chotkowski, H.L., Madigan, J.P., Wotring, M.G., and Glaser, R.L. (2000). Histone H2A.Z is widely but nonrandomly distributed in chromosomes of Drosophila melanogaster. J. Biol. Chem. *275,* 23267-23272.

Lebedeva, L.A., Nabirochkina, E.N., Kurshakova, M.M., Robert, F., Krasnov, A.N., Evgen'ev, M.B., Kadonaga, J.T., Georgieva, S.G., and Tora, L. (2005). Occupancy of the Drosophila hsp70 promoter by a subset of basal transcription factors diminishes upon transcriptional activation. Proc. Natl. Acad. Sci. U. S. A. *102,* 18087-18092.

Leduc, Y., de Murcia, G., Lamarre, D., and Poirier, G.G. (1986). Visualization of poly(ADP-ribose) synthetase associated with polynucleosomes by immunoelectron microscopy. Biochim. Biophys. Acta *885,* 248-255.

Lee, W., Tillo, D., Bray, N., Morse, R.H., Davis, R.W., Hughes, T.R., and Nislow, C. (2007). A high-resolution atlas of nucleosome occupancy in yeast. Nat. Genet. *39,* 1235-1244.

Leemans, R., Egger, B., Loop, T., Kammermeier, L., He, H., Hartmann, B., Certa, U., Hirth, F., and Reichert, H. (2000). Quantitative transcript imaging in normal and heat-shocked Drosophila embryos by using high-density oligonucleotide arrays. Proc. Natl. Acad. Sci. U. S. A. *97,* 12138-12143.

Leung, B.O., and Chou, K.C. (2011). Review of super-resolution fluorescence microscopy for biology. Appl. Spectrosc. *65,* 967-980.

Lewis, M., Helmsing, P.J., and Ashburner, M. (1975). Parallel changes in puffing activity and patterns of protein synthesis in salivary glands of Drosophila. Proc. Natl. Acad. Sci. U. S. A. *72,* 3604-3608.

Li, B., Carey, M., and Workman, J.L. (2007a). The role of chromatin during transcription. Cell *128,* 707-719.

Li, B., Gogol, M., Carey, M., Lee, D., Seidel, C., and Workman, J.L. (2007b). Combined action of PHD and chromo domains directs the Rpd3S HDAC to transcribed chromatin. Science *316,* 1050-1054.

Li, G., Levitus, M., Bustamante, C., and Widom, J. (2005). Rapid spontaneous accessibility of nucleosomal DNA. Nat. Struct. Mol. Biol. *12,* 46-53.

Li, G., and Reinberg, D. (2011). Chromatin higher-order structures and gene regulation. Curr. Opin. Genet. Dev. *21,* 175-186.

Lis, J.T. (2007). Imaging Drosophila gene activation and polymerase pausing in vivo. Nature *450,* 198-202.

Lis, J.T., Mason, P., Peng, J., Price, D.H., and Werner, J. (2000). P-TEFb kinase recruitment and function at heat shock loci. Genes Dev. *14,* 792-803.

Lorch, Y., LaPointe, J.W., and Kornberg, R.D. (1987). Nucleosomes inhibit the initiation of transcription but allow chain elongation with the displacement of histones. Cell *49,* 203-210.

Lorch, Y., Maier-Davis, B., and Kornberg, R.D. (2006). Chromatin remodeling by nucleosome disassembly in vitro. Proc. Natl. Acad. Sci. U. S. A. *103,* 3090-3093.

Lorch, Y., Zhang, M., and Kornberg, R.D. (1999). Histone octamer transfer by a chromatin-remodeling complex. Cell *96,* 389-392.

Luebben, W.R., Sharma, N., and Nyborg, J.K. (2010). Nucleosome eviction and activated transcription require p300 acetylation of histone H3 lysine 14. Proc. Natl. Acad. Sci. U. S. A. *107,* 19254-19259.

Luger, K., Mader, A.W., Richmond, R.K., Sargent, D.F., and Richmond, T.J. (1997). Crystal structure of the nucleosome core particle at 2.8 A resolution. Nature *389,* 251-260.

Luk, E., Ranjan, A., Fitzgerald, P.C., Mizuguchi, G., Huang, Y., Wei, D., and Wu, C. (2010). Stepwise histone replacement by SWR1 requires dual activation with histone H2A.Z and canonical nucleosome. Cell *143,* 725-736.

Luk, E., Vu, N.D., Patteson, K., Mizuguchi, G., Wu, W.H., Ranjan, A., Backus, J., Sen, S., Lewis, M., Bai, Y., and Wu, C. (2007). Chz1, a nuclear chaperone for histone H2AZ. Mol. Cell *25,* 357-368.

Lusser, A., Urwin, D.L., and Kadonaga, J.T. (2005). Distinct activities of CHD1 and ACF in ATP-dependent chromatin assembly. Nat. Struct. Mol. Biol. *12,* 160-166.

Madigan, J.P., Chotkowski, H.L., and Glaser, R.L. (2002). DNA double-strand break-induced phosphorylation of Drosophila histone variant H2Av helps prevent radiation-induced apoptosis. Nucleic Acids Res. *30,* 3698-3705.

Mason, P.B., and Struhl, K. (2003). The FACT complex travels with elongating RNA polymerase II and is important for the fidelity of transcriptional initiation in vivo. Mol. Cell. Biol. *23,* 8323-8333.

McKnight, S.L., and Miller, O.L.,Jr. (1979). Post-replicative nonribosomal transcription units in D. melanogaster embryos. Cell *17,* 551-563.

Mito, Y., Henikoff, J.G., and Henikoff, S. (2007). Histone replacement marks the boundaries of cis-regulatory domains. Science *315,* 1408-1411.

Mito, Y., Henikoff, J.G., and Henikoff, S. (2005). Genome-scale profiling of histone H3.3 replacement patterns. Nat. Genet. *37,* 1090-1097.

Mizuguchi, G., Shen, X., Landry, J., Wu, W.H., Sen, S., and Wu, C. (2004). ATP-driven exchange of histone H2AZ variant catalyzed by SWR1 chromatin remodeling complex. Science *303,* 343-348.

Muse, G.W., Gilchrist, D.A., Nechaev, S., Shah, R., Parker, J.S., Grissom, S.F., Zeitlinger, J., and Adelman, K. (2007). RNA polymerase is poised for activation across the genome. Nat. Genet. *39,* 1507-1511.

Nacheva, G.A., Guschin, D.Y., Preobrazhenskaya, O.V., Karpov, V.L., Ebralidse, K.K., and Mirzabekov, A.D. (1989). Change in the pattern of histone binding to DNA upon transcriptional activation. Cell *58,* 27-36.

Neumann, H., Hancock, S.M., Buning, R., Routh, A., Chapman, L., Somers, J., Owen-Hughes, T., van Noort, J., Rhodes, D., and Chin, J.W. (2009). A method for genetically installing site-specific acetylation in recombinant histones defines the effects of H3 K56 acetylation. Mol. Cell *36,* 153-163.

Ni, Z., Saunders, A., Fuda, N.J., Yao, J., Suarez, J.R., Webb, W.W., and Lis, J.T. (2007). P-TEFb is critical for the maturation of RNA Polymerase II into productive elongation in vivo. Mol. Cell. Biol.

North, J.A., Javaid, S., Ferdinand, M.B., Chatterjee, N., Picking, J.W., Shoffner, M., Nakkula, R.J., Bartholomew, B., Ottesen, J.J., Fishel, R., and Poirier, M.G. (2011). Phosphorylation of histone H3(T118) alters nucleosome dynamics and remodeling. Nucleic Acids Res. *39,* 6465-6474.

Nusinow, D.A., Hernandez-Munoz, I., Fazzio, T.G., Shah, G.M., Kraus, W.L., and Panning, B. (2007). Poly(ADP-ribose) polymerase 1 is inhibited by a histone H2A variant, MacroH2A, and contributes to silencing of the inactive X chromosome. J. Biol. Chem. *282,* 12851-12859.

O'Brien, T., and Lis, J.T. (1993). Rapid changes in Drosophila transcription after an instantaneous heat shock. Mol. Cell. Biol. *13,* 3456-3463.

O'Brien, T., Wilkins, R.C., Giardina, C., and Lis, J.T. (1995). Distribution of GAGA protein on Drosophila genes in vivo. Genes Dev. *9,* 1098-1110.

Orphanides, G., LeRoy, G., Chang, C.H., Luse, D.S., and Reinberg, D. (1998). FACT, a factor that facilitates transcript elongation through nucleosomes. Cell *92,* 105-116.

Ouararhni, K., Hadj-Slimane, R., Ait-Si-Ali, S., Robin, P., Mietton, F., Harel-Bellan, A., Dimitrov, S., and Hamiche, A. (2006). The histone variant mH2A1.1 interferes with transcription by down-regulating PARP-1 enzymatic activity. Genes Dev. *20,* 3324-3336.

Papamichos-Chronakis, M., Watanabe, S., Rando, O.J., and Peterson, C.L. (2011). Global regulation of H2A.Z localization by the INO80 chromatin-remodeling enzyme is essential for genome integrity. Cell *144,* 200-213.

Park, J.M., Werner, J., Kim, J.M., Lis, J.T., and Kim, Y.J. (2001). Mediator, not holoenzyme, is directly recruited to the heat shock promoter by HSF upon heat shock. Mol. Cell *8,* 9-19.

Pavri, R., Lewis, B., Kim, T.K., Dilworth, F.J., Erdjument-Bromage, H., Tempst, P., de Murcia, G., Evans, R., Chambon, P., and Reinberg, D. (2005). PARP-1 determines specificity in a retinoid signaling pathway via direct modulation of mediator. Mol. Cell *18,* 83-96.

Pavri, R., Zhu, B., Li, G., Trojer, P., Mandal, S., Shilatifard, A., and Reinberg, D. (2006). Histone H2B monoubiquitination functions cooperatively with FACT to regulate elongation by RNA polymerase II. Cell *125,* 703-717.

Perisic, O., Xiao, H., and Lis, J.T. (1989). Stable binding of Drosophila heat shock factor to head-to-head and tail-to-tail repeats of a conserved 5 bp recognition unit. Cell *59,* 797-806.

Peterson, C.L., and Laniel, M.A. (2004). Histones and histone modifications. Curr. Biol. *14,* R546-51.

Petesch, S.J., and Lis, J.T. (2012a). Activator-induced spread of poly(ADP-ribose) polymerase promotes nucleosome loss at Hsp70. Mol. Cell *45,* 64-74.

Petesch, S.J., and Lis, J.T. (2012b). Overcoming the nucleosome barrier during transcript elongation. Trends Genet.

Petesch, S.J., and Lis, J.T. (2008). Rapid, transcription-independent loss of nucleosomes over a large chromatin domain at Hsp70 loci. Cell *134,* 74-84.

Pinnola, A., Naumova, N., Shah, M., and Tulin, A.V. (2007). Nucleosomal core histones mediate dynamic regulation of poly(ADP-ribose) polymerase 1 protein binding to chromatin and induction of its enzymatic activity. J. Biol. Chem. *282,* 32511-32519.

Plagens, U., Greenleaf, A.L., and Bautz, E.K. (1976). Distribution of RNA polymerase on Drosophila polytene chromosomes as studied by indirect immunofluorescence. Chromosoma *59,* 157-165.

Poirier, G.G., de Murcia, G., Jongstra-Bilen, J., Niedergang, C., and Mandel, P. (1982). Poly(ADP-ribosyl)ation of polynucleosomes causes relaxation of chromatin structure. Proc. Natl. Acad. Sci. U. S. A. *79,* 3423-3427.

Pray-Grant, M.G., Daniel, J.A., Schieltz, D., Yates, J.R.,3rd, and Grant, P.A. (2005). Chd1 chromodomain links histone H3 methylation with SAGA- and SLIK-dependent acetylation. Nature *433,* 434-438.

Rabindran, S.K., Haroun, R.I., Clos, J., Wisniewski, J., and Wu, C. (1993). Regulation of heat shock factor trimer formation: role of a conserved leucine zipper. Science *259,* 230-234.

Rando, O.J., and Ahmad, K. (2007). Rules and regulation in the primary structure of chromatin. Curr. Opin. Cell Biol. *19,* 250-256.

Rasmussen, E.B., and Lis, J.T. (1993). In vivo transcriptional pausing and cap formation on three Drosophila heat shock genes. Proc. Natl. Acad. Sci. U. S. A. *90,* 7923-7927.

Ray-Gallet, D., and Almouzni, G. (2010). Nucleosome dynamics and histone variants. Essays Biochem. *48,* 75-87.

Reinke, H., and Horz, W. (2003). Histones are first hyperacetylated and then lose contact with the activated PHO5 promoter. Mol. Cell *11,* 1599-1607.

Rougvie, A.E., and Lis, J.T. (1990). Postinitiation transcriptional control in Drosophila melanogaster. Mol. Cell. Biol. *10,* 6041-6045.

Rougvie, A.E., and Lis, J.T. (1988). The RNA polymerase II molecule at the 5' end of the uninduced hsp70 gene of D. melanogaster is transcriptionally engaged. Cell *54,* 795-804.

Rouleau, M., Patel, A., Hendzel, M.J., Kaufmann, S.H., and Poirier, G.G. (2010). PARP inhibition: PARP1 and beyond. Nat. Rev. Cancer. *10,* 293-301.

Rufiange, A., Jacques, P.E., Bhat, W., Robert, F., and Nourani, A. (2007). Genome-wide replication-independent histone H3 exchange occurs predominantly at promoters and implicates H3 K56 acetylation and Asf1. Mol. Cell *27,* 393-405.

Ruthenburg, A.J., Li, H., Milne, T.A., Dewell, S., McGinty, R.K., Yuen, M., Ueberheide, B., Dou, Y., Muir, T.W., Patel, D.J., and Allis, C.D. (2011). Recognition of a mononucleosomal histone modification pattern by BPTF via multivalent interactions. Cell *145,* 692-706.

Saha, A., Wittmeyer, J., and Cairns, B.R. (2006). Chromatin remodelling: the industrial revolution of DNA around histones. Nat. Rev. Mol. Cell Biol. *7,* 437-447.

Sala, A., La Rocca, G., Burgio, G., Kotova, E., Di Gesu, D., Collesano, M., Ingrassia, A.M., Tulin, A.V., and Corona, D.F. (2008). The nucleosome-remodeling ATPase ISWI is regulated by poly-ADP-ribosylation. PLoS Biol. *6,* e252.

Sapountzi, V., Logan, I.R., and Robson, C.N. (2006). Cellular functions of TIP60. Int. J. Biochem. Cell Biol. *38,* 1496-1509.

Saunders, A., Core, L.J., and Lis, J.T. (2006). Breaking barriers to transcription elongation. Nat. Rev. Mol. Cell Biol. *7,* 557-567.

Saunders, A., Werner, J., Andrulis, E.D., Nakayama, T., Hirose, S., Reinberg, D., and Lis, J.T. (2003). Tracking FACT and the RNA polymerase II elongation complex through chromatin in vivo. Science *301,* 1094-1096.

Schmittgen, T.D., Zakrajsek, B.A., Mills, A.G., Gorn, V., Singer, M.J., and Reed, M.W. (2000). Quantitative reverse transcription-polymerase chain reaction to study mRNA decay: comparison of endpoint and real-time methods. Anal. Biochem. *285,* 194-204.

Schones, D.E., Cui, K., Cuddapah, S., Roh, T.Y., Barski, A., Wang, Z., Wei, G., and Zhao, K. (2008). Dynamic regulation of nucleosome positioning in the human genome. Cell *132,* 887-898.

Schwabish, M.A., and Struhl, K. (2007). The Swi/Snf Complex Is Important for Histone Eviction during Transcriptional Activation and RNA Polymerase II Elongation In Vivo. Mol. Cell. Biol. *27,* 6987-6995.

Schwabish, M.A., and Struhl, K. (2006). Asf1 mediates histone eviction and deposition during elongation by RNA polymerase II. Mol. Cell *22,* 415-422.

Schwabish, M.A., and Struhl, K. (2004). Evidence for eviction and rapid deposition of histones upon transcriptional elongation by RNA polymerase II. Mol. Cell. Biol. *24,* 10111-10117.

Segal, E., and Widom, J. (2009). What controls nucleosome positions? Trends Genet. *25,* 335-343.

Sekinger, E.A., Moqtaderi, Z., and Struhl, K. (2005). Intrinsic histone-DNA interactions and low nucleosome density are important for preferential accessibility of promoter regions in yeast. Mol. Cell *18,* 735-748.

Shimko, J.C., North, J.A., Bruns, A.N., Poirier, M.G., and Ottesen, J.J. (2011). Preparation of fully synthetic histone H3 reveals that acetyl-lysine 56 facilitates protein binding within nucleosomes. J. Mol. Biol. *408,* 187-204.

Shivaswamy, S., and Iyer, V.R. (2008). Stress-dependent dynamics of global chromatin remodeling in yeast: dual role for SWI/SNF in the heat shock stress response. Mol. Cell. Biol. *28,* 2221-2234.

Shogren-Knaak, M., Ishii, H., Sun, J.M., Pazin, M.J., Davie, J.R., and Peterson, C.L. (2006). Histone H4-K16 acetylation controls chromatin structure and protein interactions. Science *311,* 844-847.

Shopland, L.S., Hirayoshi, K., Fernandes, M., and Lis, J.T. (1995). HSF access to heat shock elements in vivo depends critically on promoter architecture defined by GAGA factor, TFIID, and RNA polymerase II binding sites. Genes Dev. *9,* 2756-2769.

Simic, R., Lindstrom, D.L., Tran, H.G., Roinick, K.L., Costa, P.J., Johnson, A.D., Hartzog, G.A., and Arndt, K.M. (2003). Chromatin remodeling protein Chd1 interacts with transcription elongation factors and localizes to transcribed genes. EMBO J. *22,* 1846-1856.

Simon, J.A., Sutton, C.A., Lobell, R.B., Glaser, R.L., and Lis, J.T. (1985). Determinants of heat shock-induced chromosome puffing. Cell *40,* 805-817.

Smith, S.T., Petruk, S., Sedkov, Y., Cho, E., Tillib, S., Canaani, E., and Mazo, A. (2004). Modulation of heat shock gene expression by the TAC1 chromatin-modifying complex. Nat. Cell Biol. *6,* 162-167.

Solomon, M.J., Larsen, P.L., and Varshavsky, A. (1988). Mapping protein-DNA interactions in vivo with formaldehyde: evidence that histone H4 is retained on a highly transcribed gene. Cell *53,* 937-947.

Sorger, P.K., and Pelham, H.R. (1988). Yeast heat shock factor is an essential DNA-binding protein that exhibits temperature-dependent phosphorylation. Cell *54,* 855-864.

Srinivasan, S., Armstrong, J.A., Deuring, R., Dahlsveen, I.K., McNeill, H., and Tamkun, J.W. (2005). The Drosophila trithorax group protein Kismet facilitates an early step in transcriptional elongation by RNA Polymerase II. Development *132,* 1623-1635.

Szenker, E., Ray-Gallet, D., and Almouzni, G. (2011). The double face of the histone variant H3.3. Cell Res. *21,* 421-434.

Tagami, H., Ray-Gallet, D., Almouzni, G., and Nakatani, Y. (2004). Histone H3.1 and H3.3 complexes mediate nucleosome assembly pathways dependent or independent of DNA synthesis. Cell *116,* 51-61.

Talbert, P.B., and Henikoff, S. (2010). Histone variants--ancient wrap artists of the epigenome. Nat. Rev. Mol. Cell Biol. *11,* 264-275.

Tan, M., Luo, H., Lee, S., Jin, F., Yang, J.S., Montellier, E., Buchou, T., Cheng, Z., Rousseaux, S., Rajagopal, N.*, et al.* (2011). Identification of 67 histone marks and histone lysine crotonylation as a new type of histone modification. Cell *146,* 1016-1028.

Taverna, S.D., Li, H., Ruthenburg, A.J., Allis, C.D., and Patel, D.J. (2007). How chromatin-binding modules interpret histone modifications: lessons from professional pocket pickers. Nat. Struct. Mol. Biol. *14,* 1025-1040.

Thummel, C.S., Burtis, K.C., and Hogness, D.S. (1990). Spatial and temporal patterns of E74 transcription during Drosophila development. Cell *61,* 101-111.

Tims, H.S., Gurunathan, K., Levitus, M., and Widom, J. (2011). Dynamics of nucleosome invasion by DNA binding proteins. J. Mol. Biol. *411,* 430-448.

Tolkunov, D., Zawadzki, K.A., Singer, C., Elfving, N., Morozov, A.V., and Broach, J.R. (2011). Chromatin remodelers clear nucleosomes from intrinsically unfavorable sites to establish nucleosome-depleted regions at promoters. Mol. Biol. Cell *22,* 2106-2118.

Treand, C., du Chene, I., Bres, V., Kiernan, R., Benarous, R., Benkirane, M., and Emiliani, S. (2006). Requirement for SWI/SNF chromatin-remodeling complex in Tat-mediated activation of the HIV-1 promoter. EMBO J. *25,* 1690-1699.

Trinklein, N.D., Karaoz, U., Wu, J., Halees, A., Force Aldred, S., Collins, P.J., Zheng, D., Zhang, Z.D., Gerstein, M.B., Snyder, M., Myers, R.M., and Weng, Z. (2007). Integrated analysis of experimental data sets reveals many novel promoters in 1% of the human genome. Genome Res. *17,* 720-731.

Tsukiyama, T., Becker, P.B., and Wu, C. (1994). ATP-dependent nucleosome disruption at a heat-shock promoter mediated by binding of GAGA transcription factor. Nature *367,* 525-532.

Tsukiyama, T., and Wu, C. (1995). Purification and properties of an ATP-dependent nucleosome remodeling factor. Cell *83,* 1011-1020.

Tulin, A., and Spradling, A. (2003). Chromatin loosening by poly(ADP)-ribose polymerase (PARP) at Drosophila puff loci. Science *299,* 560-562.

Udugama, M., Sabri, A., and Bartholomew, B. (2011). The INO80 ATP-dependent chromatin remodeling complex is a nucleosome spacing factor. Mol. Cell. Biol. *31,* 662-673.

Udvardy, A., Maine, E., and Schedl, P. (1985). The 87A7 chromomere. Identification of novel chromatin structures flanking the heat shock locus that may define the boundaries of higher order domains. J. Mol. Biol. *185,* 341-358.

Udvardy, A., and Schedl, P. (1991). Chromatin structure, not DNA sequence specificity, is the primary determinant of topoisomerase II sites of action in vivo. Mol. Cell. Biol. *11,* 4973-4984.

Vazquez, J., and Schedl, P. (1994). Sequences required for enhancer blocking activity of scs are located within two nuclease-hypersensitive regions. EMBO J. *13,* 5984-5993.

Virag, L., and Szabo, C. (2002). The therapeutic potential of poly(ADP-ribose) polymerase inhibitors. Pharmacol. Rev. *54,* 375-429.

Wacker, D.A., Ruhl, D.D., Balagamwala, E.H., Hope, K.M., Zhang, T., and Kraus, W.L. (2007). The DNA Binding and Catalytic Domains of Poly(ADP-ribose) Polymerase-1 Cooperate in the Regulation of Chromatin Structure and Transcription. Mol. Cell. Biol.

Walfridsson, J., Khorosjutina, O., Matikainen, P., Gustafsson, C.M., and Ekwall, K. (2007). A genome-wide role for CHD remodelling factors and Nap1 in nucleosome disassembly. EMBO J. *26,* 2868-2879.

Weake, V.M., and Workman, J.L. (2010). Inducible gene expression: diverse regulatory mechanisms. Nat. Rev. Genet. *11,* 426-437.

Westwood, J.T., Clos, J., and Wu, C. (1991). Stress-induced oligomerization and chromosomal relocalization of heat-shock factor. Nature *353,* 822-827.

Whitehouse, I., Rando, O.J., Delrow, J., and Tsukiyama, T. (2007). Chromatin remodelling at promoters suppresses antisense transcription. Nature *450,* 1031-1035.

Winegarden, N.A., Wong, K.S., Sopta, M., and Westwood, J.T. (1996). Sodium salicylate decreases intracellular ATP, induces both heat shock factor binding and chromosomal puffing, but does not induce hsp 70 gene transcription in Drosophila. J. Biol. Chem. *271,* 26971-26980.

Wu, C. (1980). The 5' ends of Drosophila heat shock genes in chromatin are hypersensitive to DNase I. Nature *286,* 854-860.

Wu, C., Wong, Y.C., and Elgin, S.C. (1979). The chromatin structure of specific genes: II. Disruption of chromatin structure during gene activity. Cell *16,* 807-814.

Wysocka, J., Swigut, T., Xiao, H., Milne, T.A., Kwon, S.Y., Landry, J., Kauer, M., Tackett, A.J., Chait, B.T., Badenhorst, P., Wu, C., and Allis, C.D. (2006). A PHD finger of NURF couples histone H3 lysine 4 trimethylation with chromatin remodelling. Nature *442,* 86-90.

Yao, J., Ardehali, M.B., Fecko, C.J., Webb, W.W., and Lis, J.T. (2007). Intranuclear Distribution and Local Dynamics of RNA Polymerase II during Transcription Activation. Mol. Cell *28,* 978-990.

Yao, J., Zobeck, K.L., Lis, J.T., and Webb, W.W. (2008). Imaging transcription dynamics at endogenous genes in living Drosophila tissues. Methods *45,* 233-241.

Yuan, G.C., Liu, Y.J., Dion, M.F., Slack, M.D., Wu, L.F., Altschuler, S.J., and Rando, O.J. (2005). Genome-scale identification of nucleosome positions in S. cerevisiae. Science *309,* 626-630.

Yun, M., Wu, J., Workman, J.L., and Li, B. (2011). Readers of histone modifications. Cell Res. *21,* 564-578.

Zhang, H., Roberts, D.N., and Cairns, B.R. (2005). Genome-wide dynamics of Htz1, a histone H2A variant that poises repressed/basal promoters for activation through histone loss. Cell *123,* 219-231.

Zhao, J., Herrera-Diaz, J., and Gross, D.S. (2005). Domain-wide displacement of histones by activated heat shock factor occurs independently of Swi/Snf and

is not correlated with RNA polymerase II density. Mol. Cell. Biol. *25,* 8985-8999.

Zhao, K., Hart, C.M., and Laemmli, U.K. (1995). Visualization of chromosomal domains with boundary element-associated factor BEAF-32. Cell *81,* 879-889.

Zhuang, Z.H., Zhou, Y., Yu, M.C., Silverman, N., and Ge, B.X. (2006). Regulation of Drosophila p38 activation by specific MAP2 kinase and MAP3 kinase in response to different stimuli. Cell. Signal. *18,* 441-448.

Zobeck, K.L., Buckley, M.S., Zipfel, W.R., and Lis, J.T. (2010). Recruitment timing and dynamics of transcription factors at the Hsp70 loci in living cells. Mol. Cell *40,* 965-975.